



Cyprus  
University of  
Technology

Faculty of Geotechnical  
Sciences and Environmental  
Management

**Doctoral Dissertation**

**RESTORATION OF SURFACE WATERS  
CONTAMINATED WITH CYANOBACTERIA HARMFUL  
BLOOMS (CYANO-HABs) THROUGH NOVEL  
CHEMICAL OXIDATION PROCESSES**

**Eleni C. Keliri**

**Limassol, December 2022**



CYPRUS UNIVERSITY OF TECHNOLOGY  
FACULTY OF GEOTECHNICAL SCIENCES AND  
ENVIRONMENTAL MANAGEMENT  
DEPARTMENT OF CHEMICAL ENGINEERING

Doctoral Dissertation

RESTORATION OF SURFACE WATERS CONTAMINATED  
WITH CYANOBACTERIAL HARMFUL BLOOMS (CYANO-  
HABs) THROUGH NOVEL CHEMICAL OXIDATION  
PROCESSES

Eleni C. Keliri

Limassol, December 2022

# Approval Form

Doctoral Dissertation

**RESTORATION OF SURFACE WATERS CONTAMINATED WITH  
CYANOBACTERIAL HARMFUL BLOOMS (CYANO-HABs)  
THROUGH NOVEL CHEMICAL OXIDATION PROCESSES**

Presented by

Eleni C. Keliri

Supervisor: Dr. Maria G. Antoniou, Assistant Professor

Signature \_\_\_\_\_

Member of the committee: prof. Ifigeneia Kagkalou (external)

Signature \_\_\_\_\_

Member of the committee: prof. RNDr. Luděk Bláha (external)

Signature \_\_\_\_\_

Cyprus University of Technology

Limassol, December 2022

## **Copyrights**

Copyright © 2022 Eleni Keliri

All rights reserved.

The approval of the dissertation by the Department of Chemical Engineering does not imply necessarily the approval by the Department of the views of the writer.

I would like to extend my sincere thanks to the supervisor of this thesis, Dr. Maria G. Antoniou, for hosting me at the Water Treatment Laboratory – AQUA, and for her unwavering support at every stage of my research. The outcomes of this thesis would not have been possible without her prompt, detailed, and constructive feedback whenever I needed it.

Acknowledgments to my Ph.D. advisory board, Dr. Konstantinos Makris, and Dr. Maria Rikkou-Kalourkoti, whose guidance positively impacted the advancement of this research. I am also grateful to the external members of the Examination Committee, prof. Ifigeneia Kagkalou and prof. RNDr. Luděk Bláha. I am sure that their insightful comments and suggestions will be crucial for the further improvement of the thesis.

A warm thank you to all the collaborators (prof. Assaf Sukenik, prof. Dariusz Dziga, prof. Hanna Mazur-Marzec, prof. Ioannis Deligiannakis, prof. Andreas Anayiotos, Dr. Ekaterina Chernova, Mr. Luc Brient, Dr. Konstantinos Kapnisis, Mrs. Despoina Kokkinidou, Dr. Claudia Wiegand, Mrs. Athena Papatheodoulou, Dr. Panayiota Demosthenous, Dr. Antonis Hadjiantonis, Dr. Evangelos Daskalakis, Mrs. Nikoletta Tsiarta, Mrs. Sinead Kinsella and Mr. Angelos Sofokleous) and to the alumni students of the Water Treatment Laboratory-AQUA (Manolis, Christia, Nektarios, and Panayiota), with whom I had a great collaboration and worked closely on several projects. I am also thankful to Mr. Loizos Constantinou of the Department of Forests, and the Division of Hydrometry of the Water Development Department, for granting access for sampling in waterbodies under their authorities.

I would also like to give my appreciation to the “Cyprus Seeds” Organization for providing funds to develop my research and the side product named “POXi kit”, for networking us with distinguished scientist and entrepreneurs, and for offering mentorship, workshops, and seminars relevant to innovative research and commercialization. The encouragement and guidance we received from our mentor, Mrs. Karen Golmer, was of a great value. Acknowledgments are also given to the Research and Innovation Foundation of Cyprus for providing research and/or travel grants to the following projects related to cyano-HABs monitoring and treatment: CYANOS «RESTART 2016-2020» (BILATERAL/France/1116/0006), CYANOBOX (ENTERPRISES/0618/157), and CYANOTECH (EXCELLENCE/0421/0212).

I would like to express my gratitude to my mum in Heaven, my supportive dad and family, my compassionate friends, and to my wonderful husband Emilios, whose love and support made the completion of this Ph.D. possible.

...Dedicated to her loving memory...

## ABSTRACT

Cyanobacteria (blue-green algae) are phototrophic microorganism that represent an essential component of the food web in all aquatic ecosystems. However, the effects of climate change and anthropogenic activities have intensely increased the load of nutrients in surface waters around the globe, making cyanobacterial harmful blooming (cyano-HABs) more persistent and prevalent, adding further pressure on the already scarce fresh water supply. Their overgrowth is causing undesirable odor, color, and taste to the water, as well as toxicity since certain strains of cyanobacteria are producing secondary metabolites, called cyanotoxins which are lethal to both humans and animals. Currently an array of methods has been applied to mitigate the negative effects of cyano-HABs, that differ in cost, efficiency, and environmental impact. Those can be categorized as physical, chemical, and biological treatment methods based on their application type. Chemical methods are the most applied ones for being efficient, cost effective, and having long-lasting treatment results. The most recently developed method is the use of liquid hydrogen peroxide ( $\text{H}_2\text{O}_2$ ) in affected surface waterbodies which is by far the least hazardous chemical, among the treatment options, used for *in-situ* treatment. However, studies have shown that its efficiency varies based on the species type and density as well as on matrix composition. In cases of high contamination, the use of higher doses of  $\text{H}_2\text{O}_2$  than the recommended  $> 5 \text{ mg L}^{-1}$  dose, are required. which negatively impact zooplankton and other non-targeted species. In this doctoral thesis, peroxide releasing compounds were utilized to test their potency to mitigate cyano-HABs as novel treatment alternatives to the high doses of liquid hydrogen peroxide. More specifically, the following oxidants were utilized: magnesium peroxide ( $\text{MgO}_2$ ) granules, calcium peroxide ( $\text{CaO}_2$ ) granules and powder,  $\text{CaO}_2$  granules enclosed in fabrics (GEF), and peroxymonosulfate (PMS). Calcium peroxide granules enclosed in textile materials and single low doses of peroxymonosulfates outperformed liquid  $\text{H}_2\text{O}_2$  treatment in terms of efficiency, required dose, and environmental friendliness.

Treatment with liquid  $\text{H}_2\text{O}_2$  in concentrations 1 to  $5 \text{ mg L}^{-1}$  had no effect on the phycocyanin fluorescence (Ft) and quantum yield of PSII (Fv/Fm) indicating an ineffective treatment for the dense ( $1 \text{ million cells mL}^{-1} \pm 20\%$ ) and naturally occurred *Merismopedia* sp. bloom, while  $1 \text{ g L}^{-1}$   $\text{CaO}_2$  granules succeeded in treating the bloom. In another study, metallic peroxide granules tested for their  $\text{H}_2\text{O}_2$  releasing capacity in

filtered St. George Lake matrix, where they released significantly higher  $\text{H}_2\text{O}_2$  concentration and therefore had better mitigation efficiency than  $\text{MgO}_2$  granules.  $\text{CaO}_2$  granules releasing capacity was also tested in three different matrixes: MQ-water, River Water and Dam water. Release kinetics results showed that matrix composition influences the  $\text{H}_2\text{O}_2$  release by granules. In extra-pure water (milli-Q) the release of  $\text{H}_2\text{O}_2$  was limited in comparison with its release in surface waters of  $\text{CaO}_2$  granules. For instance, dam water which was the least contaminated water, resulted in higher and continuous  $\text{H}_2\text{O}_2$  yield of around  $6 \text{ mg L}^{-1}$  for  $1 \text{ g L}^{-1}$   $\text{CaO}_2$  granules applied, whereas an equal  $\text{CaO}_2$  dose in river water with elevated physicochemical characteristics released around  $5 \text{ mg L}^{-1}$   $\text{H}_2\text{O}_2$ , and in lake water was around  $3 \text{ mg L}^{-1}$ . Similar release experiments were performed in surface water spiked with humics, and BG-11 medium of different concentrations. Results have shown that humics can activate  $\text{CaO}_2$  granules through an interfacial mechanism causing the simultaneous generation of hydroxyl and hydroxyalkyl radicals. Additionally, application of  $\text{CaO}_2$  granules and liquid  $\text{H}_2\text{O}_2$  in BG-11 matrices of different dilutions showed lower  $\text{H}_2\text{O}_2$  availability than what expected, indicating that the presence of micronutrients and trace elements into the water can consume and/ or interact with the available  $\text{H}_2\text{O}_2$ .

A toxicity study on invertebrate species of  $\text{CaO}_2$  granules revealed the undesirable effects on *Echinogammarus veneris* when applied in doses higher than  $1 \text{ g L}^{-1}$ . Treatment of cultivated cultures with  $\text{CaO}_2$  granules, showed that doses higher than  $0.2$  and  $1.0 \text{ g L}^{-1}$   $\text{CaO}_2$  granules were efficient to treat *Microcystis* sp. and *Aphanizomenon* sp. in Kouris Dam matrix, respectively. Finally, treatment experiments of cyano-HABs contaminated water with PMS outperformed equal doses of liquid  $\text{H}_2\text{O}_2$ . Instant oxidant quantification during treatment also showed that PMS has a residual effect while  $\text{H}_2\text{O}_2$  is rapidly being consumed or decomposed, supporting further the competence of PMS compared with  $\text{H}_2\text{O}_2$  as a novel treatment method. Treatment experiments indicated that slow  $\text{H}_2\text{O}_2$  releasing  $\text{CaO}_2$  granules, and PMS could be alternative solutions to liquid hydrogen peroxide, when applied in appropriate doses, but further investigation is needed before their field applications to ensure safety of the aquatic ecosystem.

**Keywords:** cyanobacteria, oxidant, restoration, surface water, treatment

## TABLE OF CONTENTS

ABSTRACT.....	vii
LIST OF TABLES.....	xiii
LIST OF SCHEMES.....	xviii
LIST OF ABBREVIATIONS.....	xx
1 Introduction.....	1
1.1 Cyano-HABs.....	2
1.1.1 Morphology – Taxonomy.....	2
1.1.2 Anthropogenic and environmental drivers.....	3
1.1.3 Secondary metabolites - cyanotoxins.....	4
1.2 Cyano-HABs management.....	6
1.2.1 Monitoring, prevention, and prediction.....	7
1.2.2 Mitigation of Cyano-HABs and their negative side-effects.....	11
1.2.2.1 Cyanotoxins removal.....	11
1.2.2.2 In-lake management of cyanobacteria.....	13
1.3 Research novelty.....	22
1.3.1 Research questions/ hypothesis.....	22
1.3.2 Side-projects related to cyano-HABs monitoring & treatment.....	24
1.3.3 Research outline.....	26
2 Research Methodology.....	27
2.1 Monitoring & treatment of Athalassa National Forest Park’s lakes.....	27
2.1.1 Study Area.....	27
2.1.2 Case studies.....	28
2.1.2.1 St. George Lake Case Study.....	28
2.1.2.2 Athalassa Lake Case Study.....	29
2.1.3 Sampling and monitoring.....	30
2.1.4 Physicochemical water analyses.....	31
2.1.5 Phytoplankton content.....	31
2.1.6 Cyanotoxin genes and cyanotoxins analyses.....	32
2.1.7 Treatment of naturally occurring cyano-HABs.....	33
2.1.7.1 Treatment of <i>Merismopedia</i> sp. with metallic peroxide granules vs. liquid H <sub>2</sub> O <sub>2</sub> .....	33

2.1.7.2	H <sub>2</sub> O <sub>2</sub> release kinetics by CaO <sub>2</sub> and MgO <sub>2</sub> granules in filtered St. George Lake water.....	34
2.1.7.3	Treatment of Athalassa lake surface water with liquid H <sub>2</sub> O <sub>2</sub> and PMS	34
2.2	Cyano-HABs treatment with novel chemical oxidation processes .....	36
2.2.1	Metallic peroxide granules.....	36
2.2.1.1	CaO <sub>2</sub> granules characterization .....	36
2.2.1.2	Compound type (powder, granules) effect on H <sub>2</sub> O <sub>2</sub> release kinetics	36
2.2.1.3	Matrix effect on H <sub>2</sub> O <sub>2</sub> release kinetics .....	37
2.2.1.4	Treatment of Microcystis sp. and Aphanizomenon sp. spiked in surface water with CaO <sub>2</sub> granules and liquid H <sub>2</sub> O <sub>2</sub> .....	39
2.2.1.1	Toxicity study on Echinogammarus veneris sp.....	41
2.2.2	Calcium peroxide granules enclosed in fabrics (GEF) .....	43
2.2.2.1	Fabrics characterization.....	43
2.2.2.2	H <sub>2</sub> O <sub>2</sub> release kinetics by GEF.....	44
2.2.2.3	Treatment of Microcystis sp. spiked in surface water with GEF systems	44
2.2.2.1	Toxicity study on Echinogammarus veneris sp.....	45
2.2.3	Peroxymonosulfate (PMS) – OXONE® .....	46
2.2.3.1	Development of quantification kit – POXi kit .....	46
2.2.3.2	Toxicity study on Echinogammarus veneris sp.....	47
2.2.3.3	Combined cyano-HABs treatment and toxicity study on Echinogammarus veneris sp. ....	47
2.3	Scale-up treatment.....	48
2.4	Statistical analyses .....	49
3	Results & Discussion .....	50
3.1	Monitoring and treatment of naturally occurring blooms .....	50
3.1.1	St. George Lake .....	50
3.1.1.1	Monitoring.....	50
3.1.1.2	Treatment of Merismopedia sp. in St. George Lake water.....	53
3.1.1.3	H <sub>2</sub> O <sub>2</sub> release by CaO <sub>2</sub> and MgO <sub>2</sub> granules in filtered lake water.....	56
3.1.2	Athalassa Lake .....	57
3.1.2.1	Monitoring.....	57

3.1.2.2	Treatment of contaminated Athalassa's lake water (fish-kill event).	59
3.1.2.3	Treatment of Planktothrix sp. in Athalassa Lake water .....	60
3.2	Calcium peroxide (CaO <sub>2</sub> ) granules .....	62
3.2.1	Elemental composition .....	62
3.2.2	Compound type (powder, granules) effect on H <sub>2</sub> O <sub>2</sub> yield .....	62
3.2.3	Matrix effect on CaO <sub>2</sub> granules' releasing properties .....	64
3.2.3.1	Surface water composition (MQ, River, Dam, Lake water).....	64
3.2.3.2	BG-11 matrix (25%, 50%, and 75%) .....	66
3.2.3.3	Natural Organic Matter (NOM) – humics content .....	68
3.2.4	Effect of CaO <sub>2</sub> granules dose on surface water quality characteristics ....	70
3.2.5	Cyano-HABs treatment with CaO <sub>2</sub> granules vs. liquid H <sub>2</sub> O <sub>2</sub> .....	71
3.2.6	CaO <sub>2</sub> granules toxicity on invertebrates .....	77
3.2.7	Calcium peroxide granules enclosed in fabrics – GEF systems .....	78
3.2.7.1	Fabrics characterization.....	78
3.2.7.2	H <sub>2</sub> O <sub>2</sub> Release kinetics by GEF systems.....	80
3.2.7.3	Treatment efficiency.....	82
3.2.7.4	Physicochemical water characteristics .....	85
3.2.7.5	GEF toxicity on invertebrates.....	87
3.3	Peroxymonosulfate (PMS) – OXONE® .....	88
3.3.1	Development of quantification method .....	88
3.3.2	PMS vs. H <sub>2</sub> O <sub>2</sub> (in equal peroxide doses) toxicity on invertebrates.....	90
3.3.3	Treatment of river water spiked with cultivated cultures and <i>Echinogammarus veneris</i> sp. with PMS vs. liquid H <sub>2</sub> O <sub>2</sub> (single and multiple dosing)	92
3.3.3.1	Microcystis sp.....	92
3.3.3.2	Aphanizomenon sp. ....	95
3.4	Scale-up treatment.....	98
4	Summary of Findings/ Recommendations.....	101
4.1	Monitoring and treatment of naturally occurring blooms in St. George and Athalassa Lakes .....	101
4.1.1	Monitoring .....	101
4.1.2	Treatment.....	103
4.2	Treatment with novel chemical oxidation processes .....	104

4.2.1	CaO <sub>2</sub> granules .....	104
4.2.1.1	CaO <sub>2</sub> granules properties and toxicity .....	104
4.2.1.1	Treatment with CaO <sub>2</sub> granules .....	105
4.2.1.2	Treatment with GEF systems .....	106
4.2.2	Peroxymonosulfate (PMS) – OXONE® .....	108
CONCLUSIONS .....		110
REFERENCES .....		113
APPENDIX I .....		128
APPENDIX II .....		130

## LIST OF TABLES

Table 1. Proposed surface water quality standards by OECD based on the EU Directive (2000/60/EC). .....	10
Table 2. Summary of cyano-HABs management options describing their efficiency and environmental impact. ....	14
Table 3. Physical-chemical properties of hydrogen peroxide (Sigma-Aldrich). ....	18
Table 4. Physical-chemical properties of calcium peroxide and calcium peroxide granules (Sigma-Aldrich; SOLVAY). ....	20
Table 5. Physical-chemical properties of potassium peroxydisulfate and its triple salt - OXONE <sup>®</sup> (Sigma-Aldrich). ....	21
Table 6. Repeated H <sub>2</sub> O <sub>2</sub> and PMS doses during a 72-h treatment in contaminated Athalassa's lake water. ....	35
Table 7. Repeated H <sub>2</sub> O <sub>2</sub> and PMS doses during a 96-h treatment to achieve total added concentrations of 0, 4, 8, and 12 mg L <sup>-1</sup> of each oxidant into Athalassa's lake water contaminated with <i>Planktothrix</i> sp. ....	35
Table 8. Elemental composition in CaO <sub>2</sub> granules detected by handheld XRF analysis, where [C] = concentration and L.E = light elements (e.g., Ca, O). ....	62
Table 9. Maximum accumulative concentration of H <sub>2</sub> O <sub>2</sub> released by 0.5, 1, 2 and 3 g L <sup>-1</sup> CaO <sub>2</sub> granules in different water matrixes (Mean ± SD). ....	65
Table 10. Pore size range of fabrics Type A-C, mean pore size ± SD (um), n=60 pores. ....	79

## LIST OF FIGURES

Figure 1. (A) Instantaneous fluorescence (Ft) in raw fluorescence units and (B) quantum yield measurements for phycocyanin (620 nm excitation) and chlorophyll-a (450 nm excitation) in St. George Lake samples during monitoring period. ....	50
Figure 2. Measurements of conductivity ( $\mu\text{S cm}^{-1}$ ) and salinity (ppm) throughout the monitoring period in St. George Lake. ....	51
Figure 3. The effect of liquid $\text{H}_2\text{O}_2$ concentration (0, 1, 2, 3, 5 $\text{mg L}^{-1}$ ) on (A) phycocyanin concentration (measured as raw fluorescence units – RFU) and (B) Maximal quantum efficiency of the PSII (QY) at $\lambda=620$ nm. Results are expressed as the mean $\pm$ SD. ....	54
Figure 4. The effect of $\text{CaO}_2$ granules concentration (0, 1, 2, 3 $\text{g L}^{-1}$ ) on (A) phycocyanin concentration (measured as raw fluorescence units—RFU) and (B) maximal quantum efficiency of the PSII (QY) at 620 nm. Results are expressed as the mean $\pm$ SD. ....	54
Figure 5. The effect of $\text{MgO}_2$ granules concentration (0, 1, 2, 3 $\text{g L}^{-1}$ ) on (A) phycocyanin concentration (measured as raw fluorescence units – RFU) and (B) Maximal quantum efficiency of the PSII (QY) at 620 nm. Results are expressed as the mean $\pm$ SD. ....	55
<b>Figure 6.</b> Average pH, conductivity, salinity, and TDS (mean $\pm$ SD) of St. George Lake water (pH = 8.88, conductivity = 1999 $\mu\text{S cm}^{-1}$ , salinity = 1015 ppm) after 48 h of treatment with liquid $\text{H}_2\text{O}_2$ , $\text{CaO}_2$ and $\text{MgO}_2$ granules. ....	55
Figure 7. $\text{H}_2\text{O}_2$ release curves by 1, 2 and 3 $\text{g L}^{-1}$ of (A) $\text{CaO}_2$ and (B) $\text{MgO}_2$ granules in filtered St. George Lake water matrix. ....	56
Figure 8. (A) Physicochemical water characteristics, and (B) Photosynthetic parameters of Athalassa Lake water related to cyano-HABs (August – November 2020). ....	58
Figure 9. The effect of multiple dosing of $\text{H}_2\text{O}_2$ on (A) phycocyanin fluorescence (RFU) and (B) quantum efficiency of the PSII (QY) at 620 nm during a 78-h treatment of Athalassa lake water. ....	59
Figure 10. The effect of multiple dosing of PMS on (A) phycocyanin fluorescence (RFU) and (B) QY of the PSII at 620 nm during a 78-h treatment of Athalassa lake water. ....	59
Figure 11. Ft in raw fluorescence units (RFU) and QY (Fv/Fm) at $\lambda=620$ nm during natural bloom treatment in Athalassa lake with repeated doses of 1, 2 and 3 $\text{mg L}^{-1}$ $\text{H}_2\text{O}_2$ and PMS added every 24 hours for up to 72 hours. ....	60
Figure 12. $\text{H}_2\text{O}_2$ release kinetics by 0.05, 0.3, and 0.5 $\text{g L}^{-1}$ $\text{CaO}_2$ powder and 0.5 $\text{g L}^{-1}$ $\text{MgO}_2$ powder in Milli-Q water fitted by non-linear pseudo-first order model: $Y=Y_0 + (\text{Plateau}-Y_0)*(1-\exp(-K*x))$ . ....	63

Figure 13. H <sub>2</sub> O <sub>2</sub> release kinetics by 0.5, 1, and 2 g L <sup>-1</sup> CaO <sub>2</sub> granules in Milli-Q water fitted by non-linear pseudo-first order model: $Y=Y_0 + (\text{Plateau}-Y_0)*(1-\exp(-K*x))$ . ..	63
Figure 14. Hydrogen peroxide released by 0.5 g L <sup>-1</sup> CaO <sub>2</sub> granules and CaO <sub>2</sub> powder.	64
Figure 15. H <sub>2</sub> O <sub>2</sub> release in dam, river, MQ, and lake water by 2.0 g L <sup>-1</sup> CaO <sub>2</sub> fitted by non-linear pseudo-first order model: $Y=Y_0 + (\text{Plateau}-Y_0)*(1-\exp(-K*x))$ .....	65
Figure 16. Instant H <sub>2</sub> O <sub>2</sub> concentrations released by 1g L <sup>-1</sup> CaO <sub>2</sub> granules and t= 0, 1, 4, 6, 24, and 48 h after the addition of 6 mg L <sup>-1</sup> liquid H <sub>2</sub> O <sub>2</sub> in BG-11 medium in dilutions of 25%, 50%, and 75% in Milli-Q. ....	66
Figure 17. Correlation between CaO <sub>2</sub> granules (g L <sup>-1</sup> ) added in in all tested matrixes (dam, river, milli-Q, lake, and BG-11 dilutions of 25%, 50%, and 75%) and the peak H <sub>2</sub> O <sub>2</sub> released concentration (mg L <sup>-1</sup> ). ....	67
Figure 18. Instantaneous H <sub>2</sub> O <sub>2</sub> concentration released by 1.0 g L <sup>-1</sup> CaO <sub>2</sub> in surface (dam) water enriched 0 (control), 1, 5 and 10 ppm HASS at t= 0, 2, 4, 24 hours.....	68
Figure 19. Quantification of DMPO/•OH and DMPO/Hydroxyalkyl adducts using DPPH as spin standard for the 1ppm HASS, 5ppm HASS and 10ppm HASS, respectively. ...	69
Figure 20. Recorded pH values after the addition of 0.5 - 2.0 g L <sup>-1</sup> CaO <sub>2</sub> granules in Kouris Dam surface water. ....	70
Figure 21. (A) Ft at λ=620 nm in raw fluorescence units (RFU), and (B) Quantum Yield at λ=620 nm during <i>Microcystis</i> sp. treatment with 0.5-2.0 g L <sup>-1</sup> CaO <sub>2</sub> granules. ....	71
Figure 22. pH values at t=0, 24, and 48 h of <i>Microcystis</i> sp. treatment with 0.5, 1.0 and 2.0 g L <sup>-1</sup> CaO <sub>2</sub> granules.....	72
Figure 23. Ft at λ=620 nm in raw fluorescence units (RFU) and QY (Fv/Fm) at λ=620 nm during <i>Microcystis</i> sp. treatment with 3 - 12 mg L <sup>-1</sup> H <sub>2</sub> O <sub>2</sub> . ....	72
Figure 24. Residual H <sub>2</sub> O <sub>2</sub> concentration measured during <i>Microcystis</i> sp. treatment with 1-12 mg L <sup>-1</sup> H <sub>2</sub> O <sub>2</sub> . ....	73
Figure 25. Comparison of Ft at λ=620 nm in raw fluorescence units (RFU), between equal accumulative H <sub>2</sub> O <sub>2</sub> doses of 1 g L <sup>-1</sup> CaO <sub>2</sub> granules and 6 mg L <sup>-1</sup> liquid H <sub>2</sub> O <sub>2</sub> , during <i>Microcystis</i> sp. treatment. ....	73
Figure 26. Ft at λ=620 nm in raw fluorescence units (RFU), and (B) QY (Fv/Fm) during <i>Aphanizomenon</i> sp. treatment with 0.50, 1.0, and 1.25 g L <sup>-1</sup> CaO <sub>2</sub> granules. ....	75
Figure 27. pH values at t=0, 24, and 48 h of <i>Aphanizomenon</i> sp. treatment with 0.50, 1.00 and 1.25 g L <sup>-1</sup> CaO <sub>2</sub> granules.....	75

Figure 28. (A) Ft at $\lambda=620$ nm in raw fluorescence units (RFU), and (B) QY (Fv/Fm) during <i>Aphanizomenon</i> sp. treatment with 3, 6, and 7 mg L <sup>-1</sup> H <sub>2</sub> O <sub>2</sub> . .....	76
Figure 29. Residual H <sub>2</sub> O <sub>2</sub> concentration measured during <i>Aphanizomenon</i> sp. treatment with 0.50-1.25 g L <sup>-1</sup> CaO <sub>2</sub> granules. ....	76
Figure 30. Survival of <i>Echinogammarus veneris</i> sp. at t=48 h of each CaO <sub>2</sub> granules dose (0.00, 0.50, 0.75, 1.00, 1.25, 2.00 g L <sup>-1</sup> ) to determine the LC <sub>50</sub> . ....	77
Figure 31. Release curves depicting the instantaneous H <sub>2</sub> O <sub>2</sub> concentration during a 24-h release experiment utilizing 0.5, 1.0, and 2.0 g L <sup>-1</sup> CaO <sub>2</sub> granules enclosed in fabric types (A) pocket lining, (B) interlining textile, (C) polyester netting, and (D) paper filter wrapped in tights' fabric. ....	80
Figure 32. H <sub>2</sub> O <sub>2</sub> release kinetics by 2.0 g L <sup>-1</sup> CaO <sub>2</sub> GEF types A – D, and no fabric, in a surface water (Kouris dam) fitted by non-linear pseudo-first order model: $Y=Y_0 + (\text{Plateau}-Y_0)*(1-\exp(-K*x))$ . ....	81
Figure 33. Linear correlation between H <sub>2</sub> O <sub>2</sub> yield at t=24 hours and CaO <sub>2</sub> granules' dose directly applied (no fabric) and applied enclosed in GEF types A – D. ....	82
Figure 34. Effect of 0.5, 1.0, and 2.0 g/L CaO <sub>2</sub> granules enclosed in fabric types (A) pocket lining, (B) interlining textile, (C) polyester netting, on phycocyanin Ft (left), and QY at $\lambda=620$ (right) during the treatment of <i>Microcystis</i> sp. in surface water. ....	84
Figure 35. Changes in pH during treatment of <i>Microcystis</i> sp. in surface water by 2.0 g L <sup>-1</sup> CaO <sub>2</sub> granules direct application and GEF type A – C. ....	86
Figure 36. Conductivity, TDS, and Salinity at t=48 hours of <i>Microcystis</i> sp. in surface water treatment by adding 2.0 g L <sup>-1</sup> CaO <sub>2</sub> enclosed in GEF type A – C. ....	86
Figure 37. Survival rate (%) of invertebrate species in river water at t=48 h, and doses of 0, 3, 6, and 12 mg L <sup>-1</sup> H <sub>2</sub> O <sub>2</sub> applied in the form of GEF, granules, and liquid H <sub>2</sub> O <sub>2</sub> . ....	87
Figure 38. (A) Quantification of 2 and 5 mg L <sup>-1</sup> PMS added in MQ-water at t=0 and t=25 h, (B) Absorbance at $\lambda=405$ nm of the following mixture: 2 mL of 50 uM PMS sample with 2 mL of 2 mM p-NPBA stock solution, under dark conditions. ....	89
Figure 39. Survival rate (%) of <i>Echinogammarus veneris</i> sp. in river water matrix with (A) 1 – 5 mg L <sup>-1</sup> liquid H <sub>2</sub> O <sub>2</sub> , and (B) PMS generated by OXONE (in equal molarities). ....	90
Figure 40. Residual oxidant concentration measured during toxicity study on <i>Echinogammarus veneris</i> sp. treatment with (A) 1 – 5 mg L <sup>-1</sup> liquid H <sub>2</sub> O <sub>2</sub> , and (B) PMS (in equal molarities). ....	91

Figure 41. Survival rate (%) of <i>Echinogammarus veneris</i> sp. in river water matrix with multiple doses of (A) liquid H <sub>2</sub> O <sub>2</sub> and (B) PMS (in equal molarities). [C] <sub>tot</sub> = 5 mg L <sup>-1</sup> .	91
Figure 42. Residual oxidant concentration measured during toxicity study on <i>Echinogammarus veneris</i> sp. with multiple doses of (A) liquid H <sub>2</sub> O <sub>2</sub> , and (B) PMS. [C] <sub>tot</sub> = 5 mg L <sup>-1</sup> .	92
Figure 43. Ft in raw fluorescence units (RFU) and QY (Fv/Fm) at λ=620 nm during <i>Microcystis</i> sp. treatment in river water (+ <i>Echinogammarus veneris</i> sp.) with single dose 1 – 5 mg L <sup>-1</sup> (A-B) H <sub>2</sub> O <sub>2</sub> and (C-D) PMS.	93
Figure 44. Survival rate (%) of invertebrate species during <i>Microcystis</i> sp. treatment in river water (+ <i>Echinogammarus veneris</i> sp.) with single dose 1 – 5 mg L <sup>-1</sup> (A) H <sub>2</sub> O <sub>2</sub> and (B) PMS.	93
Figure 45. Ft in raw fluorescence units (RFU) and QY at λ=620 nm during <i>Microcystis</i> sp. treatment in river water (+ <i>Echinogammarus veneris</i> sp.) with multiple doses of (A-B) H <sub>2</sub> O <sub>2</sub> and (C-D) PMS. [C] <sub>total</sub> =2, 3, 4 mg L <sup>-1</sup> .	94
Figure 46. Residual oxidant concentration measured during <i>Microcystis</i> sp. treatment in river water (+ <i>Echinogammarus veneris</i> sp.) with multiple doses with multiple doses of (A) H <sub>2</sub> O <sub>2</sub> and (B) PMS. [C] <sub>total</sub> =2, 3, 4 mg L <sup>-1</sup> .	95
Figure 47. Survival rate (%) of invertebrate species during <i>Microcystis</i> sp. treatment in river water (+ <i>Echinogammarus veneris</i> sp.) with multiple doses of (A) H <sub>2</sub> O <sub>2</sub> and (B) PMS. [C] <sub>total</sub> =2, 3, 4 mg L <sup>-1</sup> .	95
Figure 48. Ft in raw fluorescence units (RFU) and QY (Fv/Fm) at λ=620 nm during <i>Aphanizomenon</i> sp. treatment in river water (+ <i>Echinogammarus veneris</i> sp.) with single doses 1 – 3 mg L <sup>-1</sup> (A-B) H <sub>2</sub> O <sub>2</sub> and (C-D) PMS.	96
Figure 49. Residual oxidant concentration during <i>Aphanizomenon</i> sp. treatment in river water (+ <i>Echinogammarus veneris</i> species) with single dose 1 – 3 mg L <sup>-1</sup> (A) H <sub>2</sub> O <sub>2</sub> and (B) PMS.	96
Figure 50. Ft in raw fluorescence units (RFU) and QY at λ=620 nm during <i>Aphanizomenon</i> sp. treatment in river water (+ <i>Echinogammarus veneris</i> sp.) with multiple doses of 1 – 3 mg L <sup>-1</sup> (A-B) H <sub>2</sub> O <sub>2</sub> and (C-D) PMS. [C] <sub>total</sub> =2, 3, 4 mg L <sup>-1</sup> .	97
Figure 51. Residual oxidant concentration measured during <i>Aphanizomenon</i> sp. treatment in river water (+ <i>Echinogammarus veneris</i> sp.) with multiple doses of 1 – 3 mg L <sup>-1</sup> (A) H <sub>2</sub> O <sub>2</sub> and (B) PMS. [C] <sub>total</sub> =2, 3, 4 mg L <sup>-1</sup> .	98

Figure 52. (A) Ft in raw fluorescence units (RFU) and (B) QY at $\lambda=620$ nm during Athalassa up-scale treatment with multiple doses $H_2O_2$ , PMS, and $CaO_2$ granules. $[C]_{total}= 12 \text{ mg L}^{-1} H_2O_2$ equivalent.....	99
Figure 53. Residual oxidant concentration measured during Athalassa up-scale treatment with multiple doses $H_2O_2$ , PMS, and $CaO_2$ granules. $[C]_{total}= 12 \text{ mg L}^{-1} H_2O_2$ equivalent. ....	100

## LIST OF SCHEMES

Scheme 1. External factors driving cyanobacterial blooming in surface waters, and the most common side effects of cyano-HABs (created by: E. Keliri <sup>©</sup> ). ....	1
Scheme 2. A simplifies cell structure/morphology of the three main orders of cyanobacteria, left to right: Nostocales, Chroococcales, and Oscillatoriales. ....	2
Scheme 3. Photosystem II (PSII) photosynthesis processes through cyanobacterial pigments - simplified illustration (prepared by: E. Keliri). ....	3
Scheme 4. Structures of widely found cyanotoxins in surface waters, Left to right: microcystins, anatoxins, saxitoxins, nodularins, and BMMA. ....	5
Scheme 5. Managing cyano-HABs and cyanotoxins in waterbodies (created by: E. Keliri <sup>©</sup> ). ....	7
Scheme 6. Cyano-HABs water sampling, sample preparation and analysis of intra-cellular cyanotoxins (created with Biorender.com by E. Keliri <sup>©</sup> ). ....	8
Scheme 7. Main research outline .....	27
Scheme 8. Monitoring locations at the National Park of Athalassa indicated in yellow, (A) St. George Lake, (B) Athalassa Lake, retrieved by Google Maps Data, 2022 ©. ...	28
Scheme 9. Graphical abstract depicting the main research activities conducted during St. Lake monitoring and treatment in 2019 (created with Biorender.com by E. Keliri <sup>©</sup> )...	28
Scheme 10. Graphical abstract depicting the main research activities conducted during Athalassa Lake monitoring in 2020 (created with Biorender.com by E. Keliri <sup>©</sup> ). ....	29
Scheme 11. Schematic illustration depicting the comparison experiments between powdered and granulated metallic peroxide granules (created with Biorender.com by E. Keliri <sup>©</sup> ). ....	36

Scheme 12. Graphical Abstract depicting the experiments conducted for the effect of matrix load on the H <sub>2</sub> O <sub>2</sub> release kinetics by granules (created with Biorender.com by E. Keliri ©).....	37
Scheme 13. Cultivation flasks of (A) <i>Microcystis</i> sp., (B) <i>Aphanizomenon</i> sp., and (C) <i>Microcystis</i> sp. cells collected on membrane filter during filtration of the culture medium process. ....	40
Scheme 14. <i>Echinogammarus veneris</i> sp. collected from Polis Chrysochou River, and separated into various sizes, with a close-up capture for the medium sized specimens. ....	42
Scheme 15. Four different types of fabrics tested as potential delivery systems for CaO <sub>2</sub> granules: (A) pocket lining fabric, (B) non-woven interlining fabric, (C) polyester mosquito netting fabric, and (D) paper filter wrapped in 20 DEN tights. ....	43
Scheme 16. Addition of GEF system type B enclosing 0 (control), 0.5, 1.0, and 2.0 g L <sup>-1</sup> CaO <sub>2</sub> .....	45
Scheme 17. POXi™ kit; PMS quantification process. ....	46
Scheme 18. <i>Merismopedia</i> sp. captured under ECLIPSE Ci-L microscope equipped with OPTIKAM Wi-Fi camera with magnification 100x, Eleni C. Keliri ©. ....	52
Scheme 19. Samples received from Athalassa Lake Upper row: right after the fish-kill event and Lower row: <i>Planktothrix</i> sp. during the blooming period, captured under ECLIPSE Ci-L microscope equipped with OPTIKAM Wi-Fi camera with magnification from left to right 20x, 40x, and 100x, Eleni C. Keliri ©. ....	58
Scheme 20. Treatment containers during treatment of Athalassa Lake water by multiple peroxide additions with total applied concentration 3, 4, and 5 mg L <sup>-1</sup> H <sub>2</sub> O <sub>2</sub> and KHSO <sub>5</sub> . ....	61
Scheme 21. Proposed mechanism of hydroxyalkyl radicals' formation through an interfacial phenomenon between HASS with CaO <sub>2</sub> granules applied in surface water (created with Biorender.com by E. Keliri ©). ....	69
Scheme 22. SEM images of fabric types A – D, under 100x magnification and a scale of 1 mm. ....	79
Scheme 23. Treatment of <i>Microcystis</i> sp. with GEF in concentrations of 0.0 (control), 0.5, 1.0, and 2.0 g/L CaO <sub>2</sub> granules enclosed in fabric type C, at t=0, 24, and 48 hours. ....	85
Scheme 24. Experimental set-up of toxicity study on <i>Echinogammarus veneris</i> by applying 0.5, 1.0, and 2.0 g L <sup>-1</sup> GEF type C in river water matrix. Photo was taken at = 48 h and the survival of species during the experiment is visible. ....	88

Scheme 25. Reaction mechanism of <i>ipso</i> -hydroxylation of phenylboronic acid in the presence of hydrogen peroxide, that lead to the formation of phenolate ion. [105] (modified by E. Keliri ©).....	89
Scheme 26. Visual changes during treatment of naturally occurring cyano-HABs in Athalassa’s Lake (November 2021). .....	100

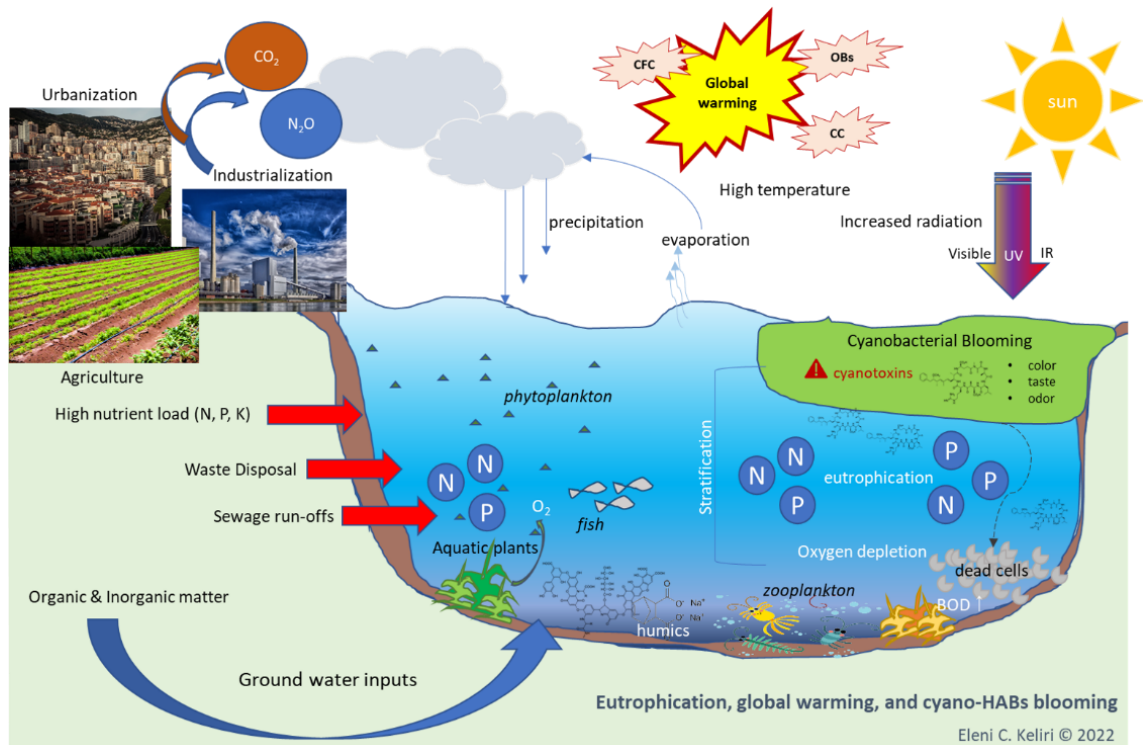
## LIST OF ABBREVIATIONS

Cyano-HABs:	Cyanobacterial Harmful Algal Blooms
Eq.	Equation
Equiv.	Equivalent
HP, H <sub>2</sub> O <sub>2</sub> :	Hydrogen Peroxide
ox	Oxone
GEF	Granules Enclosed in Fabrics
MgO <sub>2</sub>	Magnesium Peroxide
CaO <sub>2</sub>	Calcium Peroxide
PMS	Peroxymonosulfate
TP	Total phosphorus
TN	Total Nitrogen
DIN	Dissolved Inorganic Nitrogen
MC	Microcystin
NOD	Nodularin
CYL	Cylindrospermopsin
Ft	Instantaneous fluorescence
QY or (Fv/Fm)	Quantum Yield of PSII
sp.	specie
g; mg	grams; milligrams
L; mL	Liter; milliliter
m; µm; nm	Meters; millimeters; nanometers
t	time
MQ-water	Milli Quest extra pure water

PSII	Photosystem II
RFU	Raw Fluorescence Units
$\lambda$	wavelength
b.w.	Body weight
LD	Lethal dose
LC <sub>50</sub>	50% Lethal Concentration
EU	European Union
WHO	World Health Organization
OECD	Organization for Economic Co-operation and Development
DWTPs	Drinking Water Treatment Plants
AOPs	Advanced Oxidation Processes
UF	Ultra-filtration
ROS	Reactive Oxygen Species
ANFP	Athalassa National Forest Park
SR	Survival Rate
S	Salinity
TDS	Total Dissolved Solids
RPM	Revolutions per minute (rotation speed)
[C]	Concentration
Ca(OH) <sub>2</sub>	Calcium Hydroxide

# 1 Introduction

Cyanobacteria (blue-green algae) are phototrophic microorganisms and represent an essential component of the food web in all aquatic ecosystems. However, certain strains of cyanobacteria can produce secondary metabolites, also known as cyanotoxins, that have detrimental effects on human and mammalian health. The adverse effects of climate change and several anthropogenic activities are contributing towards the more frequent and prolonged presence of harmful cyanobacteria blooms (cyano-HABs) across the globe, adding further pressure on scarce fresh water supplies (Scheme 1). To better manage the water resources wellness, there are four key elements: (a) prevention, (b) monitoring, (c) mitigation, and (d) prediction. Nowadays, emphasis is given in all four practices which are highly important to safeguard water resources and supply worldwide, while mitigation techniques are applied in cases where monitoring, or prediction were insufficient to eliminate or prevent bloom formation.



**Scheme 1.** External factors driving cyanobacterial blooming in surface waters, and the most common side effects of cyano-HABs (created by: E. Keliri<sup>©</sup>).

## 1.1 Cyano-HABs

### 1.1.1 Morphology – Taxonomy

Cyanobacteria are phytoplankton microorganisms whose ability to oxygenate the atmosphere 3.5 billion years ago contributed to life formation [1]. It is a group of bacteria ranging from 1 to 100  $\mu\text{m}$  in diameter, categorized based on their structure. However, recently more advanced taxonomic methods have been applied based on the cyanobacterial genetic sequences (molecular techniques) [2]. The main orders of cyanobacteria species are: Nostocales, Chroococcales, and Oscillatoriales (Scheme 2). Nostocales are filament forming heterocystous cyanobacteria which contain specialized, differentiated, and non-photosynthetic cells called heterocysts [3]. Those organisms are capable of aerobic  $\text{N}_2$ -fixation due to their specialized cells. The most common genus of this group is *Anabaena*, *Aphanizomenon*, *Cylindrospermopsis*, and *Nostoc* [4]. Chroococcales such as *Microcystis* sp., are coccoid or rod-shaped organisms that multiply by binary fission. They can be found in loose colonies in which the constituent cells are held together by a common slime layer [5], or in well-structured layers like the pico-cyanobacterium *Merismopedia* species. Oscillatoriales, includes those filamentous taxa with a more complicated cytology, as they can be found with radial, fasciculate, or irregular thylakoid arrangement. Their single filamentous forms consist of a chain of trichome (vegetative cell), surrounded by slimy sheath [6]. In some cases, they form mats (macro-structures) on mud or rocks found in benthic environments. Some widely found Oscillatoriales species in surface water are the *Planktothrix* sp. (ex. *Oscillatoria* sp.), *Arthrospira* and *Lyngbya* [7].

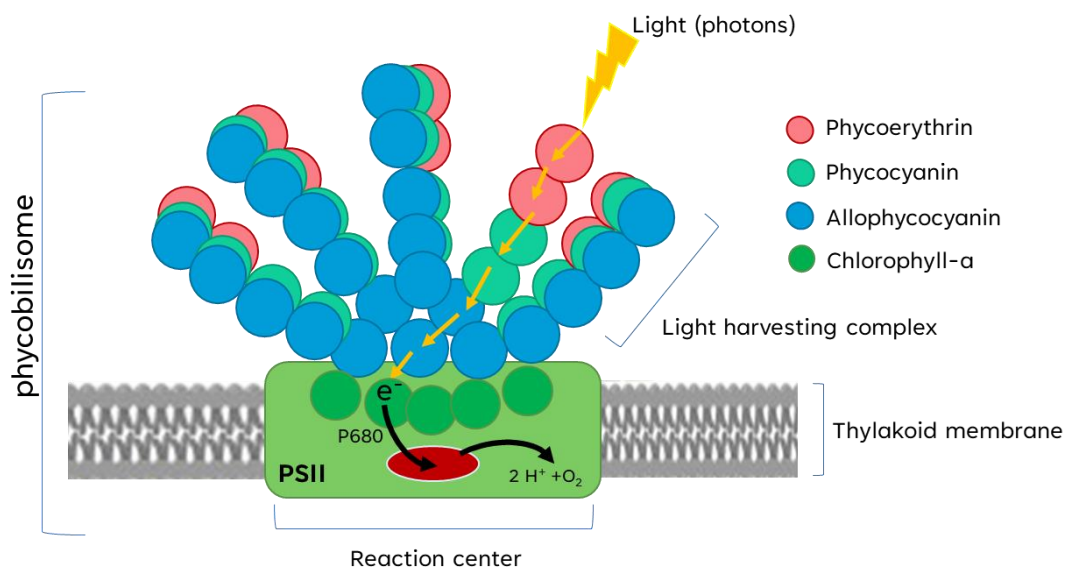


**Scheme 2.** A simplified cell structure/morphology of the three main orders of cyanobacteria, left to right: Nostocales, Chroococcales, and Oscillatoriales.

Cyanobacteria gain energy to convert carbon dioxide into oxygen through the photosynthesis process by capturing light through their light harvesting complex, including pigments. The energy is transferred through pigments to the reaction center of the Photosystem II (PSII), where the energy is utilized to excite the electron to the

primary electron acceptor in order to perform the photosynthesis reaction. The main pigments involved in their photosynthetic processes are chlorophyll-a (chl-a) and phycocyanin, whose excitation wavelengths are at  $\lambda=450$  nm and  $\lambda=620$  nm, respectively (Scheme 3). Other pigments are also present in cyanobacteria cells such as phycoerythrin and allophycocyanin. Since pigments are present in all cyanobacteria cells, the color of each cyanobacterium is based on the proportion of its pigments. Higher concentrations of phycocyanin result in a blue-green color (e.g., *Cylindrospermopsis* sp.), of phycoerythrin a brownish-red color (e.g., *Planktothrix* sp.) and chlorophyll-a a green color (*Microcystis* sp.).

Even though chl-a is present in all cyanobacterial cells, it is the dominant pigment in green-algae whereas the dominant pigment of cyanobacteria is phycocyanin, which allows the characterization of each algal taxa. The difference between the excitation wavelengths of chl-a and phycocyanin, allows the distinction between green algae and cyanobacteria, indicating their presence in freshwater and marine environments [8].



**Scheme 3.** Photosystem II (PSII) photosynthesis processes through cyanobacterial pigments - simplified illustration (prepared by: E. Keliri).

### 1.1.2 Anthropogenic and environmental drivers

Even though cyanobacteria are present in all aquatic ecosystems and comprise a key component of their food chain, increased toxicity as well as undesirable color, taste and odor occurs during their excessive growth into the waterbodies. This is caused by the excess availability of nutrients in surface water. Anthropogenic activities such as

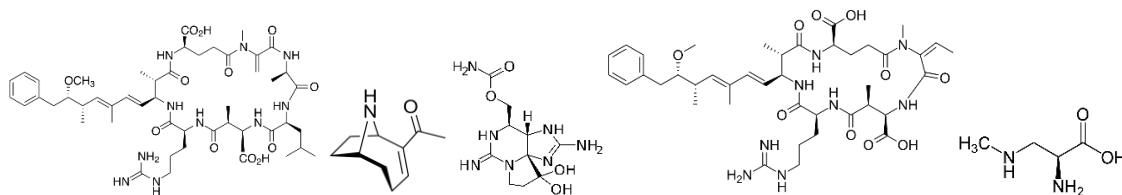
agricultural, urban, and industrial activities have intensely increased the load of nutrients in surface waters around the globe, making cyanobacterial blooming more persistent and prevalent [9]. Both nutrients and cyanobacteria are essential to maintain the aquatic balance, as nutrients support fish and shellfish production while cyanobacteria are supplying the food web of zooplankton [10]. Disruption of this balance by excess load of nutrients causes the rapid and excessive growth of cyanobacteria which leads to the formation of cyanobacteria harmful blooms (cyano-HABs). Blooming events are recorded worldwide, every year, and studies showed that nowadays cyano-HABs display an expansion in range and frequency in response to climatic and non-climatic drivers [11]. The extent to which climate change is intensifying these events is not fully understood, but recent years showed increase contamination cases along with profound consequences on water quality, biodiversity, and toxicity of the waterbodies[12].

Taste and odor compounds, distinct color, and increased toxicity, are reported during cyano-HABs events, worldwide [13]. The most well-studied and frequently met odor compounds are geosmin and 2methylisoborneol, while terpenoids, sulphides, lipid and pigment derivatives, aromatics, long-chain hydrocarbons, amines, alkaloids, lipopolysaccharides (LPS), and peptides are also released by cyanobacteria cells, causing water quality depletion. The excreted or released during cell lysis bioactive secondary metabolites of cyanobacteria – cyanotoxins, can pose a significant hazard to the aquatic ecosystem and to human/mammalian health. As a result, an increase in treatment and operational costs of water treatment plants, where cyanobacteria water is used as source water is observed [14].

### **1.1.3 Secondary metabolites - cyanotoxins**

As previously mentioned, toxic genera of cyanobacteria can excrete into the water a broad variety of bioactive metabolites, also known as cyanotoxins [15]. These metabolites can negatively impact the ecosystem and human health, making it an important environmental issue of concern [16]. Although their acute toxicity on humans is not extensively studied, mass mortalities of fishes, birds, mammals, and many other animal taxa have been reported [17]. Recent studies have correlated liver-related deaths in U.S and Serbia with several cyanotoxins [18, 19]. Cyanotoxins are divided based on their structure and/or their bioactivity. Main structural groups of cyanotoxins are the

cyclic peptides (e.g., microcystins, nodularins), alkaloids (e.g., anatoxins, saxitoxins), lipopolysaccharides and amino acids (e.g., BMMA), depicted in Scheme 4.



**Scheme 4.** Structures of widely found cyanotoxins in surface waters, Left to right: microcystins, anatoxins, saxitoxins, nodularins, and BMMA.

Based on their structure and toxicity they can act as neurotoxins, cytotoxins, endotoxins, and hepatotoxins; by targeting different organs of humans and animals. Microcystins are the most studied cyanotoxins, widespread in waterbodies all over the world (Scheme 4), and toxicity studies on mouse assays have shown that microcystin-LR (one analogue of microcystins) has an LD<sub>50</sub> of 50 µg kg<sup>-1</sup> (b.w., i.p. mouse) which is 10 times higher than the venom of cobra [20]. The most common exposure routes to humans are through the consumption of ineffectively treated drinking water, the consumption of contaminated food (accumulation of cyanotoxins in dietary products, shellfish, and fish), and direct contact with contaminated water during swimming and other recreational activities. An additional, but equally important, exposure route is inhalation of aerosols containing aerosolized cyanotoxins, hence water skiing is prohibited in cyanobacterial contaminated sites [21]. Little is known on the acute toxicity and health effects deriving from the absorption in the nasal tissue after inhalation [22], and therefore, more dedicated studies on human and animal exposure routes and their short- and long-term effects need to be conducted [23].

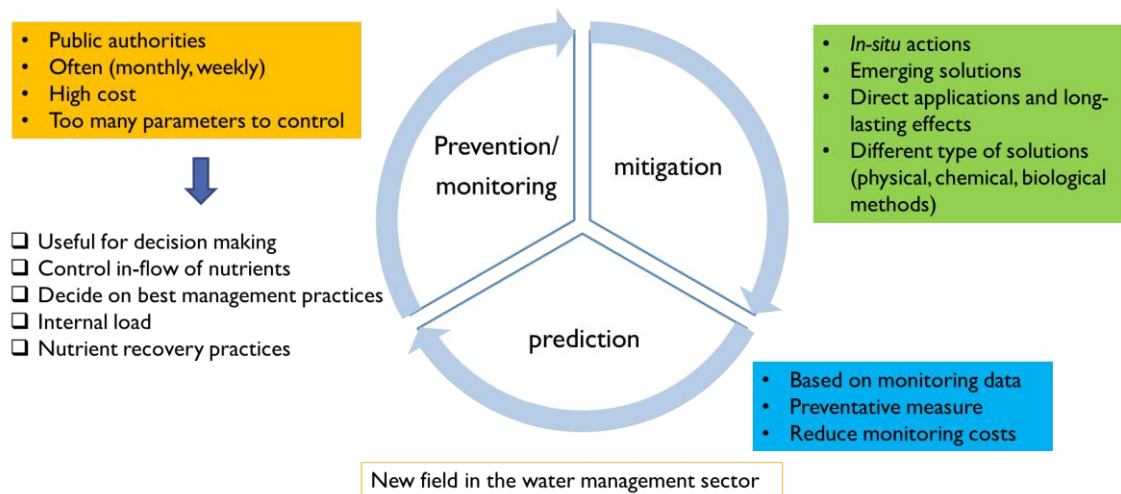
Cyanobacterial harmful algal blooms (cyano-HABs) are an increasingly pressing environmental problem affecting inland waterbodies and marine ecosystems. The first organization that officially provided guidelines for cyanotoxins in drinking water supplies was the World Health Organization (WHO) in 1984 and 1993, while in 2021 an updated version of those guidelines was published. Toxic cyanobacteria present in drinking water reservoirs pose a severe public health, recently prompting the EU to include safety levels for certain toxins in the revised Drinking Water Directive (EU) 2020/21842 [24, 25]. More specifically, the revised directive suggests that by 2026 all Member States shall take all the necessary measures to ensure that water intended for human consumption complies with the parametric values given by the Commission (1

$\mu\text{g L}^{-1}$  for microcystin-LR). Even though microcystin-LR's presence will be regulated, it comprises only 1 of the 249 officially recorded derivatives (up to 2016) from the group of the hepatotoxic microcystins [15]. This means that in a contaminated site where other derivatives such as microcystin-RR are known to be detected in higher concentrations than  $1 \mu\text{g L}^{-1}$ , the water will be regarded as safe for consumption as long as microcystin-LR is below the set allowable limit, something that scientist have pointed out during the revision process of the directive. On the other hand, WHO has issued guideline values for microcystins, cylindrospermopsin, anatoxins, and saxitoxins on their short-term and long-term exposure through the consumption of drinking-water and recreational activities [26–28].

Even though considerable progress and research outcomes have been made on the detection and treatment of these cyanotoxins, there are still many actions that need to be completed in order to achieve the new guidelines and demands of the EU Directive 2020/2184. Taking into consideration all the negative effects of cyanobacteria and cyanotoxins, it is extremely important to find effective cyano-HABs mitigation techniques to detoxify water, especially when intended for consumption, agriculture, aquaculture, and farming use.

## **1.2 Cyano-HABs management**

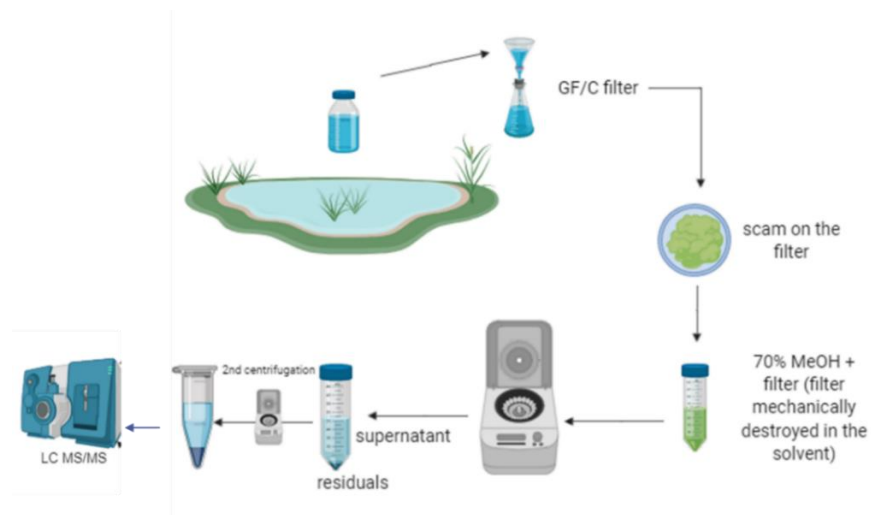
Cyano-HABs presence in freshwaters that are source of drinking water is not only a health issue, but it also raises the overall treatment and monitoring costs which are in the range of millions of euros annually [29]. A recent study estimated the overall annual amount spent by the Australian Government related to cyanobacteria contamination, including hospitalizations, monitoring and treatment costs, restrictions in recreational activities, and food contamination costs. The total amount calculated was in the range of millions of losses per year (180 – 240 million AUD) [30]. For managing the blooming of cyano-HABs and cyanotoxins in surface waters, there are four key elements: prevention prediction, monitoring, and mitigation; with the latter one being the most utilized sector for the restoration of contaminated sites (Scheme 5).



**Scheme 5.** Managing cyano-HABs and cyanotoxins in waterbodies (created by: E. Keliri<sup>©</sup>).

### 1.2.1 Monitoring, prevention, and prediction

Monitoring cyano-HABs consists of regular (daily, weekly, monthly, or annually) sampling events into a waterbody, by public authorities or private companies to ensure good water quality status. The frequency of monitoring is decided based on the characteristics of each waterbody, its overall needs, and its ecological importance, as monitoring is usually a costly process. Monitoring surface water quality, especially with regards to cyano-HABs related parameters, is a complex action, as too many parameters required evaluation. Those parameters can be physicochemical water characteristics such as pH, conductivity, total dissolved solids, salinity, nutrient load (total, dissolved salts), photosynthetic parameters (PSII quantum yield, pigments fluorescence), speciation (microscopic techniques, molecular/genetic analyses), and cyanotoxins and other emerging contaminant analyses with advanced analytical techniques. The development of advanced analytical techniques enabled the characterization and quantification of the diverse groups of cyanotoxins and their derivatives (i.e., for the hepatotoxic microcystins 249 derivatives have been isolated [15]). Conventional monitoring of cyanotoxins includes both environmental sampling and laboratory analyses [31] to decide on the quality status of the water. Usually, water is usually sampled from distinct locations of a waterbody, at various geometric coordinates, and in different heights within the water column, followed by its analysis, with highly precise, accurate, and state-of-the-art analytical techniques, like HPLC-MS/MS (Scheme 6).



**Scheme 6.** Cyano-HABs water sampling, sample preparation and analysis of intra-cellular cyanotoxins (created with Biorender.com by E. Keliri ©).

The most frequently used analytical techniques include: (a) enzyme-linked immunosorbent assays (ELISA) utilized as a screening method, (b) protein phosphatase inhibition assay (PPIA) for microcystins and nodularins, (c) chromatographic separations such as ultra or high-performance liquid chromatography-photo diode array (HPLC-PDA), HPLC with Fluorescence Derivatization (HPLC-FD), tandem mass spectroscopy, and capillary electrophoresis have been used for the separation, identification, and quantification of mixtures of cyanotoxins (within the same or different groups of cyanotoxins) [32]. Among those, LC/MS technique is mostly preferred for lab testing and even as routine analysis because it gives faster chromatographic separations with the use of UHPLC, online SPE, and MALDI-TOF. Also, multi-class toxin methods have been developed, providing the structural characterization of the parent compound as well as of its transformation products, simultaneously. It is important to note, that sampling methodology and sample preservation and handling in the lab is equally important to sample analysis, in order to avoid degradation or contamination that will cause misleading estimations of the actual concentration of cyanotoxins in the sample. To address these issues, a new generation of monitoring systems are developed to be autonomous for the *in-situ* detection of cyanobacteria and/or cyanotoxins. These systems not only give real-time monitoring results on water quality, but they can also be utilized as early-warning system for the prevention of blooming events as well as to authorities on the toxic potency on the water [33, 34].

Although the cost of properly monitoring a waterbody is high, the annual costs deriving from the cyano-HABs and its impact on health, tourism, and economy sectors are greater [14]. A new field in the water management sector, is the prediction of contaminations and cyano-HABs through advanced models that integrate data from long monitoring periods. Prediction can be the outcome of long-term monitoring, where huge datasets are being extracted and further analyzed through mathematical correlations to build prediction models [35, 36]. Those models could reduce monitoring costs and support the monitoring activities by indicating specified dates and periods that contamination is more likely to occur [37]. Currently, there is not any accredited method for the *in-situ* detection of cyanotoxins or an applicable predictive model for cyano-HABs occurrence, since not all cyanobacterial species are active toxin producers under the same conditions, and the conditions of cyano-HABs occurrence differ each blooming period. Therefore, it is imperative to find both predictive models and monitoring tools as well as efficient treatment methods to mitigate the problem and safeguard water quality while reducing the water treatment costs at source and in the waterworks.

Besides monitoring the derivatives and concentrations of cyanotoxins, monitoring the level of nutrients in waterbodies and estimating their corresponding ratios are critical for improving the applied management strategies based on the specific needs of each waterbody. This allows to better control the limiting factors in order to prevent future blooming events [38, 39]. The main input of nutrients into the waterbodies comes from the misuse of fertilizers in agriculture as well as the sewage runoffs. To eliminate the waste disposal and the chemical usage near waterbodies, the European Commission of Environment of the EU has composed the Water Framework Directive (2000/60/EC) which aims to protect surface waters from chemical pollution. Additionally, the Organization for Economic Co-operation and Development (OECD) has actively participated in the development of frameworks and guidelines by reforming the surface water quality regulations in EECCA countries [40]. Based on those, OECD proposed a surface water classification (I – V class; excellent – bad) system based on different water quality characteristics, which are presented in Table 1. The use of this water status evaluation system has been widely adopted for monitoring water quality as well as to apply restorative measures when class upgrade is needed. These limits set by OECD were extensively utilized in the present thesis to characterize the water quality status of surface waters collected from lakes, dams, reservoirs and rivers in Cyprus.

**Table 1.** Proposed surface water quality standards by OECD based on the EU Directive (2000/60/EC).

Parameter	Unit	Class I	Class II	Class III	Class IV	Class V
<b>pH</b>	[-]	6.5 – 9.5				
<b>Total Nitrogen</b>	[mg/L]	1.5	4	8	20	>20
<b>Nitrate</b>	[mg/L]	1	3	5.6	11.3	>11.3
<b>Nitrite</b>	[mg/L]	0.01	0.06	0.12	0.3	>0.3
<b>Ammonium</b>	[mg/L]	0.2	0.4	0.8	3.1	>3.1
<b>Total Phosphorus</b>	[mg/L]	0.1	0.2	0.4	1	>1
<b>Orthophosphates</b>	[mg/L]	0.05	0.1	0.2	0.5	>0.5

The concentration (total and dissolved fraction) of the main nutrients, nitrogen (N) and phosphorus (P), is a strong indicator of the eutrophic state of waterbodies, thus, several models have been developed over the years to form correlations [41]. The most applied stoichiometric reference is the Redfield ratio which describes the nutrient limitation of planktonic production in coastal waters based on the TN:TP molar ratio [42]. Even though Redfield proposed this ratio for its use on oceanic studies, it was well adopted as a universal nutrient limitation threshold with multiple citations in different types of aquatic systems. Redfield referred to an average N:P molar ratio that when exceeds 16, phosphorus becomes the limiting element for phytoplankton growth while when the ratio is below 7, nitrogen is the limiting element. Over the years, different ratios and approaches have been developed for better understanding of the limiting element based on the specific conditions of each waterbody (e.g., nutrient sources, phytoplankton species present). Based on the cited literature, lakes with different characteristics showed different correlations of nutrients with their trophic status, and the efficiency of the Redfield ratio varied in each case [43]. Recent studies indicated that higher TN:TP molar ratios (>22, P-limitation) are more suitable for surface waters while DIN:TP and  $\text{NO}_3^-$ :TP mass ratios have been used more often during the past years for determining the limiting elements in lakes [44]. Studies on dissolved nutrients mass ratios (DIN:TP,  $\text{NO}_3^-$ :TP,  $\text{NH}_4^+$ :TP) suggested that in freshwater systems the DIN:TP mass ratio is a better indicator than the TN:TP molar ratio. Also, the  $\text{NO}_3^-$ :TP mass ratio performed even better than DIN:TP as DIN includes ammonium which in some studies it showed a weak

correlation with N-limitation, resulting in a weaker model [45]. The nutrient ratios and thresholds proposed in the cited literature are presented in Table S1 (Appendix I).

Even though, surface water monitoring combined with predictive models are essential for maintaining a healthy status and protect the biodiversity of aquatic biotopes around EU, unfortunate events of high nutrient loads that lead to the formation of cyano-HABs are mostly unpredictable. Therefore, highly efficient methods are required to be applied *in-situ* for the removal of cyanobacteria and the restoration of water quality status.

## **1.2.2 Mitigation of Cyano-HABs and their negative side-effects**

### ***1.2.2.1 Cyanotoxins removal***

The increasing prevalence and persistency of cyano-HABs in surface waters comprises an ongoing challenge for the water treatment sector and public health, not only because of the aesthetic effects that are caused but also because of the release of toxic metabolites into the water column. To address this problem, multi-dimensional approaches are applied worldwide for their “at source” prevention, the remediation of impacted waterbodies and the removal or degradation of cyanobacteria and cyanotoxins [46], additional to the *in-situ* practices. Throughout the years an array of treatment processes has been implemented for the mitigation of cyanotoxins in surface waters (i.e., dams, reservoirs, lakes) and water treatment plants. The applied treatment processes can be divided into five categories: (a) physical-chemical treatment, (b) membrane processes, (c) biological treatment, (d) conventional disinfection and/ or oxidation processes, and (e) advanced oxidation processes (AOPs).

Physical methods such as coagulation and flocculation, dissolved air flotation, rapid and slow sand filtration, bank filtration, and activated carbon (particulate or powdered) are commonly used processes in water treatment plants. These methods exhibit different efficiencies for cyanobacterial cells removal, but they are found to be insufficient for the removal of soluble cyanotoxins or requiring higher adsorber doses (activated carbon) compared with the ones usually applied in water treatment. Integration of membrane processes (microfiltration, ultrafiltration, nanofiltration, and reverse osmosis) into water treatment is becoming more common when highly contaminated water with cyanobacteria requires to be treated. Micro- and ultra-filtration cannot remove soluble

cyanotoxins due to their permeability, and they can remove toxic cyanobacterial cells without causing them to lyse, hence avoiding the release of intracellular cyanotoxins. For soluble (extracellular) cyanotoxins reverse osmosis and nanofiltration are preferred as they are more efficient than UF due to their low molecular weight cut-offs [47].

Biological degradation is an evolutionary yet low-cost treatment method of detoxification, which uses naturally occurring cyanotoxin-degrading microorganisms and it can be applied at source and in drinking water treatment plants [48]. Studies suggest that biological degradation in combination with existing water treatment methods may increase treatment efficiency and maybe more advantageous for mitigating cyanotoxins in drinking water treatment compared with conventional treatment processes. Conventional disinfection and/or oxidation processes are widely and well-known methods not only for microbiological control but also for the destruction of water contaminants and in this case, cyanotoxins. Chlorine and its derivatives are extensively applied as disinfectants to ensure water purification and disinfection. Recent studies enhanced current knowledge and the state of the art on the removal of cyanotoxins from water, their possible transformation products, and the resulting toxicity of the treated water. It was shown that chlorination of several cyanotoxins decreased the overall toxicity of water, but the long-term effects of the corresponding transformation products have not been assessed yet. Therefore, further studies need to be conducted with respect to the residual toxicity of treated water with these highly efficient methods. Ozone is another well-known oxidizing agent with high oxidation potential. It is found to be effective on treating both intra and extracellular cyanotoxins leading to water detoxification but again the toxicity of their transformation products is not well-studied [46, 49].

Advanced oxidation processes (AOPs) can produce highly reactive oxygen species that readily and rapidly react with water contaminants leading to their degradation and resulting in water purification and detoxification. In recent years, AOPs are preferred to conventional treatment methods as the removal mechanisms of cyanotoxins is through degradation and not containment in an adsorber [50]. Some of the most studied AOPs are UV irradiation coupled with oxidants ( $\text{H}_2\text{O}_2$ ,  $\text{K}_2\text{S}_2\text{O}_8$ ,  $\text{KHSO}_5$ ), UV with ozone and catalytic ozonation, Fenton reaction,  $\text{TiO}_2$ -based photocatalysis, UV and visible light activation, radiolysis, and ultrasonication. During chemical oxidation, transformation

products formation should be monitored since they may possess toxicity which is not known yet. AOPs exhibit great potential for the treatment of cyanotoxins and can be introduced in the DWTPs not only as a complementary option for controlling emerging compounds, but also as a pre-treatment procedure. To do so, the scalability of AOPs also should further investigated along with their mechanistic degradation pathways, and assessments of the transformation products' toxicity.

#### ***1.2.2.2 In-lake management of cyanobacteria***

Once monitoring activities detect an on-going bloom, mitigation practices need to be applied to the contaminated waterbody, that would result in long-lasting treatment results. The serious and direct human and animal health effects posed by cyanobacterial blooms, have led to the necessity to find efficient *in-situ* mitigation techniques. Currently an array of methods is applied to mitigate the negative effects of cyano-HABs, that differ in cost, efficiency, and environmental impact. Physical, chemical, and biological methods have been developed and applied over the years with the chemical ones to be cost effective, rapid, and more efficient towards the contaminant [51]. However, chemical methods are the most invasive methods, so careful examination of the chemical properties should be conducted prior to their *in-lake* use. The most known and used methods are extensively described in Table 2, and are categorized as physical, chemical, and biological methods based on their application type. Those methods were evaluated based on their efficiency, on their application challenges, and their environmental impact. Given the wide array of methods and products available in Table 2, it is obvious that the efficiencies of the applied methods vary, they depend on several factors, and most of the methods have great or questionable impact on the environment. In addition, some technologies require the *in-field* application of devices that increases both maintenance and operational costs as well as their application can cause undesirable side effects due to invasion to the ecosystem. Also, some mitigation methods do not target cyano-HABs directly but eliminate other factors that favor cyanobacterial growth, such as nutrients load or dissolved oxygen penetration (e.g., Phoslock, Surface mixers).

Nutrient reduction through physical and chemical methods, is a preventative measure and the core of many applied physical methods. It is proven to be an effective approach for short-time control of cyano-HABs, however it is projected that it may take decades to give long-lasting effects. Controlling the availability of nutrients (N, P) comprises a

crucial factor, but it depends not only on the applied techniques in the field but also the input of nutrients from external factors that cannot always be monitored and eliminated [52]. In any case, the mitigation strategy can be challenging and requires consideration of many parameters and datasets to apply the optimum treatment in each waterbody. So far, mitigation techniques are rarely custom-made for each contamination case while most of the times, are applied without the appropriate evaluation of several factors such as physicochemical characteristics of the water, phytoplankton characterization, and zooplankton wellness.

**Table 2.** Summary of cyano-HABs management options describing their efficiency and environmental impact.

<b>Method</b>	<b>Efficiency/ Difficulties</b>	<b>Environmental Impact</b>
<b>PHYSICAL</b>		
<b>Ultrasonic</b>	Need of high-power units (difficult for in field applications), disruption of cyanobacterial cell but limited penetration through water.	High-power ultrasound is harmful to aquatic organisms. Toxins release from cell lysis, increasing the extracellular toxin concentration.
<b>Screens/ Barriers</b>	Suitable only for buoyant species, does not treat but eliminates the spread of cyano-HABs into the waterbody. Screens are easily broken up by wind.	Plastic contamination, no harm to aquatic organisms.
<b>Surface Mixers; Fountains</b>	Moderate to low efficiency, needs power supply and maintenance costs. High power usage and their operation may produce odor compounds and noise.	No harm to the aquatic organisms.
<b>Oxygenation (Aeriation)</b>	Does not target cyano-HABs but increases dissolved oxygen, causing improvement to the water quality. System installation may cause nutrient availability from soil increasing the chances of future cyano-HABs blooming.	The installation may cause change on the communities of phytoplankton, zooplankton. System causes nutrients to become more available to phytoplankton and aquatic plants, increasing their growth rate. No harm to the aquatic organisms.

<b>Dredging/ excavation</b>	Efficiency varies depending on physical, chemical, and biological conditions of the waterbody. Very expensive method and soil disposal issues.	Possible disruption of the benthic ecosystem.
<b>Surface aeration - Destratification</b>	Works only with cyanobacterial species that form surface scums and efficient when treating a small surface area portion.	Increased noise and requirement for high energy supply.
<b>Withdrawal of bottom waters</b>	It removes low-oxygen, nutrient-rich water to limit the nutrients available for cyanobacterial growth. It works only in systems where the bottom waters are cooler than the surface waters, and oxygen concentrations are low in the bottom waters (stratification conditions).	Waste of deriving from the withdrawal of waters high in nutrients, Release of nutrients in the environment can have negative effects on fish and other aquatic habitants. No direct hazard.
<b>Light exclusion technology</b>	Limited evidence of benefit. Not suitable for large water bodies.	Shade-covers and other floating devices can have unexpected consequences on enhancing sediment nutrient production.
<b>CHEMICAL</b>		
<b>Geochemical compounds (alum, Phoslock, Aqual P™, Bephos™)</b>	Forms flocks that adsorb phosphate from the water and sediments, removing one of the key nutrients that allows algae to grow to bloom proportions. Considerable literature showing benefits if dosage and background conditions are appropriate. Works when phosphorus loads are internal and only as a preventative measure.	Risk of legacy effects (e.g., chemical could remain in bottom sediments).
<b>Copper sulfate (algicides)</b>	Copper sulfate is/was a popular method for controlling cyanobacteria in reservoirs and lakes globally with high efficiency.	As knowledge of the toxicity effects of copper on food webs increases, and concern about its persistence in sediment grows, many authorities globally are

		banning or discouraging its use (EU Regulated chemical).
<b>Sediment capping</b>	A capping layer (active-carbon or passive-sand) is designed to reduce nutrient releases from the sediment to the water column. Capping is time consuming and controls only the nutrients.	Unwanted side effects on benthic organisms, such as a decrease in growth, reproduction, or diversity.
<b>Macroalgae extracts</b>	Extracts of macroalgae species such as <i>Chara vulgaris</i> , with algicidal effect applied on <i>Microcystis</i> sp. and resulted in promising results.	The effect on non-targeted species has not been explored yet, but the extracts exhibited high efficiency on treating cyanobacteria species. The application of macroalgae extracts may disrupt the chemical balance of water, hence their application necessitates further investigations
<b>Hydrogen Peroxide</b>	The amount of chemical needed for each cyanobacterial species and in each waterway varies, so it requires trials to optimize dosages. In lakes with a high abundance of eukaryotic algae, the breakdown of hydrogen peroxide may be so fast, that it will not remain long enough in the water to effectively kill cyanobacteria. Furthermore, the use of hydrogen peroxide in water bodies larger than a few hundred hectares is likely impractical and not cost effective.	When administered at the correct dose and distributed homogeneously, this chemical can preferentially kill or inhibit cyano-HABs without affecting other algae, aquatic animals, and plants. In cases where more resistant cyano-HABs such as <i>Microcystis</i> are prevalent, hydrogen peroxide may not be capable of fully removing cyano-HABs without harming zooplankton.
<b>H<sub>2</sub>O<sub>2</sub> releasing oxidants (e.g., CaO<sub>2</sub>, MgO<sub>2</sub> granules)</b>	Efficient as hydrogen peroxide, sometimes outperforms HP, but some considerations for in-situ treatment derived from their size and type (granular form)	Our preliminary results: High doses of CaO <sub>2</sub> increase pH and release Ca(OH) <sub>2</sub> in water. Doses higher than 3 g/L are lethal to zooplankton.

<b>OXONE®</b> (Peroxymonosulfate)	Highly efficient towards contaminant. Still under investigation.	Preliminary studies showed minimal effect on invertebrates on the applied doses.
<b>BIOLOGICAL</b>		
<b>Biological treatments (e.g., bacterial seeding)</b>	Very limited scientific evidence of method's efficiency.	Introduced organisms may not necessarily outcompete resident populations.
<b>Bio-manipulation of food web</b>	Only used as short-term strategy. Food web controls are notoriously difficult such as manipulating zooplankton or fish.	Disrupting the ecosystem balance within the waterbody.
<b>Aquatic plants (floating islands and wetlands)</b>	Floating and submerged plants are used. Evidence of benefit only in shallow systems.	The use of plants by birds could increase faecal contamination and nutrients load.

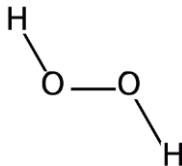
Chemical treatment methods utilizing compounds with algicidal effects is the most common and widely used mitigation strategy for both cyano-HABs and their secondary metabolites degradation [53]. In the early years of surface water treatment, copper sulfate was extensively used for its algicidal properties, resulting in various treatment efficiencies. Some lakes stated re-occurrence of the blooms just 2 months after the treatment. The observed side-effects and the advancement of knowledge regarding its environmental impact, led to the elimination of its use, while in some locations its use is regulated (EU, and some US states) [49, 54]. Among other side-effects, toxicity on aquatic organisms, accumulation in soil, oxygen depletion due to biomass coagulation, treat and increased phosphorus levels released from the sediments, were reported. [45, 46]

Later, there was a shift towards the application of biological methods, such as barley straw use, that were considered more “environmentally friendly”. Barley straw’s ability to release phenolics and carboxylic acids exhibited a mild algicidal effect in water. Even though, this method is cheap, easily applied, and safe for the aquatic environment, its treatment efficiency is low [55]. The application of natural algicides was introduced in literature, as “environmentally friendly” options for the treatment of cyano-HABs. Those chemical methods are utilizing macroalgae extracts (e.g., *Chara vulgaris*), known as allelochemicals, that exhibited high treatment efficiency towards *Microcystis*, but their

application in surface water necessitates further investigations [56]. Other biological methods were also investigated such as biomanipulation of food web, and bacterial seeds, which had minimal effect on the tested cyanobacterial species, or enormous application difficulties, leading to the reconsideration of chemical treatment methods. The need to make chemical treatment “greener” has led to the application of hydrogen peroxide (H<sub>2</sub>O<sub>2</sub>) as an alternative to copper algicides, resulting in selective reduction of cyanobacterial species among other taxa of phytoplankton [57–59].

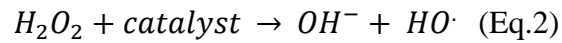
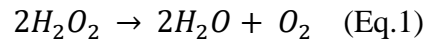
## Hydrogen peroxide

**Table 3.** Physical-chemical properties of hydrogen peroxide (Sigma-Aldrich).

<b>H<sub>2</sub>O<sub>2</sub> chemical properties</b>	
<b>Chemical structure</b>	
<b>Molecular Formula</b>	H <sub>2</sub> O <sub>2</sub>
<b>Chemical name</b>	Hydrogen Peroxide
<b>Molecular weight</b>	34.015
<b>Color/Form</b>	Colorless liquid
<b>Solubility in water</b>	1×10 <sup>6</sup> mg L <sup>-1</sup> at 25 °C
<b>Decomposition reaction</b>	$2 \text{H}_2\text{O}_2 \rightarrow 2 \text{H}_2\text{O} + \text{O}_2$
<b>Reduction reaction</b>	$\text{H}_2\text{O}_2 + 2 \text{H}^+ + 2 \text{e}^- \rightarrow 2 \text{H}_2\text{O} \text{ (E}^\circ=1.77 \text{ V)}$

Hydrogen peroxide decomposes into H<sub>2</sub>O and O<sub>2</sub>, while when it is applied in the presence of a catalyst it can form reactive oxygen species (ROS) with high oxidative potential (Equations 1-2). Its chemical and physical properties are presented in Table 3. The fact that utilization of H<sub>2</sub>O<sub>2</sub> is an advanced chemical oxidation treatment method, with the ability to generate hydroxyl radicals that target both cyanobacterial cells and

cyanotoxins, increase its treatment efficiency [60]. The hydroxyl radicals ( $\cdot\text{OH}$ ), with a high redox potential ( $E^{\circ}=2.7\text{ V}$ ), are formed by  $\text{H}_2\text{O}_2$  and can inhibit the electron transport of photosystem II, causing reduction of its photosynthetic activity, hence leading to cellular death [58, 61, 62].



The interaction mechanism between  $\text{H}_2\text{O}_2$  and cyanobacteria cells is not yet fully explored, but there are indications that  $\text{H}_2\text{O}_2$  is diffused within the cell due to the permeability of cell wall membrane, simulating  $\text{H}_2\text{O}$  diffusion. Earlier studies suggested the presence of aquaporins channels could also transfer the  $\text{H}_2\text{O}_2$  within the cell wall [63–65].

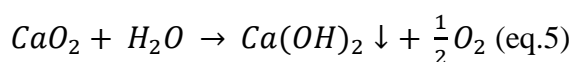
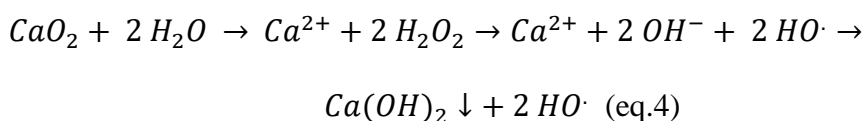
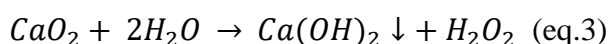
Liquid  $\text{H}_2\text{O}_2$  has been successfully applied for the mitigation of dense and resident blooms in surface waters. However, there are studies suggesting that its efficiency varies and depends on the nutrient load of the matrix, the species composition and abundance, the boom density, and light intensity. Usually high doses of  $\text{H}_2\text{O}_2$  ( $>5\text{ mg L}^{-1}$ ) are required for a complete destruction of cyanobacterial cells [66, 67]. There were blooms which demanded doses higher than  $10\text{ mg L}^{-1}$ , which are deemed harmful for the lake ecosystem. A study by Wang et. al. (2019) showed that repeated additions of liquid  $\text{H}_2\text{O}_2$  extent the residual effect of the oxidant into the water column, while resulting in successful *Microcystis* sp. mitigation [68]. It is imperative to find methods for eliminating high direct doses of oxidants into the waterbodies to safeguard non-targeted species. An alternative to liquid hydrogen peroxide is its powdered and granular form found as metallic peroxides ( $\text{CaO}_2$ ;  $\text{MgO}_2$ ), as well as the peroxide containing compound, peroxymonosulfate ( $\text{KHSO}_5$ ).

### **Metallic peroxide granules**

Calcium peroxide ( $\text{CaO}_2$ ) granules have been applied on a broad spectrum of environmental remediation processes over the last few years due to their potency to release  $\text{H}_2\text{O}_2$  and  $\text{O}_2$ , as shown in Equations 3-5 [69, 70]. Kinetic studies on their reaction pathways showed that once granules are applied into the water, they can directly react with water to form  $\text{H}_2\text{O}_2$  and oxygen without the presence of a catalyst [69].  $\text{CaO}_2$

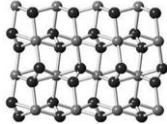
granules were previously applied for soil and groundwater remediation, as well as for odor control, chemical decomposition, and oxidation of persistent contaminants [71]. The properties of granular and powdered form of CaO<sub>2</sub> are presented in Table 4.

There are only a few studies on the application of CaO<sub>2</sub> granules for treating cyanobacteria contaminated surface water, especially for controlling *Microcystis* blooms [72–74]. Other types of granules and beads containing CaO<sub>2</sub> were fabricated and used for the mitigation of cyanobacteria resulting in high treatment efficiency [75, 76]. These studies outline the potential of this compound to be used in an array of applications due to its physical, chemical, and algicidal properties which are not yet fully understood and explored.



Their application for restoring surface waters could be useful when multiple liquid H<sub>2</sub>O<sub>2</sub> doses are required, based on their H<sub>2</sub>O<sub>2</sub> releasing properties. Other important characteristics of CaO<sub>2</sub> granules are their (a) orthorhombic structure which provides high thermal stability against its decomposition, (b) low solubility (almost insoluble) in water, and (c) inexpensive production line which requires only low-cost raw materials [77].

**Table 4.** Physical-chemical properties of calcium peroxide and calcium peroxide granules (Sigma-Aldrich; SOLVAY).

	CaO <sub>2</sub>	CaO <sub>2</sub> granules
<b>Chemical structure/ Crystal structure</b>	$\begin{array}{c} \text{O} - \text{O} \\ \backslash \ / \\ \text{Ca} \end{array}$	
<b>Molecular Formula</b>	CaO <sub>2</sub>	
<b>Chemical name</b>	calcium peroxide	calcium peroxide in the form of IXP <sup>®</sup> ER 70C

<b>Molecular weight</b>	72.1	
<b>Color/Form</b>	grayish white powder	yellowish white granules
<b>Solubility in water</b>	limited	limited
<b>Decomposition reaction</b>	$\text{CaO}_2 + \text{H}_2\text{O} \rightarrow \frac{1}{2} \text{O}_2 + \text{Ca(OH)}_2$ $\text{CaO}_2 + 2 \text{H}_2\text{O} \rightarrow \text{H}_2\text{O}_2 + \text{Ca(OH)}_2$	

### Peroxymonosulfate (PMS)

Peroxymonosulfate anion derived from peroxysulfuric acid ( $\text{H}_2\text{SO}_5$ ) is a very unstable and reactive acid, hence it had not been successfully synthesized in the form of a stable mono-salt [78], but it can be found in the market in the form of a triple salt of potassium peroxymonosulfate which is stable in room temperature [79]. The application of PMS on the removal of cyanotoxins, and other emerging contaminants of concern, showed great selectivity towards the pollutants, hence high treatment efficiencies [80]. Its properties are presented in Table 5. PMS is an unsymmetrical oxidant which can produce both hydroxyl and/or sulfate radicals, in the presence or the absence of a catalyst or an activator. Sulfate radicals ( $\text{SO}_4^{\bullet-}$ ) have strong oxidation potential ( $E_0=2.5 \text{ V}$ ), making it a powerful oxidant agent. The half-life of sulfate radicals is around  $30 \mu\text{s}$  the half-life of hydroxyl radicals is only  $20 \text{ ns}$ ; hence the selective oxidation of  $\text{SO}_4^{\bullet-}$  compared with the non-selective  $\bullet\text{OH}$  [81]. Even though its strong oxidizing potential and the high treatment efficiencies, PMS had not been explored for cyano-HABs treatment and its in-field application, except one recent study of Chen et. al (2021) [82].

**Table 5.** Physical-chemical properties of potassium peroxymonosulfate and its triple salt - OXONE<sup>®</sup> (Sigma-Aldrich).

	PMS	OXONE <sup>®</sup>
<b>Chemical structure</b>		
<b>Molecular Formula</b>	$\text{KHSO}_5$	$\text{KHSO}_5 \cdot 0.5 \text{ KHSO}_4 \cdot 0.5 \text{ K}_2\text{SO}_4$

<b>Chemical name</b>	Potassium peroxymonosulfate	Potassium peroxymonosulfate triple salt (OXONE)
<b>Molecular weight</b>	152.2	307.38
<b>Color/Form</b>	Off-white powder	White powder
<b>Solubility in water</b>	decomposes	>250 g L <sup>-1</sup>

### 1.3 Research novelty

#### 1.3.1 Research questions/ hypothesis

This doctoral thesis aimed to test novel oxidants that have the capacity to outperform current treatment methods (H<sub>2</sub>O<sub>2</sub>) in terms of application costs, cyano-HABs mitigation efficiency, and environmental impact. To do so, an experimental procedure was designed to investigate novel oxidants under comparable conditions, as based on the cited literature so far studies on cyano-HABs *in-situ* remediation, were performed under different conditions that are not comparable, making it difficult to choose between treatment options. Experiments were performed to examine the mitigation efficiencies, and the algicidal properties of the following peroxide-generating oxidants: calcium peroxide (CaO<sub>2</sub>), magnesium peroxide (MgO<sub>2</sub>), and peroxymonosulfate (KHSO<sub>5</sub>; PMS) as alternatives source of strong peroxide oxidizers.

Since metallic peroxide granules are reported in the literature as slow releasers of H<sub>2</sub>O<sub>2</sub>, we hypothesized that utilizing peroxide granules they would exhibit the same or increased treatment efficiencies compared with liquid H<sub>2</sub>O<sub>2</sub>. Both, their powdered and their granular form, were examined for their H<sub>2</sub>O<sub>2</sub> releasing capacities and their reaction kinetics in extra pure and surface water, to identify which form results in the gradual and controlled release of H<sub>2</sub>O<sub>2</sub> simulating its multiple additions.

The H<sub>2</sub>O<sub>2</sub> releasing properties of CaO<sub>2</sub> granules, in different water matrices have not been extensively studied so far, hence limited data is found for their releasing properties and treatment efficiencies. Herein, their application to mitigate dense blooms of cyanobacteria was investigated as well as their releasing properties in water matrixes of

several compositions. The effect of nutrients, microelements, and natural organic matter, on the releasing properties of granules were some of the investigations performed. The hypothesis was that  $\text{CaO}_2$  granules would have the ability to destroy cyanobacteria cells by inhibiting the PSII electron transfer in the same way as  $\text{H}_2\text{O}_2$  does, but in a more gradual and controlled manner, avoiding the instant high doses ( $>5 \text{ mg L}^{-1}$ ) of  $\text{H}_2\text{O}_2$  that disrupt the entire lake ecosystem (e.g., zooplankton and phytoplankton). Same hypothesis was applied for peroxymonosulfate application in surface water. The hypothesis was that PMS would require lower applied doses than  $\text{H}_2\text{O}_2$  (in equal molar concentrations), making it an outstanding treatment method for cyano-HABs.

Extensive monitoring activities including monthly sampling of George Lake and Athalassa Lake (National Forest Park, Nicosia, Cyprus) captured an ongoing *Merismopedia* sp. bloom during 2019, and a dense Planktothrix bloom in 2020. Therefore, preliminary studies to test the above oxidants' ability on destroying cyanocells were conducted in water collected from surface waters during naturally occurring blooms. Dedicated experiments were designed for each oxidant in order to test: (a) the released peroxide concentrations, (b) the mitigation efficiencies, (c) the effect of matrix on their treatment efficiency and peroxide generation, and (d) their effect on *Echinogammarus veneris* sp., an invertebrate specie sensitive to environmental changes.

The results of the above experiments led to additional investigations on their application method, as side products and unwanted effects were decreasing granules' efficiency. Specifically, the possibility of utilizing a delivery system to enclose the granules was explored. The granules enclosed in fabrics, proposed a holistic approach to treat cyanobacteria, which allowed the elimination of the unwanted side effects and resulted in efficient and controlled application of granules. The novelty of the present study relies not only to the use of  $\text{CaO}_2$  granules as an alternative  $\text{H}_2\text{O}_2$  source but also the investigation of its controlled application through a delivery system, using recycled textile materials and contributing to a greener economy towards the achievement of the UN SDG goals.

Apart from the above peroxide releasing chemicals, a peroxide including chemical (OXONE<sup>®</sup>) which is widely used as an oxidizing agent was tested for its mitigation efficiency, dose requirements, and environmental friendliness, always in comparison with the equal doses of liquid  $\text{H}_2\text{O}_2$ , which is the current practice. OXONE<sup>®</sup>

monopersulfate compound is a potassium triple salt mainly used as a stable, easy to handle and nontoxic oxidant. Although it was widely used as an advanced oxidation process for cyanotoxins degradation, there is only one study utilizing it as an algacide. Hence it is of high importance to study the treatment of efficiencies of PMS, and its toxicity on non-targeted organisms.

Additionally, no rapid and reliable methods were available in the literature for the quantification of PMS, thus, a quick (<1 s), reliable and easy quantification method was developed at the Water Treatment Laboratory – AQUA and a patent has been submitted to the national patent office and the United States Patent and Trademark Office. The current available method that was previously developed in our group, is an iodometric method titrated with standard sodium thiosulfate solution requiring a minimum reaction time of 15 minutes per sample [83]. Handling more than 40 samples per experiment, such methods are not feasible to be applied. The developed POXi kit requires some seconds per sample and can be determined spectrophotometrically in multiple plate reader spectrophotometers, saving time and labor.

Overall, the aim of the present study was to develop and optimize an efficient and safe for the environment treatment method for mitigating surface water quality by destroying cyanobacterial cells while keeping the wellness of the remaining ecosystem, as an additional advantage from the current approaches.

### **1.3.2 Side-projects related to cyano-HABs monitoring & treatment**

Along with the main research of this Doctoral Thesis, I was involved in the following side projects which were complimentary to the main activities of the present thesis:

- A) CYANOXI (ex. CYANOCONS): “Novel physical-chemical oxidation processes for mitigating toxic cyanobacterial blooming”. The project was funded and supported by the Cyprus Seeds Organization, and it aimed to test novel oxidants for the *in-lake* mitigation of harmful cyanobacteria blooms and with high commercialization potential. This project correlated directly to the thesis topic, and the main findings of this project are presented in Chapters 3.2-3.3.
- B) POXI “A testing kit for the rapid, accurate, and easy quantification of peroxymonosulfate compounds based on a colorimetric method” (co-PI), The project was a side-product of CYANOXI project which is funded by the Cyprus

Seeds Organization, and it aimed to develop a method for the quantification of PMS, discussed in Chapter 3.3. For the above kit a Cyprus patent application, CY202000002 (September 2020); US Provisional patent application (USPTO, October 2020); and a US patent application (USPTO, 2021) was filed through the hosting Institution, the Cyprus University of Technology. The method is explained in Chapter 3.3.1.

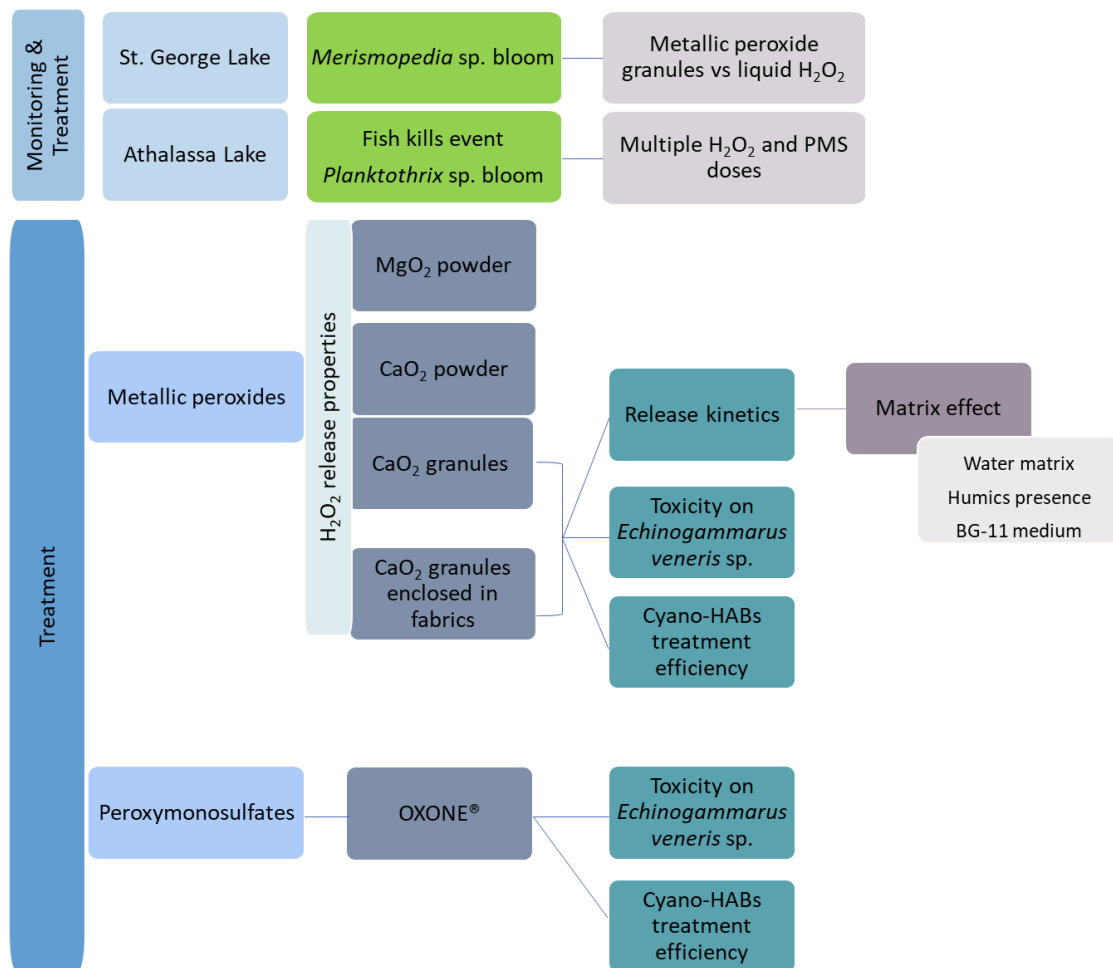
- C) CYANOS: “Monitoring and treatment of cyanobacterial contaminated surface waters in France and Cyprus”. It was a 2-year bilateral project funded by the Research Promotion Foundation of Cyprus and the Campus of France. During this project, monitoring of Polemidia Dam, Kouris Dam, Athalassa and St. George Lakes were monitored, and focus was given to St. George Athalassa Lake for monitoring and treatment with H<sub>2</sub>O<sub>2</sub> granules. The goal of this study was to examine the efficiency of treatment in a dense single-species bloom that occurred in St. George Lake of the Athalassa National Forest Park, in Cyprus with metallic peroxide granules and compare it with the traditionally used liquid hydrogen peroxide. The first objective was to determine the kinetic of the H<sub>2</sub>O<sub>2</sub> release of two types of granules (CaO<sub>2</sub> and MgO<sub>2</sub>) into an on-going bloom by monitoring its residual concentration during the treatment. The second objective was to compare the efficiency of granules in reducing the photosynthetic activity during a 48-hours treatment. This study also aimed to determine the most appropriate dose of oxidant for successful mitigation of the *Merismopedia sp.* bloom to propose an efficient treatment method for *in-lake* application that will upgrade its water quality class, as proposed by EU. Main findings of this side-project are presented in Chapter 3.1.
- D) CYANOBOX: “Automated In-situ CYANOtoxin Assessment ToolBOX for Real-Time Surface Water Monitoring” (CYanoBox). It is a 3-year project under the RESTART Enterprises call, funded by the Research and Innovation Foundation, Cyprus. Along with the Cyprus Research & Innovation Center (CyRIC), we are developing a unique water processing system that can remotely filter and lyse the cyanobacterial cells *in-situ* so that an accurate measurement is taken for both extracellular and intracellular concentration of microcystins. The project aim is to deliver an autonomous, affordable, and easy to operate water monitoring system as an early-warning tool for surface waters affected by cyano-

HABs. During the validation of “CYANOBOX” monitoring sensors a scale-up treatment of Athalassa’s lake water, was performed utilizing  $H_2O_2$ ,  $CaO_2$  granules and PMS. The experimental procedure that took place at the premises of CyRIC, is presented in Chapter 3.4.

- E) CYANOTECH: “A sustainable and innovative management system for toxic cyanobacteria blooming of surface waters with combined energy production, sustainable agriculture, and food safety”, - work packages related to the treatment of cyanobacteria with advanced oxidation processes.
- F) Mini CYANO-project: Screening of rivers in Cyprus for determining cyanobacteria speciation, toxic genes, and cyanotoxins presence in benthic macrophyte cyanobacteria masses. The project was conducted in collaboration with Mrs. Athena Papatheodoulou through I.A.CO Environmental & Water Consultants Ltd. The results of this study are not presented herein.

### **1.3.3 Research outline**

The thesis is divided in two sections based on the research topics that it tackles. The first part is on the “Monitoring and treatment of naturally occurring cyano-HABs” which includes two case studies of naturally occurring blooms in lakes located at the National Park of Athalassa (Chapter 3.1). The second part is on the “Treatment of cyano-HABs with novel peroxide releasing oxidants” and it comprises of two subsections: Investigation of metallic peroxides  $H_2O_2$  release kinetics under several conditions and their treatment efficiencies (Chapter 3.2), and cyano-HABs treatment with OXONE<sup>®</sup>, a PMS generating triple salt, and its toxicity on invertebrate species (Chapter 3.3). The breakdown of the thesis sections is depicted in Scheme 7.



**Scheme 7.** Main research outline

## 2 Research Methodology

### 2.1 Monitoring & treatment of Athalassa National Forest Park's lakes

#### 2.1.1 Study Area

Saint George Lake and Athalassa Lake are located at the Athalassa National Forest Park (ANFP) in Nicosia, the capital city of Cyprus. It is an artificial lake which covers an area of 68,000 m<sup>3</sup> with an average depth of approximately 2 m. ANFP covers an area of 8.5 km<sup>2</sup> and it is found between Aglantzia, Strovolos, Latsia, and Geri municipalities; four of the most densely populated locations in Nicosia (Scheme 8). Both lakes in the park serve as aquatic life and bird habitats, making them an extremely important biotope for the island. The present study focuses on the monitoring of the St. George Lake (February – December 2019), and Athalassa Lake (August – November 2020), in terms of nutrient concentration, cyanobacterial content, and toxicity. Moreover, treatments with novel

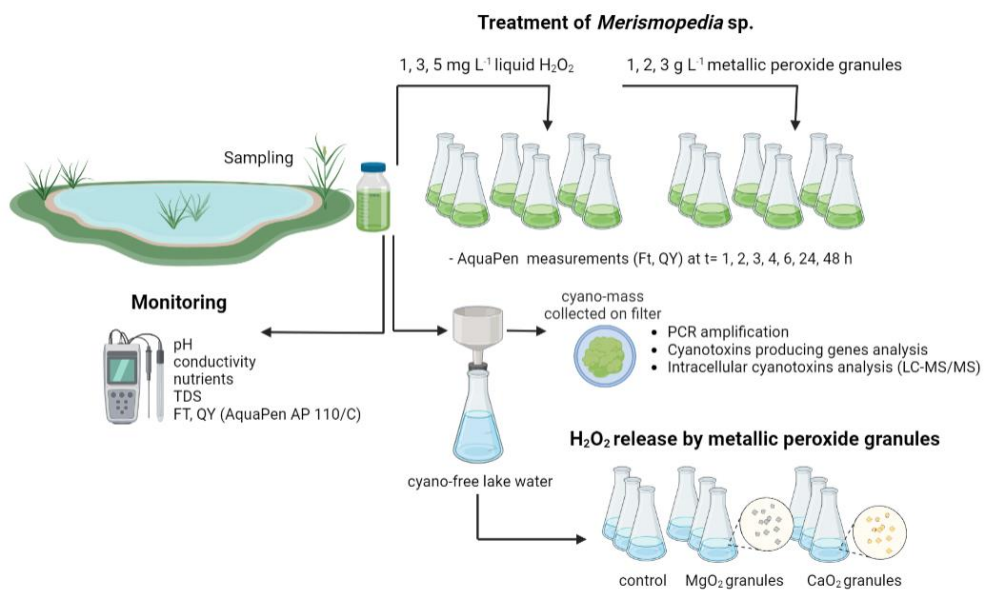
chemical oxidation processes and liquid  $H_2O_2$  were performed to investigate the potential of oxidants for treating naturally occurring cyano-HABs.



**Scheme 8.** Monitoring locations at the National Park of Athalassa indicated in yellow, (A) St. George Lake, (B) Athalassa Lake, retrieved by Google Maps Data, 2022 ©.

## 2.1.2 Case studies

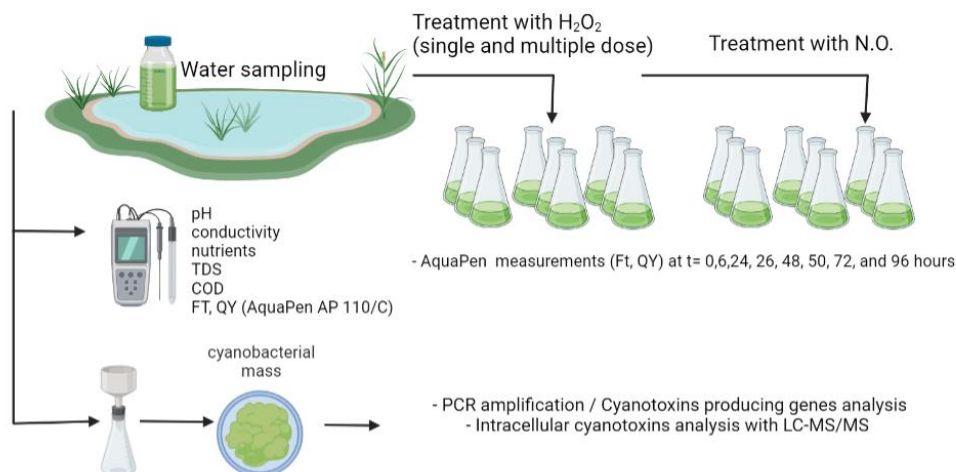
### 2.1.2.1 St. George Lake Case Study



**Scheme 9.** Graphical abstract depicting the main research activities conducted during St. Lake monitoring and treatment in 2019 (created with Biorender.com by E. Keliri ©).

Monitoring of St. George Lake occurred between February and December in 2019, and it aimed to monitor the status of St. George Lake for correlating its trophic condition with its water quality characteristics as well as to identify the limiting elements driving the cyanobacterial blooming. This was achieved by monitoring the nutrient load of the lake and calculate the nutrient ratios as proposed in literature. Another aim was to examine the treatment efficiency of metallic peroxide granules against the single high doses of liquid  $H_2O_2$ . The hypothesis made was that since peroxide granules are reported in the literature as slow  $H_2O_2$  releasers, they would have the ability to destroy cyanobacterial cells by inhibiting the PSII electron transfer in the same way as  $H_2O_2$  does. The reason of choosing granules as a potential and alternative to liquid  $H_2O_2$  treatment, is their releasing properties which may allow a graduate and controlled released of  $H_2O_2$ , simulating its multiple additions. To do so,  $CaO_2$  and  $MgO_2$  were utilized to treat a bloom occurred in August 2019, and then granules' efficiency on reducing the maximal yield of PSII (QY) during a 48-h treatment was recorded and compared between each oxidant. Then, release experiments of  $H_2O_2$  by  $CaO_2$  and  $MgO_2$  granules were performed in filtered St. George Lake water to determine the releasing capacity of granules and the maximum released concentration (Scheme 9). Since the bloom was a mono-domination of *Merismopedia* sp. that has been reported in the literature as a potential toxin producer, it was essential to determine the most appropriate dose for its successful mitigation. This study aimed to address all the above in order to investigate alternative  $H_2O_2$  applications that would avoid high instant doses of the oxidant.

### 2.1.2.2 *Athalassa Lake Case Study*



**Scheme 10.** Graphical abstract depicting the main research activities conducted during Athalassa Lake monitoring in 2020 (created with Biorender.com by E. Keliri ©).

Monitoring of Athalassa's Lake occurred between August and November 2020, based on the findings of 2019 that showed increased cyanobacterial activity during and right after the summer months. During the monitoring activities that aimed to record its water quality characteristics, a massive fish-kill event occurred (September 2020) at the lake, followed by a cyanobacteria blooming period. More than 200 fish were found dead in the shore of the lake and press-release blamed cyano-HABs for this incident. Both events raised questions regarding the toxicity of the lake and the source of its toxicity.

The present study focuses on the monitoring of Athalassa Lake, and it aimed to investigate the source of toxicity that caused the fish-kills. To do so, samples were analyzed for cyanotoxin producing genes presence (2.1.6), cyanotoxins content, and speciation. Other characteristics of the water were also determined. Another aim of this study was to treat the contaminated water in both cases (fish-kill and cyano-blooming) as an additional investigation to multiple H<sub>2</sub>O<sub>2</sub> doses and to examine the efficiency of PMS in comparison with liquid H<sub>2</sub>O<sub>2</sub> in equal active doses. The research question was to test lower repeated doses of H<sub>2</sub>O<sub>2</sub> that are considered safe for the environment (< 5 mg L<sup>-1</sup>) and record their treatment efficiency. As recent publications proposed the application of multiple H<sub>2</sub>O<sub>2</sub> doses for effective *in-situ* treatment (ref), this study aimed to test the hypothesis on a naturally contaminated surface water. In order to investigate the potential of PMS it was also employed for the treatment experiments performed in the water collected during blooming period. Both oxidants were tested under the manner of multiple additions and comparison occurred between the two (Scheme 10).

### **2.1.3 Sampling and monitoring**

Sampling was performed at a central part of St. George Lake and water was collected from a depth of 0.2–0.3 m below the surface. At Athalassa Lake water was collected at the littoral zone (depth < 0.5 m) with the use of a bucket. All water samples were stored in polyethylene (PE) bottles for the physicochemical water characterization and treatment purposes, and in amber glass bottles for cyanotoxins and cyanotoxin producing genes analyses. Bottles were stored under dark and cool conditions. In total ten samples were collected from St. George Lake during the monitoring period (25/02, 04/03, 18/04, 12/07, 06/08, 22/08, 09/09, 15/10, 12/11, and 09/12/2019), and four samples from Athalassa Lake (Aug – Nov 2020).

The main physicochemical parameters (pH, conductivity, salinity, total and dissolved nutrients, COD), the presence of cyanobacteria and green algae in terms of fluorescence signal (Ft), maximum quantum yield of PSII (Fv/Fm), microscopic observation, the content of genes for main cyanotoxins synthesis, and the concentration of cyanotoxins were determined. Samples were also collected during the cyano-blooming period (8-9/2019) from St. George as well as during the fish-kill and cyano-blooming in Athalassas. The collected samples were utilized in treatment experiments to determine the efficiencies of liquid hydrogen peroxide, hydrogen peroxide-releasing granules, and peroxide including compound (OXONE<sup>®</sup>).

#### **2.1.4 Physicochemical water analyses**

Raw samples were analyzed for total nitrogen (TN) and total phosphorus (TP) while samples filtered through cellulose nitrate membrane filter (0.45  $\mu\text{m}$ ) were analyzed for the dissolved nutrients content (ammonium— $\text{NH}_4^+$ , nitrates— $\text{NO}_3^-$ , nitrites— $\text{NO}_2^-$ , and phosphates— $\text{PO}_4^{3-}$ ). Nutrients were determined by using Spectroquant<sup>®</sup> cell test kits (Merck Millipore) equivalent to EPA and APHA standard analytical methods and the Spectroquant<sup>®</sup> Pharo 300 spectrophotometer (Merck) with method standard deviations  $\pm 0.15 \text{ mg L}^{-1}\text{-N}$ ,  $0.027 \text{ mg L}^{-1} \text{ PO}_4\text{-P}$ ,  $0.043 \text{ mg L}^{-1} \text{ NH}_4\text{-N}$ ,  $0.13 \text{ mg L}^{-1} \text{ NO}_3^- \text{ N}$ ,  $0.0027 \text{ mg L}^{-1} \text{ NO}_2\text{-N}$ , respectively. Dissolved inorganic nitrogen was calculated as the sum of dissolved nitrogen ions ( $\text{NH}_4^+$ ,  $\text{NO}_3^-$ ,  $\text{NO}_2^-$ ). Temperature, pH, conductivity, and salinity were measured at the sampling site using the ExStik<sup>®</sup> portable pH meter (EXTECH, FLIR Systems).

#### **2.1.5 Phytoplankton content**

Instantaneous fluorescence (Ft) and quantum yield (QY) of the PSII were determined using AquaPen AP 110/C (Photon Systems Instruments, Czech Republic) equipped with blue and red LED light emitters. Blue excitation wavelength at  $\lambda = 450 \text{ nm}$  represents the instantaneous chlorophyll-a fluorescence and red excitation wavelength at  $\lambda = 620 \text{ nm}$  represents the phycocyanin fluorescence, both in raw fluorescence units (RFU). The maximum quantum yield of the PSII was recorded on both wavelengths as a fraction of the maximal variable fluorescence (Fv) to the maximal fluorescence intensity in the dark-adapted (5-min adaptation) state (Fm). The instrument was used to monitor the growth

of algae and cyanobacteria in St. George Lake, as well as the effect of treatment in terms of cyano-cells' fluorescence and quantum yield.

For the characterization of cyanobacterial species in water samples, raw sample was placed directly or after filtration (cellulose nitrate filter, 0.45  $\mu\text{m}$ ) on a microscopy slide and tested under ECLIPSE Ci-L microscope (Nikon) equipped with OPTIKAM Wi-Fi camera (OPTIKA®, Italy). Phytoplankton samples were preserved with Lugol's iodine solution (2% final concentration), stored in 4–6 °C under dark conditions and used within 3 weeks.

### **2.1.6 Cyanotoxin genes and cyanotoxins analyses**

DNA isolation from the biomass collected on cellulose nitrate filters was performed as described by Rogers and Bendich (1994) with minor modifications [84]. Newly designed primers were verified using positive controls: DNA from *Anabaena lapponica* 966 for *cyrB*, *cyrJ*, DNA from *Anabaena flos-aquae* for *anaC*, DNA from *Microcystis aeruginosa* PCC for *mcyB* and *mcyE* and DNA from *Aphanizomenon flos-aquae* NIVA-CYA 689 for *sxt*. The negative control was the DNA of *Raphidiopsis raciborskii* AMU-DH-30 (non-toxic). PCRs for the identification of main genes of cyanotoxins were conducted using Dream Taq DNA polymerase (Thermo Fisher Scientific). Approximately 80 ng of isolated DNA was added to the reaction mixture (20  $\mu\text{l}$  total volume) with 0.2  $\mu\text{M}$  of each primer. PCR was performed with the following parameters: initial denaturation for 3 min at 95 °C, 30 cycles at 95 °C for 30 s, a primer-pair specific temperature for 30 s and 72 °C for 60 s; a final extension at 72 °C for 10 min. The electrophoresis of PCR products was conducted on 1% agarose gels at 100 V for 25–40 min. Gels were stained with Midori Green Advance DNA Stain (ABO).

High-performance liquid chromatography–high-resolution mass spectrometry (HPLC–HRMS) was used to detect intra-cellular cyanotoxins in the biomass stored on GF/C filters at –20 °C until extraction. Sample preparation included extraction of cyanotoxins with 1 mL of 75% methanol in an ultrasonic bath [85]. All chemicals used for analytical procedures were of analytical grade. Acetonitrile (HPLC-grade) and methanol (LiChrosolv hypergrade for LC–MS) were purchased from Merck (Darmstadt, Germany); formic acid (98–100%) was obtained from Fluka Chemika (Buchs, Switzerland). High-quality water (18.2  $\text{M}\Omega\text{ cm}^{-1}$ ) was produced by the Millipore Direct-

Q water purification system (Bedford, MA, USA). The MC-LR, MC-RR, MC-YR standards were purchased from Sigma-Aldrich. Sample preparation procedures were run according to Chernova et al. (2016). Analyses of extracts were performed using the LC-20 Prominence HPLC system (Shimadzu, Japan) coupled with LTQ Orbitrap XL Hybrid Ion Trap–Orbitrap Mass Spectrometer (Thermo Fisher Scientific, San Jose, USA). Separation of the toxins was achieved on a Thermo Hypersil Gold RP C18 column (100 mm × 3 mm, 3 μm) with a Hypersil Gold drop-in guard column (Thermo Fisher Scientific) by gradient elution (0.2 mL min<sup>-1</sup>) with a mixture of water and acetonitrile, both containing 0.05% formic acid. Mass spectrometric analysis was carried out under conditions of electrospray ionization in the positive ion detection mode. The identification of target compounds was based on the accurate mass measurement of [M + H]<sup>+</sup> or [M + 2H]<sup>2+</sup> ions (resolution of 30,000, accuracy within 5 ppm), the collected fragmentation spectrum of the ions and the retention times. Limits of the detection for different microcystin congeners (2–6 ng L<sup>-1</sup>) were evaluated in model experiments using standard compounds, natural water, and biomass as matrixes.

## **2.1.7 Treatment of naturally occurring cyano-HABs**

### ***2.1.7.1 Treatment of *Merismopedia* sp. with metallic peroxide granules vs. liquid H<sub>2</sub>O<sub>2</sub>***

Experiments on the treatment of *Merismopedia* sp. bloom in St. George Lake were performed in 250-mL sterile borosilicate glass containers and the oxidants used for this purpose were liquid hydrogen peroxide and metallic peroxide granules. Hydrogen peroxide (30%) was purchased from Sigma-Aldrich and diluted to 1000 mg L<sup>-1</sup> for the stock solution. Calcium peroxide (CaO<sub>2</sub>) and magnesium peroxide (MgO<sub>2</sub>) granules were provided in the form of IXPEN<sup>®</sup> 70CG and IXPEN<sup>®</sup> Magnesium Peroxide Granules 30MG by Solvay Chimika S.A. (free samples).

H<sub>2</sub>O<sub>2</sub> stock solution was added into each flask containing raw sample from St. George Lake to achieve the following concentrations: 0 (control), 1, 2, 3, 5 mg L<sup>-1</sup>; and a quantity calcium and magnesium peroxide granules to achieve: 0 (control), 1, 2, 3 g L<sup>-1</sup>. All the experiments were conducted in a set temperature of 20 °C, and a continuous light of about 800 (± 200) Lux. Each treatment was performed in triplicates. The oxidant concentration was monitored by the colorimetric method introduced by Sellers et al.

(1980) [86]. In brief, 5 mL of sample was filtered through a PVDF syringe filter and immediately reacted with 0.5 mL of titanium oxalate ( $[C] = 50 \text{ g L}^{-1}$ ) and 0.5 mL sulfuric acid (1 + 17 v/v) (both reagents purchased from Sigma-Aldrich). Absorbance was then measured at 400 nm by the Spectroquant® Pharo 300 spectrophotometer in a quartz cuvette and the concentration of  $\text{H}_2\text{O}_2$  was quantified based on a calibration curve ranged between 0.5 and 20  $\text{mg L}^{-1}$  (Figure S 2, Appendix II).

For determining the efficiency of oxidants on mitigating the naturally occurred cyanobacterial bloom (*Merismopedia* sp.); photosynthetic changes associated with  $\text{H}_2\text{O}_2$  additions, including instantaneous fluorescence and PSII efficiency were monitored in both wavelengths ( $\lambda = 450, 620 \text{ nm}$ ) at 1, 2, 3, 4, 6, 24, 48 h following oxidant addition. Physicochemical characteristics such as pH, conductivity, total dissolved solids, and salinity were measured before and after treatment with the use of ExStick probe (EXTECH).

#### ***2.1.7.2 $\text{H}_2\text{O}_2$ release kinetics by $\text{CaO}_2$ and $\text{MgO}_2$ granules in filtered St. George Lake water***

On a separate set-up,  $\text{H}_2\text{O}_2$  release experiments were performed by adding calcium and magnesium peroxide granule in filtered samples of St. George Lake For the determination of granules' releasing capacity in surface water. The collected water was filtered through nylon membrane filter (0.45  $\mu\text{m}$ ) to remove cyanobacteria and other contaminants found from the water and each flask was filled with 250 mL of the filtered water.  $\text{CaO}_2$  and  $\text{MgO}_2$  granules were added into the flask to achieve the following concentrations: 0 (control), 1, 2, and 3  $\text{g L}^{-1}$ .  $\text{H}_2\text{O}_2$  concentration was monitored through the previously described colorimetric reaction, for every hour the first 6 h and then at  $t = 24$ , and 48 h after the addition of granules in the matrix.

#### ***2.1.7.3 Treatment of Athalassa lake surface water with liquid $\text{H}_2\text{O}_2$ and PMS***

##### **Fish-kill event**

Water collected right after the fish-kill event in September 2020 was utilized for treatment experiments with multiple doses of liquid hydrogen peroxide in order to investigate its efficiency when single high doses are replaced with lower repeated doses. A volume of 250 mL was poured into the 9 treatment flasks (3xcontrol, 3xT<sub>1</sub>, 3xT<sub>2</sub>). Stock solution of 1000  $\text{mg L}^{-1}$  of liquid  $\text{H}_2\text{O}_2$  was prepared and added into each flask to

achieve an initial added concentration of 0 (control), 3 and 3 mg L<sup>-1</sup> H<sub>2</sub>O<sub>2</sub>. Additional doses were added at t=24 h (second dose) and t= 48 h (third dose), to achieve total additions of 7 and 9 mg L<sup>-1</sup> of oxidants (Table 6). The treatment lasted for 72 hours (3 days), and samples were taken at t=0, 24, 48, and 72 h for residual oxidant quantification and photosynthetic parameters measurements. A COD analysis performed in raw and treated water at t=0 h and t=72 h, respectively.

**Table 6.** Repeated H<sub>2</sub>O<sub>2</sub> and PMS doses during a 72-h treatment in contaminated Athalassa's lake water.

Oxidant	Liquid H <sub>2</sub> O <sub>2</sub>			units	PMS			units
Flask	Control	A	B	mg L <sup>-1</sup>	Control	A	B	mg L <sup>-1</sup> equiv. of H <sub>2</sub> O <sub>2</sub>
1 <sup>st</sup> dose (t=0 h)	0	3	3		0	3	3	
2 <sup>nd</sup> dose (t=24 h)	0	2	3		0	2	3	
3 <sup>rd</sup> dose (t=48 h)	0	2	3		0	2	3	

### Blooming period

Experiments on the treatment of *Planktothrix* sp. bloom in Athalassa Lake were performed in 250-mL sterile borosilicate glass containers and the oxidants used for this purpose were liquid H<sub>2</sub>O<sub>2</sub> and PMS. Stock solutions of 1000 mg L<sup>-1</sup> of for each oxidant was prepared and added into the flask to achieve a final concentration of 0 (control), 1, 2, 3 mg L<sup>-1</sup> H<sub>2</sub>O<sub>2</sub> and 0 (control), 1, 2, 3 mg L<sup>-1</sup> (equiv. of H<sub>2</sub>O<sub>2</sub>) PMS. The doses added in each flask was repeated every 24 h up to 72 h when the last oxidant addition occurred (Table 7). The treatment lasted for 96 hours, and samples were taken throughout the treatment for oxidant quantification, Ft, QY and physicochemical water parameters. The residual oxidant concentrations were determined by the colorimetric method introduced by Sellers for H<sub>2</sub>O<sub>2</sub>, and with POXi™ spectrophotometric method for PMS at λ=400 and 405 nm, respectively.

**Table 7.** Repeated H<sub>2</sub>O<sub>2</sub> and PMS doses during a 96-h treatment to achieve total added concentrations of 0, 4, 8, and 12 mg L<sup>-1</sup> of each oxidant into Athalassa's lake water contaminated with *Planktothrix* sp.

Oxidant	Liquid H <sub>2</sub> O <sub>2</sub>				units	PMS				units
Flask	Control	A	B	C	mg L <sup>-1</sup>	Control	A	B	C	mg L <sup>-1</sup>
1 <sup>st</sup> dose (t=0 h)	0	1	2	3		0	1	2	3	

<b>2<sup>nd</sup> dose (t=24 h)</b>	0	1	2	3		0	1	2	3	equiv. of H <sub>2</sub> O <sub>2</sub>
<b>3<sup>rd</sup> dose (t=48 h)</b>	0	1	2	3		0	1	2	3	
<b>4<sup>th</sup> dose (t=72 h)</b>	0	1	2	3		0	1	2	3	
<b>Total addition</b>	0	4	8	12		0	4	8	12	

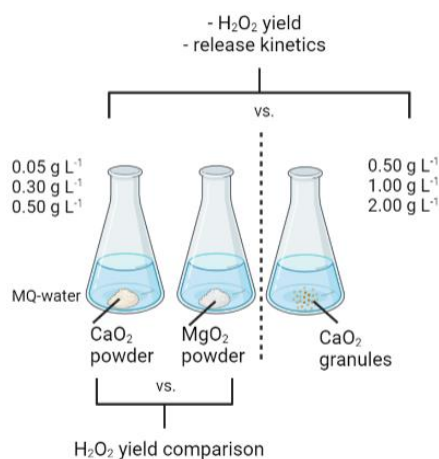
## 2.2 Cyano-HABs treatment with novel chemical oxidation processes

### 2.2.1 Metallic peroxide granules

#### 2.2.1.1 CaO<sub>2</sub> granules characterization

Calcium peroxide utilized in experiments were in the form of “IXPER<sup>®</sup> 70CG” granular compound and they were provided by Solvay Chimika S.A. free of charge. The given purity of the granules was 70 % w/w CaO<sub>2</sub>, which is equivalent to ~15.5 % available oxygen, and with particle size of 0.5 to 2 mm. Impurities reported by the manufacturer were: 10-19% Ca(OH)<sub>2</sub> and 5-19 % other inorganic calcium compounds. X-Ray Fluorescence (XRF) analysis was performed by a portable, handheld XRF analyzer (ProSpector 3, Elvatech) to determine the elemental composition of granules.

#### 2.2.1.2 Compound type (powder, granules) effect on H<sub>2</sub>O<sub>2</sub> release kinetics

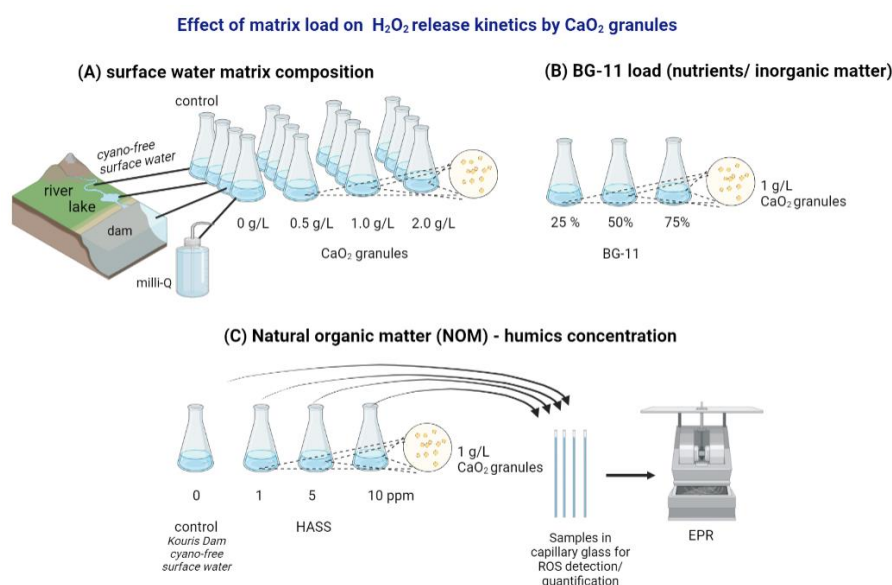


**Scheme 11.** Schematic illustration depicting the comparison experiments between powdered and granulated metallic peroxide granules (created with Biorender.com by E. Keliri<sup>©</sup>).

Two types of metallic peroxide compounds were tested for their H<sub>2</sub>O<sub>2</sub> releasing capacity in extra-pure water. Specifically, powdered form of CaO<sub>2</sub> and MgO<sub>2</sub>, purchased by Sigma-Aldrich (75%, particle size – 200 mesh), were applied in milli-Q water in

concentrations of: 0, 0.05, 0.3, and 0.5 g L<sup>-1</sup>. In a separate experiment, the H<sub>2</sub>O<sub>2</sub> release by 0.5, 1.0, and 2.0 g L<sup>-1</sup> CaO<sub>2</sub> granules was investigated, and release curves were fitted on a one-phase association kinetics model to examine the reaction kinetics. Samples were taken at t=0 ,5 ,10 ,15 ,20 ,30 ,40 ,50 ,60 ,120, and 240 minutes after oxidant addition to capture the instantaneous released concentrations of H<sub>2</sub>O<sub>2</sub>.

### 2.2.1.3 Matrix effect on H<sub>2</sub>O<sub>2</sub> release kinetics



**Scheme 12.** Graphical Abstract depicting the experiments conducted for the effect of matrix load on the H<sub>2</sub>O<sub>2</sub> release kinetics by granules (created with Biorender.com by E. Keliri ©).

#### (A) Surface water matrix composition

Experiments on the kinetics of H<sub>2</sub>O<sub>2</sub> release by CaO<sub>2</sub> granules were performed in 250 mL borosilicate glass containers filled with 200 mL of extra pure (Milli-Q) water, river water, lake water, and dam water. Extra-pure water utilized in the experiment was extracted from Milli-Q Synergy® UV remote water purification system. Surface water samples were collected from Polis Chrysochou River, St. George Lake, and Kouris Dam, with the use of bucket from a central point of each waterbody. Each water matrix was transported to the laboratory under dark and cool conditions. A volume of 200 mL was poured into 250-mL flasks and CaO<sub>2</sub> granules were added to achieve the following concentrations: 0 (control), 0.5, 1.0, 2.0, and 3.0 g L<sup>-1</sup>.

#### (B) Nutrient and inorganic matter load in BG-11

Another experiment to examine the matrix load effect on the accumulative release of H<sub>2</sub>O<sub>2</sub> by 1 g L<sup>-1</sup> CaO<sub>2</sub> granules was performed in BG-11 medium (in dilutions of 25%,

50%, and 75%). Initial TN and TP concentrations of the matrixes were determined with the use of Spectroquant® cell test kits (Merck Millipore). BG-11 medium was prepared based on the cultivation method introduced by Ruppka et. al (1979) [87], with the following composition: 10 mL Macromix, 1 mL Na<sub>2</sub>CO<sub>3</sub> (20 g L<sup>-1</sup>), 1 mL Spore solution, 1 mL K<sub>2</sub>HPO<sub>4</sub> (30.5 g L<sup>-1</sup>), and 1 mL ferric ammonium citrate (6 g L<sup>-1</sup>) in 1 L of Milli-Q water. The chemical composition of Macromix and Spore Solution is accessible in Annex II (Table S4).

### **(C) Natural Organic Matter (NOM) concentration**

Humics effect on the release kinetics were also examined by adding humic acid sodium salt (HASS) in Kouris surface water. Sampled water was poured into flasks and spiked with HASS purchased by HiMedia Laboratories to achieve 0, 1, 5, and 10 ppm. In each flask 1 g L<sup>-1</sup> CaO<sub>2</sub> granules were added. HASS stock solution was prepared 24 hours before experiment by adding 0.2 g HASS in 1 L of MQ water and placed on a stirring plate overnight to dissolve.

### **Electron Paramagnetic Resonance (EPR) Spectroscopy**

During the H<sub>2</sub>O<sub>2</sub> release experiment by 1 g L<sup>-1</sup> CaO<sub>2</sub> granules in Kouris water spiked with HASS (0, 1, 5, and 10 ppm), the EPR spectroscopy technique was employed to determine the formed Reactive Oxygen Species (ROS). A Bruker ER200D spectrometer equipped with an Agilent 5310A frequency counter was used, operating at X-band (~9.6GHz) with a modulation amplitude of 4G peak to peak. On average 20 scans of each spectrum were obtained to get an adequate signal-to-noise ratio. EPR spectra were recorded at t= 0, 2, 4, 24 and 48 h by sampling 450 µL and filtering through a PVDF of 0.45 µm. Then, a spin trap 2mM DMPO (5,5-Dimethyl-1-pyrroline-N-oxide, Aldrich) solution was mixed with the filtered sample and a suspension of 20 µL was sampled followed by its addition in glass capillaries to monitor the generation of radicals. Spin quantitation was done using DPPH (2,2-Diphenyl-1-picrylhydrazyl) as spin standard and the double integral of the EPR signals. To identify and separate the generated DMPO adducts the experimental EPR spectra were simulated using the EasySpin MATLAB add-on [88]. The typical 1:2:2:1 quartet-pattern EPR signal is attributed to DMPO/•OH [89] spin-adduct with a splitting of  $\alpha_{N=a}H \approx 15G$ , whilst the second signal is attributed to DMPO hydroxyalkyl radicals spin adduct. Nitrogen hyperfine coupling constants are approximately 16G and

proton hyperfine coupling constants are ~23G with g values around 2.00537-2.00539 [90].

Samples for determining the instant concentration of H<sub>2</sub>O<sub>2</sub> released by granules in all the above experiments, were taken every hour for up to 6 hours, and in 24, and 48 hours after the granules' addition. H<sub>2</sub>O<sub>2</sub> concentration was monitored through the colorimetric reaction introduced by Sellers et al. (1980). Experiments were performed in triplicates.

#### ***2.2.1.4 Treatment of *Microcystis* sp. and *Aphanizomenon* sp. spiked in surface water with CaO<sub>2</sub> granules and liquid H<sub>2</sub>O<sub>2</sub>***

##### **Surface water sampling**

Surface water was collected from Kouris Dam located in Limassol, Cyprus. Kouris Dam is one of the largest reservoirs in Cyprus that provide water for irrigation, enrichment, and potable purposes. Its overall catchment area is 300 kilometers with a length of approximately 550 meters which allows a capacity of 115 million cubic meters.

Water was collected from a depth of 0.3–0.5 m below the surface with the use of a bucket and a rope. Water was transferred through funnel with filter net to remove large particles, in PE bottles, and was stored under cool and dark conditions, and brought to the laboratory, for analysis and utilization in treatment experiments. The main physicochemical parameters (pH, conductivity, salinity, total dissolved solids), nutrients analysis (total and dissolved nutrients), and the presence of cyanobacteria and green algae in terms of fluorescence signal (Ft), and maximum quantum yield of the PSII (Fv/Fm), were determined within 3 hours after sampling.

##### **Cultivation of *Microcystis* sp. and *Aphanizomenon* sp.**

Pure culture of *Microcystis* sp. and *Aphanizomenon* sp., provided by the Yigal Alon Kinneret Limnological Laboratory (prof. Assaf Sukenik), were cultivated in BG-11 medium at the Water Treatment Laboratory AQUA. The growth cycle of cultures was 3-4 weeks; thus, the extraction of culture mass for experimental purposes was performed at the peak of their growth curve. Cultures were cultivated in Falcon<sup>®</sup> 75cm<sup>2</sup> rectangular canted neck cell culture flasks with vented caps containing fresh BG-11 medium and placed on an orbital shaker set at 80 RPM (Scheme 13). Cultivated culture at a mature state was spiked into surface water sampled for bench-scale treatment experiments. The

cultivated cultures were filtered through cellulose nitrate membrane filter (0.45  $\mu\text{m}$ ) and transferred into a petri dish with the use of a sterile plastic scrubber. The collected mass was then added into the Kouris surface water (free from cyanobacteria) and homogenized to achieve an initial phycocyanin variable fluorescence  $\sim 8000$  ( $\pm 200$ ) RFU, which simulates a moderate, still dense, cyano-blooming event.



**Scheme 13.** Cultivation flasks of (A) *Microcystis* sp., (B) *Aphanizomenon* sp., and (C) *Microcystis* sp. cells collected on membrane filter during filtration of the culture medium process.

#### **Intracellular cyanotoxin analysis**

To examine the toxicity of the cultivated cultures, 5 mL (x3) of *Microcystis* sp. and *Aphanizomenon* sp. passed through a GF/C filter (0.45  $\mu\text{m}$ ) and samples were extracted in 2 mL of 75:25 methanol: H<sub>2</sub>O extraction solvent, by homogenizing the filter containing cyanobacteria cells with a glass rod. Then, samples were sonicated for 10 min, vortexed for 5 min and centrifuged at 14,000 rpm for 10 min. The supernatant was transferred to a chromatographic vial and analyzed with LC-MS/MS system. Chromatographic separation of sample components was performed on Zorbax Eclipse XDB-C18 column (4.6 mm ID (inner diameter)  $\times$  150 mm, 5  $\mu\text{m}$ ; Agilent Technologies, Santa Clara, CA, USA) by gradient elution with a mixture of 5% acetonitrile in Milli-Q water and acetonitrile, both containing 0.1% formic acid. The system was composed of an Agilent 1200 (Agilent Technologies, Waldboronn, Germany) chromatograph coupled online to a hybrid triple quadrupole/linear ion trap mass spectrometer (QTRAP5500, Applied Biosystems, Sciex, Concord, ON, Canada). Mass spectrometer with a turbo ion source (550  $^{\circ}\text{C}$ , 5.5 kV) operated in positive mode [91]. Standards of microcystins used in the analysis were from Alexis Biochemicals and the detection limit for used standards was 0.1 ng mL<sup>-1</sup>. For data acquisition and processing Analyst<sup>®</sup> Software (version 1.5.1, Applied Biosystems, Concord, ON, Canada) was used.

#### **Treatment of *Microcystis* sp. with CaO<sub>2</sub> granules and liquid H<sub>2</sub>O<sub>2</sub>**

Experiments on the treatment of *Microcystis* sp. in Kouris surface water matrix were performed in 250-mL sterile borosilicate glass containers with the use of CaO<sub>2</sub> granules and liquid H<sub>2</sub>O<sub>2</sub>. Calcium peroxide (CaO<sub>2</sub>) granules were ordered by Solvay Chimika S.A. as IXPEN® 70CG (free samples). Hydrogen peroxide (30%) was purchased from Sigma-Aldrich and diluted to 1000 mg L<sup>-1</sup> for the stock solution. In each flask, stock concentration of H<sub>2</sub>O<sub>2</sub> was added to achieve: 0 (control), 3, 6, and 12 mg L<sup>-1</sup> H<sub>2</sub>O<sub>2</sub>; and a portion of granules to achieve: 0 (control), 0.5, 1, and 2 g L<sup>-1</sup> of CaO<sub>2</sub> granules.

H<sub>2</sub>O<sub>2</sub> residual concentration was monitored by the colorimetric reaction explained in above sections. For determining the efficiency of oxidants on mitigating *Microcystis* sp. in Kouris surface water, photosynthetic changes associated with H<sub>2</sub>O<sub>2</sub> and CaO<sub>2</sub> granules additions, including instantaneous fluorescence and PSII quantum efficiency were monitored with AQUAPEN instrument at  $\lambda_{\text{ex}} = 620$  nm at t = 1, 2, 3, 4, 6, 24, 48, and 120 h following oxidant addition. Physicochemical characteristics such as pH, conductivity, total dissolved solids, and salinity were measured before and after treatment with the use of ExStick probe (EXTECH).

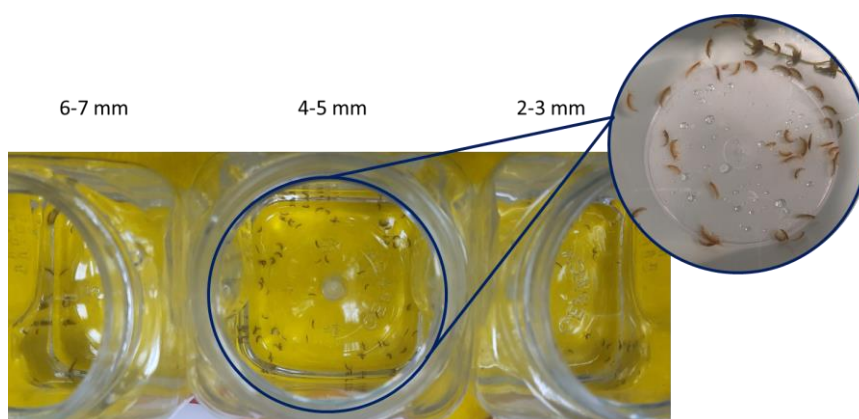
#### **Treatment of *Aphanizomenon* sp. with CaO<sub>2</sub> granules and liquid H<sub>2</sub>O<sub>2</sub>**

Experiments on the treatment of *Aphanizomenon* sp. in Kouris surface water matrix were performed in 250-mL sterile borosilicate glass containers with the use of CaO<sub>2</sub> granules and liquid H<sub>2</sub>O<sub>2</sub>. In each flask, stock concentration of H<sub>2</sub>O<sub>2</sub> was added to achieve: 0 (control), 3, 6, and 7 mg L<sup>-1</sup> H<sub>2</sub>O<sub>2</sub>; and a portion of granules to achieve: 0 (control), 0.5, 1, and 1.25 g L<sup>-1</sup> of CaO<sub>2</sub> granules. The treatment duration was 120 hours and the experimental procedure followed was the same with the one for *Microcystis* sp. treatment in Kouris water.

##### **2.2.1.1 Toxicity study on *Echinogammarus veneris* sp.**

*Echinogammarus veneris* (Gammaridae family) species were collected with the kick-sampling technique from the stream bottom of a river located in Paphos, Cyprus. Species were collected with the use of a net and transferred in a clear plastic tank with a lid along with 10 L of river water and some macrophytes to maintain their environment conditions during transportation. Samples transported to the laboratory under dark and cool conditions. The species left in the laboratory overnight to acclimatize in the conditions (T=20°C, 800 Lux) with the lid opened. Specimens were separated in different containers

based on their sizes: small (2-3 mm), medium (4-5 mm), and large (6-7 mm), as shown in Scheme 14. In each experimental bowl which contained 200 mL of river water, 10 invertebrates (3 small, 5 medium and 2 big) were added; followed by oxidant addition.



**Scheme 14.** *Echinogammarus veneris* sp. collected from Polis Chrysochou River, and separated into various sizes, with a close-up capture for the medium sized specimens.

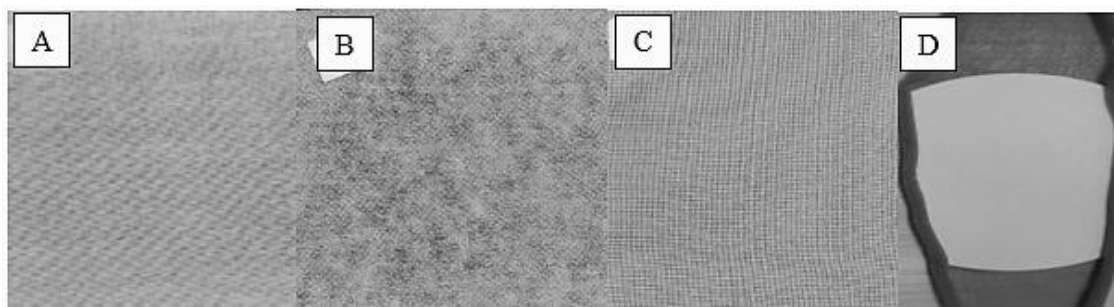
For the toxicity study of oxidants on invertebrate species, in each flask contained water matrix and *Echinogammarus veneris* sp., a portion of  $\text{CaO}_2$  granules were added to achieve: 0 (control), 0.50, 0.75, 1.00, 1.25, and 2.00  $\text{g L}^{-1}$   $\text{CaO}_2$  granules, equivalent to accumulative released concentrations of 1 – 12  $\text{mg L}^{-1}\text{H}_2\text{O}_2$ . The  $\text{H}_2\text{O}_2$  residual concentration was monitored by the colorimetric method as mentioned in previous sections. Mortality of *Echinogammarus veneris* was recorder every hour for the first 6 hours and then on 24 and 48 hours, where death was defined as the total lack of their movement. Samples were also collected for initial and residual oxidant concentrations at 0, 2, 24 and 48 hours after oxidant addition. Survival rate (%) was calculated utilizing Equation. 6.

$$SR(\%) = 100 - \left( \frac{\text{gammarus (control)} - \text{gammarus (t)}}{\text{gammarus (control)}} * 100 \right) \quad (\text{Eq. 6})$$

## 2.2.2 Calcium peroxide granules enclosed in fabrics (GEF)

### 2.2.2.1 Fabrics characterization

CaO<sub>2</sub> granules enclosed in fabrics (GEF) systems were utilized to determine their H<sub>2</sub>O<sub>2</sub> release properties in surface water matrix. The use of four types of fabrics were investigated as delivery systems for granules: Fabric “type A” = natural twill fabric for pocket lining, “type B” = non-woven interlining fabric (fusing paper), “type C” = polyester mosquito netting fabric”, and “type D” = paper filter wrapped in 20 DEN tights”, as shown in Scheme 15.



**Scheme 15.** Four different types of fabrics tested as potential delivery systems for CaO<sub>2</sub> granules: (A) pocket lining fabric, (B) non-woven interlining fabric, (C) polyester mosquito netting fabric, and (D) paper filter wrapped in 20 DEN tights.

For the characterization of woven and non-woven surfaces QUANTA 400F Field Emission high-resolution scanning electron microscope (SEM) was employed at an acceleration voltage of 10 kV. Samples were coated with 10 nm Au/Pd prior to SEM observation. Specifically, SEM - FEI Quanta 200 (Oregon, USA) scanning electron microscope with a Secondary Electrons Detector was used to evaluate the properties of the fabrics (pore area, and size). Prior to observation fabrics were deposited onto carbon tapes mounted on aluminum stubs. For determining the thickness of each textile, a cross-sectional multipurpose specimen holder was used. Obtained SEM images were processed and analyzed with the use of “ImageJ” public domain software to determine the porous area of each material [92]. The pore area was measured by determining the average surface area of 60 pores (20 pores in each image x 3).

### **2.2.2.2 *H<sub>2</sub>O<sub>2</sub> release kinetics by GEF***

Experiments on the H<sub>2</sub>O<sub>2</sub> release properties of CaO<sub>2</sub> granules were performed in 250 mL glass containers. CaO<sub>2</sub> granules were folded in fabric materials of types A – D and nylon cables were added to seal the two ends (Scheme S 3). Each fabric was cut into pieces of 5 x 5, 6 x 6, and 7 x 7 inches, which enclosed 0.5, 1.0, and 2.0 g L<sup>-1</sup> of CaO<sub>2</sub> granules, respectively. For control, a medium size fabric was folded without the addition of granules. Each fabric encapsulating the CaO<sub>2</sub> granules dose was added into a glass container with 200 mL of surface water from Kouris dam.

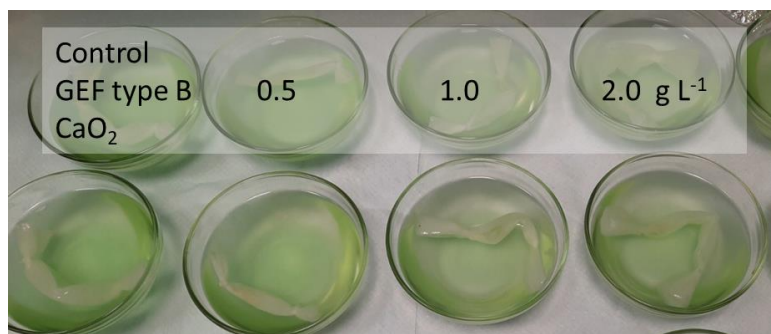
To monitor the instantaneous concentration of H<sub>2</sub>O<sub>2</sub>, 2 mL of sample was collected from each flask at t= 0, 1, 2, 4, 6, and 24 h after GEF addition. Samples were analyzed with the colorimetric method introduced by Sellers et. al (1980). The absorbance at  $\lambda=400$  nm was measured by the TECAN Infinite 200 spectrophotometer in a 96-well plate. The concentration of H<sub>2</sub>O<sub>2</sub> was quantified based on a calibration curve that ranged between 0.5 and 20 mg L<sup>-1</sup> H<sub>2</sub>O<sub>2</sub> (Appendix II, Figure S2). In addition, the physicochemical characteristics were recorded at t= 0, and 24, and 48 h including pH, conductivity, TDS, and salinity. All the experiments were performed in triplicates and conducted under the same laboratory conditions, in a set temperature of 20 °C, and a continuous light of 800 ( $\pm$  200) Lux.

### **2.2.2.3 *Treatment of Microcystis sp. spiked in surface water with GEF systems***

To examine the feasibility of applying GEF systems for the mitigation of *Microcystis* sp. in surface waters, fabric delivery systems of types A to C were utilized to encapsulate the granules, as described previously. For the matrix preparation, the collected *Microcystis* sp. mass was spiked into Kouris Dam water, slightly enriched with BG-11 medium (1% v/v), to achieve an initial Ft value ~8000 RFU. The prepared medium was stored in a PE bottle with an open lid for 12-18 hours to acclimatize, at T= 20 °C, and a continuous light source of 800 ( $\pm$  200) Lux.

Quantities of 0.0, 0.5, 1.0, and 2.0 g/L CaO<sub>2</sub> granules were enclosed in fabrics type A, B and C, and added in 200 mL of the *Microcystis* sp. medium (Scheme 16). Ft and QY values at  $\lambda= 620$  nm were recorded at t= 0, 6, 24, 48 h utilizing AquaPen AP 110/C to monitor the destruction of cyanobacterial cells and photosystem II (PSII) inactivation, thus evaluating the efficiency of the enclosed granular oxidant on mitigating *Microcystis*

sp. Physicochemical characteristics such as pH, conductivity, TDS, and salinity were measured at  $t=0$ , 24, and 48 h, with the use of ExStick probe (EXTECH). Instant  $\text{H}_2\text{O}_2$  concentrations during treatment were monitored by the colorimetric method mentioned before.



**Scheme 16.** Addition of GEF system type B enclosing 0 (control), 0.5, 1.0, and 2.0  $\text{g L}^{-1}$   $\text{CaO}_2$ .

#### **2.2.2.1 Toxicity study on *Echinogammarus veneris* sp.**

*Echinogammarus veneris* species were collected from Polis River located in Paphos (Cyprus) with the kick-sampling technique (see 2.2.1.1). For the toxicity study of GEF systems, in each bowl contained 200 mL of river water and ten *Echinogammarus veneris* sp., stock solution of liquid  $\text{H}_2\text{O}_2$  was added to achieve 0 (control), 3, 6, and 12  $\text{mg L}^{-1}$   $\text{H}_2\text{O}_2$ ; GEF enclosing 0 (control), 0.5, 1, and 2  $\text{g L}^{-1}$   $\text{CaO}_2$  granules, and directly applied 0 (control), 0.5, 1, and 2  $\text{g L}^{-1}$   $\text{CaO}_2$  granules.

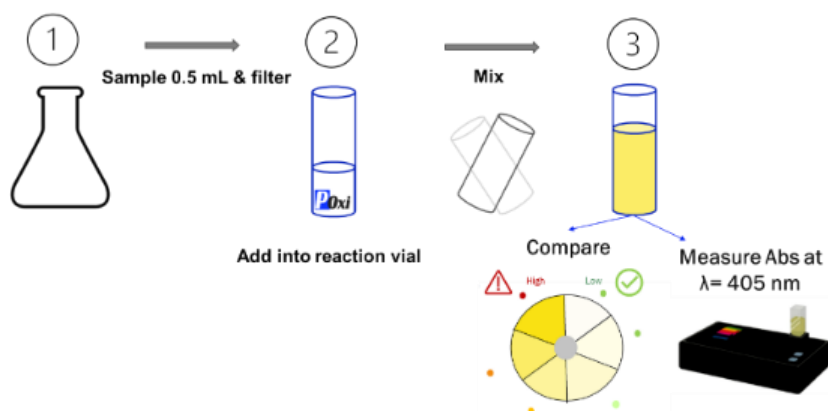
Mortality of zooplankton species was recorder every hour for the first 6 hours and then at  $t=24$  and 48 h, where death was defined as the total lack of their movement. Samples during experiments were collected for the determination of initial and residual  $\text{H}_2\text{O}_2$  concentrations at  $t=0$ , 2, 24 and 48 hours after oxidant addition. Survival rate (%) was calculated using equation 6.

## 2.2.3 Peroxymonosulfate (PMS) – OXONE®

### 2.2.3.1 Development of quantification kit – POXi kit

Peroxymonosulfate was purchased in the form of OXONE® by Sigma-Aldrich, and a stock solution (1000 mg L<sup>-1</sup> equiv. to H<sub>2</sub>O<sub>2</sub>) was prepared by adding 0.9 g OXONE® in 100 mL MQ-water right before its use. Para-nitrophenyl boronic acid (Sigma-Aldrich, Germany) was used to prepare 2 mM p-NPBA in a buffer solution (pH=9.0). The reaction solution for the quantification of PMS was prepared by mixing equal volumes of sample and p-NPBA 2mM (1:1 v/v). Spectra scan in wavelengths between 300 and 500 nm were obtained to determine the maximum absorbance wavelength of the reaction's product. Once the wavelength corresponding to its maximum absorbance was determined, stability test of the produced product was performed by allowing the reaction mixture to stand in the cuvette inside of the Spectrophotometer for 28 hours and measuring its absorbance. Photosensitivity test was also performed by measuring the absorbance of the reactions executed in direct sunlight, and in dark conditions.

The above developed and optimized quantification method for PMS (HSO<sub>5</sub><sup>-</sup>) led to the development of POXi kit™<sup>1</sup> (Scheme 17), which is a kit developed by our research group, for easy, rapid, and accurate quantification of PMS in aqueous matrixes. In general, a volume of 1 mL of sample filtered through PVDF 0.22 μm, is added in 1 mL of POXi reagent mixture in a buffer solution and the absorbance of the sample is measured under dark conditions, to determine the instant concentration of PMS.



**Scheme 17.** POXi™ kit; PMS quantification process.

<sup>1</sup> POXi kit & POXi reagent mixture are applied for US Provisional Patent (USPO, 2020) and national CY patent (CY202000002; 2020), co-PI.

### 2.2.3.2 Toxicity study on *Echinogammarus veneris* sp.

*Echinogammarus veneris* sp. were again collected with the kick sampling technique from the stream bottom of a river in Cyprus (see Section 2.2.1.1). In each experimental bowl contained 200 mL of river water, 10 invertebrates of various sizes were added. Concentrations of 1, 2, 3, 4, 5 mg L<sup>-1</sup> of H<sub>2</sub>O<sub>2</sub> and PMS (in equal molarities) were added. Multiple dosing system was also examined by adding repeated doses of: (a) 1+1+1+1+1, (b) 2+1+1+1, and (c) 3+1+1 to achieve total added concentration of 5 mg L<sup>-1</sup> H<sub>2</sub>O<sub>2</sub> and PMS.

Mortality of specimens was recorder every hour for the first 6 hours and then on 24 and 48 hours, where death was defined as the total lack of their movement. Samples were collected for initial and residual oxidant concentrations at 0, 2, 24 and 48 hours. The H<sub>2</sub>O<sub>2</sub> concentration was monitored by the colorimetric method mentioned earlier, and PMS with the aid of POXi kit, as explained in a previous section. Samples at each time point were collected, filtered, and reacted immediately in the reagent vial for measuring the solutions absorbance at  $\lambda=400$  nm and  $\lambda= 405$  nm, respectively.

### 2.2.3.3 Combined cyano-HABs treatment and toxicity study on *Echinogammarus veneris* sp.

Experiments on the treatment of *Microcystis* sp., and *Aphanizomenon* sp., in surface water matrix were performed in 250-mL sterile borosilicate glass containers with the use of liquid hydrogen peroxide and PMS stock solution in equal peroxide concentrations. Water matrixes used in this study were: (a) filtered river water, (b) Polemidia Dam, and (c) Kouris Dam waters. Cyanobacterial water matrix was prepared by spiking surface water (free from cyanobacteria) with pure cultivated cultures of *Microcystis* sp., and *Aphanizomenon* sp. Cultures were added into the water to achieve similar initial phycocyanin variable fluorescence in each treatment flask (~ 8000 RFU). In each bowl, 10 specimens of *Echinogammarus veneris* sp. were added to perform toxicological assessment of PMS on zooplankton during treatment. Photosynthetic changes associated with H<sub>2</sub>O<sub>2</sub> and PMS additions, including instantaneous fluorescence and PSII quantum efficiency, were monitored with AQUAPEN instrument in  $\lambda = 620$  nm.

For treating *Microcystis* in river water, single doses of 0 (control), 1, 2, 3, 4, and 5 mg L<sup>-1</sup> of H<sub>2</sub>O<sub>2</sub> and PMS added into the treatment bowls. Multiple dosing experiments were

conducted under the same experimental conditions, but the first dose of each oxidant applied was 1, 2 and 3 mg L<sup>-1</sup> followed by the second dose of 1 mg L<sup>-1</sup> at t=24 hours. With multiple doses, total additions of 2, 3, and 4 mg L<sup>-1</sup> H<sub>2</sub>O<sub>2</sub> and PMS were achieved. The oxidants efficiency towards *Microcystis* sp. treatment was recorded for 48 hours after the first dose of oxidant.

Treatment of *Aphanizomenon* sp. in river water was performed by applying doses of 1, 2, and 3 mg L<sup>-1</sup> of H<sub>2</sub>O<sub>2</sub> and PMS, in each to treatment bowl. Mortality and treatment efficiency were recorded for up to 48 hours. Multiple dosing experiments were conducted under the same experimental conditions. Doses of 1, 2 and 3 mg L<sup>-1</sup> were initially applied, followed by a second dose of 1 mg L<sup>-1</sup> H<sub>2</sub>O<sub>2</sub> and PMS at t=24 h. Mortality of specimens and *Aphanizomenon* sp. treatment efficiency recorded for 72 hours after the first dose of oxidant.

### **2.3 Scale-up treatment**

Experiments on the treatment of a naturally occurred *Planktothrix* bloom in Athalassa Lake (2020) were performed in 10 L plastic containers and the oxidants used for this purpose were liquid H<sub>2</sub>O<sub>2</sub>, peroxymonosulfate, and CaO<sub>2</sub> granules in concentrations 7 mg L<sup>-1</sup>, 7 mg L<sup>-1</sup> eq. to H<sub>2</sub>O<sub>2</sub>, and 1 g L<sup>-1</sup>, respectively. A second dose of each oxidant was added on day 5. Stock solutions of 1000 mg L<sup>-1</sup> H<sub>2</sub>O<sub>2</sub> and KHSO<sub>5</sub> (OXONE<sup>®</sup>) were prepared and added into surface water collected for the treatment of cyano-cells. The experiment was performed outdoors under mild environmental conditions (T=15-25 °C), with a continuous natural light exposure. (~12 h in day light: 4000 ± 1000, ~12 h in darkness: 40± 50 Lux) and the treatments were monitored for 10 days (t=240 h).

The residual oxidants were monitored with the methods mentioned before, while for the determination of each oxidant efficiency on mitigating the bloom photosynthetic changes, including instantaneous fluorescence and quantum yield of PSII, were recorded in both wavelengths ( $\lambda = 450, 620$  nm) at t= 0, 24, 48, 72, 120, 168, and 240 h following oxidant addition. Physicochemical characteristics such as pH, conductivity, total dissolved solids, and salinity were measured before and after treatment with the use of ExStick probe (EXTECH).

## **2.4 Statistical analyses**

Data processing and statistical analysis was performed with the use of PRISM®-GraphPad software. For each measurement, mean and standard deviation of the triplicates were calculated and presented on the graphs as mean with error bar and/or tables as mean  $\pm$  SD. Differences of Ft, and Fv/Fm between the comparable treatment experiments were compared using one-way ANOVA followed by a Turkey's test. All treatments and measurements were conducted in triplicates for increased reproducibility and accuracy on the outcomes.

### 3 Results & Discussion

#### 3.1 Monitoring and treatment of naturally occurring blooms

##### 3.1.1 St. George Lake<sup>2</sup>

###### 3.1.1.1 Monitoring

Lake monitoring showed that pH, salinity, total dissolved solids, and conductivity varied throughout the year, and nutrients concentration was high, which indicated a eutrophic lake. Blooming in St. George Lake was recorded from June to September with a peak cyanobacteria presence in August 2019.

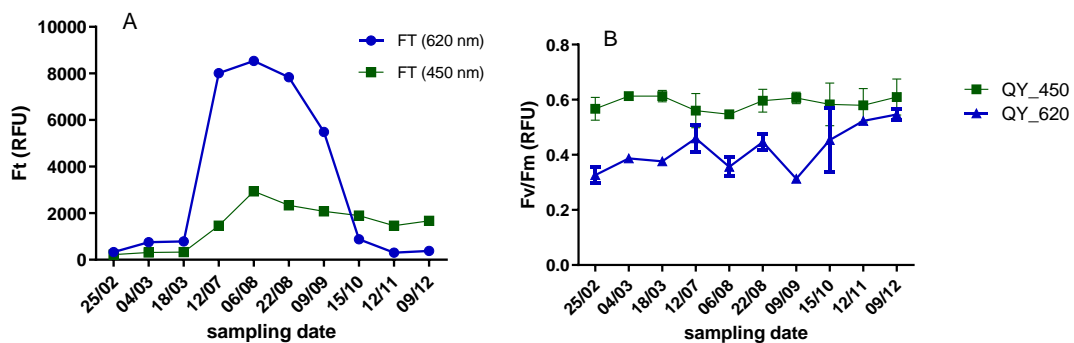


**Figure 1.** (A) Instantaneous fluorescence (Ft) in raw fluorescence units and (B) quantum yield measurements for phycocyanin (620 nm excitation) and chlorophyll-a (450 nm excitation) in St. George Lake samples during monitoring period.

Blooming was found to be a seasonal phenomenon with a maximum fluorescence recorded at  $\lambda=620$  nm at 8000-9000 RFU, indicating high phycocyanin concentration, thus increased cyanobacterial activity. After a light rainfall at the beginning of September it began dropping. Instantaneous fluorescence at  $\lambda = 450$  nm corresponding to the chl-a presence in the samples was minimal in the first 3 sampling events, but rapidly increased during blooming and maintained quite high ( $> 1000$  RFU) even after blooming period (Figure 1a). The quantum yield (Fv/Fm) of the PSII for both wavelengths ( $\lambda = 620, 450$

<sup>2</sup> The findings of this study were published in the *Journal of Environmental Sciences Europe*:

Keliri, E., et al. Occurrence of a single-species cyanobacterial bloom in a lake in Cyprus: monitoring and treatment with hydrogen peroxide-releasing granules. *Environ Sci Eur.* 33, 31 (2021).

<https://doi.org/10.1186/s12302-021-00471-5>

nm) remained high throughout the year, showing that cyanobacterial mass had a good photosynthetic activity, even before or after blooming (Figure 1b).

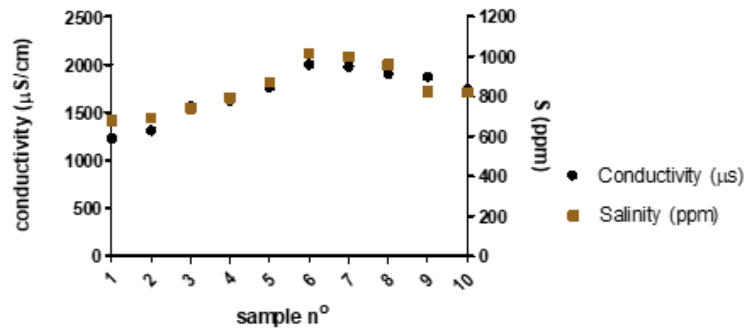


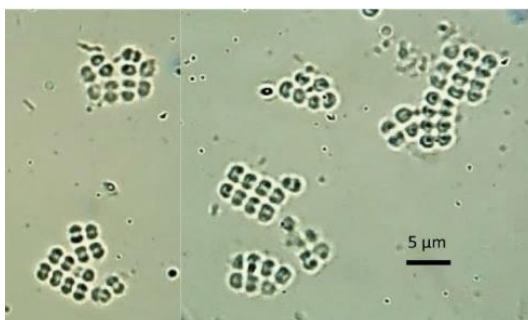
**Figure 2.** Measurements of conductivity ( $\mu\text{S cm}^{-1}$ ) and salinity (ppm) throughout the monitoring period in St. George Lake.

Physicochemical water characteristics were also monitored. Beginning with air temperature, during the summer months was as high as  $34\text{ }^{\circ}\text{C}$  while during Spring, Fall and Winter the temperature ranged between  $15 - 25\text{ }^{\circ}\text{C}$ . The pH in St. George Lake was quite stable with small variations between  $8.3 - 8.9$  during the year, and the highest pH values were recorded during and after blooming. Conductivity recorded between  $1200$  and  $2000\text{ }\mu\text{S cm}^{-1}$  and salinity between  $700$  and  $1000$  ppm (Figure 2). Conductivity and salinity followed the same trend showing a noticeable increase during the summer period; both having their peak in August and retained high even after the bloom decline.

The measured nutrient concentration as well as the calculated dissolved inorganic nitrogen and the best fitting ratios for nutrient limitation are summarized in Table S 3. In most samples phosphorus was higher than  $0.2\text{ mg L}^{-1}$  indicating St. George as a eutrophic lake. High nitrogen concentrations were detected in the early months of the year when the status of the lake was oligotrophic with low cyanobacterial content, while high phosphorus concentration was recorded during the summer period, following by its decline. Soluble reactive phosphorus (SRP) was below the MDL before summer, stable during in summer ( $0.03\text{ mg L}^{-1}$ ) and increased during the winter months ( $0.05\text{ mg L}^{-1}$ ). This may be due to heavy rainfalls that caused high nutrient run-offs to enter the lake. Dissolved inorganic nitrogen (DIN) remained high at the beginning of the year, radically decreased during summer, and increased again in winter. The concentration of phosphorus during the bloom was higher than  $0.2\text{ mg L}^{-1}$  which means that in such a eutrophic lake ( $\text{TP} > 0.2\text{ mg L}^{-1}$ ) most probably nitrogen became the limiting element.

To support these findings, different approaches on estimating nutrient limitation through nutrient ratios (DIN:TP, NO<sub>3</sub><sup>-</sup>:TP) were tested to investigate which one fits better to the studied environment (Table S 4). The ratios and thresholds used in the present study for evaluating the trophic status of the lake based on the limiting elements during the monitoring period are presented in Appendix I, Table S1.

Due to increased cyanobacterial activity in summer months, and a visible ongoing bloom in St. George Lake from July, samples were preserved for microscopic observation and species characterization. Microscopic observation showed that 99% of the phytoplankton biovolume (1 million cells mL<sup>-1</sup> ± 20%) was attributed to a single picocyanobacterial species, called *Merismopedia* sp. (Scheme 18). Cell division of *Merismopedia* always occurs along two axes, which makes groups of 4 cells within the colony.



**Scheme 18.** *Merismopedia* sp. captured under ECLIPSE Ci-L microscope equipped with OPTIKAM Wi-Fi camera with magnification 100x, Eleni C. Keliri<sup>©</sup>.

These species are reported in the literature as microcystin and nodularin producers [93, 94], which are both among the most hazardous groups of cyanotoxins detected in surface waters. Therefore, cyanotoxin genes analyses and cyanotoxin concentrations analysis were performed to examine the toxicity of this bloom. The presence of *cyrB* and *cyrJ* was recorded only in sample 1. The presence of MC genes was recorded in samples 1 (*mcyB*) and 1, 4-8 (*mcyE*). Neither *anaC* nor *sxtA* were found in analyzed samples (Scheme S 1). Analysis of samples for microcystins (MCs) occurred to identify *Merismopedia* potency to release toxins during their blooming in St. George Lake. Microcystins were not detected above the MDL, but several matrix compounds with *m/z* almost identical (2-4 ppm) to the one of microcystins were detected. However, their detection was in a very low concentration and the fragmentation patterns of their parent ions differ from ones of microcystins (Figure S 1). Lack of characteristics fragments for MCs as the *m/z* 375.27 [C<sub>11</sub>H<sub>15</sub>O – Glu – Mdha]<sup>+</sup>, *m/z* 553.36 [Mdha – Ala – Leu –

MeAsp – Arg + H]<sup>+</sup>,  $m/z$  599.42 [Arg – Adda – Glu]<sup>+</sup> confirmed the absence of microcystins in the *Merismopedia* sp. bloom.

Even though the presence of microcystin synthase encoding gene (*mcyB*, *mcyE*) was documented, microcystins were not detected by tandem mass spectroscopy. It is safe to say that most probably the gene expression was weak resulted in toxin levels below the MDL. Gene expression can be affected and regulated by an array of biotic and abiotic factors [95]. A recent study showed that iron limitation could cause the downregulation of MC synthesis [96], that is caused by lower photosynthetic activity due to lack iron. Another factor examined in the literature that is known for its effect on *mcy* expression and MC production is the light intensity [97]. Even the presence of different cultures in a medium (e.g., *M. aeruginosa* with *P. agardhii*) can regulate the expression of *mcyE* as competitive mechanism between the two. In a study, *M. aeruginosa* with *P. agardhii* suppressed growth and downregulation of *mcyE* expression [98] which suggested that the competition between two toxic strains may results in a lower MC production.

In the present study a mono-domination of one species occurred which results in the hypothesis that because of the absence of antagonists, the mono-domination excluded a strong competition with other species and therefore MC production was also inhibited. Alternatively, the presence of *mcyB* only in 1 sample and *mcyE* in 6 samples may indicate that the genetic machinery for MC synthesis is deficient and the dominant species lost the capability of MC synthesis.

### **3.1.1.2 Treatment of *Merismopedia* sp. in St. George Lake water**

The peroxide-based oxidants used for the mitigation of *Merismopedia* sp. exhibited different efficiencies and impact on the bloom. The average initial instantaneous fluorescence (Ft) and quantum yield at  $\lambda = 620$  nm, were 8500 and 0.37, respectively; while at  $\lambda = 450$  nm were 3000 and 0.6, respectively. Treatment with liquid hydrogen peroxide in concentrations 1 to 5 mg L<sup>-1</sup> had no effect on the phycocyanin fluorescence (Ft) and quantum yield of PSII (Fv/Fm) indicating an ineffective treatment for the dense *Merismopedia* bloom. At the lowest doses (1 and 2 mg L<sup>-1</sup>) cyanobacteria continued to grow steadily; making the treatment inefficient. Treatment with 3 and 5 mg L<sup>-1</sup> H<sub>2</sub>O<sub>2</sub> showed only a minor drop of the corresponding Ft values in raw fluorescence units (RFU) compared with the control (Figure 3A) which found to be insignificant ( $p > 0.05$ ). All

treated samples showed a stable average of QY around 0.37, meaning that the bloom remained unaffected during treatment with liquid H<sub>2</sub>O<sub>2</sub>, and the oxidant dose was unable to disrupt the photosystem II efficiency (Figure 3B) of the specific bloom.

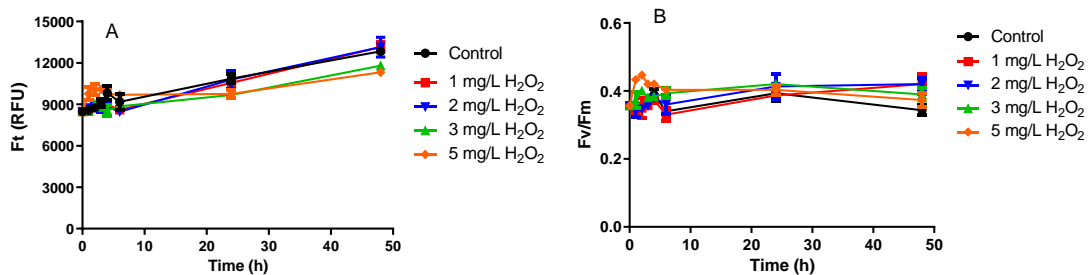


**Figure 3.** The effect of liquid H<sub>2</sub>O<sub>2</sub> concentration (0, 1, 2, 3, 5 mg L<sup>-1</sup>) on (A) phycoerythrin concentration (measured as raw fluorescence units – RFU) and (B) Maximal quantum efficiency of the PSII (QY) at  $\lambda=620$  nm. Results are expressed as the mean  $\pm$  SD.

Metallic peroxide granules exhibited different mitigation efficiencies, with MgO<sub>2</sub> to be the least efficient between the two. CaO<sub>2</sub> granules effectively decreased the photosynthetic activity of cyanobacteria (Figure 4A), as doses of 2 and 3 g L<sup>-1</sup> significantly decreased the pigment concentration measured at t= 24 h ( $p < 0.001$ ) and maintained at low levels until 48 h of treatment. Even though 2 g L<sup>-1</sup> of CaO<sub>2</sub> reduced the sample's fluorescence, but Fm/Fv was restored after 6 h of treatment, making it less efficient than its higher dose (Figure 4B).

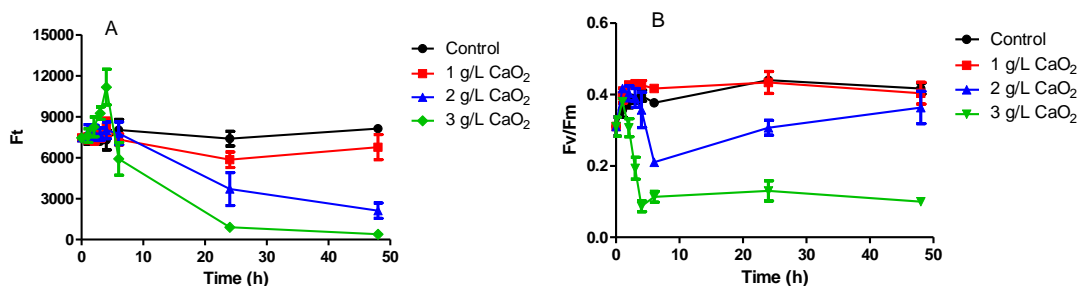


**Figure 4.** The effect of CaO<sub>2</sub> granules concentration (0, 1, 2, 3 g L<sup>-1</sup>) on (A) phycoerythrin concentration (measured as raw fluorescence units—RFU) and (B) maximal quantum efficiency of the PSII (QY) at 620 nm. Results are expressed as the mean  $\pm$  SD.

Treatment with MgO<sub>2</sub> granules was inefficient for concentrations up to 3 g L<sup>-1</sup>. Both, Ft and Fv/Fm, values at  $\lambda = 620$  nm were stable during the treatment period (Figure 5), meaning that the photosynthetic activity of *Merismopedia* cells was not affected and retained throughout the treatment. In the first 4 h of treatment, Ft values insignificantly

decreased but then were recovered within 6 h of treatment. In general, MgO<sub>2</sub> granules in equal concentrations with CaO<sub>2</sub> granules, were not able to influence the bloom, and therefore had no effect on both phycocyanin and chlorophyll a.

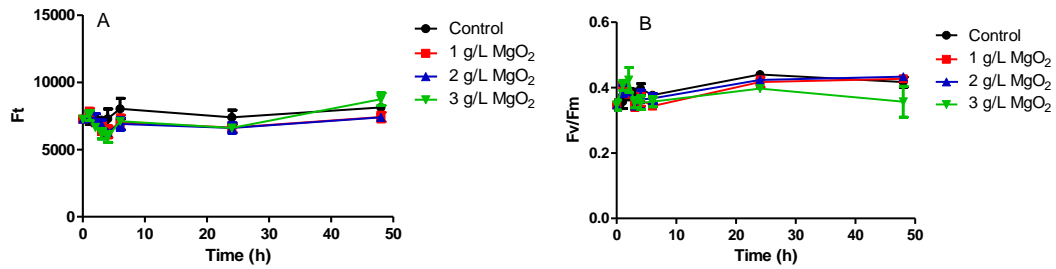


**Figure 5.** The effect of MgO<sub>2</sub> granules concentration (0, 1, 2, 3 g L<sup>-1</sup>) on (A) phycocyanin concentration (measured as raw fluorescence units – RFU) and (B) Maximal quantum efficiency of the PSII (QY) at 620 nm. Results are expressed as the mean ± SD.

Hydrogen peroxide did not affect the water quality characteristics while magnesium peroxide granules slightly increased all the recorded parameters. MgO<sub>2</sub> and CaO<sub>2</sub> granules made the solution more alkaline while H<sub>2</sub>O<sub>2</sub> had the least effect on the pH of the water matrix (Figure 6). More specifically, 3 g L<sup>-1</sup> CaO<sub>2</sub> granules increased the pH above 10, which is considered high for freshwater environments. Overall, there was no dramatic change of the remain characteristics of the water, except the pH rise above 10 which is considered as an unwanted effect in the waterbody.

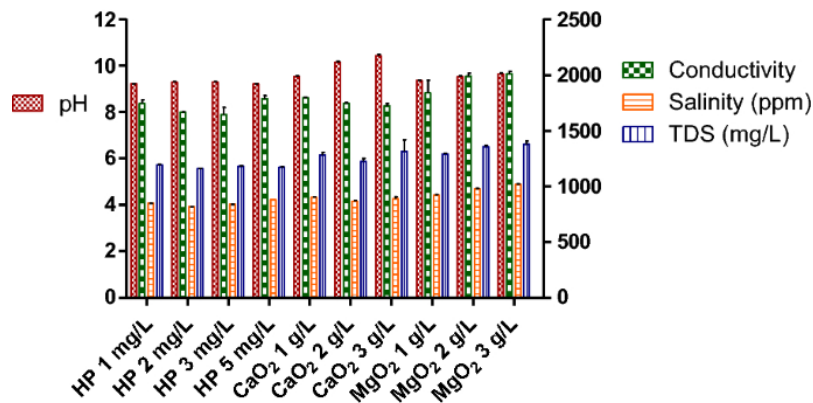


**Figure 6.** Average pH, conductivity, salinity, and TDS (mean ± SD) of St. George Lake water (pH = 8.88, conductivity = 1999 µS cm<sup>-1</sup>, salinity = 1015 ppm) after 48 h of treatment with liquid H<sub>2</sub>O<sub>2</sub>, CaO<sub>2</sub> and MgO<sub>2</sub> granules.

### 3.1.1.3 $H_2O_2$ release by $CaO_2$ and $MgO_2$ granules in filtered lake water

Metallic peroxide granules were tested for their  $H_2O_2$  releasing capacity in St. George Lake filtered water (cyano-free). As shown in Figure 8,  $MgO_2$  resulted in a much lower oxidant release than the applied  $CaO_2$  granules. Release curves in filtered St. George Lake matrix showed that maximum accumulative hydrogen peroxide concentration from 1, 2 and 3 g  $L^{-1}$  of  $CaO_2$  was 3.5, 8.0 and 11 mg  $L^{-1}$  respectively; while for 1, 2 and 3 g  $L^{-1}$  of  $MgO_2$  was as low as 0.7, 1.2, and 1.8 mg  $L^{-1}$  of  $H_2O_2$ ; respectively (Figure 7). The limited  $H_2O_2$  releasing capacity of  $MgO_2$  granules can explain their reduced efficiency as the released oxidant was not high enough to affect the bloom. Especially in cases where resistant and dense blooming events are occurred, much higher doses of  $H_2O_2$  found to be effective ( $> 5$  mg  $L^{-1}$ ). Even though a noticeable amount of  $H_2O_2$  was released in water by granules; during the treatment, oxidant was rapidly consumed we were unable to detect residual concentrations higher than 0.5 mg  $L^{-1}$ .

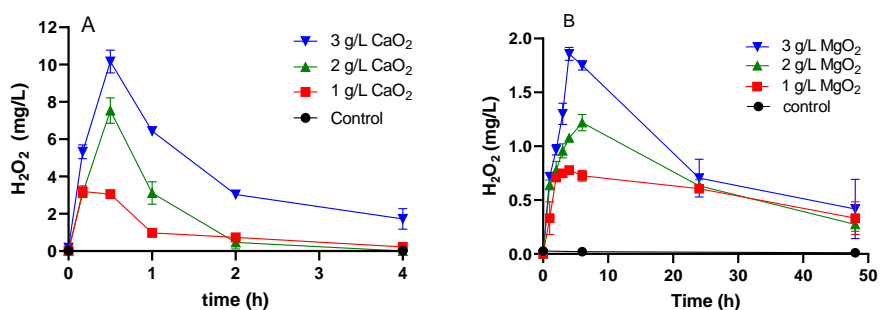


**Figure 7.**  $H_2O_2$  release curves by 1, 2 and 3 g  $L^{-1}$  of (A)  $CaO_2$  and (B)  $MgO_2$  granules in filtered St. George Lake water matrix.

### 3.1.2 Athalassa Lake

#### 3.1.2.1 Monitoring

Monitoring of Athalassa Lake occurred between August and November 2020, and a fish kill event was recorded during that period. The event was reported by the Department of Forests in Cyprus and caused the interest of the authorities to investigate the reason that drive the death of fish. The first articles released in press referred to a toxic a cyanobacteria bloom that caused acute toxicity to fish and warned the public for cyanotoxins presence into the waterbody.

Monitoring of the lake showed a continual increase in pH that started from 8.3 and reached 8.7 in November. Conductivity ranged between 2200 to 3500  $\mu\text{S}/\text{cm}$ , while TDS were quite stable the first three months but increased in November (Figure 8 A). The measured phycocyanin fluorescence in August and September was as low as 1500 RFU, which was followed by a sharp increase in October 2020. The increase in Ft indicated the beginning of a bloom, that peaked in November (Figure 8 B). The formation of the bloom was visible with a naked eye. Analysis of the chemical oxygen demand (COD) showed extremely high levels which exceeded the acceptable ranges for fresh water. Measured COD was as high as 125  $\text{mg L}^{-1}$  and 272  $\text{mg L}^{-1}$  from samples taken in September and November, respectively. Increased COD level indicate high levels of water pollution which was probably caused by organic-waste matter that leaked into the water from an unidentified point source. The total nitrogen was 2.4  $\text{mg L}^{-1}$  and 10.2  $\text{mg L}^{-1}$ , while total phosphorous was 0.21  $\text{mg L}^{-1}$  and 1.77  $\text{mg L}^{-1}$  in September and November, respectively. The nutrient levels indicated a depleted surface water quality that rapidly leapt from Class II (Mesotrophic) to Class III-V (Eutrophic).

Samples were tested under the microscope to identify the main species present in both cases. Microscopic observation showed that during fish-kill event the major species were *Planktothrix agardhii*, *Planktolyngbya limnetica*, *Limnospira*, and *Euglenophyta* sp., while *Planktothrix agardhii* became later the dominant specie (Scheme 18). Since, *Planktothrix agardhii*, previously named *Oscillatoria*, is a filamentous specie with trichomes and gas vacuoles and it is widely found in freshwater environments. Unlike other cyanobacteria species, its main pigment is phycoerythrin which is responsible for the green-brownish color of the cells, that is also reflected on the shade of the

contaminated waterbody (Scheme 20). These species are known as microcystin and several bioactive peptides producers, thereby resulting in impressive secondary metabolite structural diversity [99].

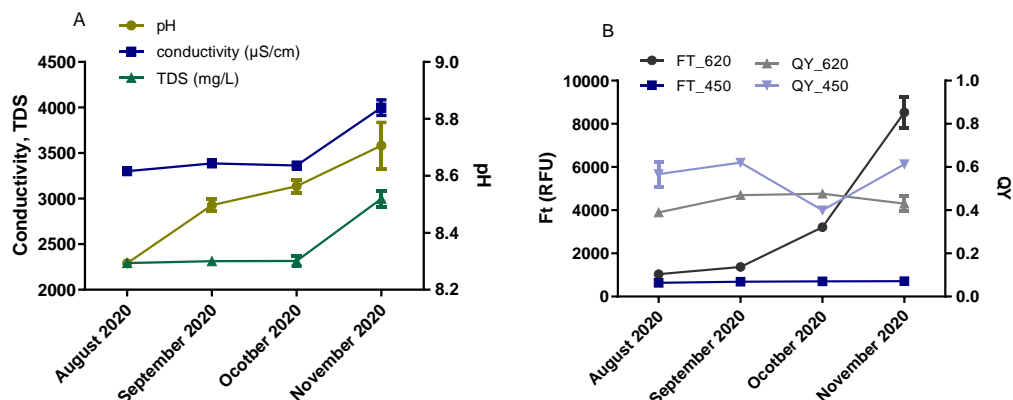
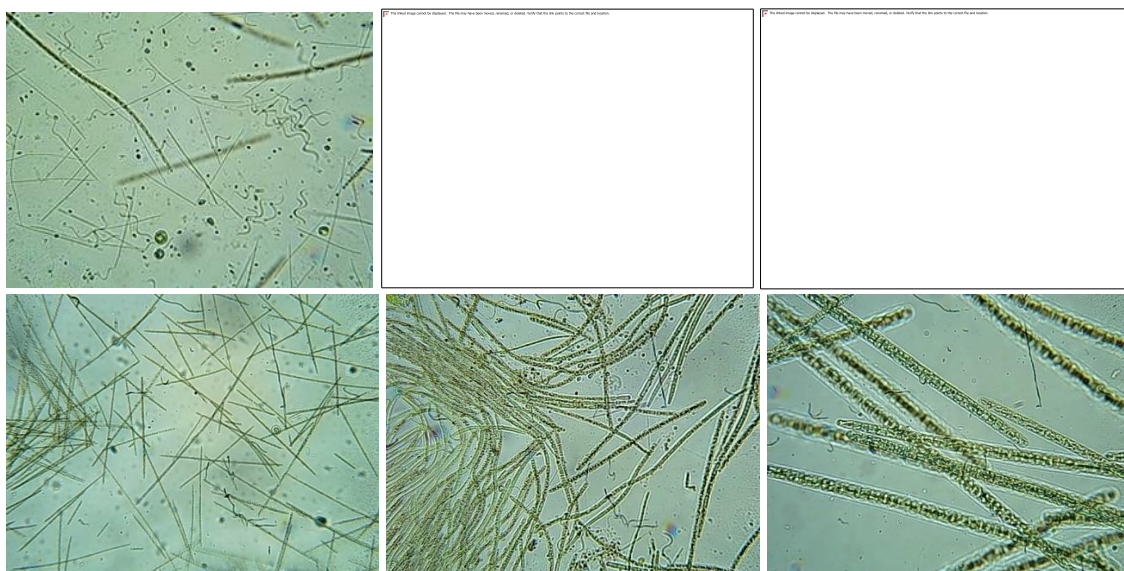


**Figure 8.** (A) Physicochemical water characteristics, and (B) Photosynthetic parameters of Athalassa Lake water related to cyano-HABs (August – November 2020).



**Scheme 19.** Samples received from Athalassa Lake **Upper row:** right after the fish-kill event and **Lower row:** *Planktothrix* sp. during the blooming period, captured under ECLIPSE Ci-L microscope equipped with OPTIKAM Wi-Fi camera with magnification from left to right 20x, 40x, and 100x, Eleni C. Keliri<sup>©</sup>.

Taking into consideration the potential toxicity of the species, water samples were collected right after the fish kill event to be analyzed for cyanotoxin producing genes (mainly *mcyE*, *mcyB*) and cyanotoxins content. The results of the above analyses did not show any correlation of the fish-kill event with cyanotoxins, as no cyanotoxin producing

genes were present into the samples nor toxins were identified with advanced analytical techniques above the MDL.

### 3.1.2.2 Treatment of contaminated *Athalassa*'s lake water (fish-kill event)

Surface water collected from Athalassa Lake with increased nutrients concentration and COD ( $=125 \text{ mg L}^{-1}$ ) ten times higher than the permissible levels for surface waters ( $10\text{--}20 \text{ mg L}^{-1}$ ) [100] was utilized for treatment experiments with liquid  $\text{H}_2\text{O}_2$  and PMS using the multiple dosing technique. A total dose of  $7_{(3+2+2)} \text{ mg L}^{-1}$  and  $9_{(3+3+3)} \text{ mg L}^{-1}$   $\text{H}_2\text{O}_2$  slightly decreased the phycocyanin content of the matrix from  $1700 \sim \text{RFU}$  to  $\sim 1000 \text{ RFU}$  (Figure 9). Quantum yield decreased from the first hours of treatment to  $\sim 0.4$  and remained stable throughout the treatment, indicating no effect on cyanobacteria photosynthetic ability. Although the cyanobacterial content into the water was not considerably high, the doses applied were not enough to destroy the cells. Also, it was observed that the oxidant was rapidly consumed by the matrix resulting in quantifications of  $\text{H}_2\text{O}_2$  lower than  $0.5 \text{ mg L}^{-1}$ , even some minutes after its addition.

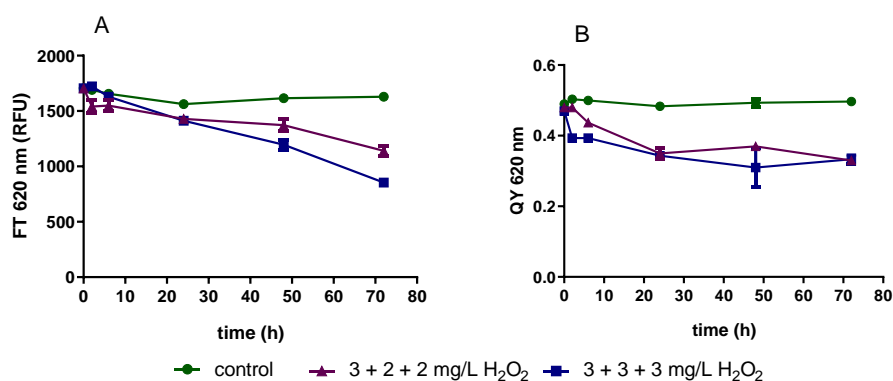


**Figure 9.** The effect of multiple dosing of  $\text{H}_2\text{O}_2$  on (A) phycocyanin fluorescence (RFU) and (B) quantum efficiency of the PSII (QY) at 620 nm during a 78-h treatment of Athalassa lake water.

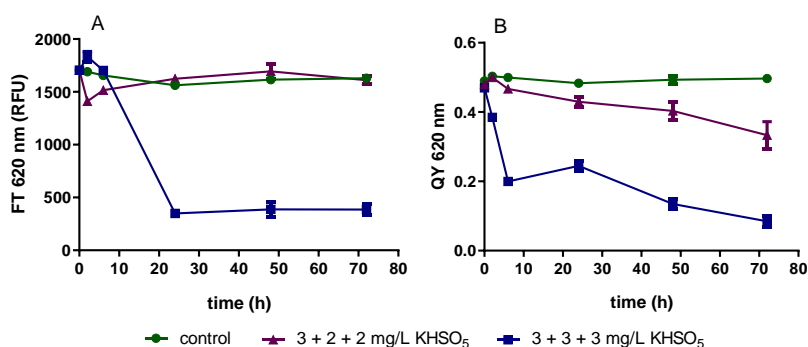


**Figure 10.** The effect of multiple dosing of PMS on (A) phycocyanin fluorescence (RFU) and (B) QY of the PSII at 620 nm during a 78-h treatment of Athalassa lake water.

PMS exhibited varied treatment efficiencies between the two dosing systems. High efficiency was only recorded when repeated doses of 3 mg L<sup>-1</sup> were applied, while the other dosing caused only a minor drop in quantum yield and had no effect on phycocyanin fluorescence. The total dose of 9<sub>(3+3+3)</sub> mg L<sup>-1</sup> KHSO<sub>5</sub>. caused a rapid decline on Ft and QY from the initial hours of treatment. Measured QY was partially restored at t=24 hours but after the 2<sup>nd</sup> and 3<sup>rd</sup> dose it dropped nearly to zero, indicating the total distraction of cyano-cells. Quantified COD at t=72 hours was 68 mg L<sup>-1</sup> and 52 mg L<sup>-1</sup> after treatment with high repeated doses of H<sub>2</sub>O<sub>2</sub> and PMS, respectively.

### 3.1.2.3 Treatment of *Planktothrix* sp. in Athalassa Lake water

Application of PMS and H<sub>2</sub>O<sub>2</sub> in equal peroxide doses (1, 2, and 3 mg L<sup>-1</sup>) resulted in different efficiencies on treating the bloom. PMS showed an increased effect on the filament bloom (*Planktothrix agardhii*) in comparison with liquid H<sub>2</sub>O<sub>2</sub>. Even though there was a reduction on the phycocyanin fluorescence when H<sub>2</sub>O<sub>2</sub> was applied, quantum yield remained unaffected, indicating no impairment on the PSII related to cyanobacteria photosynthetic activity and cell function. The application of PMS reduced both phycocyanin fluorescence and quantum yield of the PSII in all tested concentrations, while 3 mg L<sup>-1</sup> was the most effective dose, as it resulted in zero quantum yield 98 hours after oxidant addition.

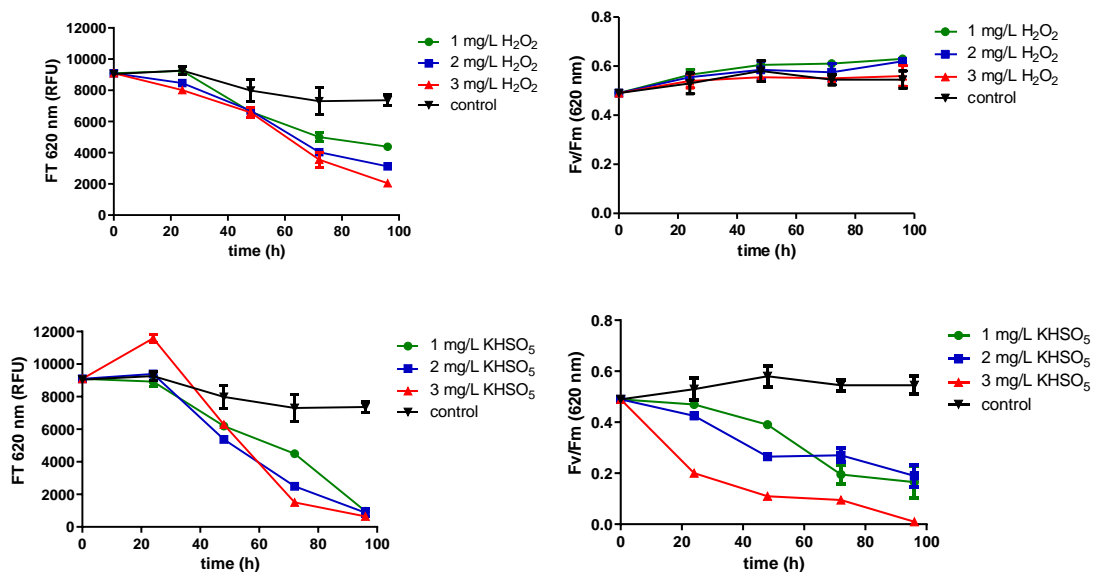
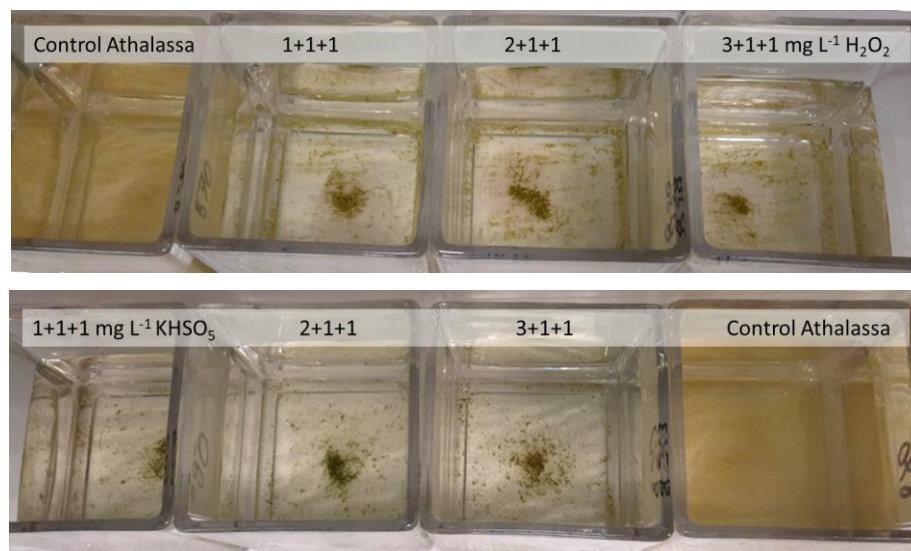


**Figure 11.** Ft in raw fluorescence units (RFU) and QY (Fv/Fm) at  $\lambda=620$  nm during natural bloom treatment in Athalassa lake with repeated doses of 1, 2 and 3 mg L<sup>-1</sup> H<sub>2</sub>O<sub>2</sub> and PMS added every 24 hours for up to 72 hours.



**Scheme 20.** Treatment containers during treatment of Athalassa Lake water by multiple peroxide additions with total applied concentration 3, 4, and 5 mg L<sup>-1</sup> H<sub>2</sub>O<sub>2</sub> and KHSO<sub>5</sub>.

Quantification of the oxidants during treatment showed no residual H<sub>2</sub>O<sub>2</sub> concentration after 6 hours of treatment while PMS remained in the matrix in concentrations > 0.5 mg L<sup>-1</sup> the first 24 h of treatment. These findings suggest that in natural environments H<sub>2</sub>O<sub>2</sub> tends to decompose or react fast with any matrix component, reducing its potential in the matrix to actively distinguish between matrix components and the target contaminant. PMS showed a long-lasting residual effect which result in a more targeted treatment and thus higher treatment efficiency. The properties of PMS and its treatment efficiencies were further explored and presented in Chapters 3.3 and 4.2.3.

The effect of novel oxidants and their application method (single, multiple dosing) were examined in naturally occurring blooms which occurred during the monitoring activities of WTL-AQUA. The above studies comprise the primary stage where the novel oxidants' behavior, their potency to perform treatments and some of their physical and chemical properties were explored. Dedicated experiments on each oxidant were performed to further investigate their individual properties, as well as to develop and optimize treatments that can be proposed for *in-lake* applications.

## 3.2 Calcium peroxide (CaO<sub>2</sub>) granules

### 3.2.1 Elemental composition

Granules utilized in the present study had a given purity of 70 % w/w CaO<sub>2</sub>, equivalent to ~15.5 % available oxygen. Granules had a particle size between 0.5 to 2 mm and a pale-yellow color. The impurities reported by the manufacturer were 10-19% Ca(OH)<sub>2</sub> and other inorganic calcium compounds of around 5-19 %. XRF analysis showed the significant presence of iron, nickel, and manganese in granules' composition. The elemental composition of CaO<sub>2</sub> granules are presented in Table 8.

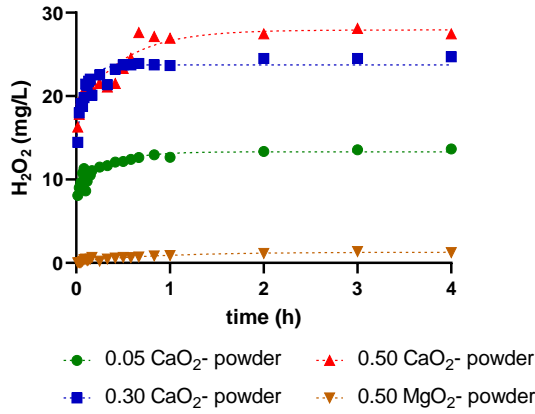
**Table 8.** Elemental composition in CaO<sub>2</sub> granules detected by handled XRF analysis, where [C] = concentration and L.E = light elements (e.g., Ca, O).

Element	[C] (ppm)	± SD
Fe	182	11
Ni	158	10
Mn	62	19
Zr	19	4
Zn	16	3
Pb	11	6
Cu	2	4
L.E	999550	14

### 3.2.2 Compound type (powder, granules) effect on H<sub>2</sub>O<sub>2</sub> yield

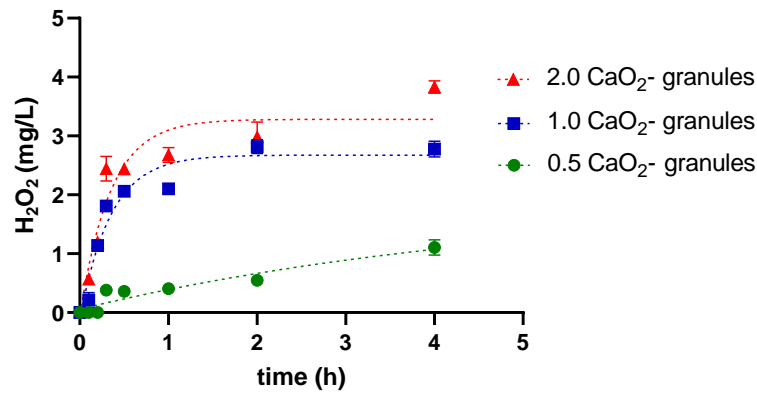
Two types of metallic peroxide granules (powder, granules) were used to examine their H<sub>2</sub>O<sub>2</sub> releasing capacity in pure water. Applied concentrations of 0.05, 0.30, and 0.5 g L<sup>-1</sup> CaO<sub>2</sub> powder resulted in the release of ~13, 24, and 28 mg L<sup>-1</sup> H<sub>2</sub>O<sub>2</sub>, respectively (Figure 12). The obtained H<sub>2</sub>O<sub>2</sub> release curves showed that CaO<sub>2</sub> powder had a much higher H<sub>2</sub>O<sub>2</sub> releasing capacity than the equal dose of MgO<sub>2</sub> powder, which only released ~1.3 mg L<sup>-1</sup> H<sub>2</sub>O<sub>2</sub>. The concentration of 0.5 g L<sup>-1</sup> of CaO<sub>2</sub> granules released much lower H<sub>2</sub>O<sub>2</sub> concentration in comparison with its powder form (Figures 13, 14), and their release kinetics were slower. The one-phase association model fitted well the release curves obtained from granules (R<sup>2</sup>>0.9), and quite less for powder (R<sup>2</sup>>0.8), meaning that H<sub>2</sub>O<sub>2</sub> release probably follows pseudo-first order kinetics. The rate of the reaction also differed between the two types of CaO<sub>2</sub>. Powdered CaO<sub>2</sub> resulted in a rapid release within the

first minutes of contact with water, reaching its maximal release at t=40 minutes, while granules required ~ 4 hours to achieve their maximum H<sub>2</sub>O<sub>2</sub> release potential. Results suggested that the use of powdered CaO<sub>2</sub> should be avoided for surface water treatment since it makes available a high quantity of H<sub>2</sub>O<sub>2</sub> in water, that can be potentially dangerous for aquatic life. The granules should be further investigated for their slow-releasing ability as this form of CaO<sub>2</sub> could be of benefit for cyano-HABs treatment.



	0.05 CaO <sub>2</sub> - powder	0.30 CaO <sub>2</sub> - powder	0.50 CaO <sub>2</sub> - powder	0.50 MgO <sub>2</sub> - powder
Best-fit values				
Y0	8.830	14.46	18.09	0.1509
Plateau	13.32	23.74	27.93	1.289
K	3.121	10.18	2.021	1.122

**Figure 12.** H<sub>2</sub>O<sub>2</sub> release kinetics by 0.05, 0.3, and 0.5 g L<sup>-1</sup> CaO<sub>2</sub> powder and 0.5 g L<sup>-1</sup> MgO<sub>2</sub> powder in Milli-Q water fitted by non-linear pseudo-first order model:  $Y=Y_0 + (\text{Plateau}-Y_0)*(1-\exp(-K*x))$ .



	0.5 CaO <sub>2</sub> - granules	1.0 CaO <sub>2</sub> - granules	2.0 CaO <sub>2</sub> - granules
Y0	0.05671	-0.1287	-0.06833
Plateau	1.913	2.675	3.282
K	0.1987	2.890	2.900

**Figure 13.** H<sub>2</sub>O<sub>2</sub> release kinetics by 0.5, 1, and 2 g L<sup>-1</sup> CaO<sub>2</sub> granules in Milli-Q water fitted by non-linear pseudo-first order model:  $Y=Y_0 + (\text{Plateau}-Y_0)*(1-\exp(-K*x))$ .

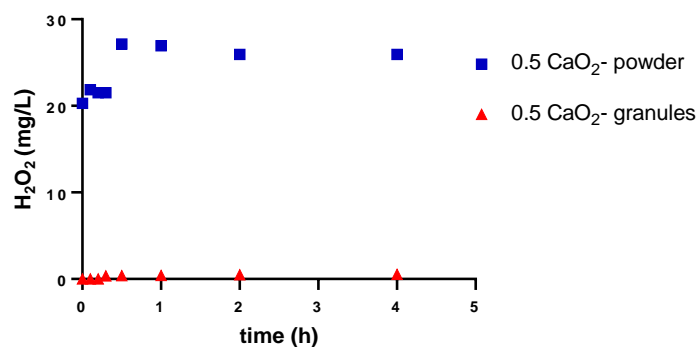


**Figure 14.** Hydrogen peroxide released by 0.5 g L<sup>-1</sup> CaO<sub>2</sub> granules and CaO<sub>2</sub> powder.

### 3.2.3 Matrix effect on CaO<sub>2</sub> granules' releasing properties<sup>3</sup>

#### 3.2.3.1 Surface water composition (MQ, River, Dam, Lake water)

An array of surface water matrixes with various physicochemical water characteristics were used to capture the release (yield) of H<sub>2</sub>O<sub>2</sub>. Surface waters collected from a river, a dam, and a lake in Cyprus, and whose water quality characteristics are shown on Table S 4, were utilized for capturing the release of H<sub>2</sub>O<sub>2</sub> by 0.5, 1, 2 and 3 g L<sup>-1</sup> CaO<sub>2</sub> granules. CaO<sub>2</sub> granules resulted in a gradual release of H<sub>2</sub>O<sub>2</sub> for up to 6 hours after their addition in the tested water matrixes. The obtained release curves (Figures 15, S 3) showed that the maximum accumulative H<sub>2</sub>O<sub>2</sub> concentration in each water matrix varied, meaning that H<sub>2</sub>O<sub>2</sub> availability is greatly affected by the matrix load. Specifically, granules in extra pure water had the lowest H<sub>2</sub>O<sub>2</sub> releasing capacity, followed by the lake water. Even though lake water collected during a blooming event, was filtered through cellulose nitrate filters, its nutrient load was much higher than the other matrixes, which may have caused the consumption of the released oxidant resulting in its limited availability. In dam water, H<sub>2</sub>O<sub>2</sub> quantification had a slightly higher accumulative concentration than in river water, achieving a release of approximately 3, 6, 12, and 17 mg L<sup>-1</sup> H<sub>2</sub>O<sub>2</sub> from 0.5, 1.0, 2.0, and 3.0 g L<sup>-1</sup> CaO<sub>2</sub> granules, respectively (Table 9). Although, the maximum accumulative concentrations between river and dam water were similar, H<sub>2</sub>O<sub>2</sub> release in river water was followed by its consumption resulting in a decreased availability H<sub>2</sub>O<sub>2</sub>

<sup>3</sup> The findings of this study will be submitted to the *Journal of Hazardous Materials* as a research article (December 2022).

in the matrix at t=48 hours. The maximum released concentrations of H<sub>2</sub>O<sub>2</sub> by each CaO<sub>2</sub> granules concentration and in each water-matrix are depicted in Table 9.

**Table 9.** Maximum accumulative concentration of H<sub>2</sub>O<sub>2</sub> released by 0.5, 1, 2 and 3 g L<sup>-1</sup> CaO<sub>2</sub> granules in different water matrixes (Mean ± SD).

CaO <sub>2</sub> granules (g L <sup>-1</sup> )	Maximum H <sub>2</sub> O <sub>2</sub> (mg L <sup>-1</sup> ) yield			
	MQ-water	Dam Water	River water	Lake water
0.5	0.7 (±0.2)	2.9 (±0.4)	2.4 (±0.3)	N/A
1.0	2.3 (±0.3)	5.7 (±0.2)	4.9 (±0.4)	3.1 (±0.2)
2.0	3.9 (±0.4)	11.9 (±0.3)	11.1 (±0.4)	7.2 (±0.3)
3.0	7.5 (±0.3)	16.7 (±0.2)	14.5 (±0.3)	10.1 (± 0.5)

Since our previous studies indicated that H<sub>2</sub>O<sub>2</sub> release may follow a pseudo-first order kinetic model, the release curves for t = 0 – 6 hours were fitted to the same model. Lake water showed no fit to the model, while river, dam and MQ water had a better fit, given the high correlation coefficients (R<sup>2</sup> = 0.95 – 0.97). The rate constant (k) obtained by the one-phase association model showed that oxidant release in dam water (k=0.28 h<sup>-1</sup>) was slower than in river (k=2.96h<sup>-1</sup>) and extra-pure water (k=2.09 h<sup>-1</sup>), but the accumulative H<sub>2</sub>O<sub>2</sub> released concentration by both surface waters were the same as the instantly measured H<sub>2</sub>O<sub>2</sub> concentration was around 12 mg L<sup>-1</sup> and did not significantly differ (p> 0.05) between river and dam water at t=6 hours, as shown in Figure 15. What was significantly higher was the initial rate of H<sub>2</sub>O<sub>2</sub> release in river water, while for dam and MQ-water did not statistically differ.

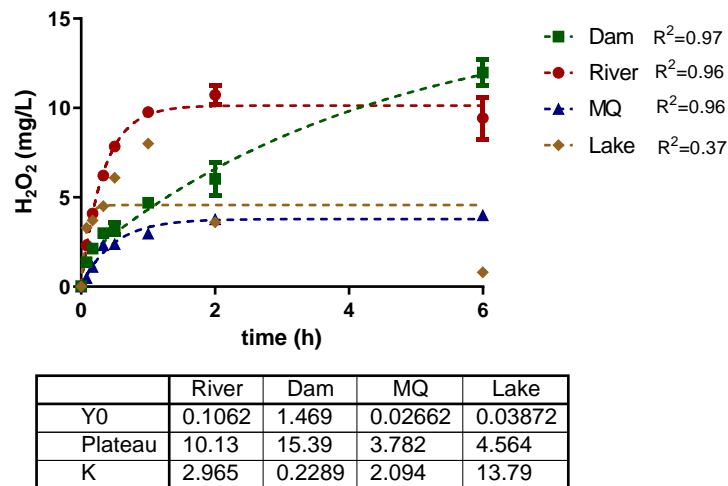


**Figure 15.** H<sub>2</sub>O<sub>2</sub> release in dam, river, MQ, and lake water by 2.0 g L<sup>-1</sup> CaO<sub>2</sub> fitted by non-linear pseudo-first order model:  $Y=Y_0 + (\text{Plateau}-Y_0)*(1-\exp(-K*x))$ .

### 3.2.3.2 BG-11 matrix (25%, 50%, and 75%)

Release in surface waters with various water characteristics showed that high nutrient load (in lake water) reacted with the released  $H_2O_2$ , resulting in its limited availability, and hence its lower accumulative concentration in the matrix. Also, the lower releasing capacity of granules in MQ-water indicated that microelements contained in the water matrix enhance the release granules. To test the above hypotheses, release experiments were conducted in BG-11 medium in dilutions of 25%, 50% and 75%, achieving an array of total nutrients', microelements' (inorganic load) concentrations into the water matrix. Total nutrient analyses prior to granules addition showed that total nitrogen and total phosphorous was as high as  $204 \text{ mg L}^{-1}$  and  $4.3 \text{ mg L}^{-1}$  in BG-11 75% solution, respectively (Table S 6).

Release curves in BG-11 matrix indicated that the higher proportion of nutrients and trace elements in the matrix, the lower accumulative  $H_2O_2$  concentration is achieved (Figure 16). For instance,  $1 \text{ g L}^{-1}$   $CaO_2$  granules in 25% BG-11 medium released up to  $5 \text{ mg L}^{-1}$   $H_2O_2$  at  $t=48 \text{ h}$ , while in 75% the released concentration was as low as  $2 \text{ mg L}^{-1}$ , indicating an immediate consumption of the released oxidant by the medium elements. To validate this outcome, an instant dose of  $6 \text{ mg L}^{-1}$   $H_2O_2$  was also added into each BG-11 medium and  $H_2O_2$  concentration was monitored at  $t=0, 1, 4, 6$  hours after its addition. Results showed that matrix load consumed  $2 - 3 \text{ mg L}^{-1}$   $H_2O_2$  right after its addition.

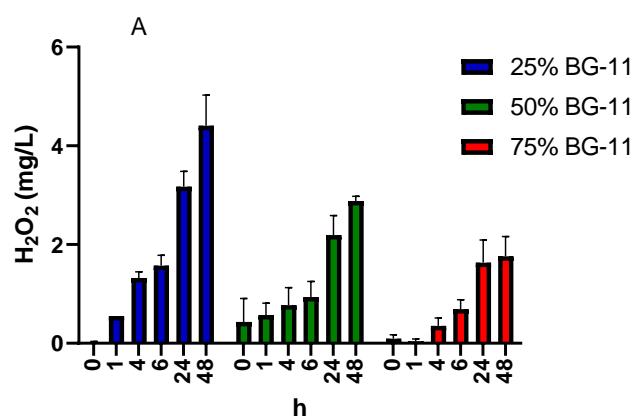


**Figure 16.** Instant  $H_2O_2$  concentrations released by  $1 \text{ g L}^{-1}$   $CaO_2$  granules and  $t=0, 1, 4, 6, 24,$  and  $48 \text{ h}$  after the addition of  $6 \text{ mg L}^{-1}$  liquid  $H_2O_2$  in BG-11 medium in dilutions of 25%, 50%, and 75% in Milli-Q.

Data points of release curves were further statistically analyzed to see whether granules dose and  $H_2O_2$  release are correlated. Linear regression analysis performed to indicate

whether the concentrations of granules added in each water matrix have a linear correlation with the released  $H_2O_2$  (Figure 16). The curves showed almost a perfect linearity in dam and lake water ( $R^2=0.99$ ), and sufficient linearity in milli-Q and lake waters ( $R^2=0.96$ ), confirming that in all tested matrixes  $H_2O_2$  release is highly depended on the granules' dose. Also, it is apparent that matrix does not affect this linear relationship, unless high nutrient and/or contamination exists which leads to the consumption of the released oxidant, hence the disturbance of the linearity. For instance, the correlation coefficients of the release in lake water and 75% BG-11 medium were slightly lower than in other less loaded matrixes. However, the matrix does affect the slope of the equation which means that the presence of matrix components (inorganic, organic load) drives the equation towards the oxidant release and in cases of highly loaded matrixes (50%, 75% BG-11) it is followed by its rapid degradation, causing slope reduction. The variation in slope values shows that higher the amount of nutrients and inorganic matter into the matrix the less availability of accumulative  $H_2O_2$  concentration in the matrix, excluding the case of milli-Q water which is an extra-pure. In that case the absence of microelements eliminated the  $H_2O_2$  releasing capability of granules, resulting similar equation (in terms of slope and  $R^2$ ) to the one obtained in highly loaded 75% BG-11 medium, where the released oxidant was consumed by the matrix components.

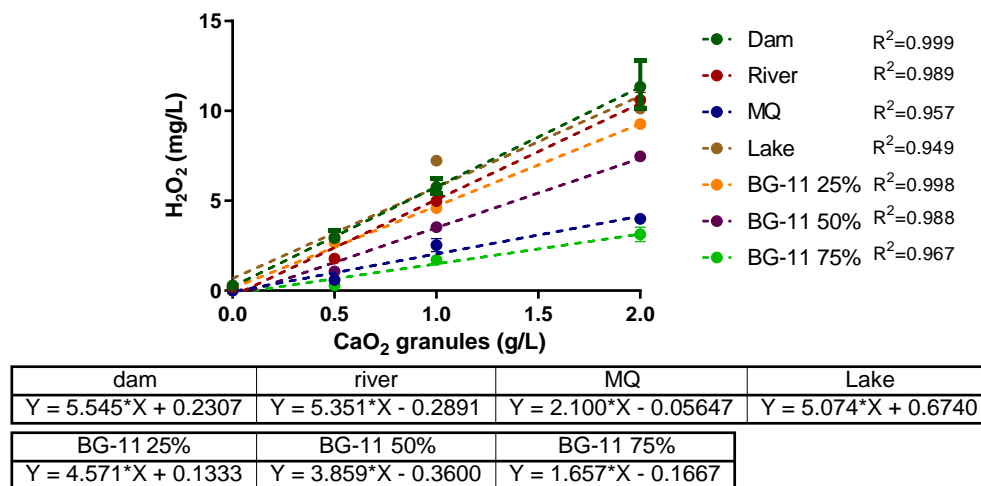


**Figure 17.** Correlation between  $CaO_2$  granules ( $g L^{-1}$ ) added in in all tested matrixes (dam, river, milli-Q, lake, and BG-11 dilutions of 25%, 50%, and 75%) and the peak  $H_2O_2$  released concentration ( $mg L^{-1}$ ).

### 3.2.3.3 Natural Organic Matter (NOM) – humics content

Besides the nutrients and inorganic elements found in surface waters, natural organic matter is also present and may influence surface water treatment. Humics in concentrations of 0, 1, 5, and 10 ppm were added into surface water (free from cyanobacteria) and the release kinetics were again investigated. In the presence of low concentration of HASS (0, 1 ppm), a release of around  $6 \text{ mg L}^{-1}$  and  $3 \text{ mg L}^{-1} \text{ H}_2\text{O}_2$ , respectively, was achieved. Surface water enriched with 5 and 10 ppm HASS showed an increased release of  $\text{H}_2\text{O}_2$  ( $> 3 \text{ mg L}^{-1}$ ) in comparison with 1 ppm, which followed by its consumption at  $t=4 \text{ h}$  and then again, its release at  $t=24 \text{ h}$  (Figure 18). It is apparent that higher concentration of humics enhanced the release of  $\text{H}_2\text{O}_2$  by the granules, but also the presence of HASS caused the simultaneous release and consumption of the oxidant, that caused disrupted release curves (Figure S 4).

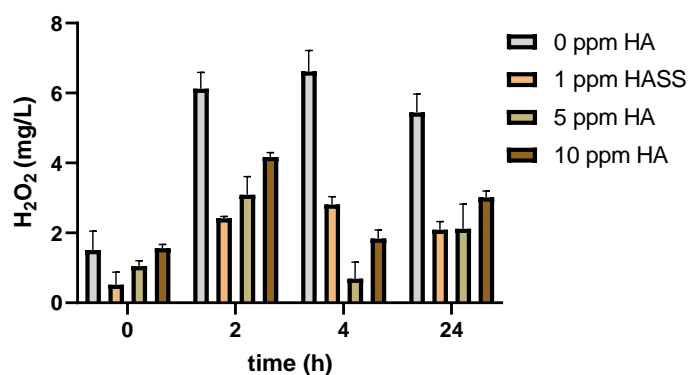


**Figure 18.** Instantaneous  $\text{H}_2\text{O}_2$  concentration released by  $1.0 \text{ g L}^{-1} \text{ CaO}_2$  in surface (dam) water enriched 0 (control), 1, 5 and 10 ppm HASS at  $t=0, 2, 4, 24$  hours.

To further investigate the reaction mechanism between granules and organic load, EPR technique was employed. Hydroxyalkyl radicals marked in red color were found in higher concentrations in water enriched with 5 and 10 ppm of HASS, reaching their peak at  $t=48$  hours (Figure 19, S 5). The lowest concentration of 1 ppm HASS, resulted an initial release of hydroxyalkyl radicals, followed by their consumption (30%) and regeneration. The concentrations of the generated hydroxyalkyl radicals in surface water contained 1, 5, and 10 ppm of HASS, were around  $1.2 \mu\text{mol L}^{-1}$  (0, 1 ppm HASS) and  $4.5 \mu\text{mol L}^{-1}$  (5, 10 ppm HASS). On the other hand, the generated hydroxyl radicals did not significantly vary between the added doses of HASS, and they ranged between  $0.8$  and  $1.0 \mu\text{mol L}^{-1}$ . Comparing the radicals formed by 1, 5, and 10 ppm of HASS, it is obvious that higher concentrations of humics (and NOM) in surface water favors the

formation of hydroxyalkyl adducts while  $\cdot\text{OH}$  radicals remain rather constant and around  $1 \mu\text{mol L}^{-1}$  in the presence of HASS (Figure 19).

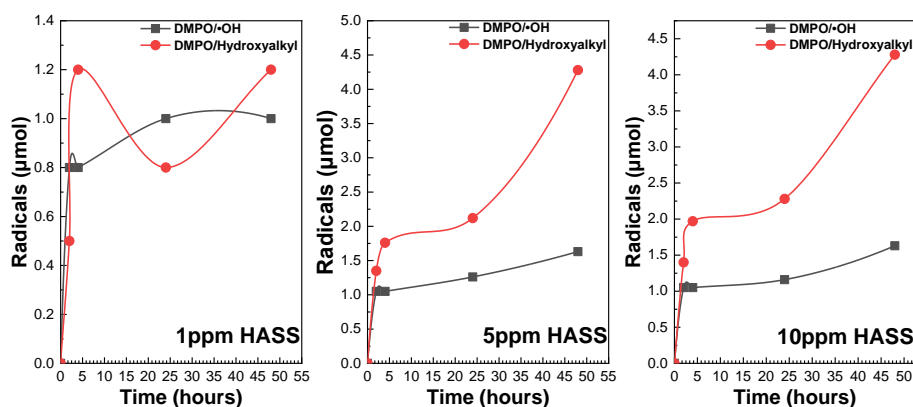
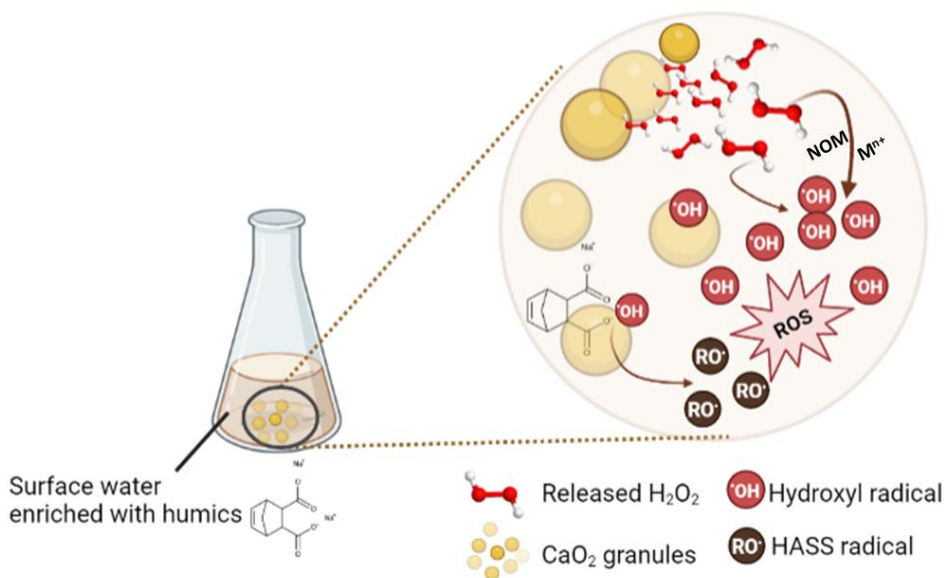


**Figure 19.** Quantification of DMPO/ $\cdot\text{OH}$  and DMPO/Hydroxyalkyl adducts using DPPH as spin standard for the 1ppm HASS, 5ppm HASS and 10ppm HASS, respectively.

The proposed mechanism of radicals' formation is described in Scheme 21, which depicts the interaction between the organic matter (HASS) and the released hydroxyl radicals to form the oxidized organic radicals (hydroxyalkyl radicals) through an interfacial phenomenon. This mechanism reveals and explains the activation of  $\text{CaO}_2$  granules in the presence of humic acids as well as the formation of side-products (hydroxyalkyl adducts) during their reaction with water enhanced with humics.



**Scheme 21.** Proposed mechanism of hydroxyalkyl radicals' formation through an interfacial phenomenon between HASS with  $\text{CaO}_2$  granules applied in surface water (created with Biorender.com by E. Keliri ©).

### 3.2.4 Effect of CaO<sub>2</sub> granules dose on surface water quality characteristics

Physicochemical water characteristics (pH, conductivity, TDS, and Salinity) were monitored during the application of CaO<sub>2</sub> granules in surface water (Kouris Dam), presented in Chapter 3.2.3.1. A noticeable increase in all measured parameters was captured, however pH exceeded the permissible limits for surface water when high CaO<sub>2</sub> concentration applied (Figure 20). The application of granules caused a quick increase of the initial pH of Kouris Dam (pH=8.8) and ranged between 9.5 and 10 after granules addition. Total dissolved solids, salinity and conductivity in all applied concentrations were found within the acceptable range for surface waters (Figure S 6 – 8) during the 48 h of granules' contact with water. Based on the results, caution should be taken when granules are applied in surface waters since the released by-product of the reaction, calcium hydroxide, significantly elevates the pH of the matrix.

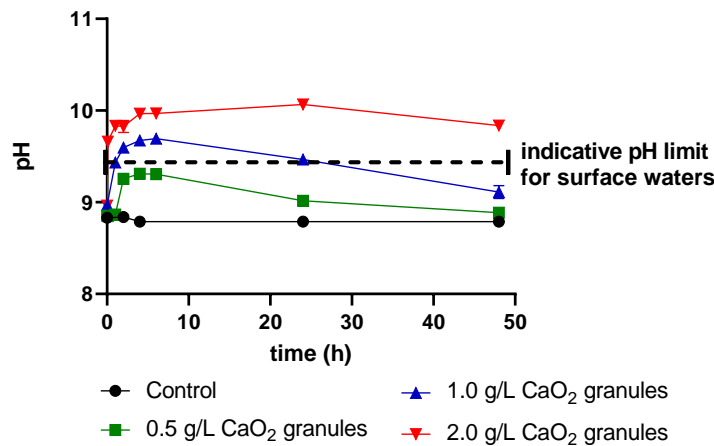


**Figure 20.** Recorded pH values after the addition of 0.5 - 2.0 g L<sup>-1</sup> CaO<sub>2</sub> granules in Kouris Dam surface water.

The obtained results revealed that humic substances and microelements found in the water matrix enhances the releasing capacity of granules (interfacial mechanisms) and result in higher accumulative concentrations of H<sub>2</sub>O<sub>2</sub> than those found in MQ-water. On the other hand, nutrients, organic and inorganic load, interact with the released oxidant leading to its rapid consumption, making it less available for other contaminants. Overall, CaO<sub>2</sub> granules showed a sufficient releasing capacity of H<sub>2</sub>O<sub>2</sub> in surface waters, making them a promising treatment option to mitigate cyano-HABs. Also, their ability to gradually release the oxidant for as long as 24 hours after addition, gives a good indication about their potency for treatment application as it can stimulate the multiple

doses of H<sub>2</sub>O<sub>2</sub>, resulting in more effective treatments than single high dose of liquid H<sub>2</sub>O<sub>2</sub>.

### 3.2.5 Cyano-HABs treatment with CaO<sub>2</sub> granules vs. liquid H<sub>2</sub>O<sub>2</sub>

#### Treatment of *Microcystis* sp.

CaO<sub>2</sub> granules concentrations (0.5 – 2 g L<sup>-1</sup>) used for cyano-HABs mitigation exhibited different efficiencies and impact on the *Microcystis* sp. (Chroococcales order) spiked in Kouris surface water matrix. The average initial instantaneous fluorescence (Ft) and quantum yield at λ = 620 nm, were 8400±200 RFU and 0.35, respectively. All the applied concentrations successfully treated the *Microcystis* sp. as the corresponding Ft values in raw fluorescence units (RFU) significantly decreased compared with the control (Figure 21 A); and the quantum yield of PSII measured as Fv/Fm was as low as 0.0 after 24 hours of treatment confirming the destruction of cyanobacterial cells (Figure 21 B). Quantified residual H<sub>2</sub>O<sub>2</sub> ranged between 0.5 and 1.2 mg L<sup>-1</sup> during the first 2 hours of treatment and then it dropped, meaning that the released oxidant was immediately reacting with the contaminant, resulting in no residual effect.

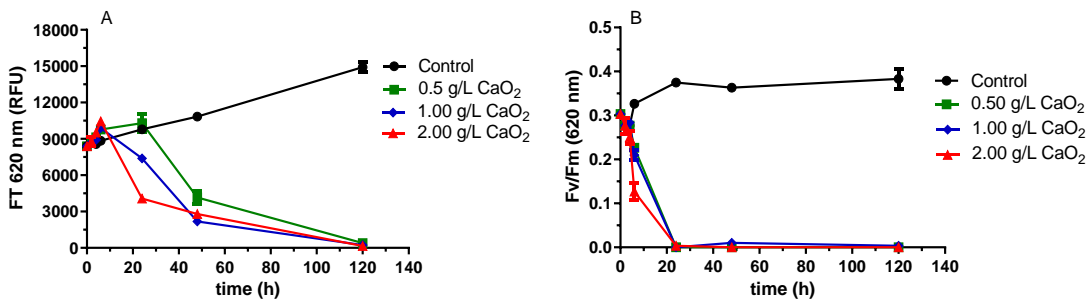


**Figure 21.** (A) Ft at λ=620 nm in raw fluorescence units (RFU), and (B) Quantum Yield at λ=620 nm during *Microcystis* sp. treatment with 0.5-2.0 g L<sup>-1</sup> CaO<sub>2</sub> granules.

The physicochemical water characteristics during treatment varied with the pH to be the most susceptible to changes. Especially, 2 g L<sup>-1</sup> CaO<sub>2</sub> granules resulted in pH higher than 9.5 at t = 24 hours, but then slightly decreased to an acceptable range at t= 48 hours (Figure 22). The rest concentrations had minimal effect on pH, conductivity increased around 60 μS/cm equally in all applied concentrations and the rest parameters were affected, however the values were within the expected ranges for surface waters.

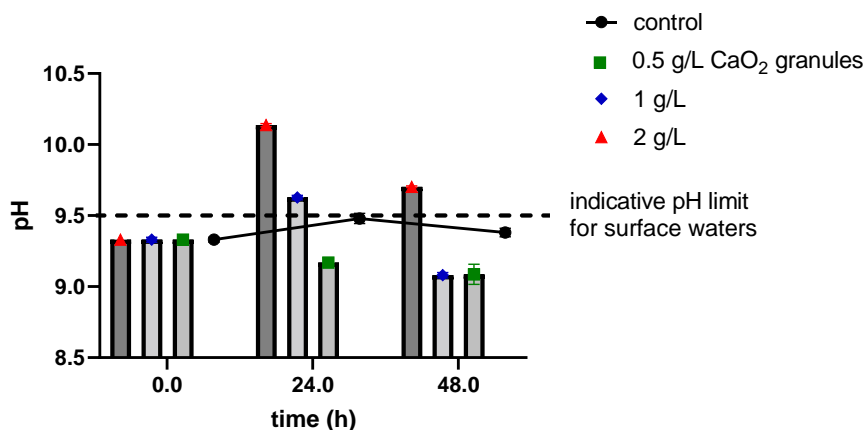


**Figure 22.** pH values at t=0, 24, and 48 h of *Microcystis* sp. treatment with 0.5, 1.0 and 2.0 g L<sup>-1</sup> CaO<sub>2</sub> granules.

To compare the treatment efficiency with the direct application of H<sub>2</sub>O<sub>2</sub>, treatment with liquid H<sub>2</sub>O<sub>2</sub> was performed under the same conditions. Treatment with 3 mg L<sup>-1</sup> H<sub>2</sub>O<sub>2</sub> was inefficient to treat the *Microcystis* sp. specie since the quantum yield of PSII was completely restored 48 hours after the oxidant addition, meaning that some cells remained unaffected and started to photosynthesize again (Figure 23). Treatment with 6 and 12 mg L<sup>-1</sup> H<sub>2</sub>O<sub>2</sub> caused significant reduction of cyano-HABs after the 48 hours of treatment. The sharp Ft increase recorded during the first 6 hours of treatment indicate the release of phycocyanin pigment into the water due to cell destruction, which can be confirmed by the simultaneous decline of its QY at t=6 h. Physicochemical parameters during liquid H<sub>2</sub>O<sub>2</sub> treatment on *Microcystis* had less variations than CaO<sub>2</sub> granules addition.

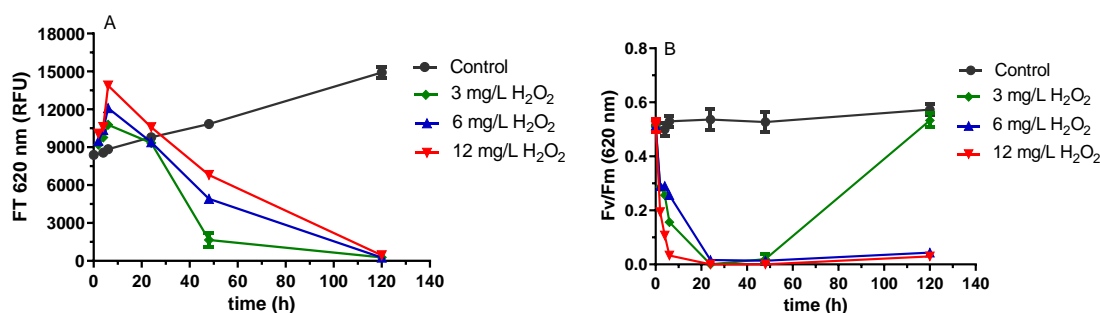


**Figure 23.** Ft at  $\lambda=620$  nm in raw fluorescence units (RFU) and QY (Fv/Fm) at  $\lambda=620$  nm during *Microcystis* sp. treatment with 3 - 12 mg L<sup>-1</sup> H<sub>2</sub>O<sub>2</sub>.

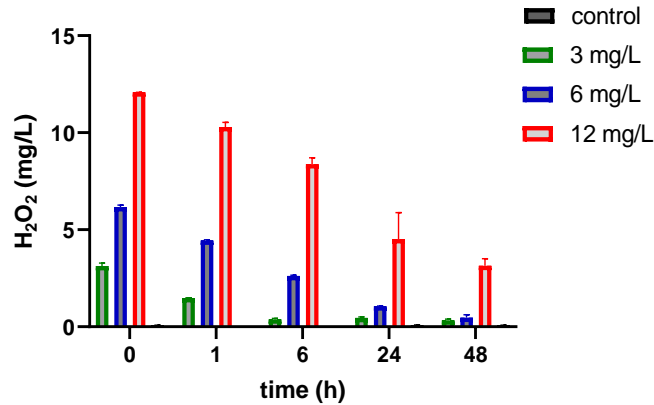


**Figure 24.** Residual H<sub>2</sub>O<sub>2</sub> concentration measured during *Microcystis* sp. treatment with 1-12 mg L<sup>-1</sup> H<sub>2</sub>O<sub>2</sub>.

Monitoring of the residual oxidant concentration during treatment showed instant consumption of the oxidant from the first hours of treatment. All added oxidant concentrations were totally consumed up to 24 hours of treatment as shown in Figure 22, except the addition of 12 mg L<sup>-1</sup> which had a residual effect of ~ 3 mg L<sup>-1</sup> H<sub>2</sub>O<sub>2</sub> after 48 hours of treatment, meaning that the oxidant was in excess (Figure 24). A slightly solution pH decrease was observed for all added H<sub>2</sub>O<sub>2</sub> concentrations. Specifically, pH decreased from 9.4 to 8.8, which means it reached a pH value close to the initial. Conductivity had similar rise as in CaO<sub>2</sub> granules treatments.

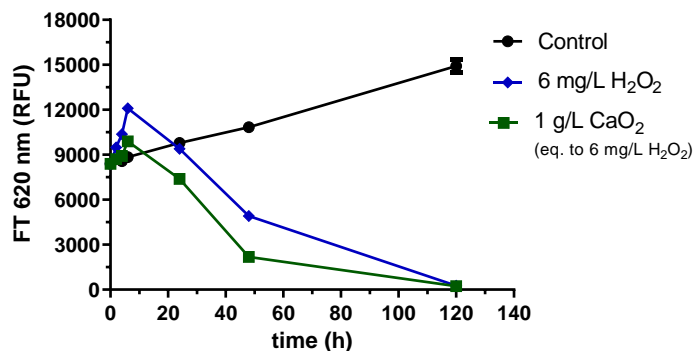


**Figure 25.** Comparison of Ft at  $\lambda=620$  nm in raw fluorescence units (RFU), between equal accumulative H<sub>2</sub>O<sub>2</sub> doses of 1 g L<sup>-1</sup> CaO<sub>2</sub> granules and 6 mg L<sup>-1</sup> liquid H<sub>2</sub>O<sub>2</sub>, during *Microcystis* sp. treatment.

Comparing the slow releasing granules with the liquid H<sub>2</sub>O<sub>2</sub> treatment in equal applied concentrations (e.g., 1.0 g L<sup>-1</sup> CaO<sub>2</sub> granules vs. 6 mg L<sup>-1</sup> H<sub>2</sub>O<sub>2</sub>) it is apparent that granules had faster response to the contaminant since it not only decreased significantly the cyano-cells into the matrix but also decomposed the released pigments from the first

few hours causing less increase in the water sample fluorescence (Figure 25). This finding supports further the increased efficiency of  $\text{CaO}_2$  for *in-lake* applications to mitigate both cyano-HABs and their side-effects (e.g., undesirable color due to pigments presence). Also, the minimum effective dose of  $\text{CaO}_2$  granules were much lower ( $0.5 \text{ g L}^{-1}$  eq. to  $3 \text{ mg L}^{-1}$  liquid  $\text{H}_2\text{O}_2$ ) than the minimum effective dose of liquid  $\text{H}_2\text{O}_2$  ( $6 \text{ mg L}^{-1}$ ). The only concern derived from the above study is the noticeably increase on the pH during  $\text{CaO}_2$  treatment due to the alkaline side product of the reaction, the  $\text{Ca}(\text{OH})_2$  precipitate.

#### **Treatment of *Aphanizomenon* sp.**

Same experimental as above was followed for the mitigation of a filamentous species, *Aphanizomenon* sp., in Kouris Dam water matrix. The  $\text{CaO}_2$  granules concentrations ( $0.50 - 1.25 \text{ g L}^{-1}$ ) used for cyano-HAB mitigation exhibited different efficiencies on the culture. The average initial instantaneous fluorescence (Ft) and quantum yield at  $\lambda = 620 \text{ nm}$ , were 7500 and 0.38, respectively. The lowest applied  $\text{CaO}_2$  granules dose ( $0.5 \text{ g L}^{-1}$ ) giving comparable Ft and QY values to the control, hence it was inefficient to treat the bloom (Figure 26). Higher concentrations of  $\text{CaO}_2$  granules significantly lower the Ft and achieved a zero measured QY, which indicates the total destruction of the cells and their photosynthetic ability. As shown in Figure 24 A, there was a noticeable increase in the phycocyanin fluorescence at  $t=24 \text{ h}$ , which indicates the presence of released pigments into water during the treatment. Even though the applied dose of  $1 \text{ g L}^{-1}$   $\text{CaO}_2$  granules resulted in a successful mitigation, it was not sufficient to also degrade the released phycocyanin, even after 120 h of treatment. In contrary,  $1.5 \text{ g L}^{-1}$   $\text{CaO}_2$  granules achieved both, making it the most effective dose for *Aphanizomenon* sp. treatment. Quantification of the residual  $\text{H}_2\text{O}_2$  released from granules during treatment is depicted in Figure 27. Oxidant was rapidly consumed after the first 6 hours of treatment, leading to no residual  $\text{H}_2\text{O}_2$  concentration after 48 h of treatment.

The physicochemical water characteristics during treatment varied with pH being once again the most affected by the  $\text{CaO}_2$  granules addition. Concentrations higher than  $0.5 \text{ g L}^{-1}$   $\text{CaO}_2$  granules resulted in a pH above 9.5, which is the OCED upper threshold limit for acceptable pH in surface water (Figure 25). The pH remained high during the treatment. Conductivity slightly decreased 20-50  $\mu\text{S}$  in all samples in all applied concentrations.

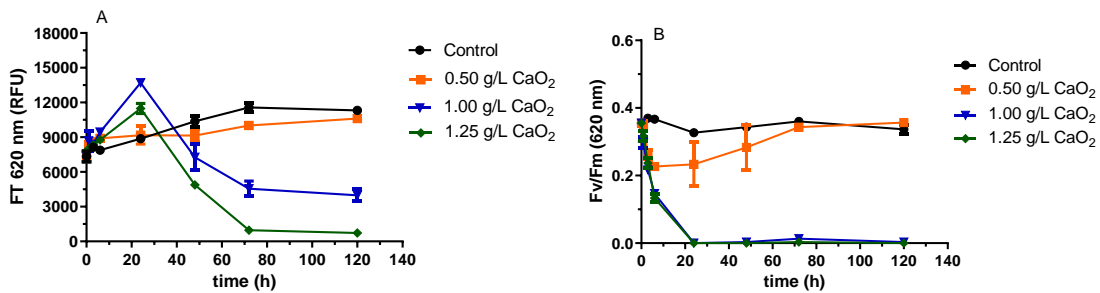


**Figure 26.** Ft at  $\lambda=620$  nm in raw fluorescence units (RFU), and (B) QY (Fv/Fm) during *Aphanizomenon* sp. treatment with 0.50, 1.0, and 1.25 g L<sup>-1</sup> CaO<sub>2</sub> granules.

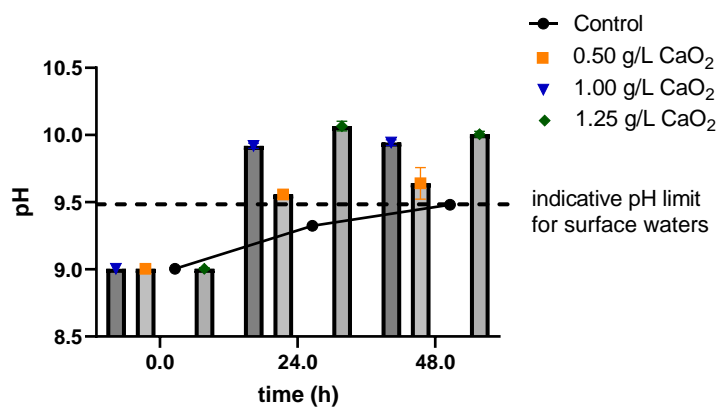


**Figure 27.** pH values at t=0, 24, and 48 h of *Aphanizomenon* sp. treatment with 0.50, 1.00 and 1.25 g L<sup>-1</sup> CaO<sub>2</sub> granules.

Again, to compare the treatment efficiency of granules with the corresponding doses of liquid H<sub>2</sub>O<sub>2</sub>, treatments with 3, 6, and 7 mg L<sup>-1</sup> H<sub>2</sub>O<sub>2</sub> were performed under the same conditions. Measured Ft values showed a sharp increase during the first 24 hours of treatment, which remained high for up to 72 hours after H<sub>2</sub>O<sub>2</sub> addition (Figure 28 A). As explained in previous experiments, this increase happens due to phycocyanin release into the water, which in this case is much higher and noticeable than in the case of *Microcystis* sp. This may be caused by the morphology of the cyanobacterium (filament vs. coccoid species). All the applied doses succeeded on reducing the QY at t=24, and 48 h, but filaments regained their photosynthetic ability after 72 hours since QY was partially restored at t=120 h of treatment. The application of liquid H<sub>2</sub>O<sub>2</sub> on *Aphanizomenon* sp. resulted in the enormous release of pigments, and doses were not sufficient to degrade both cyanobacteria and the released pigments.

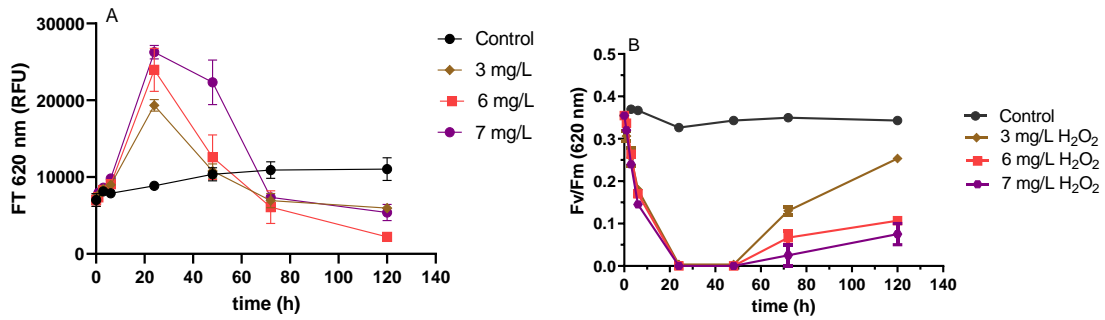


**Figure 28.** (A) Ft at  $\lambda=620$  nm in raw fluorescence units (RFU), and (B) QY (Fv/Fm) during *Aphanizomenon* sp. treatment with 3, 6, and 7 mg L<sup>-1</sup> H<sub>2</sub>O<sub>2</sub>.

Quantification of the residual H<sub>2</sub>O<sub>2</sub> in both treatments is depicted in Figure 29. The oxidant was rapidly consumed in the first 6 hours of treatment, reaching a concentration of less than 0.5 mg L<sup>-1</sup> H<sub>2</sub>O<sub>2</sub> at 24 hours of treatment.

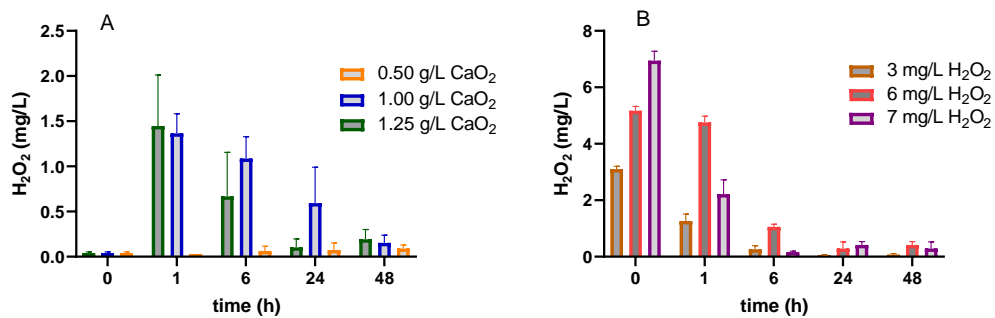


**Figure 29.** Residual H<sub>2</sub>O<sub>2</sub> concentration measured during *Aphanizomenon* sp. treatment with 0.50-1.25 g L<sup>-1</sup> CaO<sub>2</sub> granules.

Comparing granules with the liquid H<sub>2</sub>O<sub>2</sub> treatment of *Aphanizomenon* sp. in equal applied concentrations (e.g., 1.25 g L<sup>-1</sup> CaO<sub>2</sub> granules vs. 7 mg L<sup>-1</sup> H<sub>2</sub>O<sub>2</sub>) it is apparent that granules had faster response to the contaminant since it not only destructed the cyano-cells but also decomposed the released pigments from the first few hours, eliminating the fluorescence of water. Physicochemical parameters during liquid H<sub>2</sub>O<sub>2</sub> treatment on *Aphanizomenon* sp. had less variations than CaO<sub>2</sub> granules addition. Comparison between the treatment of filamentous and coccoid species, suggest that filaments demand higher doses of liquid H<sub>2</sub>O<sub>2</sub>, and they tend to release more pigments into the water matrix during the cell lysis process. Overall, a dose of 0.5 and 1 g L<sup>-1</sup> CaO<sub>2</sub> granules (eq. to 3, and 6 mg L<sup>-1</sup> H<sub>2</sub>O<sub>2</sub>) was sufficient to treat a *Microcystis* and an *Aphanizomenon* sp. bloom, respectively. As for liquid H<sub>2</sub>O<sub>2</sub>, instant doses of > 6 mg L<sup>-1</sup> were required to treat both cyano-cultures.

### 3.2.6 CaO<sub>2</sub> granules toxicity on invertebrates

When a novel chemical treatment method is proposed for *in-field* applications it is important to examine not only its efficiency towards the contaminant but also its impact on the non-targeted organisms. To decide on the optimum applied concentrations of CaO<sub>2</sub> granules for surface water treatment purposes, a toxicity study on *Echinogammarus veneris* sp. was conducted in river water matrix. The survival of species recorded at t=48 h was plotted with the added concentrations (0.50, 0.75, 1.00, 1.25, and 2.00 g L<sup>-1</sup>) of CaO<sub>2</sub> granules. The LD<sub>50</sub> was obtained by fitting the dose-respon curve on the non-linear Asymmetric EC<sub>50</sub> curve. As shown in Figure 30, 2.0 g L<sup>-1</sup> granules caused 100% mortality of Gammarus species, while 1.0 g L<sup>-1</sup> granules had a moderate effect on their survival. The LC<sub>50</sub> obtained by the survival curve proposed a lethal dose of 1.135 g L<sup>-1</sup> CaO<sub>2</sub> granules. The survival of species in each time interval is presented in Figure S 9, and the quantified H<sub>2</sub>O<sub>2</sub> during the experiment is depicted in Figure S 10. The findings of this study suggest that doses between 0.5 and 1.5 g L<sup>-1</sup> CaO<sub>2</sub> granules are considered a safe for the non-targeted species, while doses above the LC<sub>50</sub> should not be considered as treatment options.

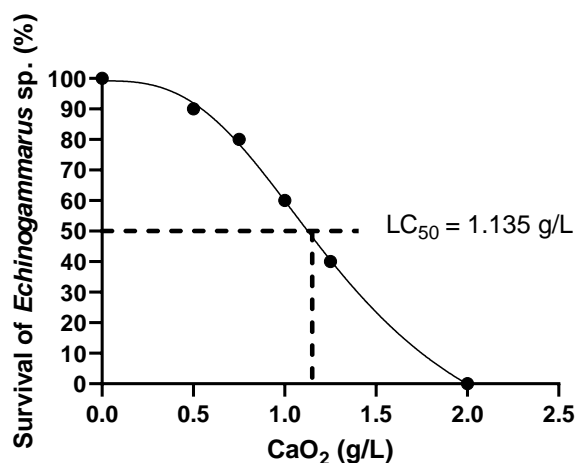


**Figure 30.** Survival of *Echinogammarus veneris* sp. at t=48 h of each CaO<sub>2</sub> granules dose (0.00, 0.50, 0.75, 1.00, 1.25, 2.00 g L<sup>-1</sup>) to determine the LC<sub>50</sub>.

Summarizing the results (Chapters 3.2.1-3.2.6), CaO<sub>2</sub> granules showed a sufficient H<sub>2</sub>O<sub>2</sub> releasing capacity and higher yield in comparison with MgO<sub>2</sub> granules, while the powdered form lacks the slow-releasing properties of granules. Dense cultures require high doses of liquid H<sub>2</sub>O<sub>2</sub>, while the gradual release by granules eliminated the residual effect. However, granules demonstrated some side effects which require further

exploration: (a) increase of matrix pH and turbidity due to  $\text{Ca}(\text{OH})_2$  precipitate, and (b) toxicity to invertebrates when doses  $> 1 \text{ g L}^{-1}$  are applied. The possibility to enclose the granules in a natural material in order to eliminate their direct contact with water and the non-targeted species as well as to capture the released precipitate, is studied in Chapter 3.2.7.

### 3.2.7 Calcium peroxide granules enclosed in fabrics – GEF systems<sup>4</sup>

#### 3.2.7.1 *Fabrics characterization*

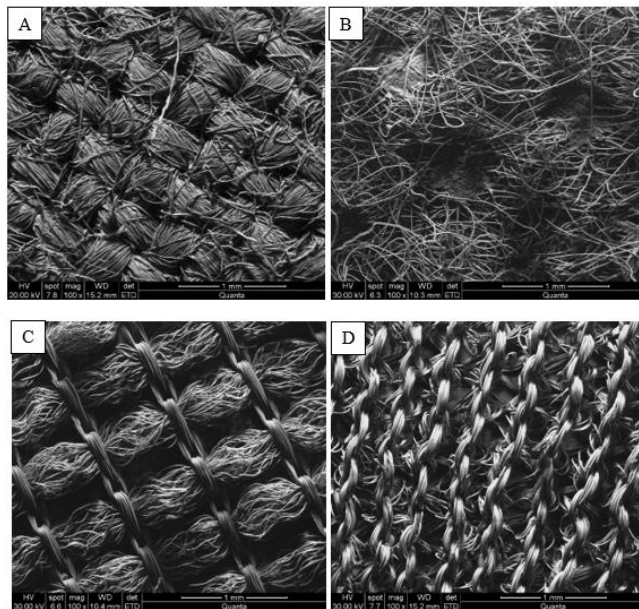
SEM was performed to characterize the morphology, pore area, and thickness of the four-textile materials utilized to enclose the granules. As shown in Scheme 22, SEM images showed fabrics of different material characteristics in regards with their morphology, pore shape and fiber networks' structure. The total surface area covered in each SEM image was measured with ImageJ software and it was  $7.7 \pm 0.1 \text{ mm}^2$ .

It can be observed from Scheme 22 (A) that fabric type A surface is smooth and clean, displaying a well-structured twilled fabric. The pores are distributed almost evenly in the surface of the fabric, resulting in a typically hierarchical pore network structure composed of cotton and polyester fibers. Scheme 22 (B) depicts the interlining fabric (fabric type B), with areas that are thermally compressed to shape visible dots on the fusing paper. Those spots have zero porosity and cover around 18% of its surface area. The fibers were not structurally distributed in the non-woven fabric and therefore pores are being shaped by the available spaces between the tangled fibers. Fabric type C depicted in Scheme 22 (C), had the most strict and repeatable structure with rectangle spaces between the twilled fabric that shape its pores. Parallel horizontal lines of fabric bundles are observed with vertically braided fabrics that are shaping knots to keep its fabric network. Scheme 22 (D) shows the 20 DEN tights comprised by knitted nylon fiber networks with nodes that allow the formation of pores between the intersected fabric lines.

---

<sup>4</sup> The findings of this study were published at *Chemical Engineering Journal Advances*: E. Keliri, et. al., Calcium peroxide ( $\text{CaO}_2$ ) granules enclosed in fabrics as an alternative  $\text{H}_2\text{O}_2$  delivery system to combat *Microcystis* sp., *Chemical Engineering Journal Advances*, Volume 11, 2022, 100318, <https://doi.org/10.1016/j.ceja.2022.100318>

The regular pore area ( $\text{mm}^2$ ) of each material was defined with the use of “ImageJ” software by measuring the surface area of 60 pores for each fabric and then calculating the average pore size, the standard deviation as well as identifying the minimum and maximum pore size to determine a surface area range (Table 10). For Fabric type C, pore radius and diameter are not available (N/A) since the shape of the pores were selected to be rectangular instead of circular, as it fitted better the pore shape. The total coverage of pores on the surface of each material was calculated and found to be 5.7%, 19%, 12% for fabric type A, C, and D, respectively (Scheme S 2, Appendix II).



**Scheme 22.** SEM images of fabric types A – D, under 100x magnification and a scale of 1 mm.

**Table 10.** Pore size range of fabrics Type A-C, mean pore size  $\pm$  SD ( $\mu\text{m}$ ), n=60 pores.

	Average pore surface area	$\pm$ SD	min	max	R	D	Thickness
Fabric	$\text{mm}^2$				mm		$\mu\text{m}$
<b>A</b>	0.016	0.006	0.007	0.033	0.07	0.14	260
<b>B</b>	0.004	0.003	0.001	0.020	0.04	0.08	200
<b>C</b>	0.113	0.022	0.072	0.157	N/A	N/A	170
<b>D</b>	0.009	0.005	0.003	0.024	0.5	0.1	554

### 3.2.7.2 H<sub>2</sub>O<sub>2</sub> Release kinetics by GEF systems

Following the same experimental procedure as in the direct application of CaO<sub>2</sub> granules in surface water, H<sub>2</sub>O<sub>2</sub> release curves were obtained for the GEF systems. As shown in Figure 31, all the enclosed concentrations in all fabrics except from GEF type D, exhibited a high H<sub>2</sub>O<sub>2</sub> releasing capacity. For instance, GEF systems resulted in a continuous release similar to their direct application in water and confirmed that granules can retain their ability to release H<sub>2</sub>O<sub>2</sub> when enclosed in fabric materials.

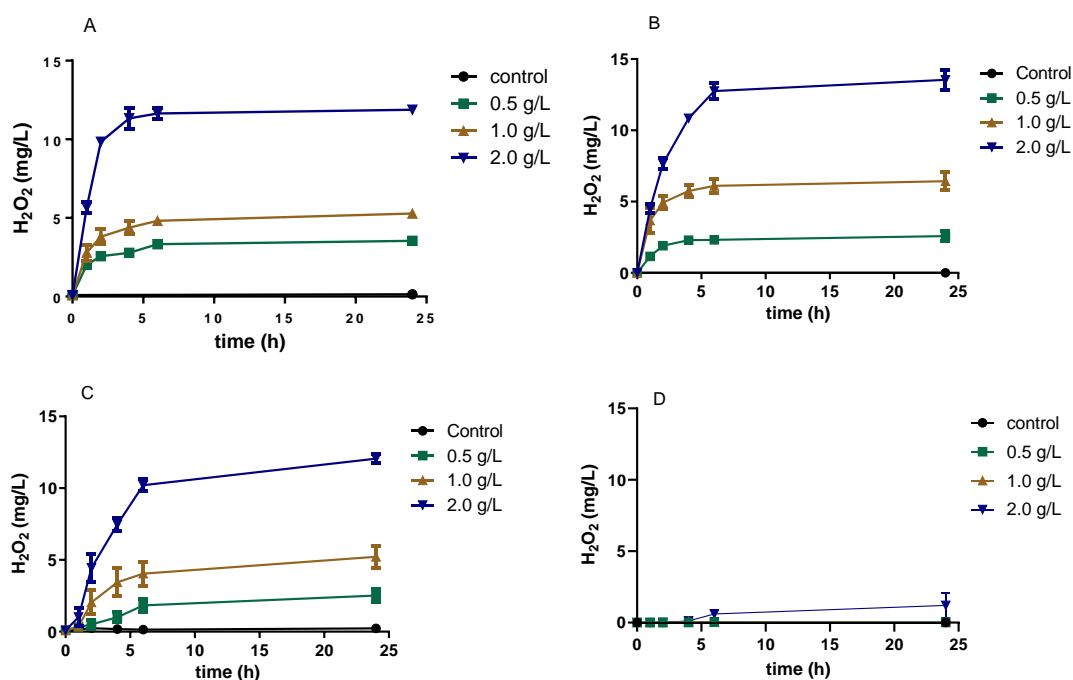


**Figure 31.** Release curves depicting the instantaneous H<sub>2</sub>O<sub>2</sub> concentration during a 24-h release experiment utilizing 0.5, 1.0, and 2.0 g L<sup>-1</sup> CaO<sub>2</sub> granules enclosed in fabric types (A) pocket lining, (B) interlining textile, (C) polyester netting, and (D) paper filter wrapped in tights' fabric.

The release curves follow a pseudo-first order association kinetics model and the calculated correlation coefficients showed that R<sup>2</sup> derived from the pseudo-zero-order model were much lower than the ones from the non-linear pseudo-first order model (Figure S 11), which is against the findings in literature which propose a pseudo-zero-order kinetics model for H<sub>2</sub>O<sub>2</sub> release by CaO<sub>2</sub> granules [69]. Correlation coefficients ranged between 0.63 and 0.99 for the non-linear pseudo-first order model (Figures 32, S 11) exhibiting a sufficient fit to the model for GEF types A, B and C. Those systems released similar H<sub>2</sub>O<sub>2</sub> concentrations compared with the ones released by the direct application of CaO<sub>2</sub> granules. In contrast, GEF type D released significantly lower H<sub>2</sub>O<sub>2</sub>

concentrations than the other GEF types ( $p < 0.05$ ), hence it was the only system that had a poor fit to the model. It also indicates a not as favorable delivery system for granules as the rest systems. The inability of  $\text{H}_2\text{O}_2$  to diffuse from the filter to the bulk of the solution could be either a result of its reaction with the filter itself or the porosity of the combined system (filter enrolled in tights). For GEF type D, the highest tested concentration of  $2 \text{ g L}^{-1}$  resulted in a maximum release of just  $1.2 \pm 0.9 \text{ mg L}^{-1} \text{ H}_2\text{O}_2$  at  $t=24$  hours, while GEF systems of type A, B and C released up to  $11.9 \pm 0.4 \text{ mg L}^{-1} \text{ H}_2\text{O}_2$ ,  $13.5 \pm 1.2 \text{ mg L}^{-1} \text{ H}_2\text{O}_2$ , and  $12.0 \pm 0.5 \text{ mg L}^{-1} \text{ H}_2\text{O}_2$ , respectively (Figures 31-32, Table S 7).

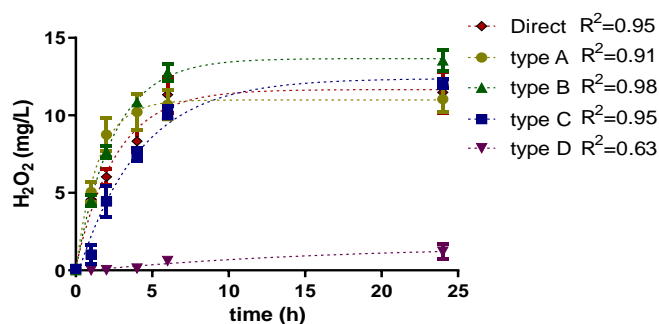


**Figure 32.**  $\text{H}_2\text{O}_2$  release kinetics by  $2.0 \text{ g L}^{-1} \text{ CaO}_2$  GEF types A – D, and no fabric, in a surface water (Kouris dam) fitted by non-linear pseudo-first order model:  $Y=Y_0 + (\text{Plateau}-Y_0) \cdot (1-\exp(-K \cdot x))$ .

#### Linear correlation between $\text{H}_2\text{O}_2$ yield and $\text{CaO}_2$ granules dose

The overall released concentration in GEF type A-C was the same ( $p > 0.1$ ) for each added dose. Therefore, a linear regression analysis was employed to find the correlation between  $\text{H}_2\text{O}_2$  yield and the applied  $\text{CaO}_2$  granules dose. The analysis showed a linear relationship between the two ( $R^2=0.97-0.98$ ), meaning that GEF exhibit the same behaviour as their direct application in water. The linear relationship shows that the  $\text{H}_2\text{O}_2$  yield depends on the  $\text{CaO}_2$  dose, hinting that the  $\text{H}_2\text{O}_2$  yield per  $\text{CaO}_2$  weight unit applied in water remains constant. Specifically,  $0.5$ ,  $1.0$ , and  $2.0 \text{ g L}^{-1} \text{ CaO}_2$  granules released around  $3.0 \text{ mg L}^{-1} \text{ H}_2\text{O}_2$ ,  $6.0 \text{ mg L}^{-1} \text{ H}_2\text{O}_2$ , and  $12.0 \text{ mg L}^{-1} \text{ H}_2\text{O}_2$ , respectively. Those yields were obtained by all tested fabrics except type D that gave a significantly lower  $R^2$  value, which was anticipated based on its minimal  $\text{H}_2\text{O}_2$  releasing potential (Figure 33, Table S 7).

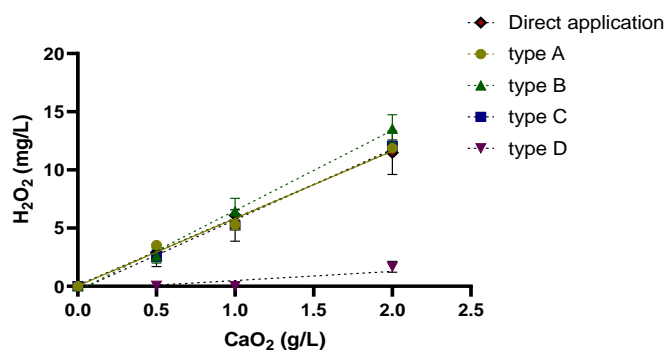


**Figure 33.** Linear correlation between H<sub>2</sub>O<sub>2</sub> yield at t=24 hours and CaO<sub>2</sub> granules' dose directly applied (no fabric) and applied enclosed in GEF types A – D.

The obtained linear equation could be a useful tool on deciding on the CaO<sub>2</sub> granules doses during an *in-lake* application if the required overall H<sub>2</sub>O<sub>2</sub> concentration is known, estimated, or indicated by previous experiments. These results confirm previous studies that suggested a linear relationship between the H<sub>2</sub>O<sub>2</sub> yield and the added CaO<sub>2</sub> granules dose [72] and support the findings of the present study that the release is not following a pseudo-zero-order but pseudo-first-order kinetics model, as explained in section 3.2.7.2.

### 3.2.7.3 Treatment efficiency

The effectiveness of the proposed H<sub>2</sub>O<sub>2</sub> delivery systems (GEF types A to C) on the treatment of a *Microcystis* sp. bloom was investigated. Each GEF system was evaluated by recording the phycocyanin instantaneous fluorescence (Ft) and quantum yield (QY) of the photosystem II at  $\lambda = 620$  nm throughout a treatment that lasted for 3 days. The experimental conditions were kept the same in all experiments, with the initial fluorescence and QY to be at  $8000 \pm 700$  RFU, and  $0.45 \pm 0.05$ , respectively.

Starting from the highest enclosed dose of  $2.0 \text{ g L}^{-1}$  in GEF type A, it was not sufficient to significantly reduce the Ft and QY, while in GEF types B and C a major reduction of Ft (87.5 – 91%) at t=48 h was observed. This reduction was also reflected in the respective quantum yields of GEF type B and C, where the recorded QY reached almost zero value (Figure 34). Also, a noticeable rise in Ft values can be observed in the first hours of treatment with high concentration of granules. This can be explained by the released pigments from the lysed cells, as although the recorded Ft values showed an increase in phycocyanin concentration, the QY significantly declined. The measured QY represents the ability of the cells to photosynthesize, thus rapid decline of QY verified

that the increase in Ft was due to phycocyanin release into the matrix, while the decline in Ft afterwards is a result of simultaneous cyanobacteria and their pigments' degradation by the excess or residual oxidant. The remaining concentrations enclosed in GEF type A did not affect the photosynthetic parameters, as the obtained values were identical to the control. The lowest concentration enclosed in GEF type B ( $0.5 \text{ g L}^{-1}$ ) was not sufficient to destroy the cells, while  $1.0 \text{ g L}^{-1}$  GEF type B released enough  $\text{H}_2\text{O}_2$  to destroy the cells ( $\text{QY} < 0.2$ ) but not sufficient to degrade the pigmentation released from lysed cells ( $\text{Ft} > 5000 \text{ RFU}$ ). As for the GEF type C, even the lower concentration caused a significant reduction to the Ft values, as well as the photosynthetic activity. Even though, QY initially dropped when  $0.5 \text{ g L}^{-1}$  were applied, it was completely restored after 24 h of treatment, indicating the regrowth of cyano-cells. Overall, GEF type C in concentrations  $1.0$  and  $2.0 \text{ g L}^{-1} \text{ CaO}_2$  achieved the higher treatment efficiency in terms of both photosynthetic parameters, while GEF type A was the least efficient delivery system since it only caused a slight decrease at the highest applied dose of  $2.0 \text{ g L}^{-1} \text{ CaO}_2$  granules.

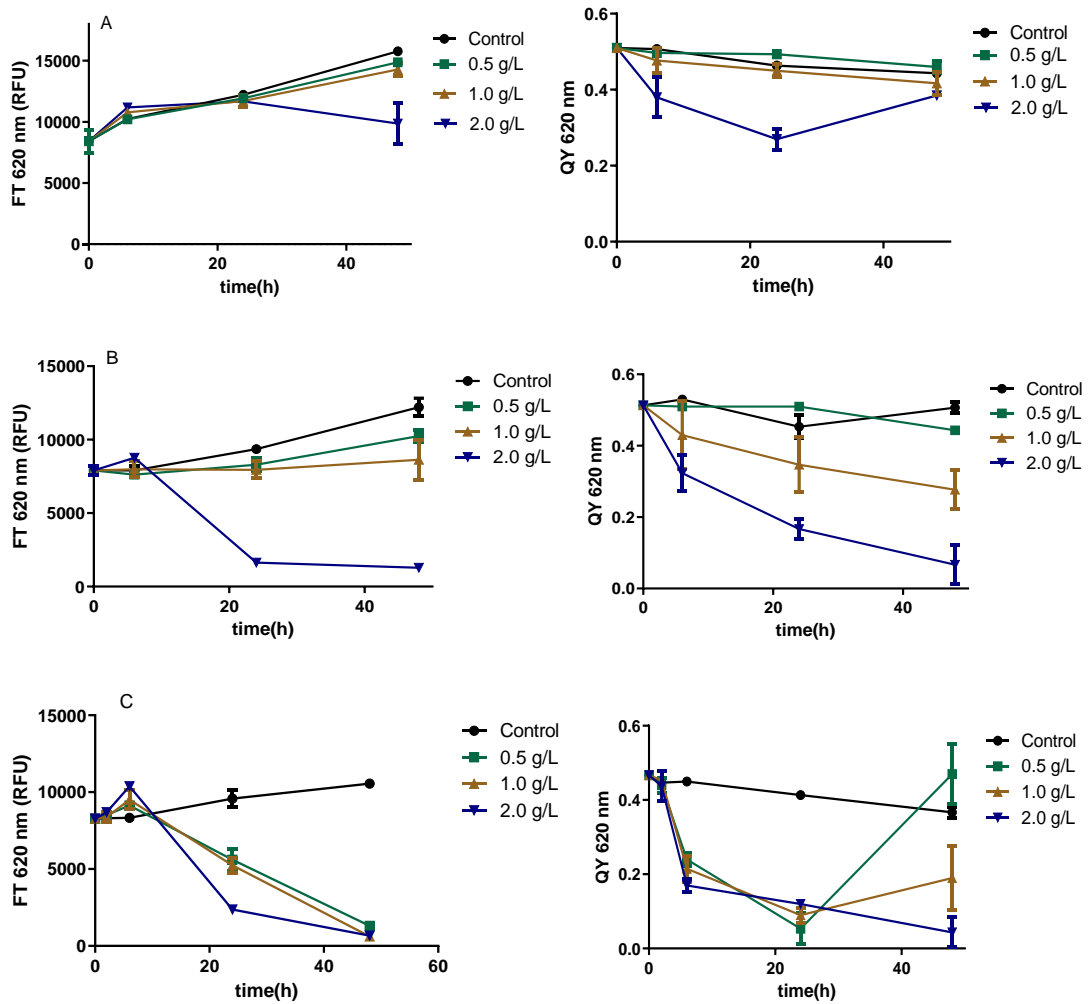
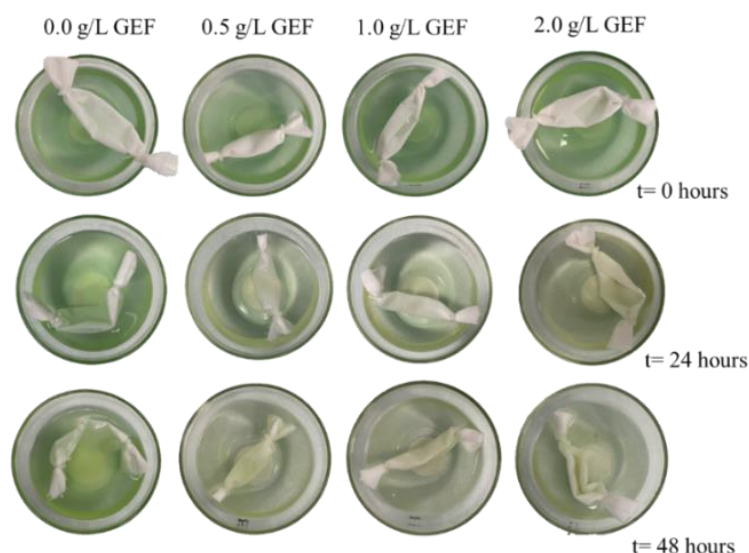


**Figure 34.** Effect of 0.5, 1.0, and 2.0 g/L CaO<sub>2</sub> granules enclosed in fabric types (A) pocket lining, (B) interlining textile, (C) polyester netting, on phycocyanin Ft (left), and QY at  $\lambda=620$  (right) during the treatment of *Microcystis* sp. in surface water.

During the bench-scale experiments, attention was given to ensure that granules were folded as a monolayer inside the fabric material, to be totally submerged into the water which allowed their continuous contact through the pores of the material (Scheme 23). The percentage of the upper layer of surface water covered by GEF system in the experiments were 5.3%, 14.2%, and 29.5% for GEF 0.5, 1.0, and 2.0 g L<sup>-1</sup> CaO<sub>2</sub> granules, respectively. Based on the obtained results, the surface area of GEF systems applied on the upper layer of surface water (floating on the top) is sufficient to mitigate a dense Chroococcales bloom.



**Scheme 23.** Treatment of *Microcystis* sp. with GEF in concentrations of 0.0 (control), 0.5, 1.0, and 2.0 g/L CaO<sub>2</sub> granules enclosed in fabric type C, at t=0, 24, and 48 hours.

The concentration of H<sub>2</sub>O<sub>2</sub> was monitored throughout the treatment to determine the instantaneous residual oxidant concentration. Even though a noticeable amount of accumulative H<sub>2</sub>O<sub>2</sub> was quantified during the release experiments by all GEF doses, instantaneous H<sub>2</sub>O<sub>2</sub> concentrations at t=6, 24, and 48 hours were below 1.0 mg L<sup>-1</sup>, showing that the oxidant was rapidly consumed by the contaminant and/or the matrix, once was released.

#### 3.2.7.4 Physicochemical water characteristics

Physicochemical water parameters were monitored during treatment with GEF to evaluate their effect on matrix pH, conductivity, salinity, and TDS. Matrix pH is one of the most important parameters that required monitoring since it is important to avoid high pH values that caused by the side-product of the reaction which is released Ca(OH)<sub>2</sub> into the waterbody. This type of side-effects when applying a chemical treatment method can disrupt the ecosystem and potentially reduce water quality making it inappropriate for drinking purposes. A slight increase in water pH (pH=9.5) was observed in matrix where fabric type A and B were added, while where type A was added no evident increase was recorded (Figure 35). Still, all the encapsulated systems kept the pH lower than 10, while the directly applied granules significantly increased the pH above 11, which is exceeding the expected limits for surface water. Salinity, TDS, and conductivity were found to be

within acceptable ranges for freshwater during the treatment, and the Salinity and TDS were found to be the least affected parameters (Figures 36).

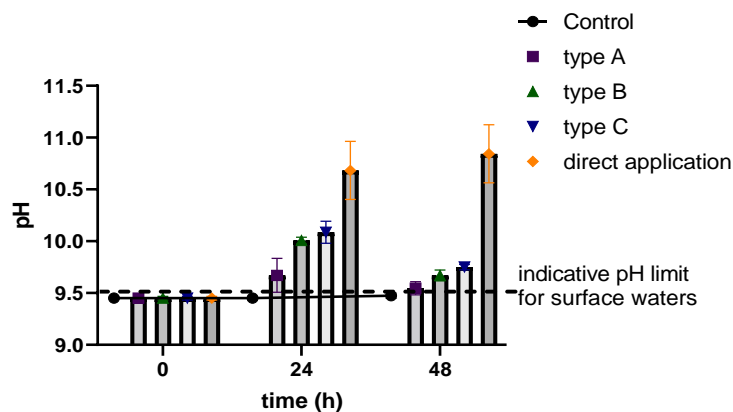


**Figure 35.** Changes in pH during treatment of *Microcystis* sp. in surface water by  $2.0 \text{ g L}^{-1} \text{ CaO}_2$  granules direct application and GEF type A – C.

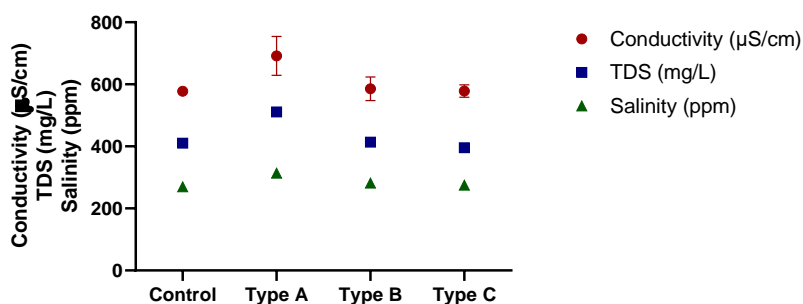


**Figure 36.** Conductivity, TDS, and Salinity at  $t=48$  hours of *Microcystis* sp. in surface water treatment by adding  $2.0 \text{ g L}^{-1} \text{ CaO}_2$  enclosed in GEF type A – C.

The surface area of fabric type C was visibly higher than the other textiles, which may have caused the partial release of  $\text{Ca(OH)}_2$  precipitate into the water. The particle size of the  $\text{Ca(OH)}_2$  powder ranges from  $0.5$  to  $20 \mu\text{m}$  with the most common ones to be around  $15 \mu\text{m}$  [101]. The pores of material A ( $16 \pm 0.6 \mu\text{m}$ ) could barely limit the the release of  $\text{Ca(OH)}_2$  into the water, while the pores of type B ( $4 \pm 0.3 \mu\text{m}$ ) had higher chances to restrict the release of the powder into the bulk. Differences between the direct application of  $\text{CaO}_2$  granules and GEF when  $2 \text{ g L}^{-1}$  were applied can be observed in Figure 35, where all GEF systems had minimal variations, while direct application caused a steep increase to pH above 11. Since all GEF systems affected pH similarly, it is likely that  $\text{Ca(OH)}_2$  powder had particle size close to the pores' surface area of the materials, that allowed its capture into the fiber networks, where the knots were.

### 3.2.7.5 GEF toxicity on invertebrates

The toxicity effect of CaO<sub>2</sub> granules directly applied in surface water showed that LD<sub>50</sub> is slightly above 1 g L<sup>-1</sup>. GEF systems enclosing 0.5, 1.0 and 2.0 g L<sup>-1</sup> CaO<sub>2</sub> granules were examined for their lethal effect on Gammarus species, in comparison with equal doses H<sub>2</sub>O<sub>2</sub>. Figure 37 summarizes the survival (%) of tested organisms during their 48 hours contact with the applied oxidants (Figure S 12). Results showed that GEF systems caused no significant mortality of the species (<10%), thus the curve was well above the LD<sub>50</sub> value. It is important to note that the granules allowed for higher tolerance of the gammarus species to H<sub>2</sub>O<sub>2</sub>, as LC<sub>50</sub> values were around 5 mg L<sup>-1</sup> and 7 mg L<sup>-1</sup> for liquid H<sub>2</sub>O<sub>2</sub> and released by free granules, respectively. Enclosing the granules in fabrics eliminated the toxicity of the granules, which was mostly coming from the precipitate of the reaction. In general, concentrations higher than 5 mg L<sup>-1</sup> H<sub>2</sub>O<sub>2</sub> (released or directly applied) effect the zooplankton wellness.

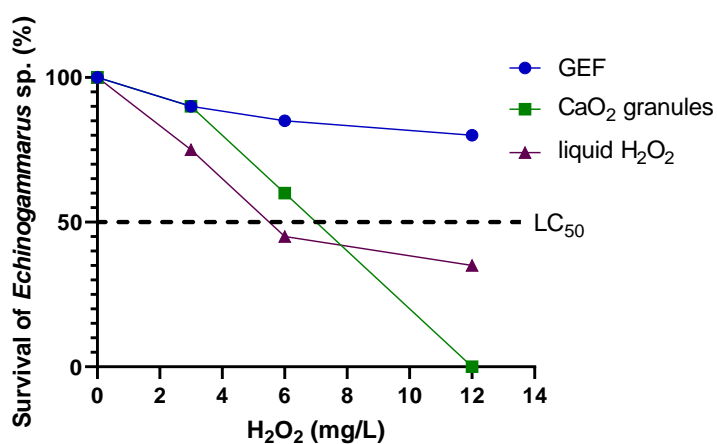
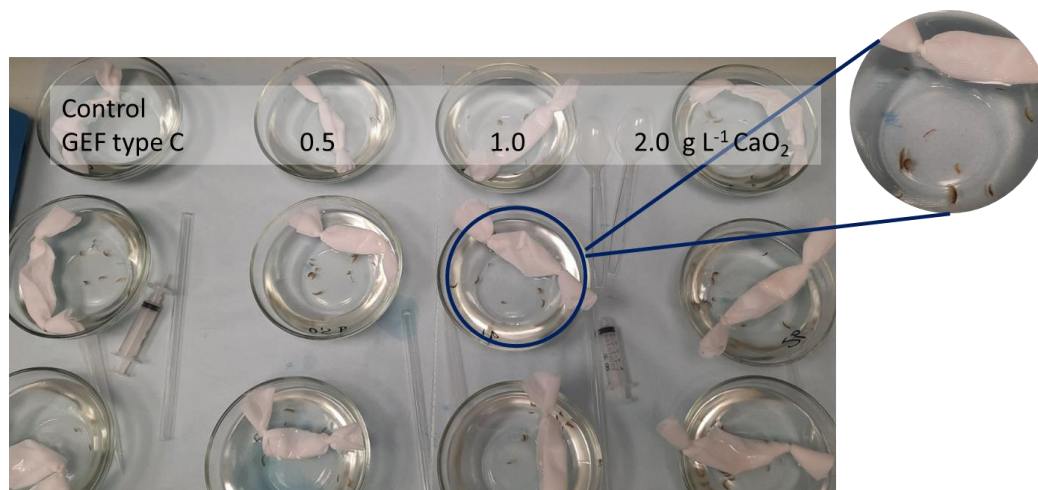


**Figure 37.** Survival rate (%) of invertebrate species in river water at t=48 h, and doses of 0, 3, 6, and 12 mg L<sup>-1</sup> H<sub>2</sub>O<sub>2</sub> applied in the form of GEF, granules, and liquid H<sub>2</sub>O<sub>2</sub>.



**Scheme 24.** Experimental set-up of toxicity study on *Echinogammarus veneris* by applying 0.5, 1.0, and 2.0 g L<sup>-1</sup> GEF type C in river water matrix. Photo was taken at = 48 h and the survival of species during the experiment is visible.

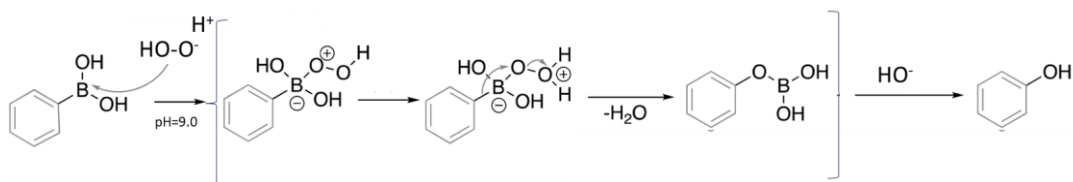
### 3.3 Peroxymonosulfate (PMS) – OXONE<sup>®</sup>

#### 3.3.1 Development of quantification method<sup>5</sup>

Arylboronic acids are derivatives of the boric acid, in which one of the hydroxyl bonds breaks, yielding a new Boron-Carbon bond. As proposed in literature, phenylboronic acids react with peroxides under mild alkaline conditions to generate phenolates (Scheme 25). This reaction is extensively studied as an easy, efficient, and “green” method to produce phenolates in chemical synthesis processes [102]. Recently, the reaction was utilized for the development of H<sub>2</sub>O<sub>2</sub> chemo-selective probes to detect residual H<sub>2</sub>O<sub>2</sub> in food and agriculture products [103]. Specifically, nitrophenyl boronic acids (NPBA) were firstly introduced by Su et. al. (2011) [104] for the direct colorimetric determination of H<sub>2</sub>O<sub>2</sub> due to the generation of 4-Nitrophenol which is in the visible spectrum.

---

<sup>5</sup> For the method a Cyprus patent application, CY202000002 (September 2020); US Provisional patent application (USPTO, October 2020); and a US patent application (USPTO, 2021) was filed through the hosting Institution, Cyprus University of Technology. The patent application fees were funded by Cyprus Seeds, the Research and Innovation Foundation and the Cyprus University of Technology.



**Scheme 25.** Reaction mechanism of *ipso*-hydroxylation of phenylboronic acid in the presence of hydrogen peroxide, that lead to the formation of phenolate ion. [105] (modified by E. Keliri <sup>©</sup>).

Our research group aimed to explore the reaction between p-NPBA and HO-O<sup>•</sup> derived from peroxymonosulfates as a possible quantification method in aquatic samples. Other studies also employed this reaction to determine peroxide-containing chemicals (e.g., urea-hydrogen peroxide). Reaction between p-NPBA and PMS showed that peroxymonosulfates react with para-nitrophenyl boronic acid to form para-nitrophenol, with peak absorbance at  $\lambda=405$  nm. The product of the reaction has a pKa of 7.15 in water, thus when deprotonated, gives the recorded absorbance at 405 nm, explained by the yellowish color of the solution. The reaction time was initially ~ 5-10 minutes but changing the molarities of p-NPBA solution and the volume proportions of the reagents, we achieved a rapid reaction (<1 sec) with accurate results. The accuracy was tested by adding known concentrations of PMS in pure water matrix and quantifying the residual concentration through the proposed reaction. Stability tests showed a stable UV-read at  $\lambda=405$ nm during a 28-hrs monitoring of p-nitrophenol in the reaction medium (Figure 38), under dark conditions, whereas an unstable reaction was detected in the presence of solar light. The findings indicate a photosensitive reaction, that it can be utilized only in the absence of radiation, where the reaction product is stable.

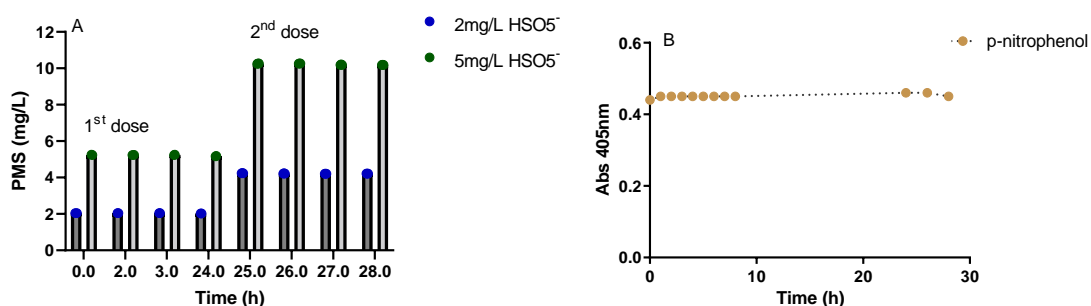


**Figure 38.** (A) Quantification of 2 and 5 mg L<sup>-1</sup> PMS added in MQ-water at t=0 and t=25 h, (B) Absorbance at  $\lambda=405$  nm of the following mixture: 2 mL of 50 uM PMS sample with 2 mL of 2 mM p-NPBA stock solution, under dark conditions.

### 3.3.2 PMS vs. H<sub>2</sub>O<sub>2</sub> (in equal peroxide doses) toxicity on invertebrates

Toxicity study on invertebrates' species, *Echinogammarus veneris* sp., was conducted in river water matrix - their surviving environment - by applying doses of 1 - 5 mg L<sup>-1</sup> H<sub>2</sub>O<sub>2</sub> and PMS (equal to H<sub>2</sub>O<sub>2</sub> molarity)<sup>6</sup>. To test if the application method is also affecting their wellness, single dose and multiple doses experiments were performed under the same experimental conditions. Both oxidants showed a moderate effect on the zooplankton species, recording mortalities of less than 50%. Liquid H<sub>2</sub>O<sub>2</sub> doses of 3 and 4 mg L<sup>-1</sup> showed a slight decrease on the survival rate of the species at t=6 h after oxidant addition, while 5 mg L<sup>-1</sup> H<sub>2</sub>O<sub>2</sub> caused an obvious reduction close to 50% (Figure 39 A). PMS had no effect in any of the concentrations tested, as it maintained a survival rate of 90-100% in all added concentrations (Figure 39 B).

Quantification of residual oxidant during the toxicity study showed that H<sub>2</sub>O<sub>2</sub> was rapidly consumed by the components of the matrix (and/or interacted with zooplankton species), while the retention of KHSO<sub>5</sub> in the matrix was longer, causing a residual effect. In terms of treatment, the residual effect of PMS indicates a possibly higher treatment efficiency. Comparing the survival of gammarus between 5 mg L<sup>-1</sup> of H<sub>2</sub>O<sub>2</sub> and KHSO<sub>5</sub>, the latter one is considered safer for surface water applications in respect to the non-targeted species.

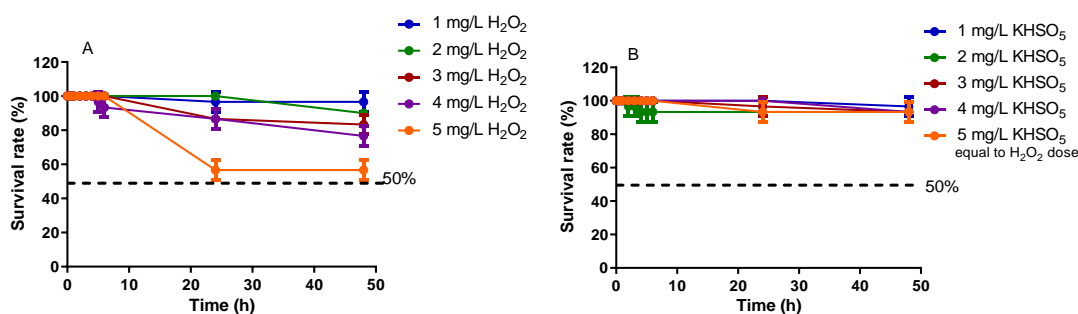


**Figure 39.** Survival rate (%) of *Echinogammarus veneris* sp. in river water matrix with (A) 1 – 5 mg L<sup>-1</sup> liquid H<sub>2</sub>O<sub>2</sub>, and (B) PMS generated by OXONE (in equal molarities).

<sup>6</sup> Calculated molarities of PMS equal to 1 – 5 mg L<sup>-1</sup> of peroxide are presented in Table S 8, Annex II.

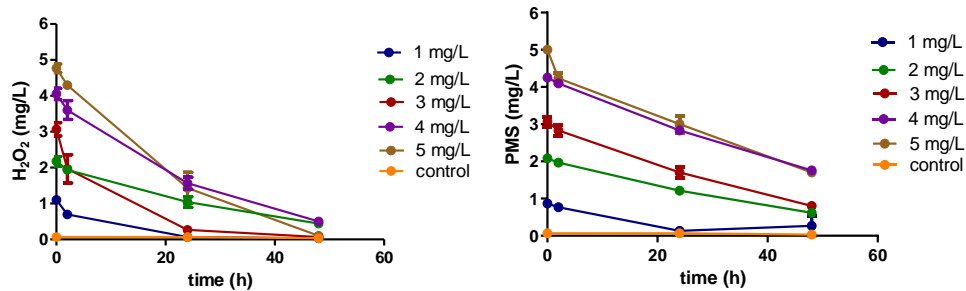


**Figure 40.** Residual oxidant concentration measured during toxicity study on *Echinogammarus veneris* sp. treatment with (A) 1 – 5 mg L<sup>-1</sup> liquid H<sub>2</sub>O<sub>2</sub>, and (B) PMS (in equal molarities).

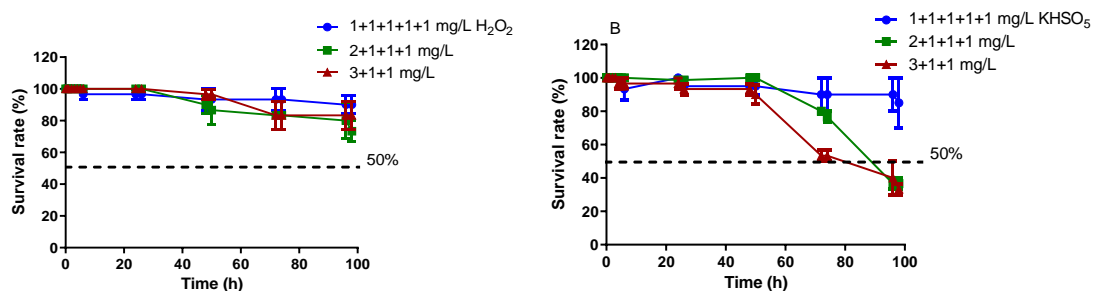


**Figure 41.** Survival rate (%) of *Echinogammarus veneris* sp. in river water matrix with multiple doses of (A) liquid H<sub>2</sub>O<sub>2</sub> and (B) PMS (in equal molarities). [C]<sub>tot</sub> = 5 mg L<sup>-1</sup>.

Repeated doses of each tested oxidant on *Echinogammarus veneris* sp. resulted in distinct differences compared to their single high doses. As shown in Figure 41, the survival rate of gammarus when multiple doses of H<sub>2</sub>O<sub>2</sub> were applied remained high (70-90%), while multiple doses of KHSO<sub>5</sub> caused higher mortality to the species (S.R.=30-50%). The effect on Gammarus was noticeable after the 3<sup>rd</sup> dose of KHSO<sub>5</sub> (1 mg L<sup>-1</sup>), as the survival rate dropped from 100% at t= 48 h to 30% at t=96 h. This can be attributed to the residual effect of PMS which causes its higher cumulative concentration into the matrix, hence longer contact with the tested organisms (Figure 42 B).

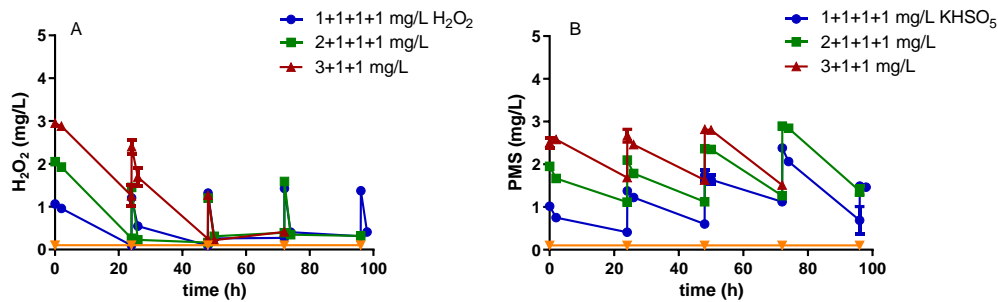


**Figure 42.** Residual oxidant concentration measured during toxicity study on *Echinogammarus veneris* sp. with multiple doses of (A) liquid H<sub>2</sub>O<sub>2</sub>, and (B) PMS. [C]<sub>tot</sub> = 5 mg L<sup>-1</sup>.

### 3.3.3 Treatment of river water spiked with cultivated cultures and *Echinogammarus veneris* sp. with PMS vs. liquid H<sub>2</sub>O<sub>2</sub> (single and multiple dosing)

#### 3.3.3.1 *Microcystis* sp.

##### Single dose treatment

All H<sub>2</sub>O<sub>2</sub> concentrations were effective towards the coccoid specie, *Microcystis* sp. with initial Ft =9000 RFU at λ=620 nm and QY=0.46. Increased phycocyanin release by the cells was again captured during the treatment with liquid H<sub>2</sub>O<sub>2</sub>, especially when 5 mg L<sup>-1</sup> were added. All concentrations except 1 mg L<sup>-1</sup> H<sub>2</sub>O<sub>2</sub> resulted in significant decline on the Ft and QY values, however water samples treated with 1 - 3 mg L<sup>-1</sup> restored their quantum yield at t=48 hours, resulting in an inefficient treatment (Figure 43).

PMS effectively treated the bloom in concentrations higher than 3 mg L<sup>-1</sup> KHSO<sub>5</sub> moalr equiv. of H<sub>2</sub>O<sub>2</sub>. During the treatment, PMS demonstrated again a longer residual effect, compared to liquid H<sub>2</sub>O<sub>2</sub> which declined rapidly at 24 hours of treatment. Both oxidants were consumed by the end of the experiment, meaning that none was in excess at t=48 h and that *Microcystis* at the specific conditions demanded higher doses for better mitigation efficiencies.

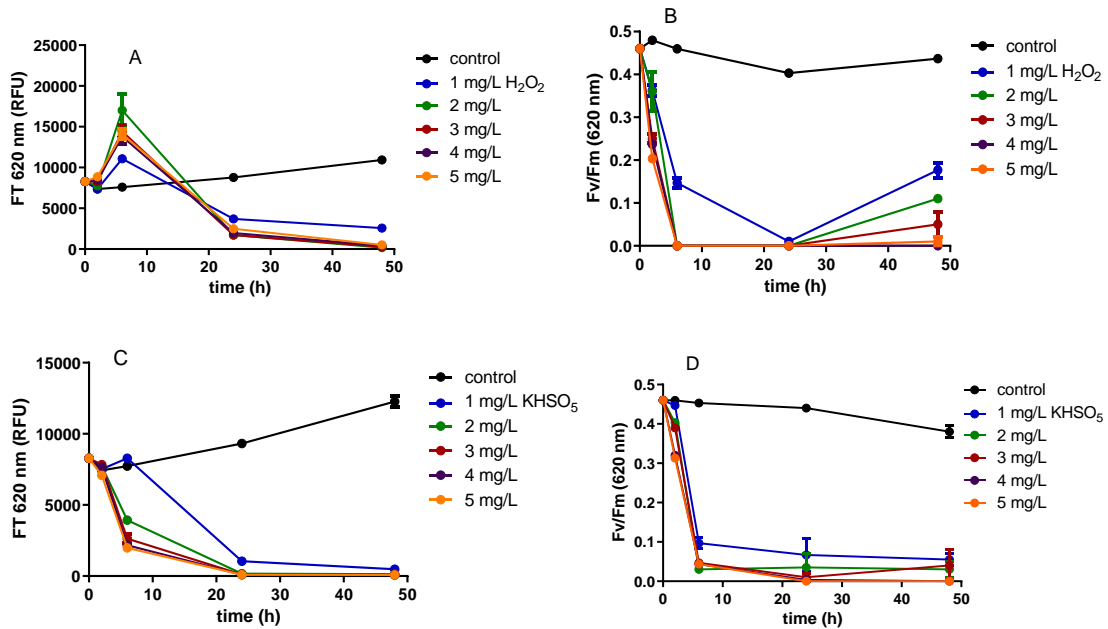


**Figure 43.** Ft in raw fluorescence units (RFU) and QY (Fv/Fm) at  $\lambda=620$  nm during *Microcystis* sp. treatment in river water (+ *Echinogammarus veneris* sp.) with single dose 1 – 5 mg L<sup>-1</sup> (A-B) H<sub>2</sub>O<sub>2</sub> and (C-D) PMS.

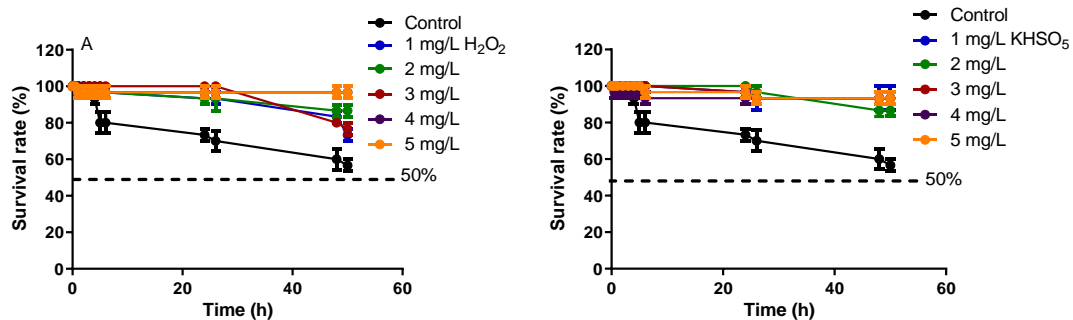


**Figure 44.** Survival rate (%) of invertebrate species during *Microcystis* sp. treatment in river water (+ *Echinogammarus veneris* sp.) with single dose 1 – 5 mg L<sup>-1</sup> (A) H<sub>2</sub>O<sub>2</sub> and (B) PMS.

Application of H<sub>2</sub>O<sub>2</sub> and KHSO<sub>5</sub> in cyano-HABs surface water with invertebrates exhibited opposite results from their application in “clean” surface water. The applied concentrations of 1-3 mg L<sup>-1</sup> H<sub>2</sub>O<sub>2</sub> resulted in slightly reduced survival rate of *Echinogammarus veneris* species. However, treatment with higher doses resulted in higher survival rates than the ones of the control (untreated water), indicating that gammarus species are more susceptible to cyano-HABs than to the applied oxidant (Figure 44). All tested doses during treatment did not affect the *Echinogammarus veneris* sp. which remained alive in the treated matrixes rather in the control. We speculate that the oxidant “cleans-up” the matrix and turns it into a more welcoming environment for

the species, in contrary to the control which is heavily contaminated. Also, the oxidant was consumed by matrix contaminants (in this case *Microcystis* sp.), making it less available to invertebrates.

### Multiple doses treatment

Applied concentrations of  $H_2O_2$  and  $KHSO_5$  effectively decreased phycocyanin fluorescence of the treated samples at  $t=48$  h, during the multiple dose treatment of *Microcystis* sp. in river water along with *Echinogammarus veneris* sp. Treatment with  $H_2O_2$  caused the excessive release of phycocyanin into the water, hence the demand for oxidant was increased during the treatment. Even though at  $t=24$  h the measured QY yield dropped to zero, indicating a successful treatment, post the 48 hours mark it was partially restored. All added doses of  $KHSO_5$  responded faster to the contaminant since treatment with PMS achieved Ft values lower than 1000 RFU during the first 6 hours. A minor increase of QY at  $t=24$  h was captured, but the 2<sup>nd</sup> dose at  $t=24$  h was sufficient to reduce again the QY at  $t=48$  h. It is apparent that PMS outperformed  $H_2O_2$  treatment since quantum yield of all treated samples remained low throughout the treatment (Figure 45).

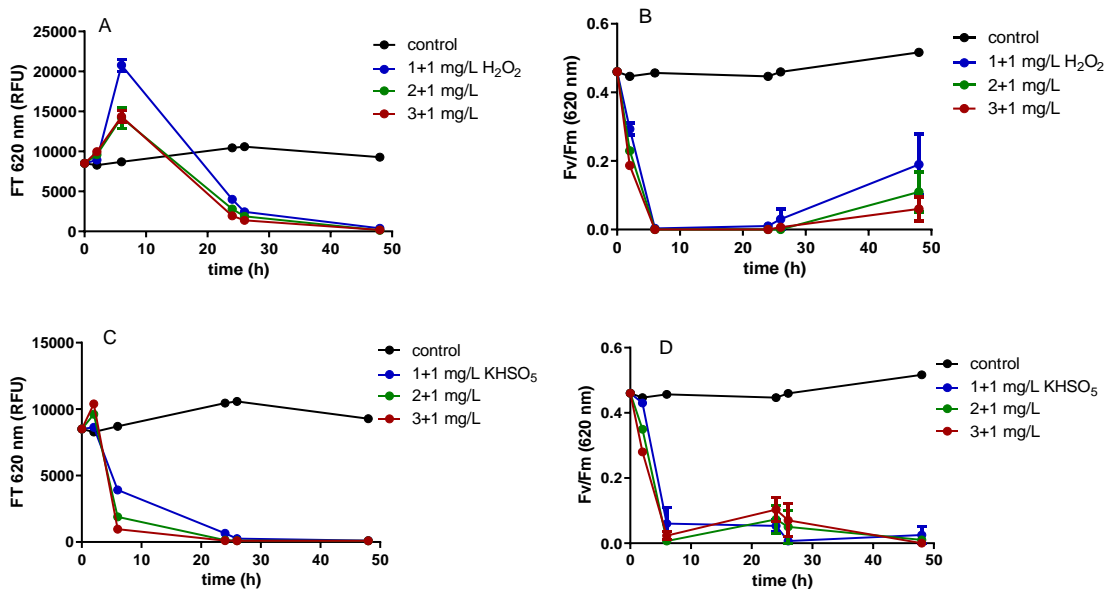


**Figure 45.** Ft in raw fluorescence units (RFU) and QY at  $\lambda=620$  nm during *Microcystis* sp. treatment in river water (+ *Echinogammarus veneris* sp.) with multiple doses of (A-B)  $H_2O_2$  and (C-D) PMS.  $[C]_{total}=2, 3, 4$  mg  $L^{-1}$ .

Quantification of residual oxidant concentration during treatments showed that both oxidants were completely consumed by the end of the experiment (Figure 46). *Echinogammarus veneris* species survival rate followed the same trend with the single dose experiments, where in treated samples a higher survival rate was obtained, compared with the untreated samples (Figure 47).

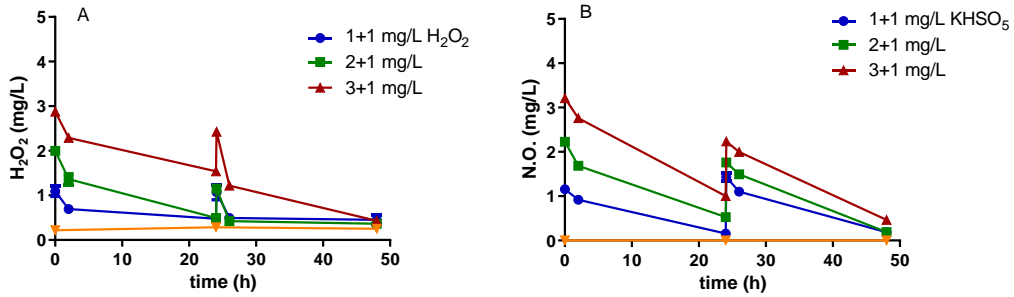


**Figure 46.** Residual oxidant concentration measured during *Microcystis* sp. treatment in river water (+ *Echinogammarus veneris* sp.) with multiple doses with multiple doses of (A) H<sub>2</sub>O<sub>2</sub> and (B) PMS. [C]<sub>total</sub>=2, 3, 4 mg L<sup>-1</sup>

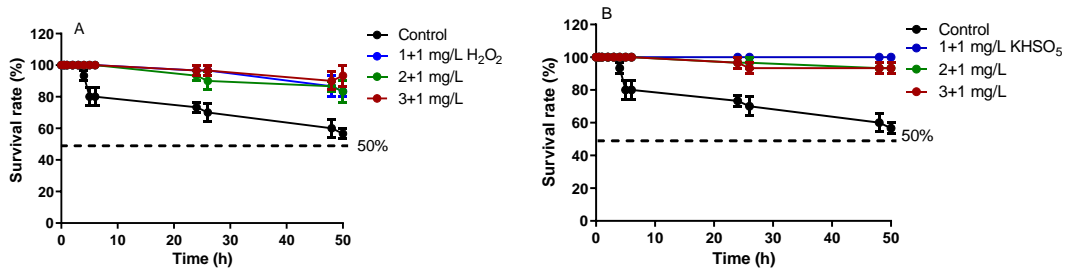


**Figure 47.** Survival rate (%) of invertebrate species during *Microcystis* sp. treatment in river water (+ *Echinogammarus veneris* sp.) with multiple doses of (A) H<sub>2</sub>O<sub>2</sub> and (B) PMS. [C]<sub>total</sub>=2, 3, 4 mg L<sup>-1</sup>.

### 3.3.3.2 *Aphanizomenon* sp.

#### Single dose treatment

Single doses of 3 mg L<sup>-1</sup> of H<sub>2</sub>O<sub>2</sub> and KHSO<sub>5</sub> was efficient to reduce both Ft and QY of the treated samples, resulting in an effective treatment. However, lower doses were not sufficient to treat *Aphanizomenon*, as 1 mg L<sup>-1</sup> H<sub>2</sub>O<sub>2</sub> caused minor effect on Ft and QY values, and 2 mg L<sup>-1</sup> succeeded on reducing the Ft, but the quantum yield of the treated sample was partially restored at t=48 h. The results indicate increased dosing

requirements of filamentous species, *Aphanizomenon* sp., over the coccoid specie, *Microcystis* sp. (Figures 45, 48).

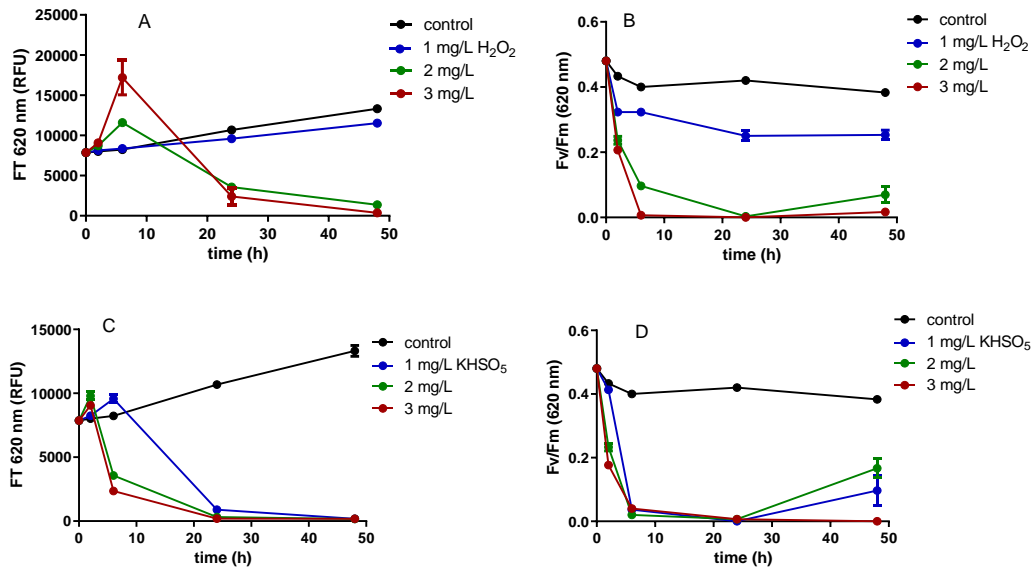


**Figure 48.** Ft in raw fluorescence units (RFU) and QY (Fv/Fm) at  $\lambda=620$  nm during *Aphanizomenon* sp. treatment in river water (+ *Echinogammarus veneris* sp.) with single doses 1 – 3 mg L<sup>-1</sup> (A-B) H<sub>2</sub>O<sub>2</sub> and (C-D) PMS.

Quantification of oxidants during the single dose treatment of *Aphanizomenon* sp., was consistent with previous experiments, confirming the residual effect of PMS, although both oxidants were utilized by the matrix, giving no excess concentration by t=48 h (Figure 45). Survival rates were as high as 100% when 1, and 2 mg L<sup>-1</sup> of each oxidant applied. A minor drop of about 10-15% was recorded for the applied concentration of 3 mg L<sup>-1</sup>, meaning that 85-90% of *Gammarus* species survived during treatment (Figure 46), which is comparable to the previously obtained results.

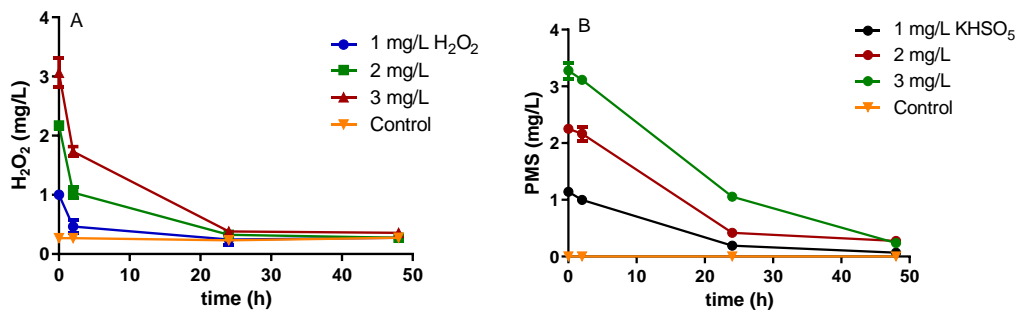


**Figure 49.** Residual oxidant concentration during *Aphanizomenon* sp. treatment in river water (+ *Echinogammarus veneris* species) with single dose 1 – 3 mg L<sup>-1</sup> (A) H<sub>2</sub>O<sub>2</sub> and (B) PMS.

## Multiple doses treatment

Treatment with multiple doses of  $\text{KHSO}_5$  outperformed liquid  $\text{H}_2\text{O}_2$  since the overall added concentrations of  $3_{(2+1)}$  and  $4_{(3+1)}$   $\text{mg L}^{-1}$  significantly reduced QY and maintained low throughout the treatment. Corresponding doses of  $\text{H}_2\text{O}_2$  were not sufficient to mitigate *Aphanizomenon* sp. as the measured QY initially dropped but then it was followed by a steady increase even after the 2<sup>nd</sup> dose. The added dose at  $t=24$  h failed to reduce again the QY of the treated samples, meaning that the effect of 2<sup>nd</sup> dose was minimal. PMS was effective to treat the species even before the addition of the extra dose, yet the 2<sup>nd</sup> dose it possibly contributed on retaining low quantum yield throughout the treatment (Figure 46, C-D). Only the overall concentration of  $2_{(1+1)}$   $\text{mg L}^{-1}$  PMS showed a slight increase of QY, making it the least effective treatment dose.

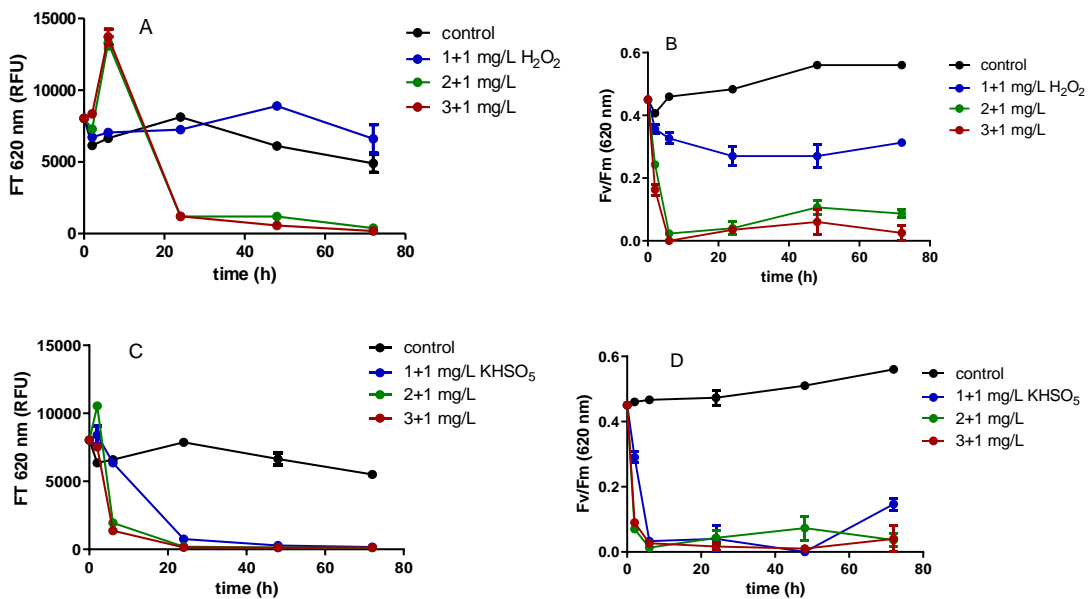


**Figure 50.** Ft in raw fluorescence units (RFU) and QY at  $\lambda=620$  nm during *Aphanizomenon* sp. treatment in river water (+ *Echinogammarus veneris* sp.) with multiple doses of 1 – 3  $\text{mg L}^{-1}$  (A-B)  $\text{H}_2\text{O}_2$  and (C-D) PMS.  $[\text{C}]_{\text{total}}=2, 3, 4$   $\text{mg L}^{-1}$ .

Quantification of residual oxidant concentrations were aligned with the previously obtained results. Same results were also observed on the toxicity study, where high survival rates (80-100%) were recorder during the treatment of *Aphanizomenon* sp. in river water, whereas cyano-HABs presence in control (untreated water) caused increased mortality to the tested species.

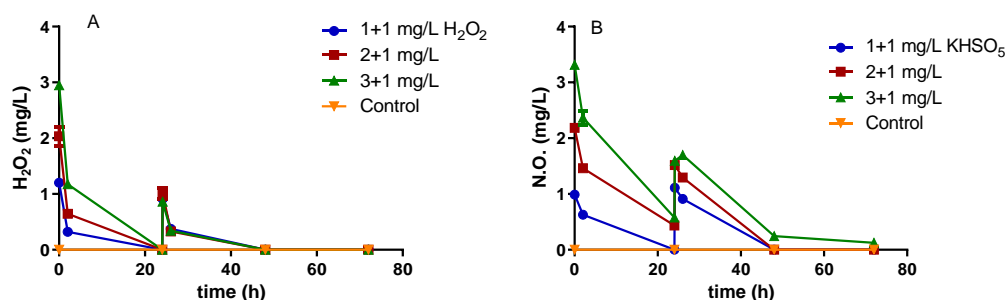


**Figure 51.** Residual oxidant concentration measured during *Aphanizomenon* sp. treatment in river water (+ *Echinogammarus veneris* sp.) with multiple doses of 1 – 3 mg L<sup>-1</sup> (A) H<sub>2</sub>O<sub>2</sub> and (B) PMS. [C]<sub>total</sub>=2, 3, 4 mg L<sup>-1</sup>.

Additional to the above investigations, experiments on: (a) the treatment of *Microcystis* sp. spiked in Kouris Dam and (b) Polemidia Dam, were performed and resulted in similar findings. The outcomes of those experiments are presented in Appendix II (Figures S 13 – 16).

### 3.4 Scale-up treatment

Surface water collected from Athalassa lake showed elevated level of nutrients and physicochemical water characteristics. Total nitrogen was as high as 9.1 mg L<sup>-1</sup>, TP was 0.11 mg L<sup>-1</sup>, while pH, conductivity, salinity, and TDS were 10.05, 4.61 mS/cm, 3.23 ppt, and 3.24 g L<sup>-1</sup>, respectively. The high measured values indicated a hypereutrophic lake, with decreased water quality. The bloom was detectable with a naked eye as species formed visible mats on the surface of the water, while measured Ft and QY values confirmed the presence of an on-going and dense bloom. Microscopic observation showed a diverse composition of matrix, but the dominant species was once again *Planktothrix* sp.

The initial Ft and QY values at  $\lambda=620$  nm were  $17560 \pm 500$  RFU, and 0.42, respectively. Application of liquid H<sub>2</sub>O<sub>2</sub>, PMS, and CaO<sub>2</sub> granules, exhibited various efficiencies on treating the bloom as well as different visual changes on the water matrix. Scheme 26 depicts the treatment vessels at t= 0, 120, and 240 h before and after oxidant addition. Treatment with multiple doses of KHSO<sub>5</sub> outperformed liquid H<sub>2</sub>O<sub>2</sub> and CaO<sub>2</sub> granules since the overall added concentrations of 12<sub>(7+5)</sub> mg L<sup>-1</sup> equiv. of H<sub>2</sub>O<sub>2</sub>, significantly reduced QY at  $\lambda=620$  nm and maintained low throughout the treatment (Figure 52). Corresponding doses of H<sub>2</sub>O<sub>2</sub> were not sufficient to mitigate the bloom as the measured

QY initially dropped, then retrieved and then again dropped after the 2<sup>nd</sup> dose at t=120 h. Even though the extra dose succeeded in reducing the QY, it was restored after 1 day meaning that higher than 5 mg L<sup>-1</sup> H<sub>2</sub>O<sub>2</sub> dose was required. Although, calcium peroxide granules showed a significant reduction on both FT, and QY, that resulted in the successful elimination of the bloom, it caused several unexpected side-effects. CaO<sub>2</sub> granules were initially floating on the water surface top allowing the gradual release of H<sub>2</sub>O<sub>2</sub>. The peroxide released was sufficient to destroy some cyanobacterial cells, but some filaments of *Planktothrix* were attached on the surface of granules forming a coagulant mass on the surface of each vessel. Also, the addition of granules increased the pH above 11 which exceeded the allowable limit for surface waters. Treatments with liquid H<sub>2</sub>O<sub>2</sub> and PMS did not significantly affect the physicochemical water characteristics, while PMS lower the initial pH from 10.05 to 9.5.

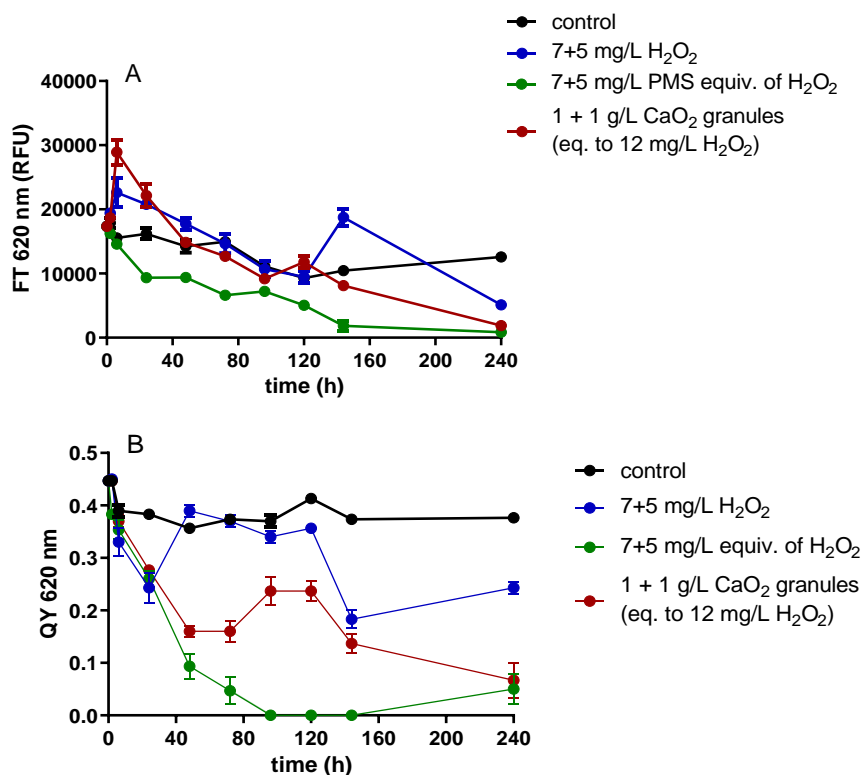
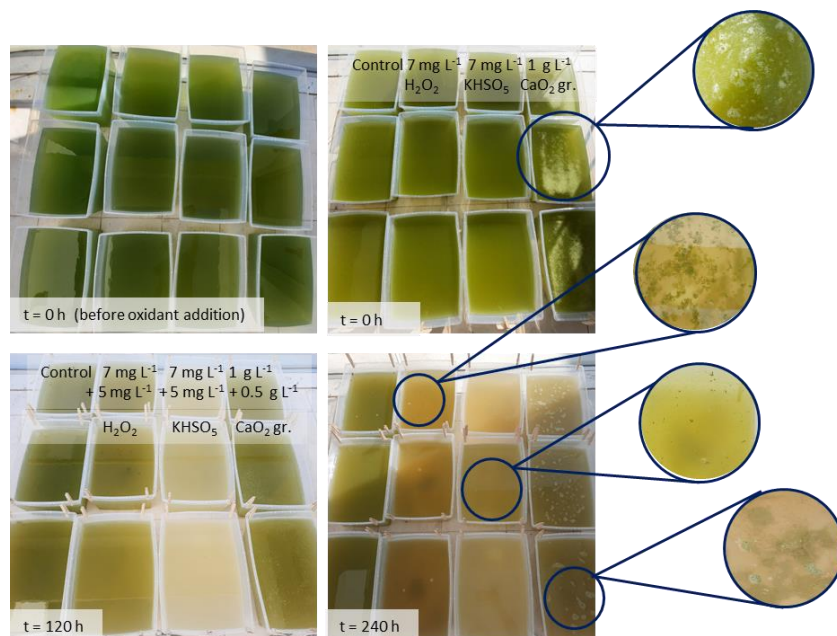


**Figure 52.** (A) Ft in raw fluorescence units (RFU) and (B) QY at  $\lambda=620$  nm during *Athalassa* up-scale treatment with multiple doses H<sub>2</sub>O<sub>2</sub>, PMS, and CaO<sub>2</sub> granules. [C]<sub>total</sub>= 12 mg L<sup>-1</sup> H<sub>2</sub>O<sub>2</sub> equivalent.



**Scheme 26.** Visual changes during treatment of naturally occurring cyano-HABs in Athalassa's Lake (November 2021).

Quantification of residual oxidant showed a rapid consumption of  $\text{H}_2\text{O}_2$ , since its residual concentration was lower than  $1 \text{ mg L}^{-1}$  after 6 hours of treatment, while PMS had a residual effect higher than  $1 \text{ mg L}^{-1}$   $\text{KHSO}_5$  eq. of  $\text{H}_2\text{O}_2$ , after 24 hours of treatment. Granules had no residual effect, since the  $\text{H}_2\text{O}_2$  release and consumption happened simultaneously due to the high oxidant demand of the heavily contaminated matrix.

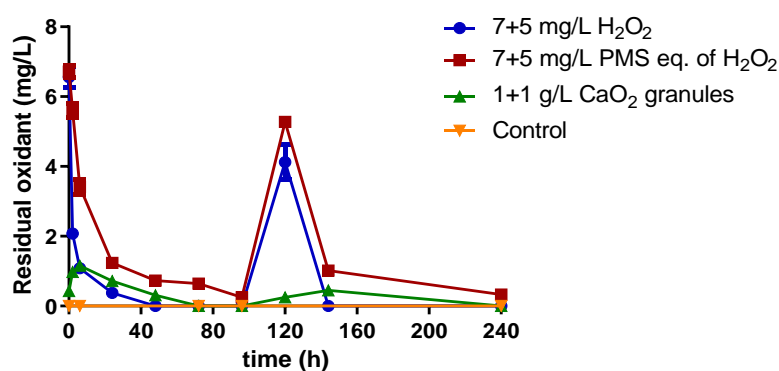


**Figure 53.** Residual oxidant concentration measured during Athalassa up-scale treatment with multiple doses  $\text{H}_2\text{O}_2$ , PMS, and  $\text{CaO}_2$  granules.  $[\text{C}]_{\text{total}} = 12 \text{ mg L}^{-1} \text{H}_2\text{O}_2$  equivalent.

## 4 Summary of Findings/ Recommendations

### 4.1 Monitoring and treatment of naturally occurring blooms in St. George and Athalassa Lakes

#### 4.1.1 Monitoring

Monitoring of St. George Lake indicated the formation of *Merismopedia* picocyanobacterial bloom that lasted for 4 months during summer and early autumn (June–September 2019). The increase of the water temperature and the low turbidity during summer in combination with nutrient load and/or release from the sediments may be the reasons for the observed seasonal blooming of cyanobacteria. In St. George Lake, high nutrient content recorded throughout the year, which favored *Merismopedia* sp. to form a mono-dominated bloom. The concentration of TP during blooming was above 0.2 mg L<sup>-1</sup> which means that most probably nitrogen became the limiting element, which was also found in lower levels during blooming than in the rest samples. The high correlation of nutrient levels and the trophic status indicates the need of monitoring for the early detection of cyanobacterial blooms.

Monitoring with conventional techniques, such as Secchi Depth, microscopy, and other assist the preliminary screening, however parameters directly related to cyano-HABs, and their toxins should be monitored as well. Photosynthetic parameters of water samples such as instantaneous fluorescence and quantum yield of the PSII are strong indicators of the bloom density, as well as the wellness of the blooming cultures. Instantaneous fluorescence (Ft) of water samples at 620 nm with higher than 3000 RFU usually indicate an on-going bloom or the primary stage of a bloom. During monitoring, the steep increase of fluorescence at  $\lambda=620$  nm, revealed the increase of cyanobacterial mass into the water, hence the phycocyanin concentration, which is a unique pigment of cyanobacteria cells. Instantaneous fluorescence of the water samples showed increased phycocyanin levels even after the bloom. This can be explained with the release of pigments after the cell lysis which occurred at the end of the blooming period, caused high fluorescence signal at 620 nm (phycocyanin) and 450 nm (chlorophyll-a).

Microscopic observation of samples during the bloom indicated a mono-domination of a picocyanobacterial species *Merismopedia* (most probably *Merismopedia minutissima*

based on their 2-D sheets morphology), a known MC and NOD producer. However, even though genes involved in MC and NOD synthesis were present (*mcyB* and *mcyE*), these cyanotoxins were not detectable in any sample. Based on previous studies, the monodomination of one species can trigger a strong competition with other species and under these conditions the production of MC may be also inhibited. Alternatively, the presence of *mcyB* only in 1 sample and *mcyE* in 6 samples may indicate that the genetic machinery for MC synthesis by *Merismopedia* sp. is deficient and that the dominant species lost their capability of MC synthesis.

Nevertheless, it should be underlined that any applied genetic method should be complemented and accompanied with analytical confirmation. The level of *mcy* transcripts is often not correlated with MC concentration. The toxicity based on the *mcy* levels might be both under- and overestimated [60, 106]. Therefore, these assays should not be considered as good indicators of the toxicity of the bloom, but rather as a complementary tool in risk assessments. Similarly, it can be assumed that the detection of *mcy* does not ensure MC presence, which should be proven through advanced analytical methods (LC–MS/MS). In this case, advanced analytical techniques conformed that no toxins were produced above MDL during blooming. Attention should also be paid on the obtained *m/z* and the corresponding fragmentation patterns so that cyanotoxin concentration is not overestimated.

The second case study on Athalassa Lake, showed some other important considerations during contamination events and their assessment. Nutrient levels as well as COD, rapidly increased after a heavy rainfall in September, followed by a massive fish-kill event a week after. Even though cyano-HABs were the first to blame, a more thorough examination of the fish-kill event showed that the probability of cyano-HABs toxicity over the fish was low, given the absence of toxin producing genes, and cyanotoxins in the water samples. Also, microscopic observation showed a low density of cyanobacteria, and a good diversity of algal species in water that was sampled right after the fish kill event. This excludes the hypothesis of fish deaths due to blooming that caused water stratification, and anoxia in the bottom layers due to absence of light. In surface waters with high contamination status and increased COD, the possibility of external sources of contamination should be considered, as the increased levels of COD reduce the available dissolved oxygen that leads to hypoxia, hence to fish deaths.

#### 4.1.2 Treatment

Dense blooms of *Merismopedia sp.* in a eutrophic lake inferred the necessity to apply extremely high doses of  $\text{H}_2\text{O}_2$  for the treatment to be effective. Since in those cases, direct application of  $\text{H}_2\text{O}_2$  doses over  $5 \text{ mg L}^{-1}$  are considered potentially harmful for the other components of microbial communities (bacteria, phytoplankton, and zooplankton) [107], alternative solutions are needed.  $\text{CaO}_2$  and  $\text{MgO}_2$  granules studied herein, are an alternative to the traditionally used liquid hydrogen peroxide [108]. In order to determine the most efficient dose, the ability of the oxidant to destroy cyanobacterial cells by measuring changes in the photosynthetic parameters as well as the effects that it may had on the physicochemical parameters of the sample (pH, conductivity, TDS, and salinity) were taken into consideration.

Treatments with 2 and  $3 \text{ g L}^{-1}$  of  $\text{CaO}_2$  were the most effective in bloom elimination, but they both caused an increase of pH which was slightly above 10 after 48-h of treatment (limit is 9.5). Overall,  $\text{CaO}_2$  shows higher releasing capacity than  $\text{MgO}_2$  granules. The lower  $\text{H}_2\text{O}_2$  release by  $\text{MgO}_2$  may be caused by the dissolution product of  $\text{MgO}_2$  (magnesium hydroxide) which is less soluble than the dissolution product of  $\text{CaO}_2$ , at the same pH. The lower solubility may not allow for the reaction equilibrium to shift towards the products. This also affected the suspended solids content of the treated water. Calcium peroxide granules caused drastic change of pH as while decomposing it releases highly basic  $\text{Ca}(\text{OH})_2$ .

Taking into consideration both the treatment efficiency and the releasing capacity, direct application of liquid  $\text{H}_2\text{O}_2$  and  $\text{MgO}_2$  granules is less efficient compared with  $\text{CaO}_2$  granules. For the effective restoration of contaminated sites by high-density cyanobacterial blooms, doses higher than  $5 \text{ mg L}^{-1}$  of liquid  $\text{H}_2\text{O}_2$  should be applied and in the case of magnesium peroxide granules it would require higher than  $3 \text{ g L}^{-1}$  of granular compound. In both cases the required applied doses will have undesirable side-effects for *in-situ* application. Therefore,  $\text{CaO}_2$  which can release  $\text{H}_2\text{O}_2$  more effectively could be introduced as a suitable treatment method in concentrations no more than  $3 \text{ g L}^{-1}$  for high-density blooms. The effects on the physicochemical parameters of treated freshwaters need to be accounted as well when deciding on the type of oxidant and its dosing to avoid possible side-effects in the lake ecosystem during treatment.

## 4.2 Treatment with novel chemical oxidation processes

### 4.2.1 CaO<sub>2</sub> granules

#### 4.2.1.1 CaO<sub>2</sub> granules properties and toxicity

The first assessment of the H<sub>2</sub>O<sub>2</sub> releasing properties of metallic peroxide compounds showed that powdered form of CaO<sub>2</sub> releases high instant doses of H<sub>2</sub>O<sub>2</sub>, while MgO<sub>2</sub> had significantly less peroxide releasing capacity. CaO<sub>2</sub> granules, on the other hand, resulted in the gradual and controlled release of H<sub>2</sub>O<sub>2</sub> which followed a pseudo-first-order kinetics model. This property of granules inhibits the accumulative concentrations of H<sub>2</sub>O<sub>2</sub> into the waterbody and lowers the initial applied concentrations that do not “shock” or disrupt the aquatic environment. The continues release of H<sub>2</sub>O<sub>2</sub> by granules, positioned the granules as a promising chemical treatment method for *in-lake* cyano-HABs mitigation. Overall, a releasing concentration of ~ 3, 6, and 12 mg L<sup>-1</sup> is achieved by 0.5, 1.0 and 2.0 g L<sup>-1</sup> CaO<sub>2</sub> granules in a “clean” surface water matrix.

To further examine their releasing properties in relevant environments, H<sub>2</sub>O<sub>2</sub> release curves were obtained by adding CaO<sub>2</sub> granules in surface waters with various physicochemical characteristics. Results showed that the releasing capacity of granules is greatly affected by water matrix composition. Specifically, the presence of microelements enhances (inorganic content) the release of H<sub>2</sub>O<sub>2</sub> while nutrients and natural organic matter consume a portion of the released oxidant. Humics had a dual effect on the granules’ H<sub>2</sub>O<sub>2</sub> releasing capacity, as higher humic concentrations enhanced the release of hydroxyl radicals, but also reacted with the released H<sub>2</sub>O<sub>2</sub>. Therefore, caution should be applied when deciding on the effective treatment doses, since the matrix may enhance and/or suppress the releasing properties of granules. There are some studies testing the mitigation efficiencies of liquid H<sub>2</sub>O<sub>2</sub> on cyanobacterial species, which were performed in BG-11 matrixes [109–112]. This may lead to misleading conclusions on the efficiency of the applied oxidant, as the complex matrix of BG-11 contains transition metals that activate H<sub>2</sub>O<sub>2</sub> through electron transfer mechanism[113]. Nevertheless, the effect of nutrients and nutrient limitation on the sensitivity of *Microcystis* to H<sub>2</sub>O<sub>2</sub> was examined by Sandrini et. al. (2020) [114].

In this study, a linear correlation between the applied dose of CaO<sub>2</sub> granules and the released H<sub>2</sub>O<sub>2</sub> concentration was found. The obtained curves confirmed previous studies that suggested a linear relationship between the H<sub>2</sub>O<sub>2</sub> yield and the added granules' dose [77, 115]. The linear equation of each water matrix tested herein could be a useful tool on deciding on the best doses of CaO<sub>2</sub> granules during an *in-lake* application when the overall H<sub>2</sub>O<sub>2</sub> concentration requirements are known.

The follow-up investigation was on the toxicity of CaO<sub>2</sub> granules on invertebrate species, *Echinogammarus* sp., that showed a 100% loss of non-targeted organisms when doses  $\geq 2 \text{ g L}^{-1}$  of CaO<sub>2</sub> granules were applied. The calculated LC<sub>50</sub> was around  $1 \text{ g L}^{-1}$  CaO<sub>2</sub> granules, meaning that applied doses for cyano-HABs treatments should not exceed that indicative limit. Despite the effect on zooplankton, the granular form may cause unwanted side effects as it can be easily consumed by fish or higher animals (birds, ducks, etc.) due to the size and morphology of granules. Also, granules can be sunk to the bottom of the lake causing oxidation of benthos (soil, invertebrates), or float on the top (like coagulants) which could inhibit light to the lower levels of a waterbody. All these should be taken into consideration when the direct application of granules is considered for *in-lake* treatment, although it is not recommended based on the findings of this study.

#### **4.2.1.1 Treatment with CaO<sub>2</sub> granules**

Treatment of surface water spiked with cyanobacterial species utilizing  $0.5 - 2.0 \text{ g L}^{-1}$  CaO<sub>2</sub> granules, were conducted to investigate the treatment efficiency of granules and the dose requirements based on the cyanobacterial specie. Corresponding doses of liquid H<sub>2</sub>O<sub>2</sub> were applied in the same water matrixes in order to compare the efficiencies of the two oxidants. Treating *Microcystis* and *Aphanizomenon* sp. with peroxide granules showed an increased mitigation efficiency in comparison with equal accumulative doses of liquid H<sub>2</sub>O<sub>2</sub>. However, application of doses higher than  $1.0 \text{ g L}^{-1}$  granules in water resulted in elevated pH values, which exceeded the allowable limit for surface water. For the effective suppression of *Microcystis* sp., doses of  $0.5 \text{ g L}^{-1}$  and  $6 \text{ mg L}^{-1}$  CaO<sub>2</sub> granules and liquid H<sub>2</sub>O<sub>2</sub> were needed, respectively. Treatment of *Aphanizomenon* sp. required double the doses of *Microcystis* sp. It is apparent that filamentous species (e.g., Nostocales) has higher dose requirements than coccoid species (e.g., Chroococcales). Hence, it is important to consider the type of the bloom (species) when deciding on the

dose of the oxidant as not all oxidants and doses respond in the same way in all the blooms. An additional study to this, could be the test of a range of initial FT of the blooms to determine the dose requirements not only based on the speciation but also on the maturity and the phase of blooming. Early stages of the bloom require lower doses of oxidant, which is beneficial for the rest of the ecosystem when treatments are applied.

#### **4.2.1.2 Treatment with GEF systems**

To eliminate the side-effects of CaO<sub>2</sub> granules (elevated pH, turbidity from precipitate, and availability of granules for consumption), textile materials were employed to enclose the granules during treatment. Granules enclosed in fabrics (GEF) exhibited various treatment efficiencies which are highly depended on the material characteristics of each fabric (pore size, thickness, etc.). H<sub>2</sub>O<sub>2</sub> release kinetics experiments showed that GEF can release comparable H<sub>2</sub>O<sub>2</sub> concentrations to the direct application of CaO<sub>2</sub> granules in a surface water. Only GEF type D, comprising of paper filter and tights, had minimal H<sub>2</sub>O<sub>2</sub> release and that it was probably caused by the reaction of H<sub>2</sub>O<sub>2</sub> with the paper and/or its adsorption on the filter, that eventually inhibited its diffusion to the bulk of the solution. GEF types A – C resulted in similar H<sub>2</sub>O<sub>2</sub> releasing capacity and followed a pseudo-first order release kinetics model. A pseudo-zero-order equation was firstly employed to study the release kinetics - as proposed by the literature [69, 116], but the correlation coefficients were not indicating a good fit to the model. By fitting the curves to a pseudo-first-order kinetics model, the correlation coefficients were as high as 0.94 – 0.97. Two studies [14, 29] in the cited literature reported a “good fit” to the pseudo-zero-order model for the release of H<sub>2</sub>O<sub>2</sub> by CaO<sub>2</sub> granules, which was not compatible with the obtained results herein as well as with the fact that our release curves reached a distinct plateau after 6 hours of release. The obtained linear equation between CaO<sub>2</sub> granules doses and H<sub>2</sub>O<sub>2</sub> yield confirm previous studies that suggested a linear relationship between the H<sub>2</sub>O<sub>2</sub> yield and the added CaO<sub>2</sub> granules dose [115] and support the findings that the release is not following a pseudo-zero-order kinetics model.

Treatment of dense *Microcystis* sp. with GEF exhibited various efficiencies on reducing Ft and QY of the PSII. Their difference could be explained by the textile properties of each fabric type utilized. Fabric type A was thicker than the other textiles (Fabric A=260>B=200>C=170 μm) caused cyanobacteria cells to “adhere” on its external surface, which clogged the pores of the fabric. This may have caused restrictions between

the cyanobacteria cells that were in the bulk of the treated water and the oxidant released, which kept the Ft and QY at elevated levels compared with the other GEF at equivalent treatment times. Fabric type B, which is widely used for fusing purposes, was quickly submerged into the water after its application on the surface. This property allowed a better diffusion of oxidant into the water matrix, which caused a high treatment efficiency for the applied dose of  $2 \text{ g L}^{-1}$ . The textile utilized for GEF type C was thinner than the rest, but its water-resistant properties did not allowed a full submerged into the water. Therefore, it was floating on the surface for the first 6 hours (Scheme 21). Even though it was not fully submerged, granules were in the submerged side and in contact with the water surface which allowed water exchange between the internal and external of the fabric – hence the diffusion of the released  $\text{H}_2\text{O}_2$ . This fabric being thinner, allowed a smooth and gradient release of oxidant in concentrations that were enough to result in effective treatments.

Overall, granules retained their ability to release  $\text{H}_2\text{O}_2$  due to the permeability of the porous textile materials used to encapsulated them. Based on the above findings, fabrics of non-woven interline and polyester netting materials can be used as delivery systems since they partially restricted the release of  $\text{Ca}(\text{OH})_2$ , retained pH levels at acceptable levels, and did not affect the survival of invertebrates in matrix during release and treatment experiments ( $\text{LD}_{50} > 2 \text{ g L}^{-1}$ ). Especially in cases were multiple  $\text{H}_2\text{O}_2$  doses are required for the effective removal of a contaminant, GEF may offer a novel and alternative  $\text{H}_2\text{O}_2$  delivery system. Considering that doses of  $1.0$  and  $2.0 \text{ g L}^{-1}$   $\text{CaO}_2$  granules enclosed in textile material were required to fully combat the *Microcystis* species, which corresponds to an accumulative release of  $12 \text{ mg L}^{-1}$   $\text{H}_2\text{O}_2$ , the requirement for  $\text{H}_2\text{O}_2$  in this case was high. If such doses of liquid  $\text{H}_2\text{O}_2$  were used directly, it would probably have cause adverse effects to the remaining aquatic organisms of the waterbody and especially on zooplankton mobility. Studies showed that  $\text{H}_2\text{O}_2$  concentrations above  $9 \text{ mg L}^{-1}$  can cause mortalities to *Calanus spp.*, a dominant zooplankton species in the North Atlantic [117], while many studies showed that high  $\text{H}_2\text{O}_2$  doses ( $>10 \text{ mg L}^{-1}$   $\text{H}_2\text{O}_2$ ) are required for an efficient *Microcystis* sp. treatment [118]. As a global trend to switch to multiple or repeated doses of  $\text{H}_2\text{O}_2$  was detected in order to avoid the adverse effects of single high  $\text{H}_2\text{O}_2$  dose [119, 120], GEF system can be considered as a safer and more environmentally friendly application method of the granules.

#### 4.2.2 Peroxymonosulfate (PMS) – OXONE®

Peroxymonosulfate deemed a highly efficient treatment towards cyanobacteria as it outperformed liquid H<sub>2</sub>O<sub>2</sub> in all treatments with equal applied doses (based on peroxide molarities). PMS, resulted in outstanding results on its ability to mitigate the *Microcystis* and *Aphanizomenon* sp., even in very low applied concentrations of 2 mg L<sup>-1</sup> KHSO<sub>5</sub>, that liquid H<sub>2</sub>O<sub>2</sub> and CaO<sub>2</sub> granules failed to achieve. Even at in the case of highly contaminated water sampled from Athalassa Lake during a fish-kill event and *Planktothrix* sp. blooming, it was the only peroxide-based compound that achieved the targeted oxidation of contaminant, resulting in reduced COD levels and water clarity. One of the most important findings is the residual effect of PMS which allows for longer retention in the water matrix and therefore better mitigation efficiency. PMS had a noticeable residual effect in all the conducted experiments, having a much lower consumption rate than that of H<sub>2</sub>O<sub>2</sub>. Liquid H<sub>2</sub>O<sub>2</sub> is being consumed faster under the same experimental conditions meaning that H<sub>2</sub>O<sub>2</sub> is either reacting with matrix compounds and non-targeted organisms or is being degraded faster making it less available to the contaminant.

The fact that PMS persists longer in the matrix allows it to react slower but more targeted towards cyanobacteria, making it the most efficient oxidant tested so far. During treatment with PMS, the increase of Ft due to cell lysis was minimal in comparison with the one of H<sub>2</sub>O<sub>2</sub>, indicating that PMS has higher oxidative potential that result in the degradation of the released pigment-protein complexes. This can be explained based on PMS ability to rapidly react with organic matter, such as amino acids and carboxylic acids [121]. Also, it may indicate that PMS caused cell rupture through a different mechanism than H<sub>2</sub>O<sub>2</sub>, which is expected based on their different chemical structure and charge. PMS is an asymmetrical peroxide producing salt, with a large negatively charged sulfate group that enhance its selective oxidation due to the caused steric hindrance. The mechanism of PMS action on cells was recently investigated by Chen et.al. (2021), through SEM imaging. The proposed mechanism is that PMS destroys the out-layer of cell membrane by reacting and oxidizing the elements of the membrane which consist of lipids, and proteins [82]. However, those mechanisms were only derived by the morphology of the destroyed cell, thus more advanced imaging techniques need to be employed for revealing the reaction mechanisms with cells. Considering the low

pigmentation release during treatments with PMS in comparison with the extremely high Ft values during H<sub>2</sub>O<sub>2</sub> treatment, the proposed mechanism is reasonable.

Toxicity study on *Echinogammarus veneris* sp. showed an excellent survival of species when 1-5 mg L<sup>-1</sup> PMS applied, but survival rates reached the indicative limit when multiple doses of PMS were applied. Hence, multiple dosing of PMS is not advised for surface waters, while for liquid H<sub>2</sub>O<sub>2</sub> multiple dosing is advisable. The residual effect of PMS and the low mortality of invertebrates during single doses suggest that PMS should be applied in low direct doses. The ability of PMS to destroy the released pigments, may indicate that the residual oxidant could be available to also oxidize released cyanotoxins after the cell lysis. This should be further examined with experiments in toxified samples, even though the ability of PMS to degrade cyanotoxins such as Microcystin-LR is extensively studied [122]. Thus, it is expected that PMS treatments could result in a holistic contaminant removal from surface waters.

### **Overall remarks**

Upscale treatment in a naturally occurring bloom in Athalassa's lake water validated the undesirable side-effects of CaO<sub>2</sub> granules direct application in water. Some of them were the increased turbidity of water, the floating masses on the top of the surface and the difficulty of removing the granules from the water matrix after the treatment. The application of CaO<sub>2</sub> granules through a delivery system can eliminate most of these effects, while it can prevent the formation of coagulants between granules surface and filaments. Overall, treatment experiments with all novel oxidants showed that filamentous cyanobacteria require higher doses of oxidant than coccoid colonies. Density of the bloom increases the demand of oxidant in water; thus, it is preferable to detect and treat the bloom at initial stages [123]. Lastly, water matrix plays a key role on treatment efficiency as organic and inorganic load can consume oxidant before reaching targeted cells. Consequently, the demand of oxidant by each matrix should be determined prior to deciding on dosing requirements for an *in-field* treatment application. However, this was not the case with PMS, which outperformed all tested oxidant, making it the most efficient, cost-effective (lower oxidant demand = less cost), and environmentally friendly approach. Future studies by the Water Treatment Laboratory – AQUA group, on the utilization of PMS in surface waters, under various environmental conditions will support these findings.

## CONCLUSIONS

Conventional monitoring tools can give limited information on the factors driving cyanobacterial blooming. Therefore, additional characterization of the lake ecosystem including cyanobacterial and green algae content; identification of cyanotoxin producing genes, and cyanotoxins analyses were found to be essential. Customized monitoring strategies based on the needs of each waterbody are essential for adequately protecting the water quality of surface waters. An example of the development of a data-driven real-time risk characterization tool is the monitoring strategy including predictive models created by the US Environmental Protection Agency to monitor cyano-HABs in Ohio river [124]. Besides monitoring, which is found to be extremely important for the early detection of a bloom to decide on proactive measures or respond with an *in-lake* strategy, treating cyanobacteria effectively, without harming the remaining ecosystem is also essential. Mitigation methods are an additional to the monitoring measure, that should complement and support the overall strategy of the waterbody restoration to safeguard surface water quality.

Currently, liquid H<sub>2</sub>O<sub>2</sub> is widely used for the mitigation of cyano-HABs, as an alternative to copper algicides and an eco-friendly method. However, the treatment of dense blooms, such as the ones occurred in St. George and Athalassa Lakes, requires the application of high doses (> 5 mg L<sup>-1</sup>) of liquid H<sub>2</sub>O<sub>2</sub> at once, which in turn affects other aquatic organisms in the waterbody. Recent studies showed that only mild treatments (< 2 mg L<sup>-1</sup>) avoid side effects on non-targeted species, while moderate treatments (2-4 mg L<sup>-1</sup>) are likely to have negative effects on some zooplankton taxa (particularly rotifers and small Cladocera's)[107]. This means that application of liquid H<sub>2</sub>O<sub>2</sub> must be performed on low biomasses, at the beginning of a bloom cycle and not on high-density blooms, to avoid severe doses (4-10 mg L<sup>-1</sup>) that cause undesirable side-effects, including the release of potential cyanotoxins into the waterbody. Metallic peroxide granules and peroxymonosulfate, as alternative sources of peroxides (R-O-O-R), were tested herein for their algicidal properties. Both oxidants were proposed, for the first time in literature, as cyano-HABs mitigation processes, thus their unexplored chemical and algicidal properties were investigated in the present PhD study. Calcium peroxide granules resulted in efficient treatment, but their effect on non-targeted species necessitate the application through a delivery system. Treatment with granules enclosed in fabrics

exhibited various efficiencies on treating cyanobacteria, and its efficiency was highly depended on the porous and morphology of the textile material utilized. Nevertheless, GEF systems had minimal effect on zooplankton in all tested concentrations. Investigations of PMS application in surface waters showed that it has limited impact on zooplankton (SR>90%), its residual effect allows for highly efficient treatments that result in not only the treatment of cyanobacteria but also the degradation of the released pigments, and potentially of cyanotoxins. The above results showed that PMS outperformed all current treatment options.

Taking into consideration the findings of this thesis, caution should be applied when *in-situ* chemical treatments are delivered to contaminated waterbodies. Known and unknown side-effects may cause the irreversible deterioration of aquatic environments. Hence, chemical treatment methods proposed for the restoration of surface waters should be extensively studied in terms not only of treatment efficiency, but also of its effect on non-targeted species. Toxicity studies on phytoplankton, zooplankton, and other biological factors (aquatic plants, fish, and benthic organisms), should be conducted along with the treatment efficiencies of any tested and applied chemical /method, in order to decide on their appropriateness in respect with their environmental friendliness. The evaluation of treatment matrix (cyano-HABs surface water) as well as the properties of each oxidant applied in that matrix, are also important to decide on the minimum effective dose. The bench-scale evaluations of the emerging treatment methods have provided important information towards their optimization; however, it is important to investigate their scalability potential [125] as well as their suitability for *in-situ* applications. Further studies will provide a clearer view on their potential, as both metallic peroxide granules and peroxymonosulfate deemed promising mitigation techniques which allowed a “green” and effective cyano-HABs treatment.

### ***Future studies***

For the continuity of the present study, the degradation of cyanotoxins during the treatment with novel oxidants, as well as the fate of the released pigments, and T&O compounds should be examined. Also, novel oxidant treatments should be applied on more cyanobacteria species, with diverse morphologies, densities, and cultivation ages, in order to test the susceptibility of cultures based on their bloom type, mass and maturity. Further to this, the effect of application methods on the oxidants’ efficiency should be

explored, while the investigation of more delivery systems and types will expand the treatment options of these oxidants for *in-lake* applications. The above experiments will enable the development of a data platform comprising of the water matrix characteristics and the oxidant demand, which can become the ultimate tool for deciding on chemical doses based on each waterbody characteristics prior to their in-filed application. This will allow for a controlled chemical dosing application that corresponds to the needs of each waterbody based on its specific water characteristics. By doing so, a holistic mitigation practice for the *in-situ* treatment of cyano-HABs based on the novel oxidants could be proposed. Further to this, more delivery systems, preferable bio-degradable or naturally fabricated materials, can be investigated as alternative delivery systems for CaO<sub>2</sub> granules.

## REFERENCES

1. Altermann W, Kazmierczak J, Oren A, Wright DT (2006) Cyanobacterial calcification and its rock-building potential during 3.5 billion years of Earth history. *Geobiology* 4:147–166
2. Casamatta DA, Johansen JR, Vis ML, Broadwater ST (2005) MOLECULAR AND MORPHOLOGICAL CHARACTERIZATION OF TEN POLAR AND NEAR-POLAR STRAINS WITHIN THE OSCILLATORIALES (CYANOBACTERIA)1. *J Phycol* 41:421–438. <https://doi.org/10.1111/J.1529-8817.2005.04062.X>
3. Heimann K, Cirés S (2015) N<sub>2</sub>-Fixing Cyanobacteria: Ecology and Biotechnological Applications. *Handbook of Marine Microalgae: Biotechnology Advances* 501–515. <https://doi.org/10.1016/B978-0-12-800776-1.00033-9>
4. Lee H, Depuydt S, Choi S, et al (2021) Potential use of nuisance cyanobacteria as a source of anticancer agents. *Natural Bioactive Compounds* 203–231. <https://doi.org/10.1016/B978-0-12-820655-3.00010-0>
5. Stanier RY, Kunisawa R, Mandel M, Cohen-Bazire G (1971) Purification and Properties of Unicellular Blue-Green Algae (Order Chroococcales). *BACTERIOLOGICAL REVIEWS* 171–205
6. Komárek J, Kaštovský J, Mareš J, Johansen JR (2014) Taxonomic classification of cyanoprokaryotes (cyanobacterial genera) 2014, using a polyphasic approach. *Preslia* 86:295–335
7. Marie B, Huet H, Marie A, et al (2012) Effects of a toxic cyanobacterial bloom (*Planktothrix agardhii*) on fish: insights from histopathological and quantitative proteomic assessments following the oral exposure of medaka fish (*Oryzias latipes*). *Aquat Toxicol* 114–115:39–48. <https://doi.org/10.1016/J.AQUATOX.2012.02.008>
8. Thomas J (1972) Relationship between age of culture and occurrence of the pigments of photosystem II of photosynthesis in heterocysts of a blue-green alga. *J Bacteriol* 110:92–95. <https://doi.org/10.1128/jb.110.1.92-95.1972>

9. Moss B, Jeppesen E, Søndergaard M, et al (2013) Nitrogen, macrophytes, shallow lakes and nutrient limitation: Resolution of a current controversy? *Hydrobiologia* 710:3–21
10. Bachmann RW, Jones BL, Fox DD, et al (1996) Relations between trophic state indicators and fish in Florida (U.S.A.) lakes. *Canadian Journal of Fisheries and Aquatic Sciences* 53:842–855. <https://doi.org/10.1139/f95-236>
11. Gobler CJ (2020) Climate Change and Harmful Algal Blooms: Insights and perspective. *Harmful Algae* 91:101731. <https://doi.org/10.1016/J.HAL.2019.101731>
12. Paerl HW, Barnard MA (2020) Mitigating the global expansion of harmful cyanobacterial blooms: Moving targets in a human- and climatically-altered world. *Harmful Algae* 96:. <https://doi.org/10.1016/J.HAL.2020.101845>
13. Krztoń W, Kosiba J, Pocięcha A, Wilk-Woźniak E (2019) The effect of cyanobacterial blooms on bio- and functional diversity of zooplankton communities. *Biodivers Conserv* 28:1815–1835. <https://doi.org/10.1007/s10531-019-01758-z>
14. Algal bloom and its economic impact - Publications Office of the EU. <https://op.europa.eu/en/publication-detail/-/publication/4d384d1b-1804-11e6-ba9a-01aa75ed71a1/language-en>. Accessed 29 Nov 2022
15. Meriluoto J, Spoof L, Codd GA (2016) *Handbook of Cyanobacterial Monitoring and Cyanotoxin Analysis*. John Wiley & Sons, Ltd, Chichester, UK
16. Souza NR, Metcalf JS (2020) Cyanobacterial toxins and their effects on human and animal health. In: *Handbook of Algal Science, Technology and Medicine*. Elsevier, pp 561–574
17. Stewart I, Seawright AA, Shaw GR (2008) Cyanobacterial poisoning in livestock, wild mammals and birds--an overview. *Adv Exp Med Biol* 619:613–637
18. Zhang F, Lee J, Liang S, Shum C (2015) Cyanobacteria blooms and non-alcoholic liver disease: Evidence from a county level ecological study in the United States. *Environ Health* 14:. <https://doi.org/10.1186/s12940-015-0026-7>

19. Svirčev Z, Krstić S, Miladinov-Mikov M, et al (2009) Freshwater cyanobacterial blooms and primary liver cancer epidemiological studies in Serbia. *J Environ Sci Health C Environ Carcinog Ecotoxicol Rev* 27:36–55. <https://doi.org/10.1080/10590500802668016>
20. Bouaïcha N, Miles CO, Beach DG, et al (2019) Structural Diversity, Characterization and Toxicology of Microcystins. *Toxins* 2019, Vol 11, Page 714 11:714. <https://doi.org/10.3390/TOXINS11120714>
21. Wood SA, Dietrich DR (2011) Quantitative assessment of aerosolized cyanobacterial toxins at two New Zealand lakes. *Journal of Environmental Monitoring* 13:1617–1624. <https://doi.org/10.1039/c1em10102a>
22. Facciponte DN, Bough MW, Seidler D, et al (2018) Identifying aerosolized cyanobacteria in the human respiratory tract: A proposed mechanism for cyanotoxin-associated diseases. *Science of the Total Environment* 645:1003–1013. <https://doi.org/10.1016/j.scitotenv.2018.07.226>
23. (2021) *Toxic Cyanobacteria in Water*. CRC Press
24. Revision of the Drinking Water Directive (RECAST 2017). <https://ec.europa.eu/info/law/better-regulation/have-your-say/initiatives/1563-Revision-of-the-Drinking-Water-Directive-RECAST-2017->. Accessed 30 Oct 2020
25. EUR-Lex - 32020L2184 - EN - EUR-Lex. <https://eur-lex.europa.eu/eli/dir/2020/2184/oj>. Accessed 11 Jul 2021
26. (2020) Cyanobacterial toxins: saxitoxins Background document for development of WHO
27. (2020) Cyanobacterial toxins: cylindrospermopsins Background document for development of WHO
28. (2020) Cyanobacterial toxins: microcystins Background document for development of WHO
29. Hamilton DP, Wood SA, Dietrich DR, Puddick J (2013) Costs of harmful blooms of freshwater cyanobacteria. In: *Cyanobacteria*. John Wiley & Sons, Ltd, Chichester, UK, pp 245–256
30. Cost of algal blooms | Land and Water Australia. <http://lwa.gov.au/products/pr990308>. Accessed 11 Jul 2021

31. Triantis T, Tsimeli K, Kaloudis T, et al (2010) Development of an integrated laboratory system for the monitoring of cyanotoxins in surface and drinking waters. *Toxicon* 55:979–989. <https://doi.org/10.1016/j.toxicon.2009.07.012>
32. Cyanotoxins - Publications Office of the EU. <https://op.europa.eu/en/publication-detail/-/publication/c61665a1-45ab-11e7-aea8-01aa75ed71a1/language-en>. Accessed 11 Jul 2021
33. Recknagel F, Orr PT, Bartkow M, et al (2017) Early warning of limit-exceeding concentrations of cyanobacteria and cyanotoxins in drinking water reservoirs by inferential modelling. *Harmful Algae* 69:18–27. <https://doi.org/10.1016/J.HAL.2017.09.003>
34. CyanoBox - CYRIC. <https://www.cyric.eu/project/cyanobox/>. Accessed 11 Jul 2021
35. Pyo JC, Park LJ, Pachevsky Y, et al (2020) Using convolutional neural network for predicting cyanobacteria concentrations in river water. *Water Res* 186:116349. <https://doi.org/10.1016/J.WATRES.2020.116349>
36. Shahmuradov IA, Mohamad Razali R, Bougouffa S, et al (2017) bTSSfinder: a novel tool for the prediction of promoters in cyanobacteria and *Escherichia coli*. *Bioinformatics* 33:334–340. <https://doi.org/10.1093/BIOINFORMATICS/BTW629>
37. Zhao CS, Shao NF, Yang ST, et al (2019) Predicting cyanobacteria bloom occurrence in lakes and reservoirs before blooms occur. *Science of The Total Environment* 670:837–848. <https://doi.org/10.1016/J.SCITOTENV.2019.03.161>
38. Kim T-J (2018) Prevention of Harmful Algal Blooms by Control of Growth Parameters. *Advances in Bioscience and Biotechnology* 09:613–648. <https://doi.org/10.4236/ABB.2018.911043>
39. Li J, Hansson LA, Persson KM (2018) Nutrient Control to Prevent the Occurrence of Cyanobacterial Blooms in a Eutrophic Lake in Southern Sweden, Used for Drinking Water Supply. *Water* 2018, Vol 10, Page 919 10:919. <https://doi.org/10.3390/W10070919>
40. Caspers H (1984) OECD: Eutrophication of Waters. Monitoring, Assessment and Control. — 154 pp. Paris: Organisation for Economic Co-

- Operation and Development 1982. (Publié en français sous le titre «Eutrophication des Eaux. Méthodes de Surveillance, d'Evaluation et de Lutte»). Internationale Revue der gesamten Hydrobiologie und Hydrographie 69:200–200. <https://doi.org/10.1002/iroh.19840690206>
41. Verburg P, Horrox J, Chaney E, et al (2013) Nutrient ratios, differential retention, and the effect on nutrient limitation in a deep oligotrophic lake. *Hydrobiologia* 718:119–130. <https://doi.org/10.1007/s10750-013-1609-3>
  42. On the Proportions of Organic Derivatives in Sea Water and Their Relation to ... - Alfred Clarence Redfield - Βιβλία Google. [https://books.google.com.cy/books/about/On\\_the\\_Proportions\\_of\\_Organic\\_Derivative.html?id=N6VEnQEACAAJ&redir\\_esc=y](https://books.google.com.cy/books/about/On_the_Proportions_of_Organic_Derivative.html?id=N6VEnQEACAAJ&redir_esc=y). Accessed 30 Oct 2020
  43. Ptacnik R, Andersen T, Tamminen T (2010) Performance of the Redfield Ratio and a Family of Nutrient Limitation Indicators as Thresholds for Phytoplankton N vs. P Limitation. *Ecosystems* 13:1201–1214. <https://doi.org/10.1007/s10021-010-9380-z>
  44. Guildford SJ, Hecky RE (2000) Total nitrogen, total phosphorus, and nutrient limitation in lakes and oceans: Is there a common relationship? *Limnol Oceanogr* 45:1213–1223. <https://doi.org/10.4319/lo.2000.45.6.1213>
  45. Bergström AK (2010) The use of TN:TP and DIN:TP ratios as indicators for phytoplankton nutrient limitation in oligotrophic lakes affected by N deposition. *Aquat Sci* 72:277–281. <https://doi.org/10.1007/s00027-010-0132-0>
  46. Water Treatment for Purification from Cyanobacteria and Cyanotoxins | Wiley. <https://www.wiley.com/en-us/Water+Treatment+for+Purification+from+Cyanobacteria+and+Cyanotoxins-p-9781118928615>. Accessed 1 Mar 2021
  47. Gijssbertsen-Abrahamse AJ, Schmidt W, Chorus I, Heijman SGJ (2006) Removal of cyanotoxins by ultrafiltration and nanofiltration. *J Memb Sci* 276:252–259. <https://doi.org/10.1016/j.memsci.2005.09.053>
  48. Dziga D, Wasylewski M, Wladyka B, et al (2013) Microbial degradation of microcystins. *Chem Res Toxicol* 26:841–852

49. Antoniou MG, de La Cruz AA, Pelaez MA, et al (2013) Practices that Prevent the Formation of Cyanobacterial Blooms in Water Resources and Remove Cyanotoxins During Physical Treatment of Drinking Water. In: Comprehensive Water Quality and Purification. Elsevier Inc., pp 173–195
50. Sharma VK, Triantis TM, Antoniou MG, et al (2012) Destruction of microcystins by conventional and advanced oxidation processes: A review. *Sep Purif Technol* 91:3–17
51. Paerl HW, Xu H, McCarthy MJ, et al (2011) Controlling harmful cyanobacterial blooms in a hyper-eutrophic lake (Lake Taihu, China): The need for a dual nutrient (N & P) management strategy. *Water Res* 45:1973–1983. <https://doi.org/10.1016/j.watres.2010.09.018>
52. Kibuye FA, Zamyadi A, Wert EC (2021) A critical review on operation and performance of source water control strategies for cyanobacterial blooms: Part II-mechanical and biological control methods. *Harmful Algae* 109:102119. <https://doi.org/10.1016/J.HAL.2021.102119>
53. Pêczuła W, Stosowane M, Kontroli W, et al METHODS APPLIED IN CYANOBACTERIAL BLOOM CONTROL IN SHALLOW LAKES AND RESERVOIRS. [https://doi.org/10.2428/ecea.2012.19\(07\)079](https://doi.org/10.2428/ecea.2012.19(07)079)
54. Greenfield DI, Duquette A, Goodson A, et al The Effects of Three Chemical Algaecides on Cell Numbers and Toxin Content of the Cyanobacteria *Microcystis aeruginosa* and *Anabaenopsis* sp. <https://doi.org/10.1007/s00267-014-0339-2>
55. Pęczuła W (2013) Influence of barley straw (*Hordeum vulgare* L.) extract on phytoplankton dominated by *Scenedesmus* species in laboratory conditions: the importance of the extraction duration. *J Appl Phycol* 25:661. <https://doi.org/10.1007/S10811-012-9900-7>
56. Bouaidi -el (2021) ALGICIDAL EFFECT OF EXTRACTS FROM A GREEN MACROLAGAE (*CHARA VULGARIS*) ON THE GROWTH OF THE POTENTIALLY TOXIC CYANOBACTERIUM (*MICROCYSTIS AERUGINOSA*). [https://doi.org/10.15666/aeer/1906\\_47814794](https://doi.org/10.15666/aeer/1906_47814794)

57. Drábková M, Matthijs HCP, Admiraal W, Maršálek B (2007) Selective effects of H<sub>2</sub>O<sub>2</sub> on cyanobacterial photosynthesis. *Photosynthetica* 45:363–369. <https://doi.org/10.1007/s11099-007-0062-9>
58. Piel T, Sandrini G, White E, et al (2019) Suppressing cyanobacteria with hydrogen peroxide is more effective at high light intensities. *Toxins (Basel)* 12:. <https://doi.org/10.3390/toxins12010018>
59. Matthijs HCP, Visser PM, Reeze B, et al (2012) Selective suppression of harmful cyanobacteria in an entire lake with hydrogen peroxide. *Water Res* 46:1460–1472. <https://doi.org/10.1016/j.watres.2011.11.016>
60. Santos AA, Guedes DO, Barros MUG, et al (2021) Effect of hydrogen peroxide on natural phytoplankton and bacterioplankton in a drinking water reservoir: Mesocosm-scale study. *Water Res* 197:117069. <https://doi.org/10.1016/J.WATRES.2021.117069>
61. Samuilov VD, Timofeev KN, Sinitsyn S V., Bezryadnov D V. (2004) H<sub>2</sub>O<sub>2</sub>-induced inhibition of photosynthetic O<sub>2</sub> evolution by *Anabaena variabilis* cells. *Biochemistry (Moscow)* 69:926–933. <https://doi.org/10.1023/B:BIRY.0000040227.66714.19>
62. Bouchard JN, Roy S, Campbell DA (2006) UVB Effects on the Photosystem II-D1 Protein of Phytoplankton and Natural Phytoplankton Communities. *Photochem Photobiol* 82:936. <https://doi.org/10.1562/2005-08-31-ir-666>
63. Bienert GP, Schjoerring JK, Jahn TP (2006) Membrane transport of hydrogen peroxide. *Biochim Biophys Acta Biomembr* 1758:994–1003. <https://doi.org/10.1016/J.BBAMEM.2006.02.015>
64. Bienert GP, Møller ALB, Kristiansen KA, et al (2007) Specific aquaporins facilitate the diffusion of hydrogen peroxide across membranes. *Journal of Biological Chemistry* 282:1183–1192. <https://doi.org/10.1074/JBC.M603761200>
65. Zhang H, Meng G, Mao F, et al (2019) Use of an integrated metabolomics platform for mechanistic investigations of three commonly used algacides on cyanobacterium, *Microcystis aeruginosa*. *J Hazard Mater* 367:120–127. <https://doi.org/10.1016/J.JHAZMAT.2018.12.069>

66. Sandrini G, Piel T, Xu T, et al (2020) Sensitivity to hydrogen peroxide of the bloom-forming cyanobacterium *Microcystis* PCC 7806 depends on nutrient availability. *Harmful Algae* 99:101916. <https://doi.org/10.1016/j.hal.2020.101916>
67. Menezes I, Maxwell-McQueeney D, Capelo-Neto J, et al (2020) Oxidative stress in the cyanobacterium *Microcystis aeruginosa* PCC 7813: Comparison of different analytical cell stress detection assays. *Chemosphere* 269:128766. <https://doi.org/10.1016/j.chemosphere.2020.128766>
68. Wang B, Song Q, Long J, et al (2019) Optimization method for *Microcystis* bloom mitigation by hydrogen peroxide and its stimulative effects on growth of chlorophytes. *Chemosphere* 228:503–512. <https://doi.org/10.1016/J.CHEMOSPHERE.2019.04.138>
69. Wang H, Zhao Y, Li T, et al (2016) Properties of calcium peroxide for release of hydrogen peroxide and oxygen: A kinetics study. *Chemical Engineering Journal* 303:450–457. <https://doi.org/10.1016/j.cej.2016.05.123>
70. Keliri E, Paraskeva C, Sofokleous A, et al (2021) Occurrence of a single-species cyanobacterial bloom in a lake in Cyprus: monitoring and treatment with hydrogen peroxide-releasing granules. *Environmental Sciences Europe* 2021 33:1 33:1–14. <https://doi.org/10.1186/S12302-021-00471-5>
71. Lu S, Zhang X, Xue Y (2017) Application of calcium peroxide in water and soil treatment: A review. *J Hazard Mater* 337:163–177. <https://doi.org/10.1016/J.JHAZMAT.2017.04.064>
72. Hu Y, Shen L, Ren X, et al (2020) Properties of CaO<sub>2</sub> for H<sub>2</sub>O<sub>2</sub> release and phosphate removal and its feasibility in controlling *Microcystis* blooms. *Environmental Science and Pollution Research* 27:35239–35248. <https://doi.org/10.1007/S11356-020-09738-5/FIGURES/6>
73. Controlling cyanobacterial blooms through effective flocculation and sedimentation with combined use of flocculants and phosphorus adsorbing natural soil and modified clay | Elsevier Enhanced Reader. <https://reader.elsevier.com/reader/sd/pii/S0043135415303833?token=ED4CC24D88799DC45E01880ABBD1143F461B3773F8820581D31E74182>

- F7FFE4742918E551D22F3F9385209FAB723D723&originRegion=eu-west-1&originCreation=20211215175646. Accessed 15 Dec 2021
74. Cho I, Lee K (2002) Effect of calcium peroxide on the growth and proliferation of *Microcystis aeruginosa*, a water-blooming cyanobacterium. *Biotechnol Bioproc E* 7:231–233. <https://doi.org/10.1007/bf02932976>
  75. An optimized CaO<sub>2</sub>-functionalized alginate bead for simultaneous and efficient removal of phosphorous and harmful cyanobacteria | Elsevier Enhanced Reader. <https://reader.elsevier.com/reader/sd/pii/S0048969721054590?token=92D91A784423439C464BC79CA7C88E63D1F636F8672F63A02DC543B04646C24DCB99094CFC5AFF7B7EEAF46F39A9CFF5&originRegion=eu-west-1&originCreation=20211215171348>. Accessed 15 Dec 2021
  76. Wang B, Zheng S, Huang Z, et al (2021) Fabrication of H<sub>2</sub>O<sub>2</sub> slow-releasing composites for simultaneous *Microcystis* mitigation and phosphate immobilization. *Science of The Total Environment* 798:149164. <https://doi.org/10.1016/J.SCITOTENV.2021.149164>
  77. Keliri E, Adamou P, Efstathiou N, et al (2022) Calcium peroxide (CaO<sub>2</sub>) granules enclosed in fabrics as an alternative H<sub>2</sub>O<sub>2</sub> delivery system to combat *Microcystis* sp. *Chemical Engineering Journal Advances* 11:100318. <https://doi.org/10.1016/J.CEJA.2022.100318>
  78. Teixeira LAC, Andia JPM, Yokoyama L, et al (2013) Oxidation of cyanide in effluents by Caro's Acid. *Miner Eng* 45:81–87. <https://doi.org/10.1016/J.MINENG.2013.01.008>
  79. IXPER® Calcium Peroxide 75C | Solvay. <https://www.solvay.com/en/product/ixper-calcium-peroxide-75c>. Accessed 27 Feb 2022
  80. Ghanbari F, Moradi M (2017) Application of peroxymonosulfate and its activation methods for degradation of environmental organic pollutants: Review. *Chemical Engineering Journal* 310:41–62. <https://doi.org/10.1016/J.CEJ.2016.10.064>
  81. Tay KS, Ismail NSB (2016) Degradation of  $\beta$ -blockers in water by sulfate radical-based oxidation: kinetics, mechanism and ecotoxicity assessment.

- International Journal of Environmental Science and Technology 13:2495–2504. <https://doi.org/10.1007/S13762-016-1083-3/TABLES/5>
82. Chen Z, Li J, Chen M, et al (2021) Microcystis aeruginosa removal by peroxides of hydrogen peroxide, peroxymonosulfate and peroxydisulfate without additional activators. *Water Res* 201:. <https://doi.org/10.1016/J.WATRES.2021.117263>
  83. Wahba N, el Asmar MF, el Sadr MM (1959) Iodometric Method for Determination of Persulfates. *Anal Chem* 31:1870–1871. [https://doi.org/10.1021/AC60155A059/ASSET/AC60155A059.FP.PNG\\_V03](https://doi.org/10.1021/AC60155A059/ASSET/AC60155A059.FP.PNG_V03)
  84. Rogers SO, Bendich AJ (1994) Extraction of total cellular DNA from plants, algae and fungi. In: *Plant Molecular Biology Manual*. Springer Netherlands, pp 183–190
  85. Chernova E, Russkikh I, Voyakina E, Zhakovskaya Z (2016) Occurrence of microcystins and anatoxin-a in eutrophic lakes of Saint Petersburg, Northwestern Russia. *Oceanol Hydrobiol Stud* 45:466–484. <https://doi.org/10.1515/ohs-2016-0040>
  86. Sellers RM (1980) Spectrophotometric determination of hydrogen peroxide using potassium titanium(IV) oxalate. *Analyst* 105:950–954. <https://doi.org/10.1039/an9800500950>
  87. Rippka R, Deruelles J, Waterbury JB (1979) Generic assignments, strain histories and properties of pure cultures of cyanobacteria. *J Gen Microbiol* 111:1–61. <https://doi.org/10.1099/00221287-111-1-1/CITE/REFWORKS>
  88. Stoll S, Schweiger A (2005) EasySpin, a comprehensive software package for spectral simulation and analysis in EPR. <https://doi.org/10.1016/j.jmr.2005.08.013>
  89. Harbour JR, Chow V, Bolt On^ JR, et al (2011) An Electron Spin Resonance Study of the Spin Adducts of OH and HO2 Radicals with Nitrones in the Ultraviolet Photolysis of Aqueous Hydrogen Peroxide Solutions. <https://doi.org/10.1139/v74-527> 52:3549–3553. <https://doi.org/10.1139/V74-527>
  90. Taniguchi H, Madden KP (2000) DMPO-Alkyl Radical Spin Trapping: An In Situ Radiolysis Steady-State ESR Study. <https://doi.org/10.1667/0033->

7587(2000)153[0447:DARSTA]20CO;2 153:447–453.

[https://doi.org/10.1667/0033-7587\(2000\)153](https://doi.org/10.1667/0033-7587(2000)153)

91. Khomutovska N, Sandzewicz M, Łach Ł, et al (2020) Limited Microcystin, Anatoxin and Cylindrospermopsin Production by Cyanobacteria from Microbial Mats in Cold Deserts. *Toxins* (Basel) 12:.. <https://doi.org/10.3390/TOXINS12040244>
92. Schneider CA, Rasband WS, Eliceiri KW (2012) NIH Image to ImageJ: 25 years of image analysis. *Nature Methods* 2012 9:7 9:671–675. <https://doi.org/10.1038/nmeth.2089>
93. Jakubowska N, Szelaż-Wasielewska E (2015) Toxic Picoplanktonic Cyanobacteria—Review. *Mar Drugs* 13:1497–1518. <https://doi.org/10.3390/md13031497>
94. Mazur-Marzec H, Sutryk K, Kobos J, et al (2013) Occurrence of cyanobacteria and cyanotoxin in the Southern Baltic Proper. Filamentous cyanobacteria versus single-celled picocyanobacteria. *Hydrobiologia* 701:235–252. <https://doi.org/10.1007/s10750-012-1278-7>
95. Ngwa FF, Madramootoo CA, Jabaji S (2014) Comparison of cyanobacterial microcystin synthetase (mcy) E gene transcript levels, mcy E gene copies, and biomass as indicators of microcystin risk under laboratory and field conditions. *Microbiologyopen* 3:411–425. <https://doi.org/10.1002/mbo3.173>
96. Wang X, Wang P, Wang C, et al (2018) Microcystin biosynthesis in *Microcystis aeruginosa*: Indirect regulation by iron variation. *Ecotoxicol Environ Saf* 148:942–952. <https://doi.org/10.1016/j.ecoenv.2017.11.059>
97. Salvador D, Churro C, Valério E (2016) Evaluating the influence of light intensity in mcyA gene expression and microcystin production in toxic strains of *Planktothrix agardhii* and *Microcystis aeruginosa*. *J Microbiol Methods* 123:4–12. <https://doi.org/10.1016/j.mimet.2016.02.002>
98. Zuo J, Chen L, Shan K, et al (2018) Assessment of different mcy genes for detecting the toxic to non-toxic *Microcystis* ratio in the field by multiplex qPCR. *J Oceanol Limnol* 36:1132–1144. <https://doi.org/10.1007/s00343-019-7186-1>

99. Kurmayer R, Deng L, Entfellner E (2016) Role of toxic and bioactive secondary metabolites in colonization and bloom formation by filamentous cyanobacteria *Planktothrix*. *Harmful Algae* 54:69–86. <https://doi.org/10.1016/J.HAL.2016.01.004>
100. Altansukh O, Davaa G (2011) Application of Index Analysis to Evaluate the Water Quality of the Tuul River in Mongolia. *J Water Resour Prot* 3:398–414. <https://doi.org/10.4236/jwarp.2011.36050>
101. Renedo MJ, Fernández J, Garea A, Irabien JA (2007) INFLUENCE OF PARTICLE SIZE AND STRUCTURAL PROPERTIES OF SORBENTS PREPARED FROM FLY-ASH AND Ca(OH)<sub>2</sub> ON THE SO<sub>2</sub> REMOVAL ABILITY. <http://dx.doi.org/101080/00986440008912828> 182:69–80. <https://doi.org/10.1080/00986440008912828>
102. Henry Kuivila BG, Snyder HR, Kuck JA, Johnson JR (1952) Quantitative Organic Analysis via Functional Groups. *J Gen Chem (USSR)* 870:327
103. Lu C-P, Lin C-T, Chang C-M, et al (2011) Nitrophenylboronic Acids as Highly Chemoselective Probes To Detect Hydrogen Peroxide in Foods and Agricultural Products. *J Agric Food Chem* 59:11403–11406. <https://doi.org/10.1021/jf202874r>
104. Su G, Wei Y, Guo M (2011) Direct Colorimetric Detection of Hydrogen Peroxide Using 4-Nitrophenyl Boronic Acid or Its Pinacol Ester. *Am J Analyt Chem* 2:879–884. <https://doi.org/10.4236/ajac.2011.28101>
105. Elumalai V, Hansen JH (2020) A scalable and green one-minute synthesis of substituted phenols †. <https://doi.org/10.1039/d0ra08580d>
106. Beversdorf LJ, Chaston SD, Miller TR, McMahon KD (2015) Microcystin mcyA and mcyE Gene Abundances Are Not Appropriate Indicators of Microcystin Concentrations in Lakes. *PLoS One* 10:e0125353. <https://doi.org/10.1371/journal.pone.0125353>
107. Weenink EFJ, Kraak MHS, van Teulingen C, et al (2022) Sensitivity of phytoplankton, zooplankton and macroinvertebrates to hydrogen peroxide treatments of cyanobacterial blooms. *Water Res* 225:119169. <https://doi.org/10.1016/J.WATRES.2022.119169>
108. Lu S, Zhang X, Xue Y (2017) Application of calcium peroxide in water and soil treatment: A review. *J Hazard Mater* 337:163–177

109. Wang B, Song Q, Long J, et al (2019) Optimization method for Microcystis bloom mitigation by hydrogen peroxide and its stimulative effects on growth of chlorophytes. *Chemosphere* 228:503–512. <https://doi.org/10.1016/J.CHEMOSPHERE.2019.04.138>
110. Asaeda T, Rahman M, Damitha H, Abeynayaka L (2020) Hydrogen peroxide can be a plausible biomarker in cyanobacterial bloom treatment. <https://doi.org/10.1038/s41598-021-02978-6>
111. Piel T, Sandrini G, White E, et al Suppressing Cyanobacteria with Hydrogen Peroxide Is More Effective at High Light Intensities. <https://doi.org/10.3390/toxins12010018>
112. Weenink EFJ, Matthijs HCP, Schuurmans JM, et al (2021) Interspecific protection against oxidative stress: green algae protect harmful cyanobacteria against hydrogen peroxide. *Environ Microbiol* 23:2404–2419. <https://doi.org/10.1111/1462-2920.15429>
113. Oszejca M, Brindell M, Orzeł Ł, et al (2016) Mechanistic studies on versatile metal-assisted hydrogen peroxide activation processes for biomedical and environmental incentives. *Coord Chem Rev* 327–328:143–165. <https://doi.org/10.1016/J.CCR.2016.05.013>
114. Sandrini G, Piel T, Xu T, et al (2020) Sensitivity to hydrogen peroxide of the bloom-forming cyanobacterium *Microcystis* PCC 7806 depends on nutrient availability. *Harmful Algae* 99:101916. <https://doi.org/10.1016/J.HAL.2020.101916>
115. Hu Y, Shen L, Ren X, et al (2020) Properties of CaO<sub>2</sub> for H<sub>2</sub>O<sub>2</sub> release and phosphate removal and its feasibility in controlling *Microcystis* blooms. *Environmental Science and Pollution Research* 27:35239–35248. <https://doi.org/10.1007/S11356-020-09738-5/FIGURES/6>
116. Hu Y, Shen L, Ren X, et al (2020) Properties of CaO<sub>2</sub> for H<sub>2</sub>O<sub>2</sub> release and phosphate removal and its feasibility in controlling *Microcystis* blooms. *Environmental Science and Pollution Research* 27:35239–35248. <https://doi.org/10.1007/S11356-020-09738-5>
117. Escobar-Lux RH, Fields DM, Browman HI, et al (2019) The effects of hydrogen peroxide on mortality, escape response, and oxygen consumption

- of *Calanus* spp. *Facets* 2019:626–637. <https://doi.org/10.1139/FACETS-2019-0011/ASSET/IMAGES/MEDIUM/FACETS-2019-0011F2.GIF>
118. Huang IS, Zimba P v. (2020) Hydrogen peroxide, an ecofriendly remediation method for controlling *Microcystis aeruginosa* toxic blooms. *J Appl Phycol* 32:3133–3142. <https://doi.org/10.1007/S10811-020-02086-4/FIGURES/3>
  119. Lusty MW, Gobler CJ (2023) Repeated hydrogen peroxide dosing briefly reduces cyanobacterial blooms and microcystin while increasing fecal bacteria indicators in a eutrophic pond. *Journal of Environmental Sciences* 124:522–543. <https://doi.org/10.1016/J.JES.2021.11.031>
  120. Daniel E, Weiss G, Murik O, et al (2019) The response of *Microcystis aeruginosa* strain MGK to a single or two consecutive H<sub>2</sub>O<sub>2</sub> applications. *Environ Microbiol Rep* 11:621–629. <https://doi.org/10.1111/1758-2229.12789>
  121. Ruiz M, Yang Y, Lochbaum CA, et al (2019) Peroxymonosulfate Oxidizes Amino Acids in Water without Activation. *Environ Sci Technol* 53:10845–10854. [https://doi.org/10.1021/ACS.EST.9B01322/ASSET/IMAGES/LARGE/ES9B01322\\_0002.JPEG](https://doi.org/10.1021/ACS.EST.9B01322/ASSET/IMAGES/LARGE/ES9B01322_0002.JPEG)
  122. Antoniou MG, Boraei I, Solakidou M, et al (2018) Enhancing photocatalytic degradation of the cyanotoxin microcystin-LR with the addition of sulfate-radical generating oxidants. *J Hazard Mater* 360:461–470. <https://doi.org/10.1016/J.JHAZMAT.2018.07.111>
  123. Mouchet P, Bonnelye V (1998) Solving algae problems: French expertise and world-wide applications. *Journal of Water Supply: Research and Technology-Aqua* 47:125–141. <https://doi.org/10.2166/AQUA.1998.19>
  124. Nietch CT, Gains-Germain L, Lazorchak J, et al (2022) Development of a Risk Characterization Tool for Harmful Cyanobacteria Blooms on the Ohio River. *Water* 2022, Vol 14, Page 644 14:644. <https://doi.org/10.3390/W14040644>
  125. Sukenik A, Kaplan A (2021) Cyanobacterial Harmful Algal Blooms in Aquatic Ecosystems: A Comprehensive Outlook on Current and Emerging

Mitigation and Control Approaches. *Microorganisms* 2021, Vol 9, Page  
1472 9:1472. <https://doi.org/10.3390/MICROORGANISMS9071472>

## APPENDIX I

Recent studies indicated that higher TN:TP molar ratios (>22, P-limitation) are more suitable for surface waters while DIN:TP (Dissolved Inorganic Nitrogen: Total Phosphorus) and NO<sub>3</sub><sup>-</sup>:TP mass ratios have been used more often during the past years for determining the limiting elements in lakes [44]. Studies on dissolved nutrients mass ratios (DIN:TP, NO<sub>3</sub><sup>-</sup>:TP, NH<sub>4</sub><sup>+</sup>:TP suggested that in freshwater systems the DIN:TP mass ratio is a better indicator than the TN:TP molar ratio. Also, the NO<sub>3</sub><sup>-</sup>:TP mass ratio performed even better than DIN:TP as DIN includes ammonium which in some studies it showed a weak correlation with N-limitation, resulting in a weaker model [45]. The nutrient ratios and thresholds proposed by researchers are presented in Table S1, as well as the water environment that they were studied.

**Table S 1.** Nutrient limitation approaches and thresholds based on TN:TP, DIN:TP and NO<sub>3</sub><sup>-</sup>:TP ratios in different aquatic environments.

Ratio	Units	Threshold	Nutrient Limitation	Reference	Aquatic environment studied
TN:TP	Molar	<7	N – limitation	[34,35]	Ocean
		>22	P – limitation		
TN:TP	Molar	<20	N – limitation	[36]	Lakes; Ocean
		20-50	N or P limitation		
		>50	P – limitation		
DIN:TP	Mass	<9	N – limitation	[37]	Lakes; ponds
		9-22	N or P co-limitation		
		>22	P – limitation		
NO <sub>3</sub> <sup>-</sup> :TP	Mass	<9	N – limitation	[37,38]	Lakes
		9-22	N or P co-limitation		
		>22	P – limitation		

**Table S 2.** Primers used in the detection of cyanotoxin producing genes in St. George Lake samples and amplification parameters of PCR. The primers were designed using deposited sequences or taken from references. *Cyr*, *sxt*, *ana* and *mcy* genes are involved in cylindrospermopsin, saxitoxin, anatoxin and microcystin synthesis, respectively.

<b>Targeting gene</b>	<b>Primer name</b>	<b>Sequence 5'-3'</b>	<b>Amplicon size (bp)</b>	<b>Annealing temperature (°C)</b>
<i>cyrJ</i>	cyrJ_F	AGTAATCCCGCCTGTCATAGA	109	60
	cyrJ_R	ACTGAGCATTGTCTCGGTAAAC		
<i>cyrB</i>	cyrB_F	GCCTGAGTACCTATCTGCTTAAC	95	60
	cyrB_R	AGCCTGAAACTGCTCCATATC		
<i>sxtA</i>	sxtA_F	GCGTACATCCAAGCTGGACTCG	683	55
	sxtA_R	GTAGTCCAGCTAAGGCACTTGC		
<i>anaC</i>	anaC_F	TCTGGTATTCAGTCCCCTCTAT	366	58
	anaC_R	CCCAATAGCCTGTCATCAA		
<i>mcyB</i>	mcyB_F	CCTCAGACAATCAACGGTTAGT	119	60
	mcyB_R	AAAGGCAGAAGGCACCATATAA		
<i>mcyE</i>	mcyE_F	CTGGTGGGAAAGGACTGATTTA	95	60
	mcyE_R	CGCCCTCAAGTCAAGAAAGA		

## APPENDIX II

### Water quality characteristics

Water characterization before each experiment was performed to estimate the load of the matrix and to ensure similar water characteristics of each complete set of experiments.

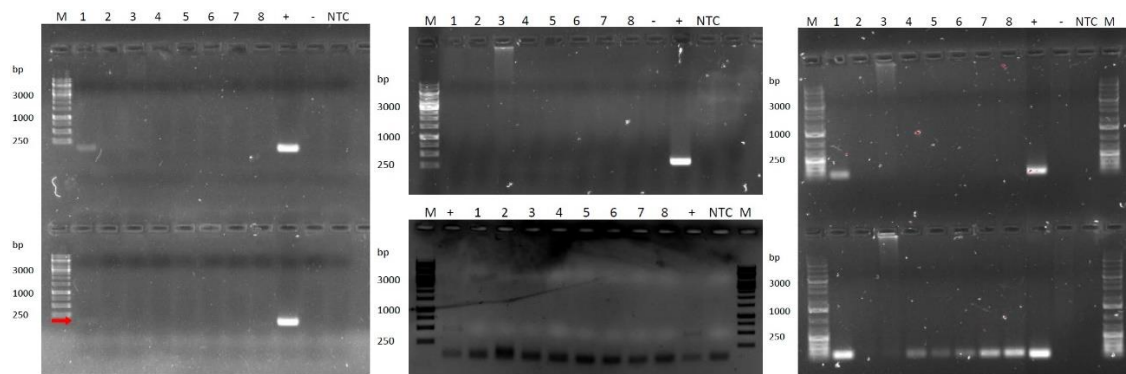
**Table S 3.** Summary of main physicochemical water characteristics of matrixes used in the experiments of this thesis.

<b>Water matrix</b>	<b>pH</b>	<b>conductivity</b>	<b>TDS mg/L</b>	<b>S ppm</b>	<b>TN mg/L</b>	<b>TP mg/L</b>	<b>FT620 RFU</b>	<b>FT 450 RFU</b>
<b>MQ</b>	6.99	18 $\mu\Omega$ cm <sup>-1</sup>	-	-	<LD	<LD	0	0
<b>Polis River</b>	8.20	1512 $\mu$ S cm <sup>-1</sup>	1028	1135	0.25	0.03	57	52
<b>Kouris Dam</b>	8.81	605 $\mu$ S cm <sup>-1</sup>	400	285	0.8	0.04	111	79
<b>Kouris Dam</b>	8.79	581	405	272	0.25	0.025	59	80
<b>Polemida Dam</b>	8.79	1170 $\mu$ S cm <sup>-1</sup>	824	579	0.8	0.04	266	350
<b>St. George Lake (blooming)</b>	8.88	1999	1835	950	2.6	0.28	7800	2390
<b>St. George Lake – Filtered (blooming)</b>	8.75	750	1318	891	0.7	0.10	78	101
<b>Athalassa Lake (fish kills)</b>	8.46	3300 $\mu$ S cm <sup>-1</sup>	2310	1640	2.4	0.21	1375	686
<b>Athalassa Lake (blooming)</b>	8.89	2954 $\mu$ S cm <sup>-1</sup>	2500	1214	2.1	0.19	6780	741

## St. George Lake monitoring

**Table S 4.** Average total and dissolved nutrient concentration (mg L<sup>-1</sup>) in St. George Lake during monitoring period, and best fitting nutrient ratios explaining limitation.

D/M/2019	TN	TP	N-NO <sub>3</sub>	N-NO <sub>2</sub>	N-NH <sub>4</sub>	DIN	DIN:TP	NO <sub>3</sub> :TP	Limiting element
25/02	6.0	0.06	4.6	0.10	0.10	4.8	80	77	P
04/03	4.7	0.11	3.4	0.09	0.10	3.6	33	31	P
18/04	6.9	0.06	5.8	0.11	0.10	6.0	100	97	P
12/07	6.6	0.20	2.4	0.08	0.20	2.7	13	12	Co-limitation
06/08	7.9	0.36	0.0	0.08	0.29	0.4	1	0	N
22/08	2.6	0.28	1.9	0.06	0.13	2.1	7	7	N
09/09	5.3	0.19	0.0	0.14	0.94	1.1	6	0	N
15/10	4.1	0.14	1.8	0.08	0.10	2.0	14	13	Co-limitation
09/12	6.4	0.28	4.9	0.09	0.10	5.1	18	18	Co-limitation



**Scheme S 1.** Agarose gel electrophoresis of DNA extracted from St. George Lake samples: (A) *cyrB* (upper row) and *cyrJ* (lower row); (B) *anaC* (upper row) and *sxtA* (lower row); (C) *mcyB* (upper row) and *mcyE* (lower row). M means marker, numbers 1-8 are the samples from St. George Lake, (+) positive control, (-) negative control, NTC (non-template control) is the control without DNA.

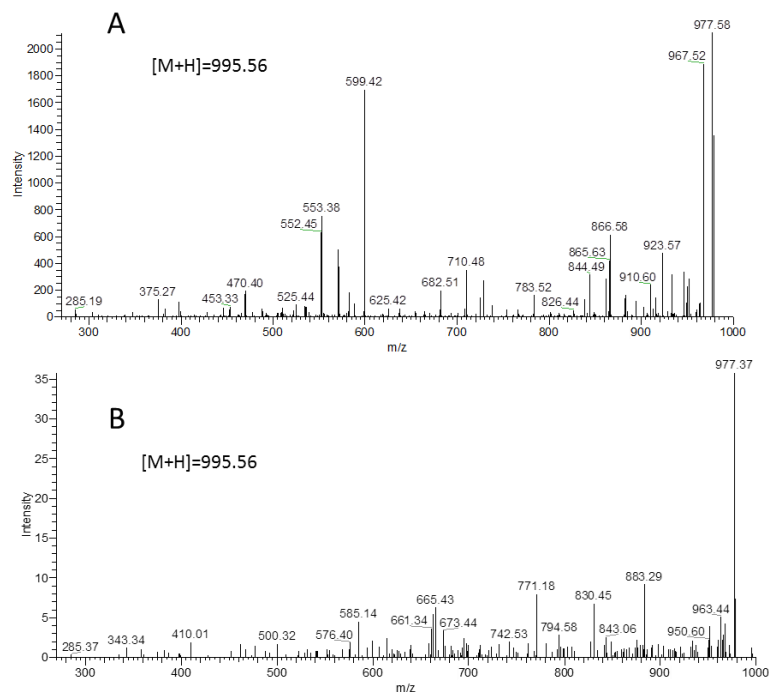


**Figure S 1.** MS/MS spectra of the (A) MC-LR standard compound and (B) compound detected in samples with  $[M+H] = 995.56$  but different fragmentation pattern.

## Novel oxidant treatments

### ➤ Calibration curves

Linear equations derived from calibration curves were utilized to translate absorbance read into concentrations.

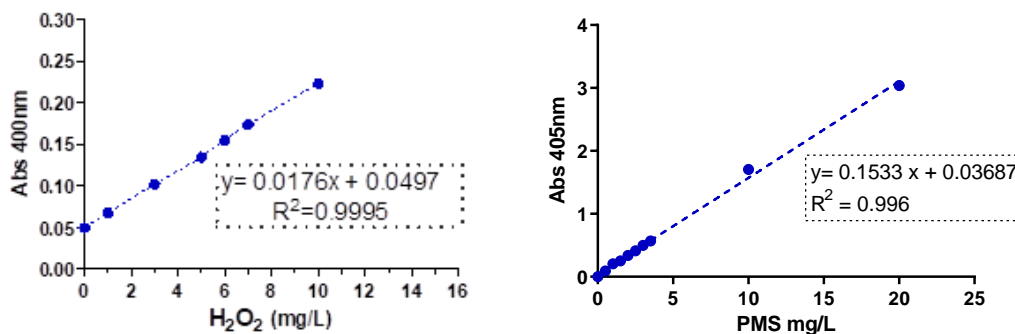


**Figure S 2.** Calibration curve of  $H_2O_2$  (left) and PMS (right).

➤ **Effect of surface water matrix**

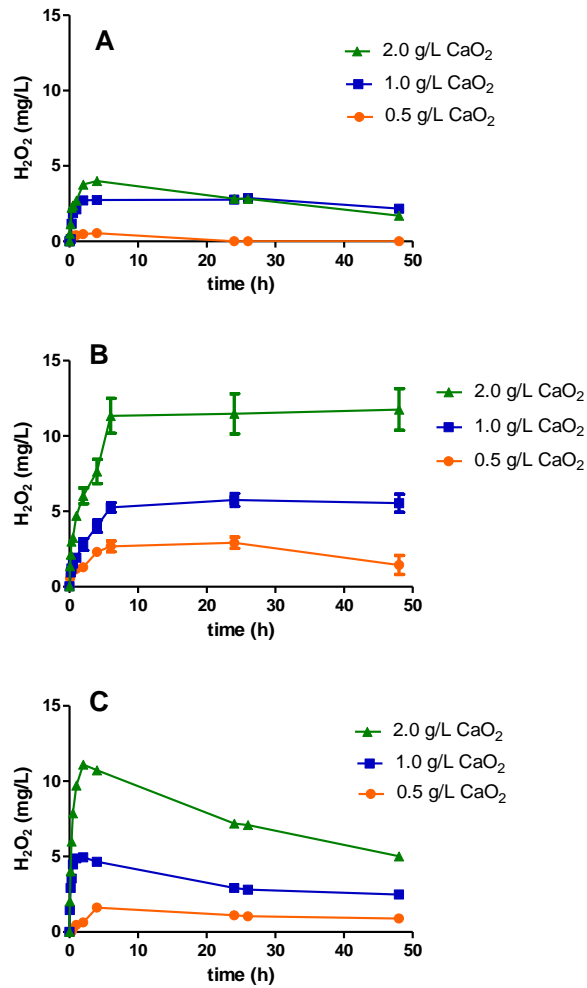


**Figure S 3.** H<sub>2</sub>O<sub>2</sub> release kinetics by CaO<sub>2</sub> granules in: (A) MQ-water, (B) River water, and (C) Kouris Dam water.

➤ **Effect of BG-11 medium**

**Table S 5.** BG-11 100%, 50%, and 25% matrix composition.

<b>Components</b>	<b>Stock solution (g/L)</b>	<b>[C] in 100 % BG-11 medium (mg/L)</b>	<b>[C] in 50 % BG-11 medium (mg/L)</b>	<b>[C] in 25 % BG-11 medium (mg/L)</b>
<b>Macromix</b>				
<b>NaNO<sub>3</sub></b>	500	500	250	125
<b>Na<sub>2</sub>EDTA</b>	1.1	1	0.50	0.25
<b>Citric acid</b>	6	6	3.00	1.50
<b>MgSO<sub>4</sub>.7H<sub>2</sub>O</b>	75	75	37.5	18.7
<b>CaCl<sub>2</sub>.2H<sub>2</sub>O</b>	36	36	18.0	9.00
<b>Na<sub>2</sub>CO<sub>3</sub></b>	20	20	10.0	5.00
<b>Spore solution</b>				
<b>H<sub>3</sub>BO<sub>3</sub></b>	2.86	0.715	0.357	0.178
<b>MnCl<sub>2</sub>.4H<sub>2</sub>O</b>	1.81	0.452	0.226	0.113
<b>ZnSO<sub>4</sub>.7H<sub>2</sub>O</b>	0.22	0.055	0.027	0.014
<b>(NH<sub>4</sub>)<sub>6</sub>Mo<sub>7</sub>O<sub>24</sub>.4H<sub>2</sub>O</b>	1.13	0.282	0.141	0.070
<b>CuSO<sub>4</sub>.5H<sub>2</sub>O</b>	0.078	0.019	0.009	0.005
<b>Co(NO<sub>3</sub>)<sub>2</sub>.6H<sub>2</sub>O</b>	0.049	0.012	0.006	0.003
<b>K<sub>2</sub>HPO<sub>4</sub></b>	30.5	3	1.5	0.75
<b>Fe(NH<sub>4</sub>)<sub>3</sub>-citrate</b>	6	0.6	0.3	0.15

**Table S 6.** Measured total nutrients in BG-11 medium (25%, 50%, and 75%).

<b>Total nutrients (mg L<sup>-1</sup>)</b>	<b>BG-11 dilutions</b>		
	<b>25%</b>	<b>50%</b>	<b>75%</b>
<b>TN</b>	68	133	204
<b>TP</b>	1.4	2.8	4.3

➤ **Effect of humics**

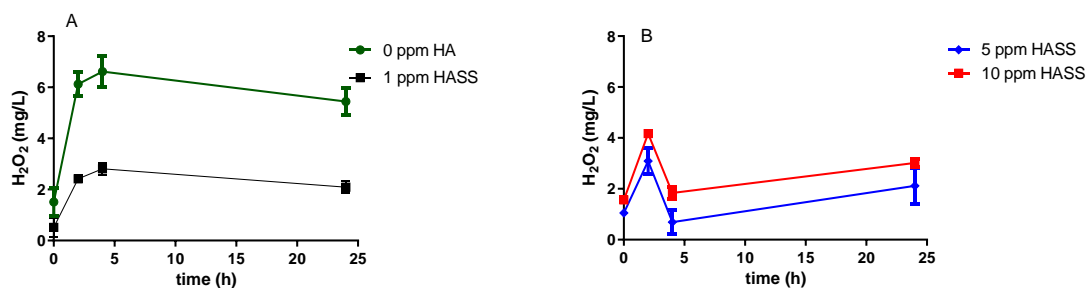


**Figure S 4.** H<sub>2</sub>O<sub>2</sub> release curves by 1.0 g L<sup>-1</sup> CaO<sub>2</sub> in surface (dam) water enriched (A) 0 and 1 ppm, and (B) 5 and 10 ppm of HASS at t= 0, 2, 4, 24 hours.

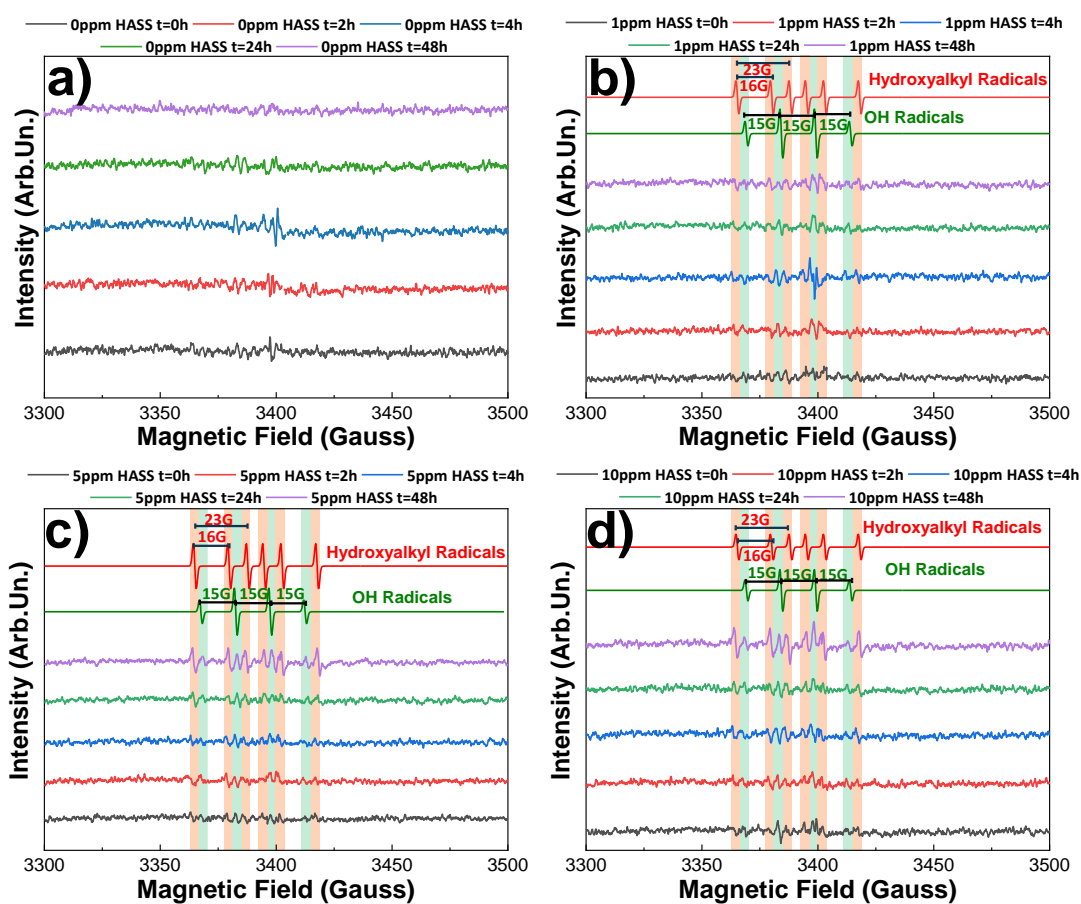


**Figure S 5.** EPR measurements of the four flasks at different time intervals. With green color we mark the DMPO/•OH adduct while with red color we mark the DMPO hydroxyalkyl adduct as they resulted from our simulations using the Easy Spin MATLAB add-on.

## H<sub>2</sub>O<sub>2</sub> release kinetics by CaO<sub>2</sub> granules / physicochemical water characteristics

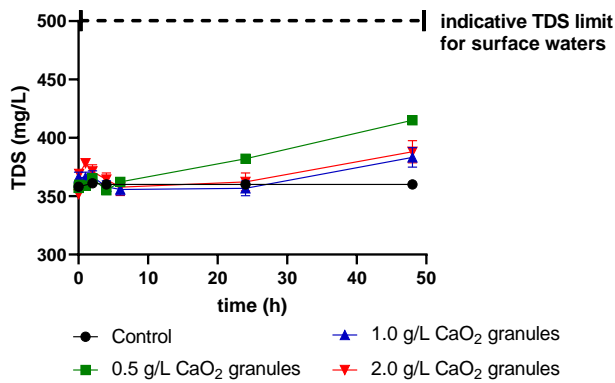


**Figure S 6.** Recorded TDS (mg/L) values after the addition of 0, 0.5, 1.0, and 2.0 g L<sup>-1</sup> CaO<sub>2</sub> granules in Kouris Dam surface water.

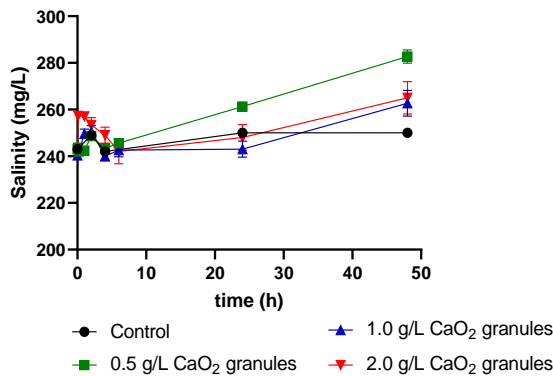


**Figure S 7.** Recorded Salinity (mg/L) values after the addition of 0, 0.5, 1.0, and 2.0 g L<sup>-1</sup> CaO<sub>2</sub> granules in Kouris Dam surface water.

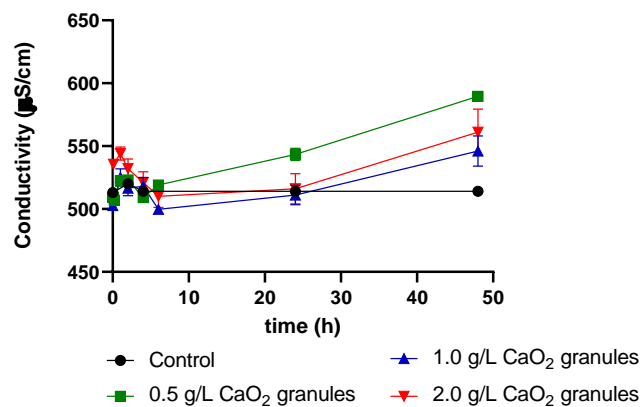


**Figure S 8.** Recorded Conductivity (µS/cm) values after the addition of 0, 0.5, 1.0, and 2.0 g L<sup>-1</sup> CaO<sub>2</sub> granules in Kouris Dam surface water.

### CaO<sub>2</sub> granules toxicity study on *Echinogammarus veneris* sp.

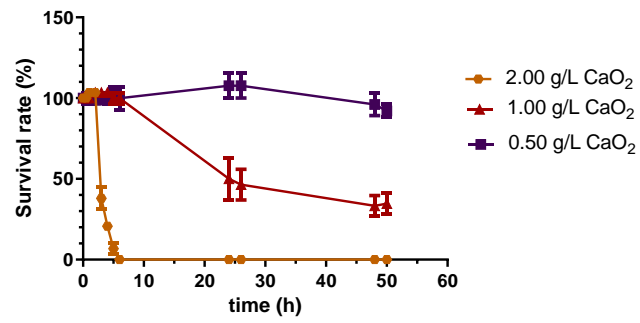


**Figure S 9.** Survival rate (%) of invertebrate species in river water matrix with addition of 0.5, 1.0, and 2.0 g L<sup>-1</sup> CaO<sub>2</sub> granules.

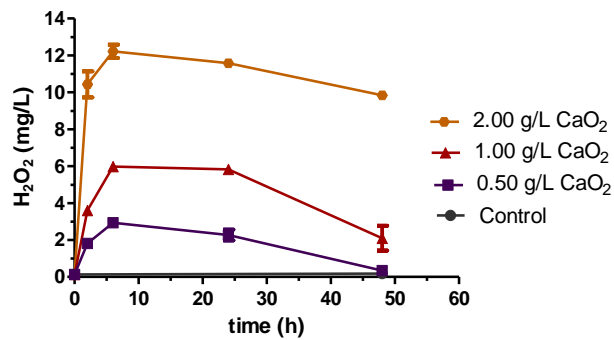
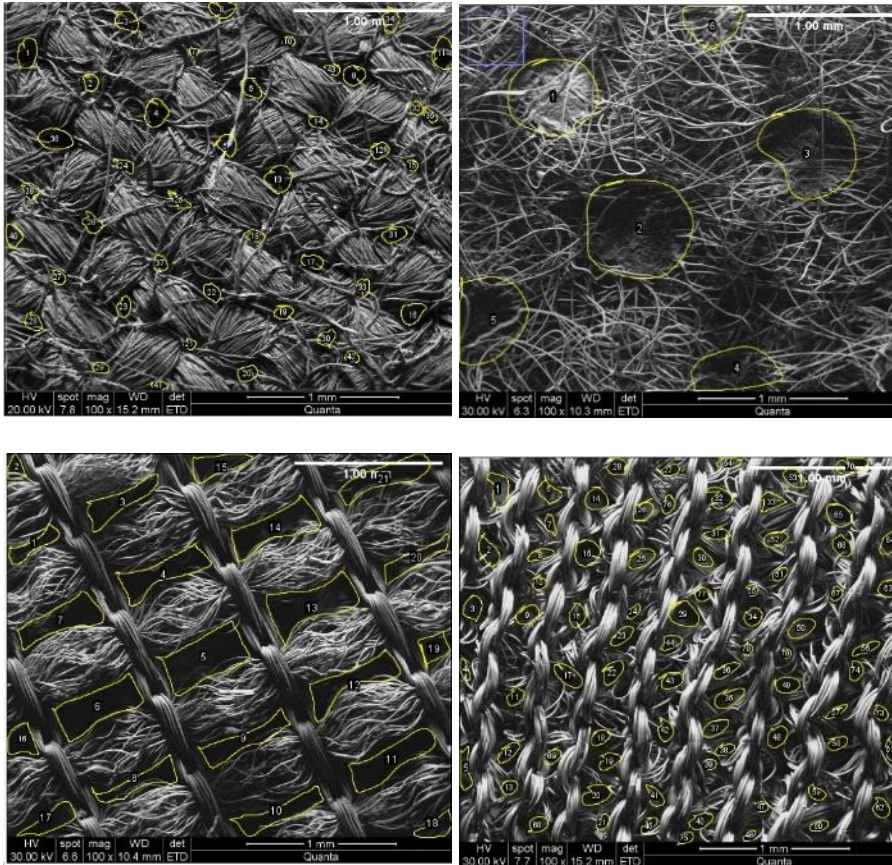


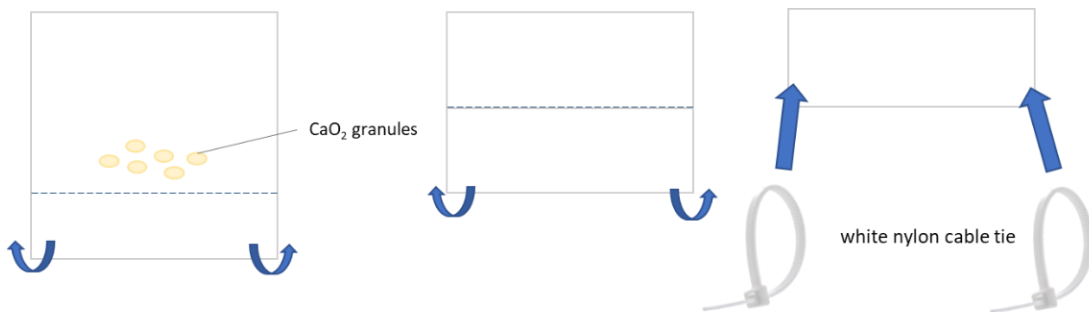
**Figure S 10.** Residual H<sub>2</sub>O<sub>2</sub> concentration measured during CaO<sub>2</sub> granules 0.5, 1 and 2.0 g L<sup>-1</sup> application in Kouris water with *Echinogammarus veneris* sp.

## Granules enclosed in fabrics (GEF)

### Fabrics characterization (SEM, Image J analysis)



**Scheme S 2.** SEM images of fabric types A-D processed with “Image J” software to determine to the pore size and pore surface area of each fabric.



**Scheme S 3.** Illustration explaining the process of folding  $\text{CaO}_2$  granules into a fabric material. The granules were placed into the middle of a square cut fabric and the fabric was folded two times. The fabric ends were tightly closed with white nylon cable tie.

➤ **H<sub>2</sub>O<sub>2</sub> release kinetics by GEF**

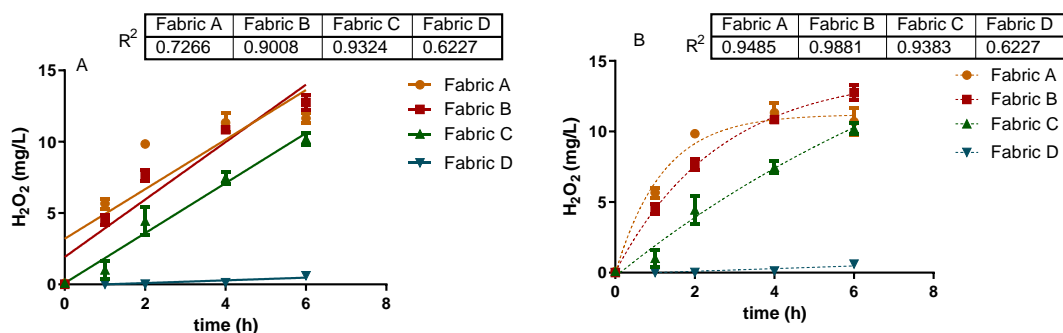


**Figure S 11.** H<sub>2</sub>O<sub>2</sub> released by GEF type A-D curves fitted by (A) Linear Regression Analysis and (B) one-phase association release.

**Table S 7.** Maximal H<sub>2</sub>O<sub>2</sub> yield (mg L<sup>-1</sup>) at t=24 hours by direct application of CaO<sub>2</sub> granules delivery system = none) and by GEF types A – D delivery systems, presented as value ± SD. Correlation coefficients and slope derived from the linear regression analysis between H<sub>2</sub>O<sub>2</sub> yield and CaO<sub>2</sub> granules dose applied in surface water (Kouris Dam) is presented at the right side.

H <sub>2</sub> O <sub>2</sub> yield (mg/L)				Linear Regression Analysis		
Delivery system	CaO <sub>2</sub> granules (g/L)	0.5	1.0	2.0	Correlation coefficient (R <sup>2</sup> )	Slope
	None		2.9 ±0.4	6.1 ±0.4	11.5 ±1.9	0.98
Type A		3.5 ±0.2	5.3 ±0.4	11.9 ±0.4	0.98	5.8 ±0.2
Type B		2.6 ±0.6	6.4 ±1.1	13.5 ±1.2	0.98	6.9 ±0.3
Type C		2.5 ±0.8	5.2 ±1.3	12.0 ±0.5	0.97	6.1 ±0.3
Type D		0.0 ±0.00	0.4 ±0.06	1.7 ±0.5	0.69	0.8 ±0.2

➤ **Comparison between peroxide-compounds on their toxicity on *Echinogammarus veneris* sp.**

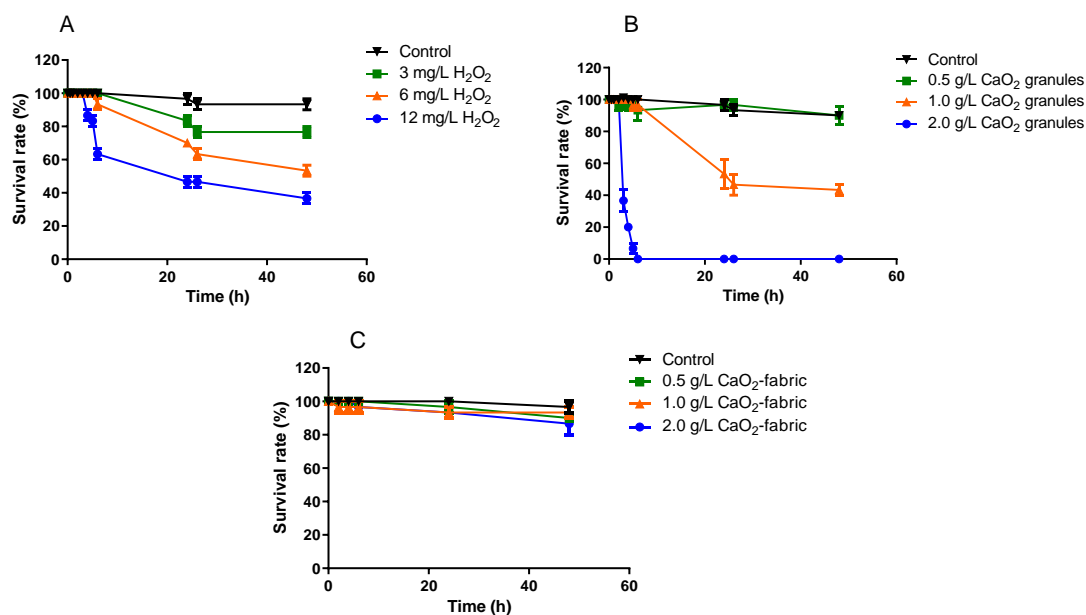


**Figure S 12.** Survival rate (%) of invertebrate species in river water matrix with (A) 0 (control), 3, 6, 12 mg/L liquid  $H_2O_2$  0, 3, 6, 12 mg/L (B) 0.5, 1 and 2.0 g/L  $CaO_2$  granules, and (C) 0.5, 1 and 2.0 g/L  $CaO_2$  granules enclosed in fabric.

➤ **Peroxymonosulfate**

**Table S 8.** Equal molarities of  $H_2O_2$  and PMS applied in treatments.

Oxidant	$H_2O_2$	PMS	OXONE	Sulfates Quantified in samples
mM	0.029	0.029	0.014	
mg L <sup>-1</sup>	1000	4410	9960	
	5	220.5	498	19-22
	3	132.3	298.8	
	1	44.1	99.6	

## Treatment of dam water spiked with cultivated *Microcystis* sp. PMS vs. liquid H<sub>2</sub>O<sub>2</sub> (single dosing)

### Polemídia Dam

Treatments in surface waters with various characteristics were performed to examine the effect of matrix on treatment efficiencies of KHSO<sub>5</sub> and H<sub>2</sub>O<sub>2</sub>. The results are presented in Figure S11. Water was collected from Polemídia Dam and spiked with cultivated *Microcystis* sp. cultures.

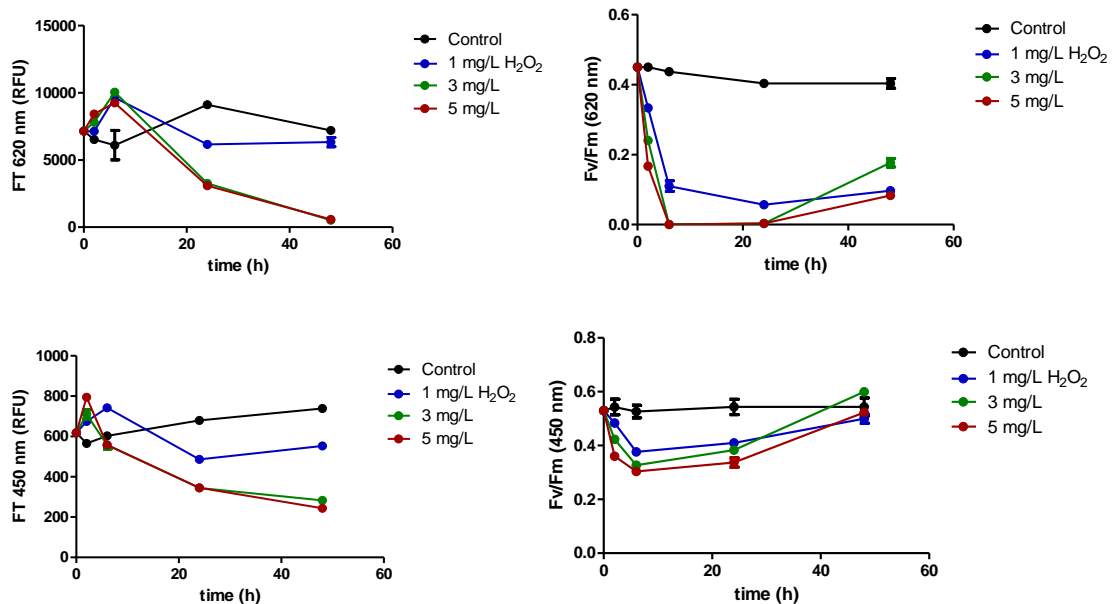


**Figure S 13.** Ft in raw fluorescence units (RFU) and QY (Fv/Fm) at  $\lambda=620$  and 450 nm during *Microcystis* sp. treatment in Polemídia Dam water with single doses of 1, 3, 5 mg L<sup>-1</sup> H<sub>2</sub>O<sub>2</sub>.

Treatment of *Microcystis* sp. with liquid H<sub>2</sub>O<sub>2</sub> and PMS single dose conducted for 48 hours to test the treatment efficiency, and residual oxidant concentration during treatment. Doses of 1, 3, and 5 mg L<sup>-1</sup> of H<sub>2</sub>O<sub>2</sub> and PMS added to treatment flasks and treatment efficiency was recorded as Ft and QY values in both wavelengths. For both oxidants, 5 mg L<sup>-1</sup> was the best treatment option since that dose eliminated the FT at  $\lambda=620$  nm and decreased dramatically QY of PSII, while keeping in a good status chl-a fluorescence recorded at  $\lambda=450$  nm. Increased pigmentation release was again captured during the treatment with liquid H<sub>2</sub>O<sub>2</sub>, with the highest concentration (5 mg L<sup>-1</sup>) reaching a phycocyanin fluorescence at  $\lambda= 620$  nm, around 10000 RFU (Figure S 11). Visual changes in the color of the treated waters were visible with the naked eye, since there was a fading of the distinct cyano- color during the 48 hours of treatment in all flasks.

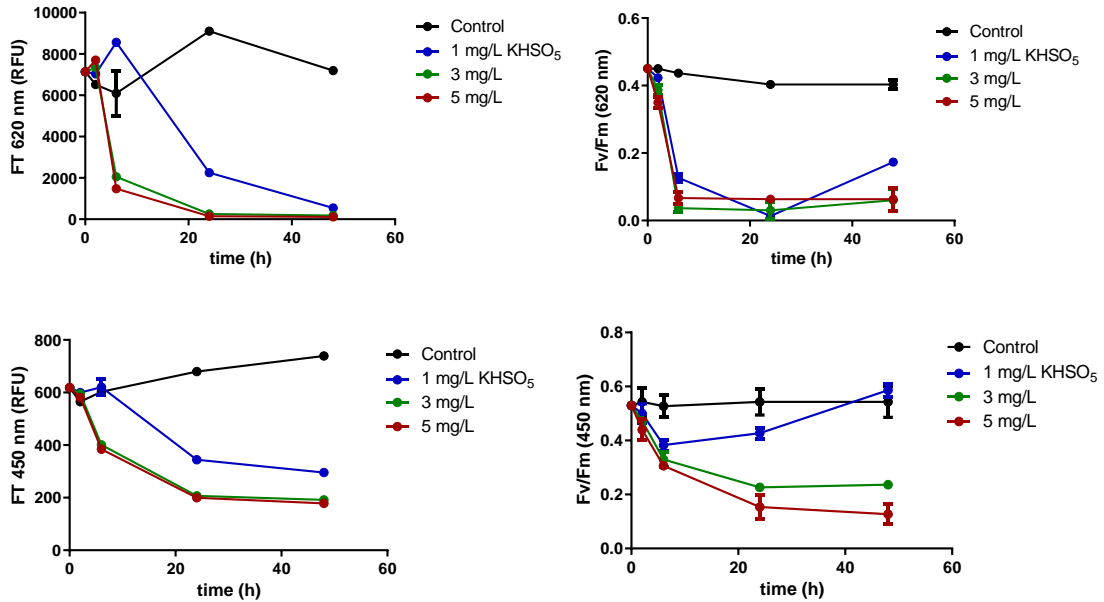


**Figure S 14.** Ft in raw fluorescence units (RFU) and QY (Fv/Fm) at  $\lambda=620$  and 450 nm during *Microcystis* sp. treatment in Polemidia Dam water with single doses of 1, 3, 5 mg L<sup>-1</sup> N.O.

Quantification of oxidants during the single dose treatment of *Microcystis* sp., was consistent with previous experiments, confirming the residual effect of N.O. into the matrix. Liquid H<sub>2</sub>O<sub>2</sub> declined rapidly at 24 hours of treatment (Figure S 13). Both oxidants were consumed by the end of the experiment, meaning that none was in excess and available for other non-targeted species; or that higher was needed.

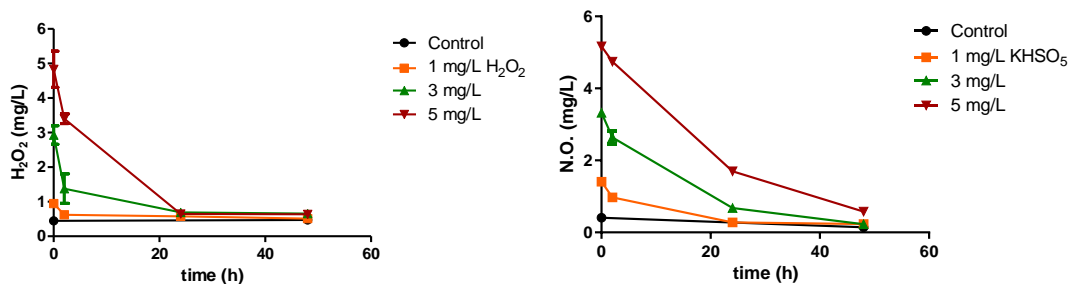


**Figure S 15.** Residual oxidant concentration measured during *Microcystis* sp. treatment in Polemidia Dam water with single doses of 1, 3, and 5 mg L<sup>-1</sup> H<sub>2</sub>O<sub>2</sub> (left) and PMS (right).

## Kouris Dam

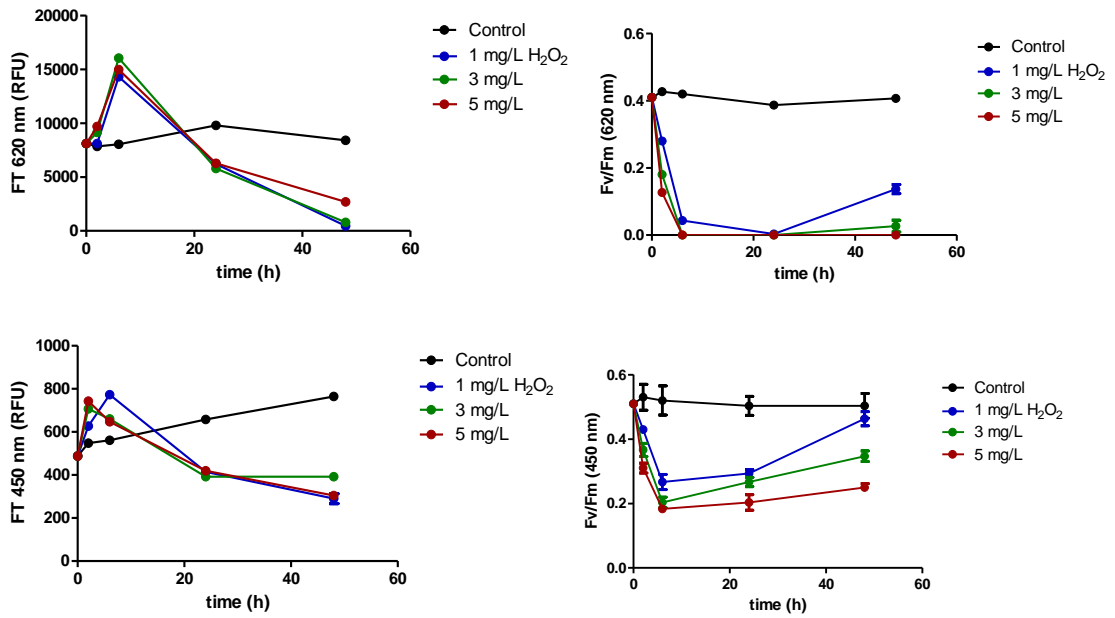


**Figure S 16.** Ft in raw fluorescence units (RFU) and QY (Fv/Fm) at  $\lambda=620$  and 450 nm during *Microcystis* sp. treatment in Kouris Dam water with single doses of 1, 3, 5 mg L<sup>-1</sup> H<sub>2</sub>O<sub>2</sub>.

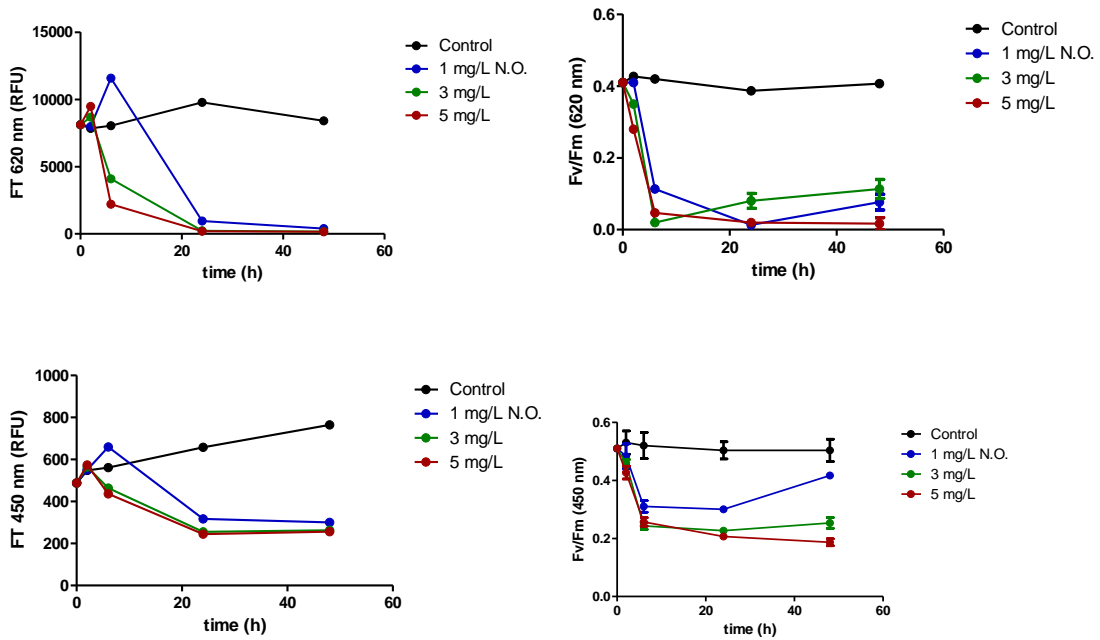


**Figure S 17.** Ft in raw fluorescence units (RFU) and QY (Fv/Fm) at  $\lambda=620$  and 450 nm during *Microcystis* sp. treatment in Kouris Dam water with single doses of 1, 3, 5 mg L<sup>-1</sup> PMS.

Treatment of Kouris spiked with *Microcystis* sp. utilizing equal doses of liquid H<sub>2</sub>O<sub>2</sub> and PMS gave supplementary to the other experiments results. The findings of these experiments are similar with treatment in Polemidia Dam matrix, which is expected since the two matrixes have similar water characteristics (Table S 3).